AD-A147 549 POTENTIAL EFFECTS OF NEW ENTRANCE CHANNEL TO BOLSA CHICA BAY CALIFORNIA O..(U) COASTAL ENGINEERING RESEARCH CENTER VICKSBURG MS L Z HALES OCT 84 1/3

UNCLASSIFIED CERC-MP-84-10 F/G 13/2 NL

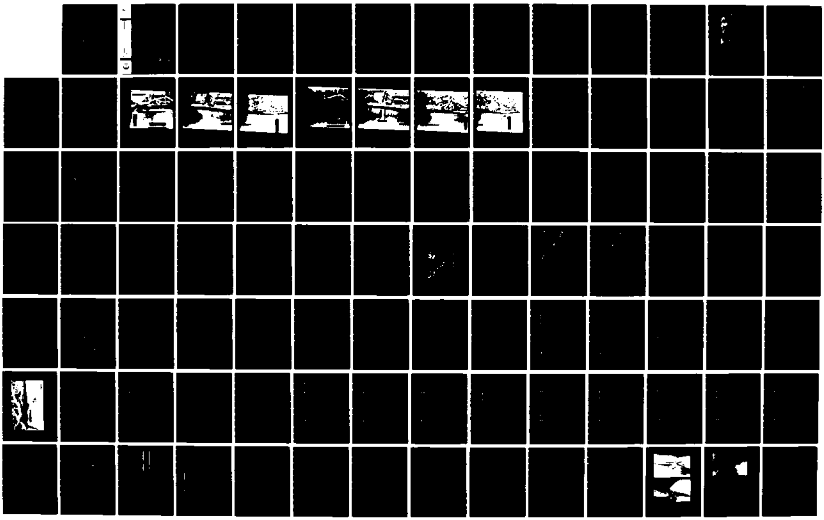

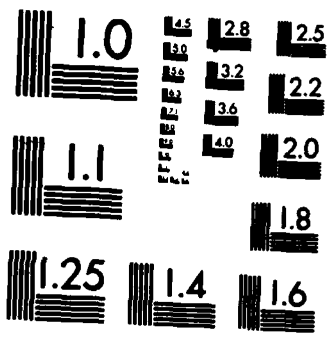
1.0
2.8
2.5
3.2
2.2
3.6
1.1
4.0
2.0
1.8
1.25
1.4
1.6

MISCELLANEOUS PAPER CERC-84-10

POTENTIAL EFFECTS OF NEW ENTRANCE CHANNEL TO BOLSA CHICA BAY, CALIFORNIA, ON UNSTABILIZED ADJACENT SHORELINES

by

Lyndell Z. Hales

Coastal Engineering Research Center

DEPARTMENT OF THE ARMY
Waterways Experiment Station, Corps of Engineers
PO Box 631
Vicksburg, Mississippi 39180-0631

October 1984
Final Report

Prepared for US Army Engineer District, Los Angeles
Los Angeles, California 90053

Monitored by Hydraulics Laboratory
US Army Engineer Waterways Experiment Station
PO Box 631, Vicksburg, Mississippi 39180-0631

Unclassified

SECURITY CLASSIFICATION OF THIS PAGE (When Data Entered)

REPORT DOCUMENTATION PAGE

READ INSTRUCTIONS BEFORE COMPLETING FORM

1. REPORT NUMBER Miscellaneous Paper CERC-84-10	2. GOVT ACCESSION NO.	3. RECIPIENT'S CATALOG NUMBER
4. TITLE (and Subtitle) POTENTIAL EFFECTS OF NEW ENTRANCE CHANNEL TO BOLSA CHICA BAY, CALIFORNIA, ON UNSTABILIZED ADJACENT SHORELINES		5. TYPE OF REPORT & PERIOD COVERED Final report 6. PERFORMING ORG. REPORT NUMBER
7. AUTHOR(s) Lyndell Z. Hales		8. CONTRACT OR GRANT NUMBER(s)
9. PERFORMING ORGANIZATION NAME AND ADDRESS US Army Engineer Waterways Experiment Station Coastal Engineering Research Center PO Box 631, Vicksburg, Mississippi 39180-0631		10. PROGRAM ELEMENT, PROJECT, TASK AREA & WORK UNIT NUMBERS
11. CONTROLLING OFFICE NAME AND ADDRESS US Army Engineer District, Los Angeles PO Box 2711 Los Angeles, California 90053		12. REPORT DATE October 1984 13. NUMBER OF PAGES 188
14. MONITORING AGENCY NAME & ADDRESS(if different from Controlling Office) US Army Engineer Waterways Experiment Station Hydraulics Laboratory PO Box 631, Vicksburg, Mississippi 39180-0631		15. SECURITY CLASS. (of this report) Unclassified 15a. DECLASSIFICATION/DOWNGRADING SCHEDULE

16. DISTRIBUTION STATEMENT (of this Report)

Approved for public release; distribution unlimited.

17. DISTRIBUTION STATEMENT (of the abstract entered in Block 20, if different from Report)

18. SUPPLEMENTARY NOTES

Available from National Technical Information Service, 5285 Port Royal Road, Springfield, Virginia 22161.

19. KEY WORDS (Continue on reverse side if necessary and identify by block number)

Bolsa Chica Bay (Calif.) (LC)
Channels (Hydraulic engineering) (LC)
Littoral drift--California--Simulation methods (LC)
Shore-lines--California (LC)

CA

20. ABSTRACT (Continue on reverse side if necessary and identify by block number)

Access to the open ocean from Huntington Harbor, ~~California,~~ is obtained by passage through Anaheim Bay which is heavily used by US Naval Weapons Station, Seal Beach. Concern has existed for many years about the possibility of accidental encounters between civilian and military craft in this area where ammunition off-loading and storage are routine practices. Local interests have requested US Army Engineer District, Los Angeles, to investigate the practicality of the construction of a new navigation entrance channel connecting Bolsa Chica Bay with the Pacific Ocean. Functional requirements of such a new entrance channel will necessitate stabilization by the use of a parallel or arrowhead jetty system, otherwise, the large net downcoast drift of littoral material will rapidly close the entrance channel and preclude navigation. At the same time, any jetty system will interrupt the transport of littoral material in
(Continued)

DD FORM 1 JAN 73 1473 EDITION OF 1 NOV 65 IS OBSOLETE

Unclassified

SECURITY CLASSIFICATION OF THIS PAGE (When Data Entered)

20. ABSTRACT (Continued).

the surf zone and deplete the downcoast (in terms of net transport) beaches of their nourishment from upcoast sources. Consequently, a sand bypassing concept must be developed to operate in concert with a weir jetty system. The jetty system is necessary for navigational channel stabilization and a sand bypassing system is required to mitigate effects of the jetties on the recreational beaches of Bolsa Chica Beach State Park.

The purposes of this study were to: (a) estimate the nearshore wave climate in the vicinity of potential new navigation entrance channel construction for structure design wave determination, and (b) to adapt computer simulation modeling of longshore transport of littoral material to estimate the resulting unstabilized shoreline evolution from jetty construction and example representative material bypassing at Bolsa Chica Beach State Park, California.

The wave heights and their frequency of occurrence were determined at five locations along the potential new structure site (10-, 15-, 20-, 25-, and 30-ft water depths). The maximum wave height at the structure for all waves is less than the breaking wave height for water depths of 30, 25, and 20 ft, and the proposed structure will be subjected to nonbreaking waves in these water depths. In shallower water, however, the combined effect of refraction and shoaling increases and the waves may break. These portions of the structure will be subjected to breaking waves of various periods from certain directions of approach. These data are presented in tabular form.

In order to estimate the effects of a weir jetty system and sand bypassing techniques on the adjacent unstabilized shorelines, it is necessary to have an understanding of the potential longshore transport of littoral material in the surf zone. The refraction analysis and wave hindcast data used for estimating the structure design wave were extended to calculate the potential longshore transport for the region of coastline extending from Surfside-Sunset Beach to Huntington Harbor. It was determined that on the average, approximately 376,600 cu yd of material moves toward the southeast each year, and about 100,700 cu yd of material is transported northwesterly each year, resulting in a net southerly transport of about 275,900 cu yd/yr.

A computer simulation model for shoreline evolution was adapted to this region and calibrated for known movement of material from the feeder beach located at Surfside-Sunset Beach. Because the renourishment interval for the feeder beach is expected to be about 5 years, the numerical model was operated for this period of time (with a time increment for computational purposes of 1 hr). The two critical times of the year in this region are toward the end of May (following a large volume of southerly transport movement) and toward the end of December (at the end of the northerly transport season). At these times, the shoreline will have advanced or retreated to its farthest position during the year's oscillations. The length of the sandtight landward section of the proposed navigation entrance channel west jetty between the preconstruction existing shoreline and the weir determines the extent of fillet formation that will evolve and ultimately the volume of material that will be available for transport back upcoast toward the erosional beach area.

Results of this study into the potential effects of a new entrance channel (and the necessary stabilizing structural measures) to Bolsa Chica Bay, California, on the unstabilized adjacent shorelines are detailed in tabular and graphical form.

PREFACE

The study reported herein was authorized by Intra-Army Order Number CIV-81-13 for Reimbursable Services dated 29 October 1980, from the US Army Engineer District, Los Angeles (SPL).

This investigation was conducted during the period 1 December 1980 through 30 September 1981 by personnel of the Hydraulics Laboratory of the US Army Engineer Waterways Experiment Station (WES) under the general supervision of Mr. H. B. Simmons, Chief of the Hydraulics Laboratory; Mr. F. A. Herrmann, Jr., Assistant Chief of the Hydraulics Laboratory; Dr. R. W. Whalin and Mr. C. E. Chatham, former and Acting Chiefs of the Wave Dynamics Division, respectively; and Mr. D. D. Davidson, Chief of the Wave Research Branch. The Wave Dynamics Division was transferred to the Coastal Engineering Research Center (CERC) of WES on 1 July 1983 under the direction of Dr. R. W. Whalin, Chief.

Mr. Claude Wong and Ms. Jane Fulton were the SPL Technical Monitors during the preparation and publication of this report. Coordination of this effort with other SPL investigations was maintained through discussions with Mr. Robert Nathan, Moffatt and Nichol, Consulting Engineers, Long Beach, California. Dr. L. Z. Hales, Research Hydraulic Engineer, performed the investigations described herein and prepared this report.

Commanders and Directors of WES during the conduct of the investigation and the preparation and publication of this report were COL Nelson P. Conover, CE, and COL Tilford C. Creel, CE. Technical Director was Mr. F. R. Brown.

CONTENTS

CONVERSION FACTORS, U. S. CUSTOMARY TO METRIC (SI) UNITS OF MEASUREMENT

U. S. customary units of measurement used in this report can be converted to metric (SI) units as follows:

Multiply	By	To Obtain
acre-feet	1233.482	cubic metres
acres	4046.856	square metres
cubic yards	0.7645549	cubic metres
feet	0.3048	metres
feet per second	0.3048	metres per second
feet per second per second	0.3048	metres per second per second
foot-pounds per foot per second	45.35924	kilogram-centimetres per metre per second
miles (U. S. statute)	1.609344	kilometres
pounds-second-second per foot per foot per foot per foot	52.5540137	kilograms-second-second per metre per metre per metre per metre

POTENTIAL EFFECTS OF NEW ENTRANCE CHANNEL TO BOLSA CHICA BAY, CALIFORNIA, ON UNSTABILIZED ADJACENT SHORELINES

PART I: INTRODUCTION

Project Location

1. Bolsa Chica Bay, California, is located south of the Los Angeles-Long Beach Harbor complex and north of Newport Beach (Figure 1). The specific portion of California coastline encompassed by this study begins at approximately the eastern jetty of Anaheim Bay and extends east and southeasterly for a distance of approximately 6 miles* to the city of Huntington Beach (Figure 2). Bolsa Chica Bay is connected to the Pacific Ocean through Anaheim Bay. Tidal flows have access to Bolsa Chica Bay from Anaheim Bay through Huntington Harbor at the Warner Avenue Bridge. Currently, tidal flow is controlled by three tide gates at the entrance to Bolsa Chica Bay. General concepts for increased marsh area subject to tidal action have been developed by the U. S. Army Engineer District, Los Angeles (SPL), in coordination with other Federal, State, and local agencies. These general concepts include plans that maintain tidal access through the existing channel, through a new ocean entrance, or by a combination of a new entrance channel and the existing channel. Proposed marina developments are included in plans with a new navigable entrance channel, and proposed saltwater marsh restoration only is included in plans with a new nonnavigable channel.

2. This study region consists of a portion of the San Pedro littoral cell as defined by Inman (1976) (Figure 3), which extends from Point Fermin on the northwest to the Newport Submarine Canyon on the southeast. The direction of net longshore transport of material in this vicinity is considered to be southerly by most researchers, for example, Emery (1960), Shepard and Wanless (1971), and Inman (1976). Any material that may be drifting southerly pass Point Fermin will be deposited in the deep water of San Pedro Bay outside the Los Angeles-Long Beach Harbor breakwaters.

---

* A table of factors for converting U. S. customary units of measurement to metric (SI) units is presented on page 4.

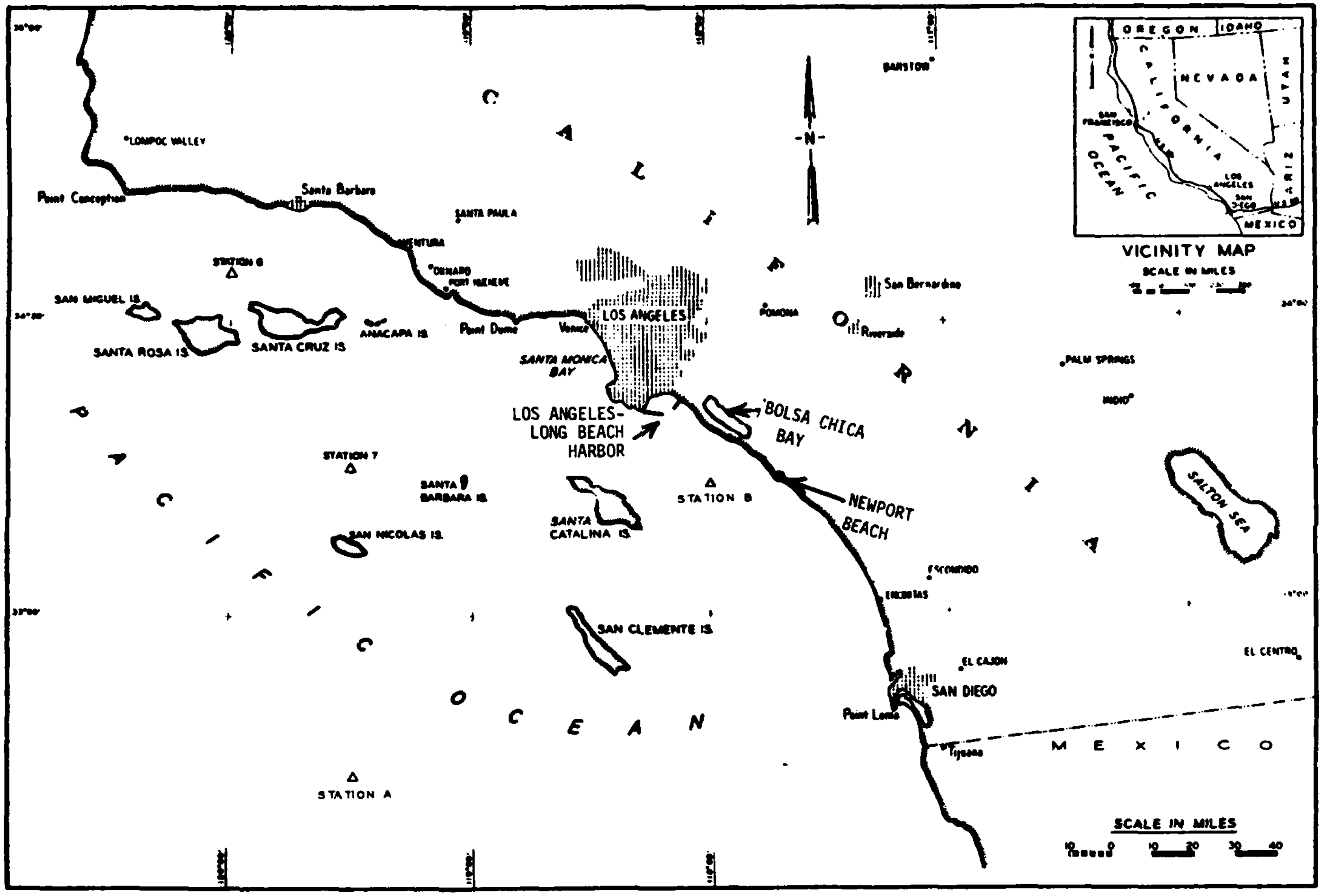

Figure 1. Bolsa Chica Bay, California, project location, and deepwater wave hindcasting stations

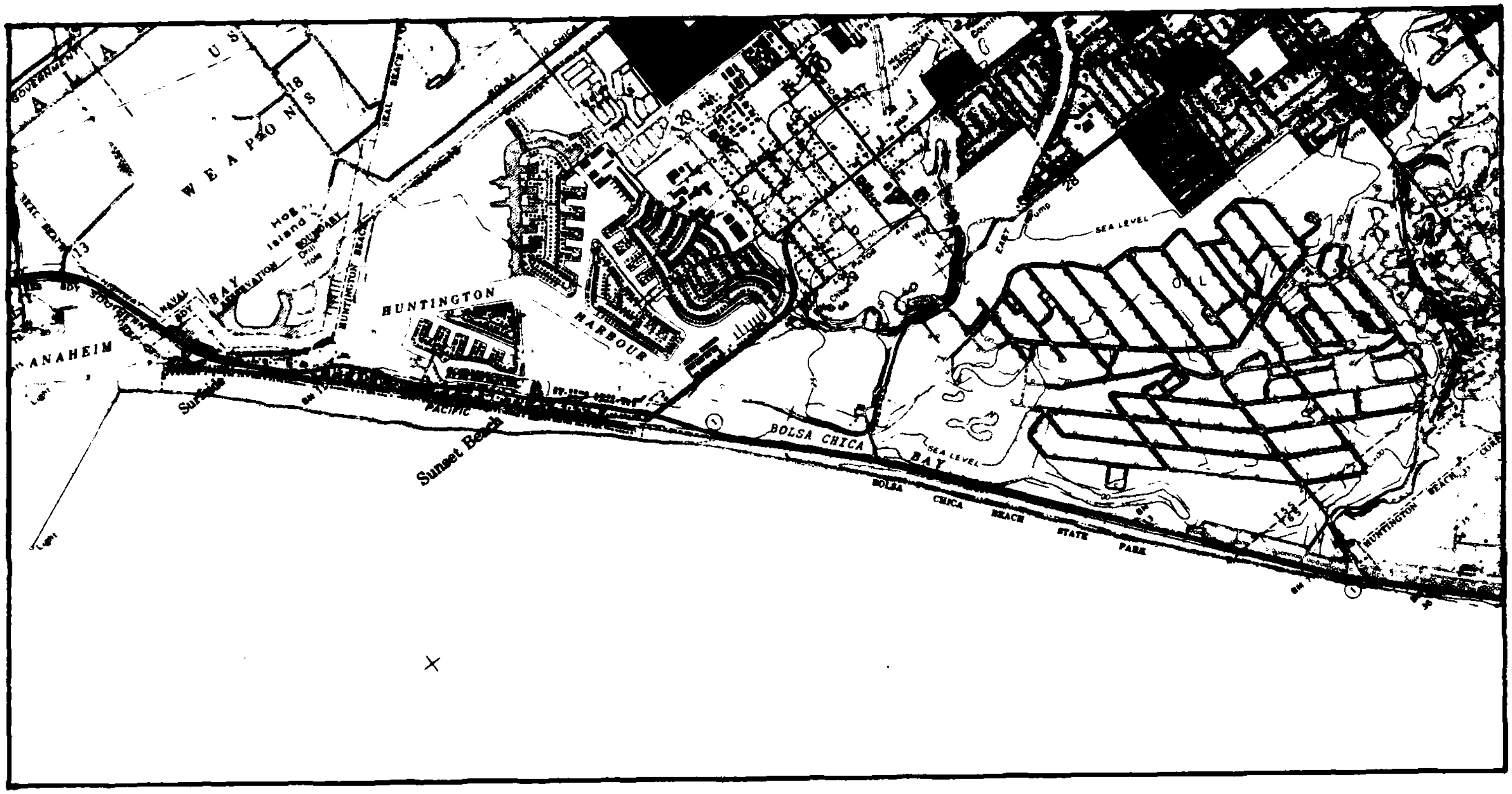

Figure 2. Bolsa Chica Bay, California, study region, extending from Anaheim Bay east jetty to the city of Huntington Beach, California

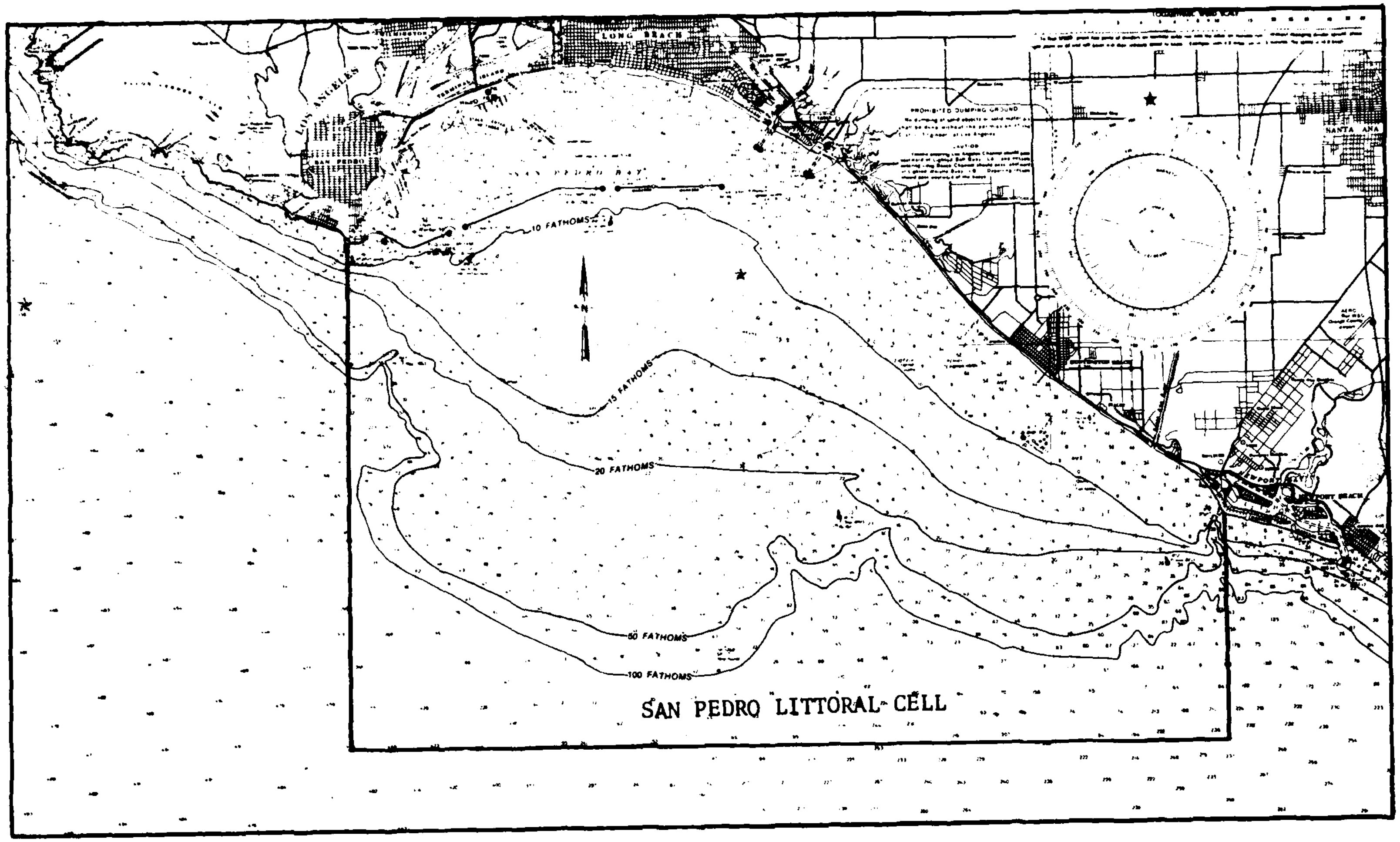

Figure 3. San Pedro littoral cell, *California*, as *defined* by Inman (1976), extending from Point Fermin on the northwest to the Newport Submarine Canyon on the southeast

Correspondingly, any littoral material drifting southerly pass Newport Beach will be lost from the system, as it is either moved offshore into deep water or trapped by the Newport Submarine Canyon.

3. A littoral cell is defined as a coastal segment that contains a complete sedimentation cycle including sources, transport paths, and sinks. The San Pedro littoral cell satisfies these requirements; i.e., the source being the feeder beach located immediately east of Anaheim Bay (Surfside-Sunset Beach) and infrequent transport to the beach by flooding of the Santa Ana River to the south of Huntington Beach, the transport path being the surf zone energized by breaking waves, and the ultimate sink to the southeast being either the Newport Submarine Canyon or the steeper nearshore bathymetry of the Newport Beach region. No firm quantitative figures exist to define precisely what happens to the sand, and this question contributed to the establishment in 1978 of a 5-year monitoring program by SPL (U. S. Army Engineer District, Los Angeles, 1978b). The monitoring program consisted of biological monitoring and physical monitoring (wave gage program, hydrographic surveys, and sand sampling and analysis). The entire beach between Anaheim Bay and Newport Bay Harbors (about 90,000 ft) had hydrographic and topographic surveys made on a quarterly basis. Sinks also exist to the north in the form of Anaheim Bay (for material potentially transported into the bay by tidal currents) and the beaches sheltered by the Long Beach breakwater from wave energy which could transport material back to the southeast. Sources of material for transport to the northwest are the beaches along the entire cell and the infrequent transport to the beach by the Santa Ana River.

4. The Santa Ana River enters the Pacific Ocean at approximately the midpoint of the San Pedro littoral cell and has historically contributed a significant amount of sediment to the surf zone. An analysis of U. S. Geological Survey sediment discharge data for the Santa Ana River for the period 1941-1971 by Kroll (1975) indicated the mean annual volume of coarse-sediment discharge to be 190,000 cu yd of material. Howver, in recent years, periods of prolonged drought and the construction of floodwater retarding structures on the river have drastically reduced the amount of river-transported sediment to the ocean (Brownlie and Taylor 1981). Reduction in the supply of sand to the beaches has resulted in severe erosion, beginning at Surfside and propagating downcoast. This has necessitated extensive beach nourishment and creation of a feeder beach in the Surfside-Sunset Beach area

(U. S. Army Engineer District, Los Angeles, 1978a), with a renourishment interval of approximately 5 years.

Statements of the Problems

5. The problems of this region are multifaceted and interrelated. Huntington Harbor, California, is an intensely concentrated recreational boating complex. Access to the open ocean is obtained by passage through Anaheim Bay, which is heavily used by the U. S. Naval Weapons Station, Seal Beach, California. Concern has existed for many years about the possibility of accidental encounters between civilian and military craft in this area where ammunition off-loading and storage are routine practices. Local interests have requested SPL to investigate the practicality of the construction of a new entrance channel connecting Bolsa Chica Bay with the Pacific Ocean. Additionally, in August 1972, the State of California executed a land agreement with Signal Property, Incorporated, regarding tidal lands in Bolsa Chica Bay. Points of the agreement pertinent to this study were that: (a) the State receive fee title to a 327.5-acre area of the Bolsa Chica Bay along the Pacific Coast Highway, (b) Signal Property, Incorporated, provided to the State the right to use, starting in 1973 and for a period of 14 years, an additional 230-acre area of Bolsa Chica Bay adjacent to the 327.5-acre area, and (c) the State will receive fee title to the 230-acre area provided a navigational channel with a minimum width of 300 ft be constructed connecting the Pacific Ocean to the Signal Property land during the 14-year period. In 1973, the State of California developed a conceptual plan utilizing the 557.5-acre area of the Bolsa Chica Bay for a public marina and saltwater marsh restoration. Navigable entrances located at two possible sites along the Bolsa Chica Bay shoreline (Figures 4 and 5), and a nonnavigable entrance for the purpose of tidal exchange with a saltwater marsh, are considered in this study.

6. Functional requirements of such a proposed new entrance channel will necessitate stabilization by the use of a parallel or arrowhead jetty system. Otherwise, the large net downcoast drift of littoral material will rapidly close the entrance channel and preclude navigation. At the same time, any jetty system will interrupt the transport of littoral material in the surf zone and deplete the downcoast (in terms of net transport) beaches of their nourishment from upcoast sources. Consequently, a sand bypassing concept must

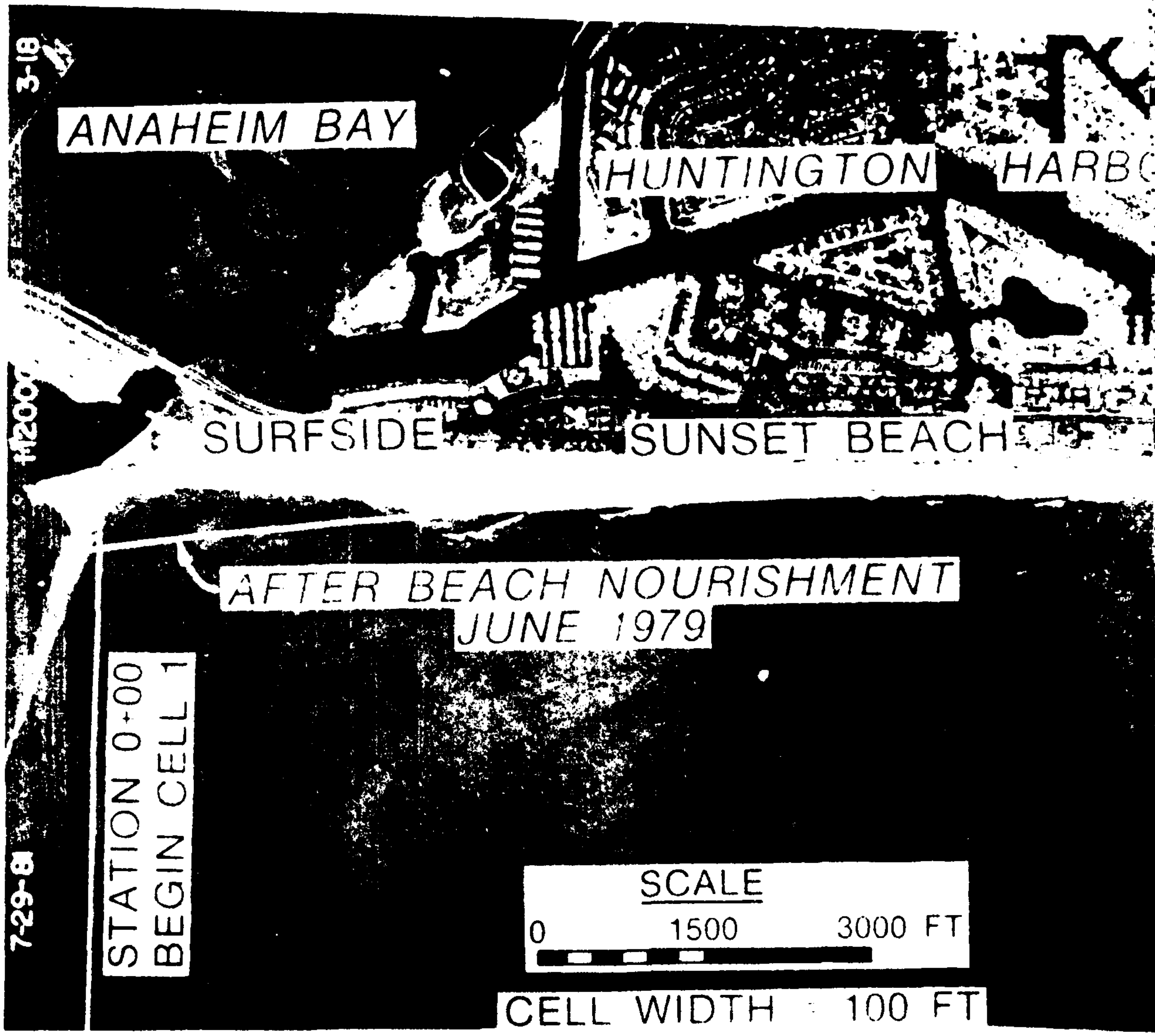
3-18
ANAHEIM BAY
HUNTINGTON
HARB
SURFSIDE
SUNSET BEACH
AFTER BEACH NOURISHMENT
JUNE 1979
STATION 0+00
BEGIN CELL 1
7-29-81
SCALE
0
1500
3000 FT
CELL WIDTH 100 FT

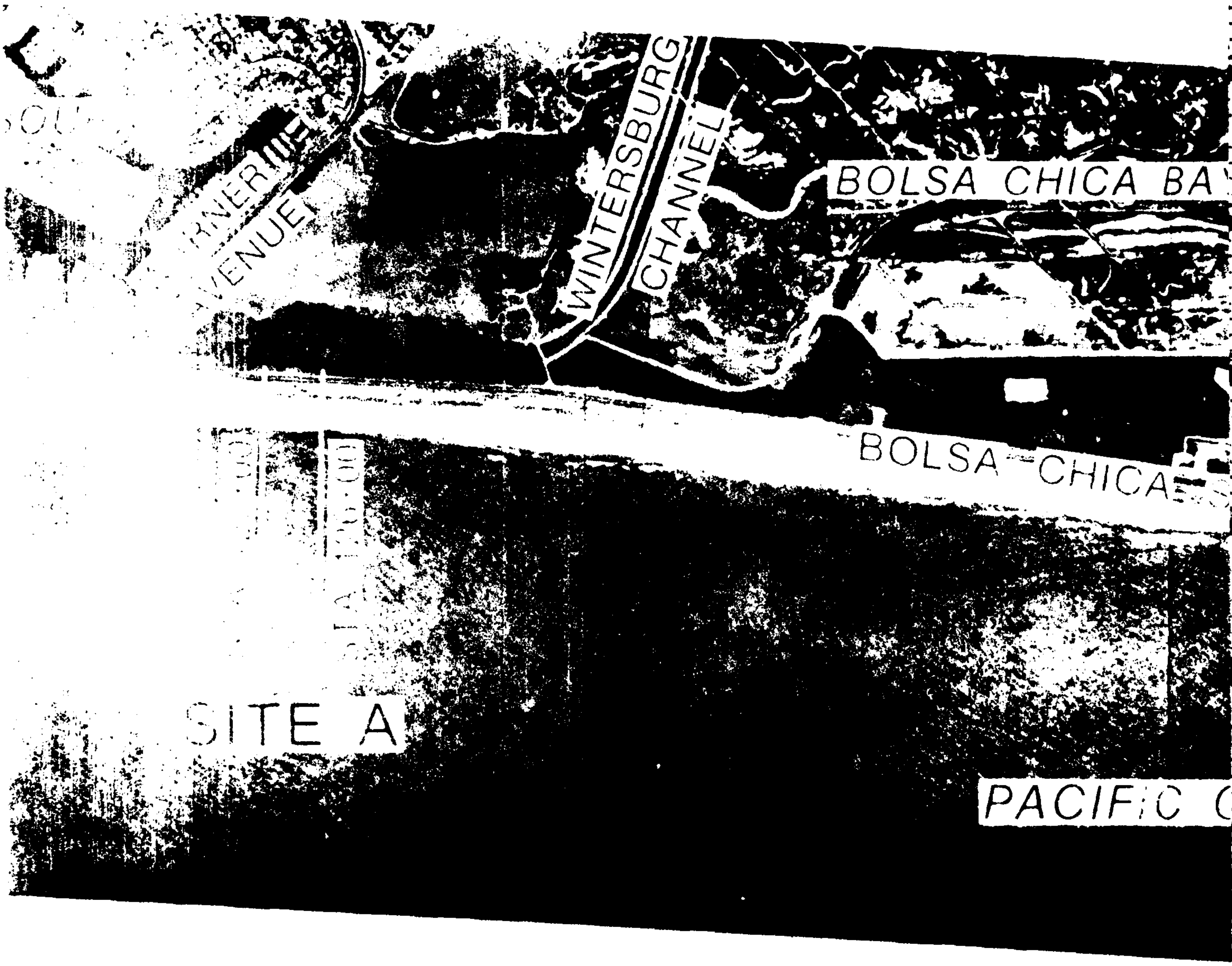

Figure 4. Potential new navigation entrance channel connecting Bolsa Chica Bay, California, with Pacific Ocean, Site A. Jetty structures incorporate a weir sand bypassing concept

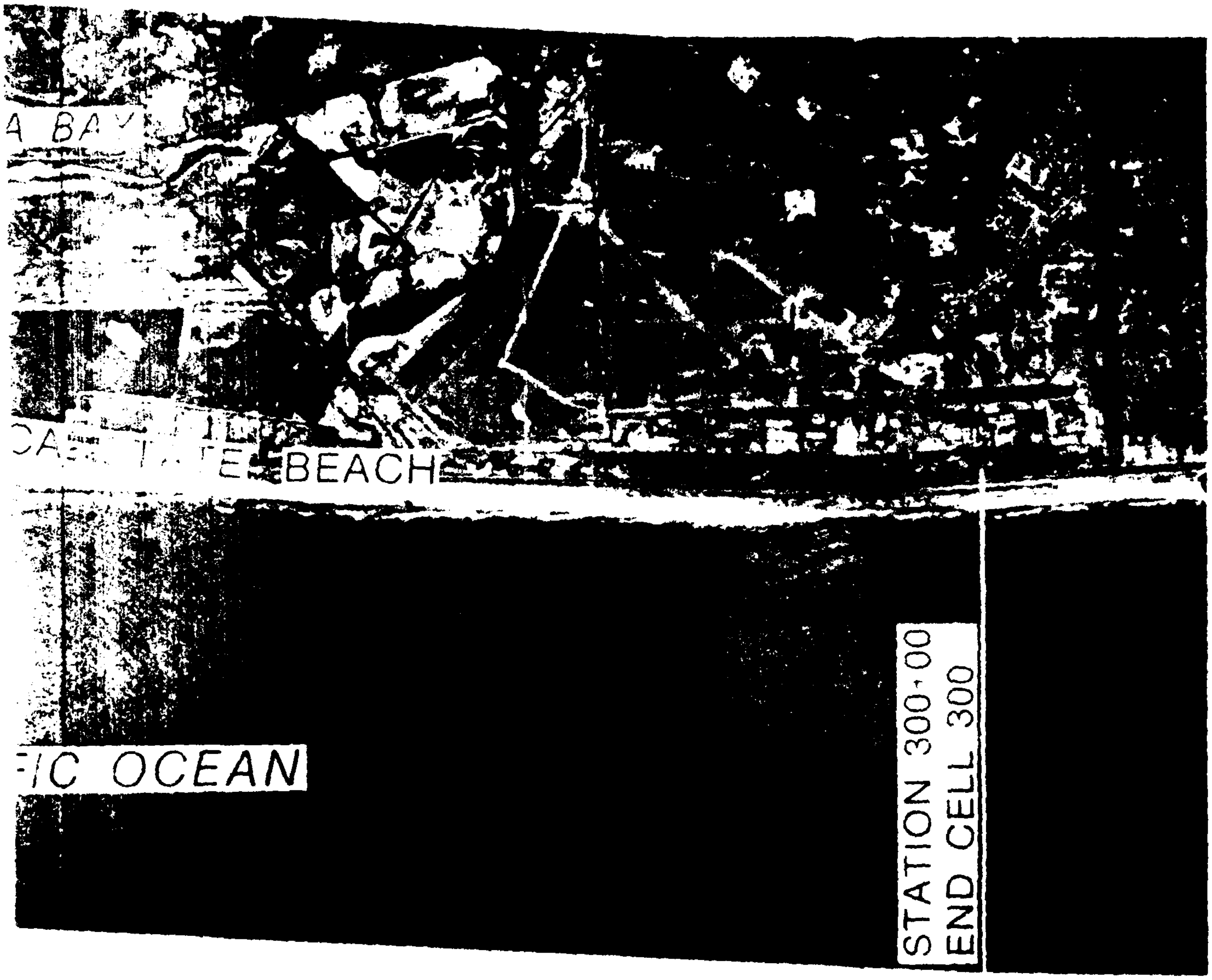

ia, with the
ept

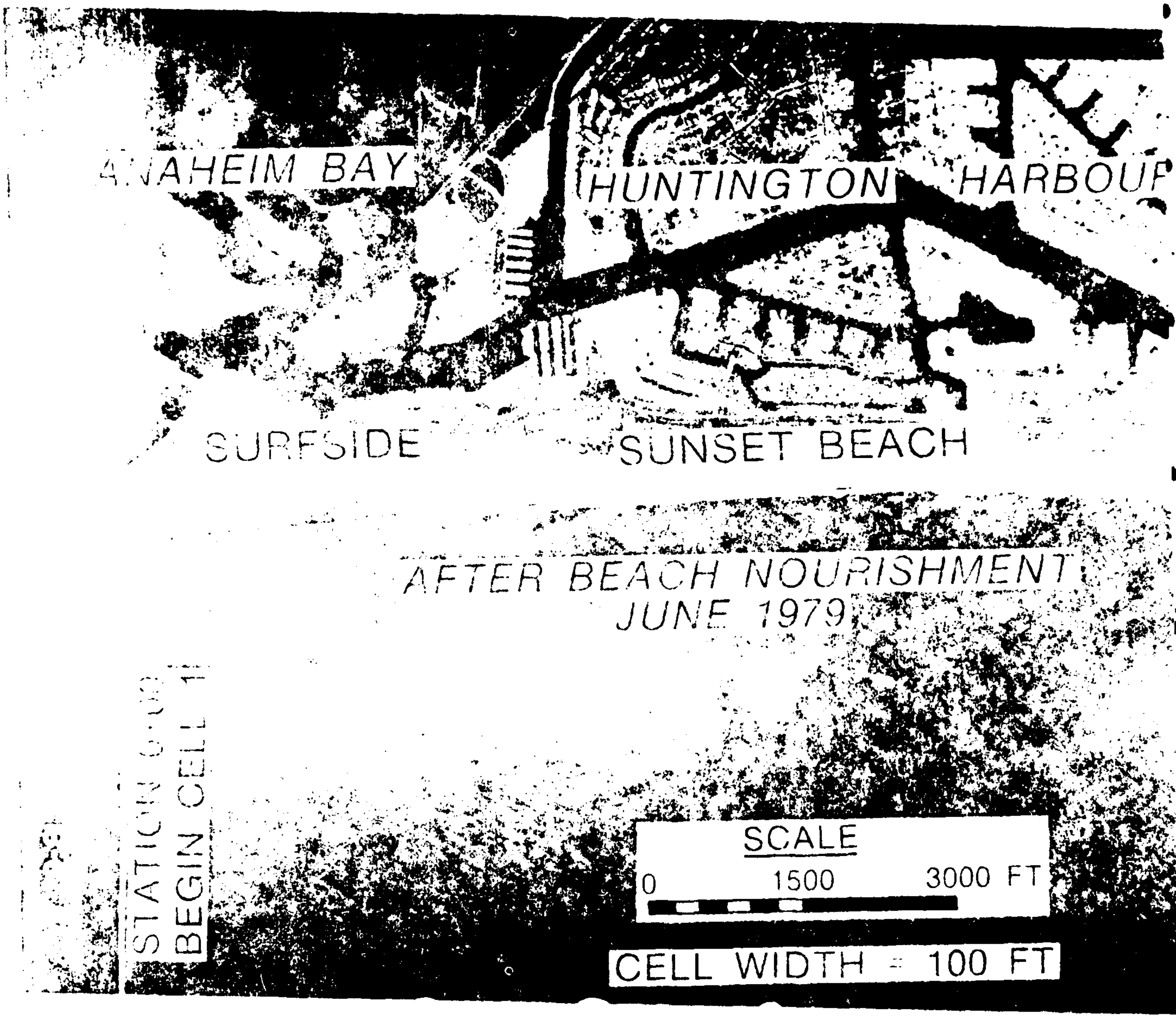

ANAHEIM BAY
HUNTINGTON HARBOUR
SURFSIDE
SUNSET BEACH
AFTER BEACH NOURISHMENT
JUNE 1979
STATION 0+00
BEGIN CELL 1
SCALE
0
1500
3000 FT
CELL WIDTH = 100 FT

Figure

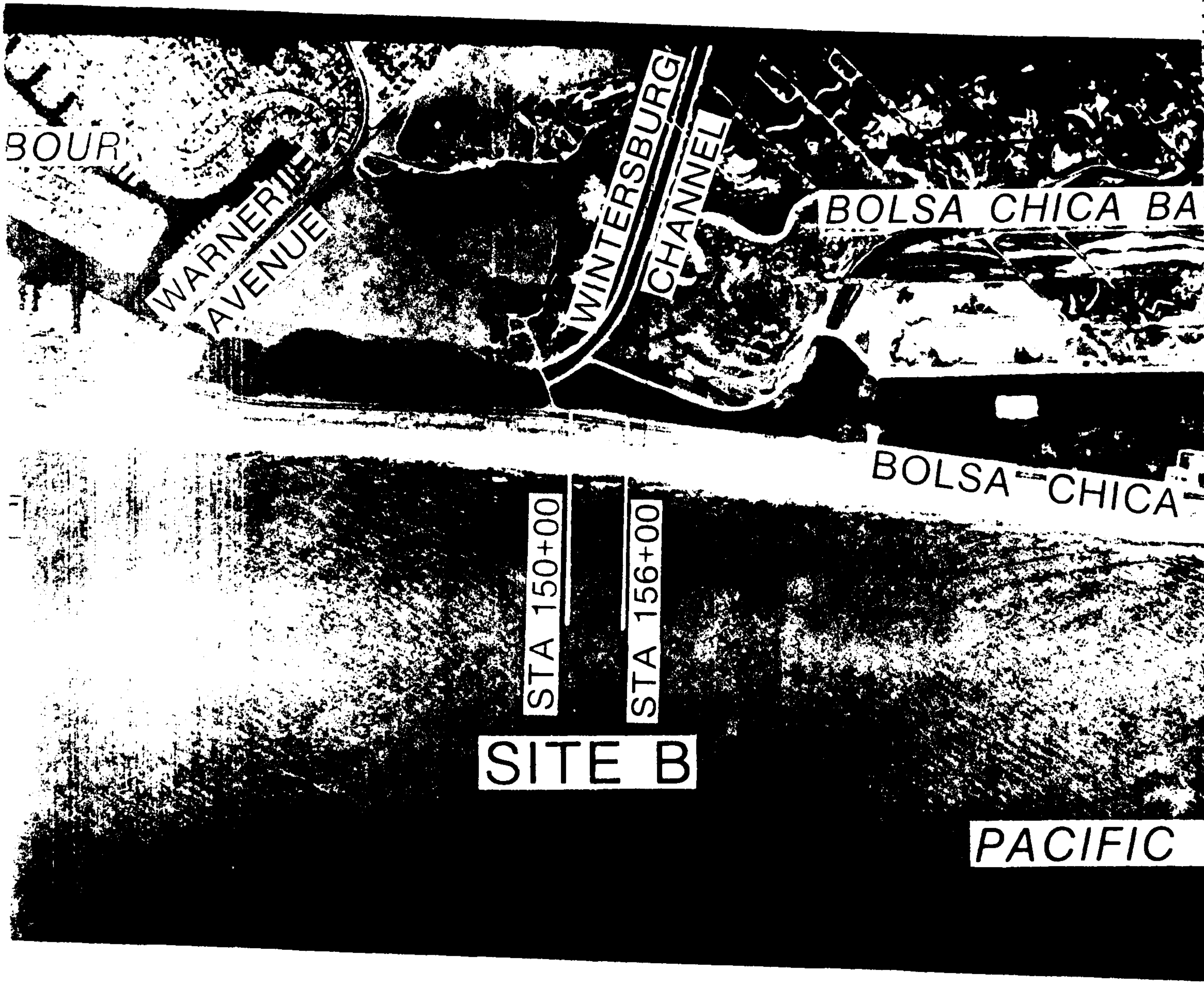

Figure 5. Potential new navigation entrance channel connecting Bolsa Chica Bay, California, wit Pacific Ocean, Site B. Jetty structures incorporate a weir sand bypassing concept

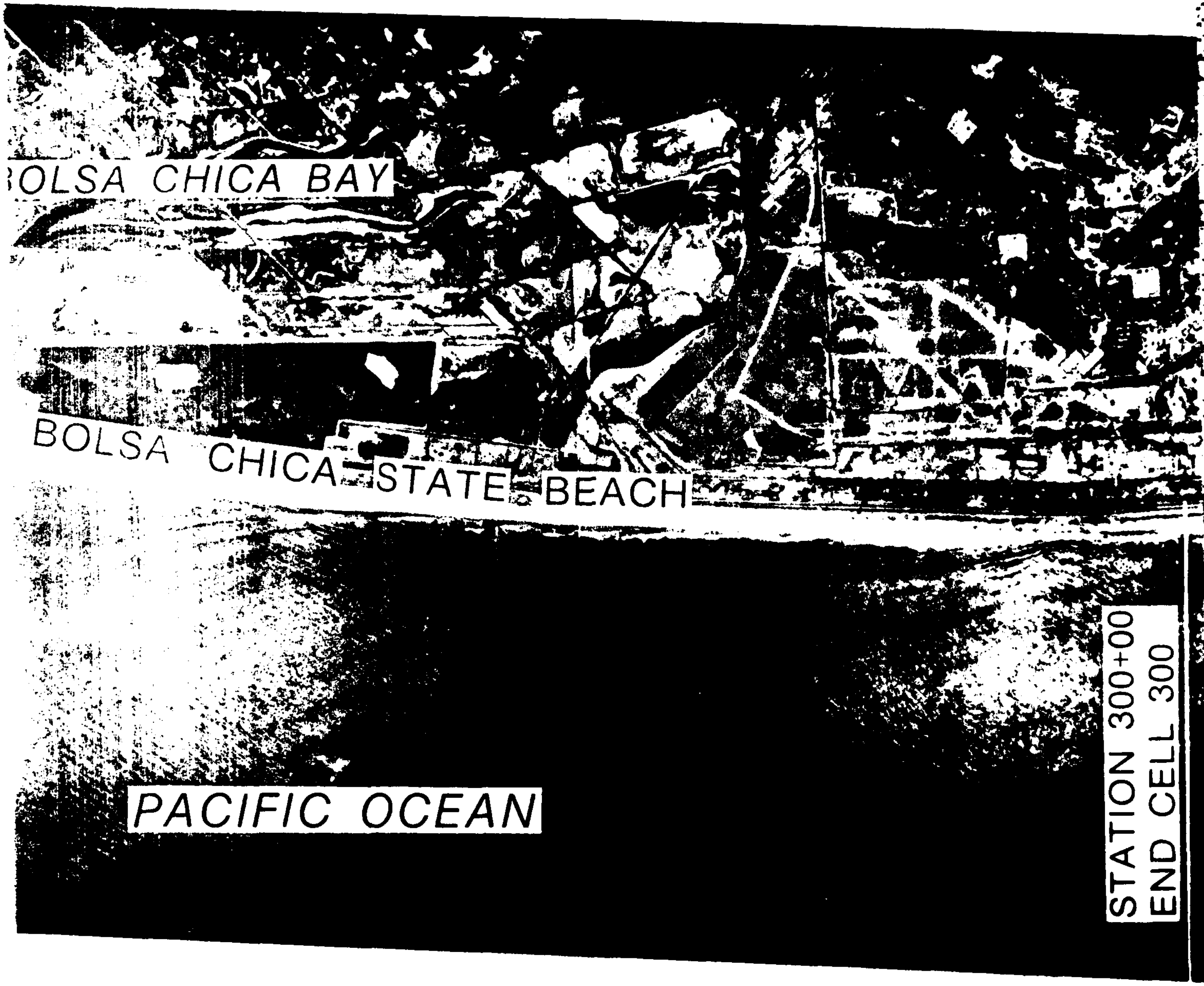

sa Chica Bay, California, with the
ir sand bypassing concept

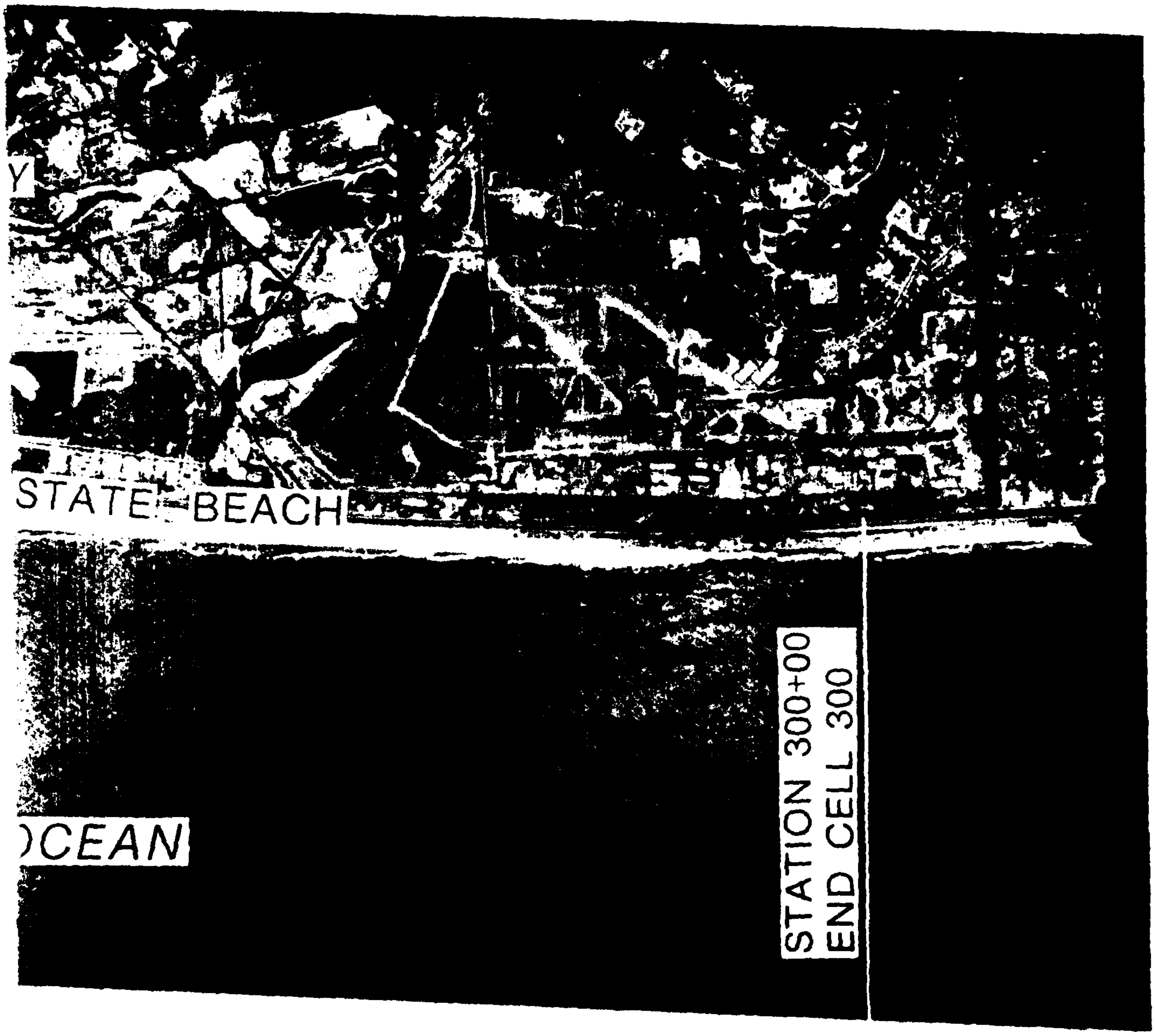

the

be developed to operate in concert with a jetty system. The jetty system is necessary for navigational channel stabilization and the sand bypassing system can be designed to mitigate effects of the jetties on the recreational beaches of Bolsa Chica Beach State Park.

Project Authorization

7. The Bolsa Chica Bay project was authorized by two congressional resolutions. The first of these two resolutions was requested by Congressman Richard T. Hanna, adopted in 1964, and reads in part:

> ....Resolved by the Committee on Public Works of the House of Representatives, United States, that the Board of Engineers for Rivers and Harbors is hereby requested to review the reports on the coast of southern California, with a view to determining the need for a harbor for light-draft vessels in the Bolsa Chica-Sunset Bay area, California....

The second resolution was requested by Congressman Mark W. Hannaford, adopted in 1976, and reads in part:

> ....Resolved by the Committee on Public Works and Transportation of the House of Representatives, United States, that the Board of Engineers for Rivers and Harbors is hereby requested to review the reports on the coast of southern California for light-draft vessels with a view to determining whether any modifications therein are warranted in the Bolsa Chica-Sunset Bay area, California, and to conduct a study to determine the feasibility and desirability of creating a tidal marsh upon the state-controlled lands in Bolsa Chica Bay for increasing its value for fish and wildlife. This study is to include evaluation and investigation of levees, jetties, breakwaters, and other works needed to provide and maintain tidal waters within the proposed marsh....

Purposes of the Study

8. Wind-generated ocean waves produce the most critical forces to which coastal structures are subjected (except possibly for seismic sea waves), according to the U. S. Army Coastal Engineering Research Center (CERC 1977). The wave height that a structure should be designed to withstand depends in part on whether the structure is subjected to nonbreaking, breaking, or broken

waves. The type of wave action experienced by a structure may vary with position along the structure and with water level and time at a given structure section. Critical wave conditions that result in maximum forces on structures such as jetties may be found at a location other than the seaward end of the structure. Jetties constructed of rubble-mound stone are considered to be flexible structures (CERC 1977), and their design wave height is usually the significant wave height, H_s,* at various locations along the structure (various water depths in the absence of the structure, at the site where the structure is intended to be constructed). The significant wave height (or wave spectrum) at a site includes the effects of refraction and shoaling. Statistical wave data are normally available only for deepwater hindcast stations, and refraction/shoaling analyses are necessary to determine wave characteristics at a nearshore site. The direction of approach, θ, and wave period, T, of the highest significant wave height (or wave spectrum) defines the direction of approach and period of the design wave (or spectrum).

9. When jetties are constructed across the littoral zone, where a substantial portion of the total transport takes place, the downcoast beach will experience erosion unless bypassing techniques are employed. At the same time, sand will accumulate on the updrift side of the jetty, and the accumulation may progress to such an extent that material passes around the seaward end of the jetty and into the navigation (or nonnavigable) channel. The Bolsa Chica Bay region appears to exist in such a littoral environment; hence it is imperative that portions of littoral drift which accumulate in the fillet and on the adjacent shoreline on the updrift side of the jetty system be systematically and timely transported to the downdrift beach in order to prevent detrimental accumulation on the updrift side and erosion downcoast. A temporal fillet will also develop on the downcoast side of the jetty system, and sand may occasionally have to be bypassed to the updrift side of the jetty system during periods of prolonged upcoast transport. The resulting shoreline configuration that develops will be in response to the blocking ability of the jetty system and the effectiveness of the bypassing system.

10. The purposes of this study are to: (a) estimate the nearshore wave climate in the vicinity of potential new entrance channel construction for

---

* For convenience, symbols are listed and defined in the Notation (Appendix E).

structure design wave determination, and (b) to adapt computer simulation modeling of longshore transport of littoral material to estimate the resulting shoreline evolution from jetty construction and material bypassing at Bolsa Chica Beach State Park region, California.

PART II: WAVE CLIMATE ESTIMATE FOR STRUCTURE DESIGN WAVE DETERMINATION

General Considerations

11. Incoming surface gravity waves not only directly affect the operation of marinas and harbors but also affect longshore transport of littoral material in the surf zone and erosion of adjacent shorelines, and are potentially damaging to structural engineering works of improvement. Wave height, period, direction of travel, frequency of occurrence, and energy of wave groups are wave characteristics that affect the nearshore processes. In turn, these wave characteristics are directly influenced by such physical factors as wave exposure, island sheltering, refraction, and shoaling. All these factors determine the height and angle of the incoming deepwater waves at the specific nearshore site.

12. Damage to flexible rubble-mound structures is usually progressive, and an extended period of destructive wave action is required before a structure ceases to provide protection. Waves higher than the significant wave height, H_s, impinging on flexible structures seldom create serious damage for short durations of extreme wave action. When an individual stone is displaced by a larger wave, smaller waves of the train tend to move it to a more stable position on the slope. It is necessary in selecting a design wave to consider both frequency of occurrence of damaging waves and economics of construction, protection, and maintenance. On the Atlantic and Gulf coasts of the United States, hurricanes may provide the design criteria. However, it may be uneconomical to build a structure that would withstand the hurricane conditions without damage; hence H_s is a more reasonable design wave height (CERC 1977). The Pacific coast of southern California is somewhat shielded by the offshore Islands of San Nicholas, San Clemente, Santa Catalina, and Santa Barbara from the extreme wave conditions generated on the open ocean. The resulting nearshore wave climate for this region is strikingly similar to that of the Gulf coast of the United States (CERC 1977) (Figure 6). Therefore H_s appears to be a reasonable design wave height for the Bolsa Chica Bay region, and is used as the design wave in this study.

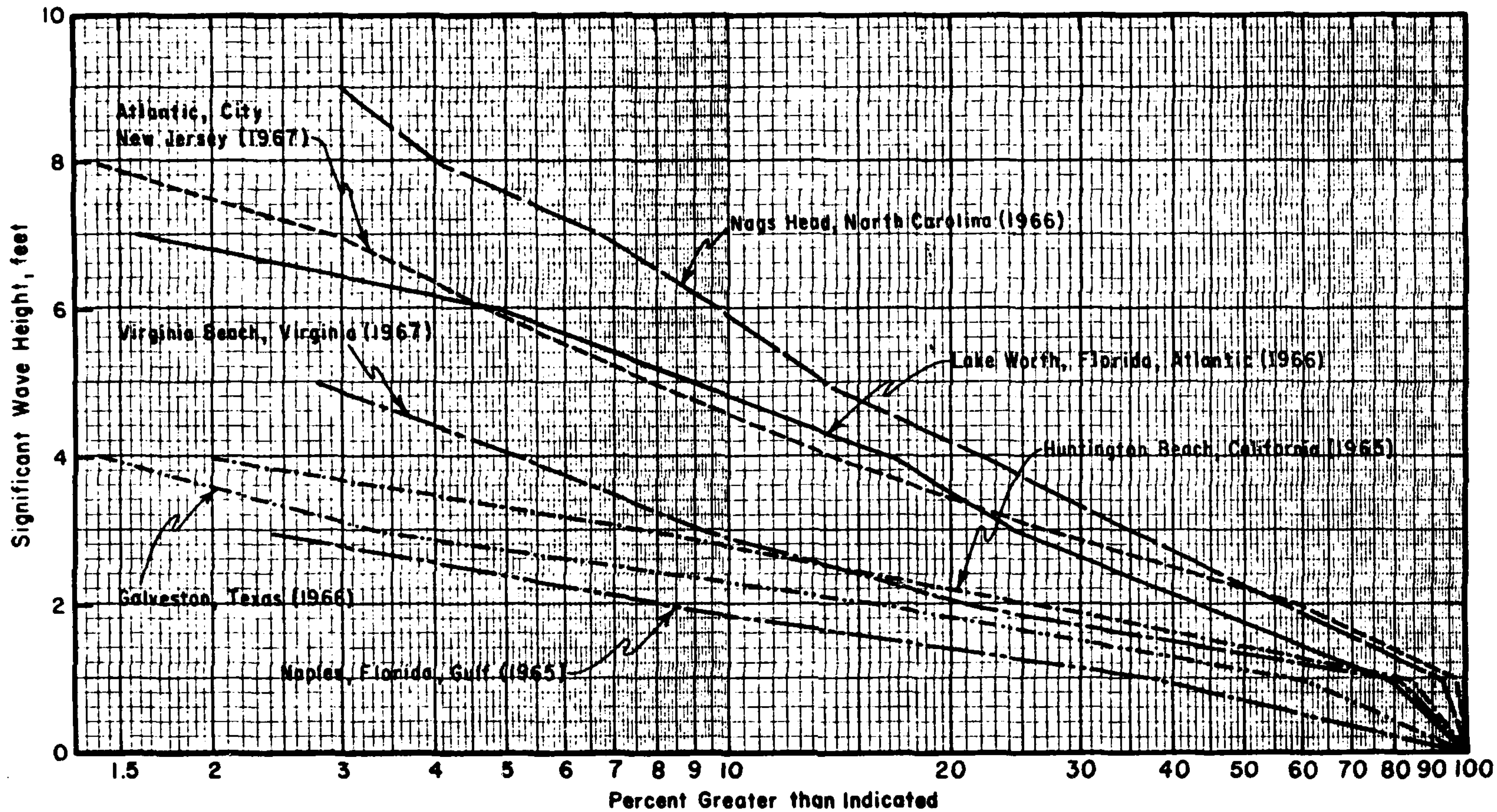

Figure 6. Distribution of significant wave heights, H_s, from coastal wave gages for 1-year records (after CERC 1977)

Wave Exposure

13. The degree to which a site is open to the directional spectrum of wave energy from distant and local storms is called wave exposure. The amount of wave exposure along the coastline of southern California from Anaheim Bay to Huntington Beach is dependent on the configuration of the mainland and on the location of the offshore islands. Wave exposure from the northwest is reduced by the shielding effect of the orientation of the coastline south of Point Conception. The Los Coronados Islands off the coast of Mexico have a minimal effect, and the Tanner Banks and Cortes Banks probably do not affect the wave transmission to the coast of interest since they lie directly in front of San Clemente and Santa Catalina Islands.

14. Different locations along the coastline are exposed to different wave climates due to the fact that the physical orientation of the coastlines and the islands permit wave exposure windows to vary as one proceeds southerly from Point Fermin to Huntington Beach. In general, the study area is exposed to open ocean swell from two different directions. Southern hemisphere swell penetrates the Gulf of Santa Catalina through the southern window which extends from San Clemente Island to the mainland (Figure 7). Some swell generated in the northern hemisphere also propagates northward through this window, but the predominant wave energy that enters this window is southern swell which produces a northward transport of littoral material in the region of interest. The western exposure window between Santa Catalina Island and Point Fermin allows a large amount of northern hemisphere swell to propagate directly down the San Pedro Channel and onto the shores of the study area. According to Emery (1960), the highest waves of the region ordinarily occur in the area between Point Arguello and San Nicolas Island, and these waves are commonly up to 2 m in height although larger waves up to 6 m high have occurred with some regularity. The northern hemisphere swell propagating through the western wave exposure window causes a significant amount of southern transport of littoral material along the coast of interest. Local sea breezes also generate shorter period waves (up to 10 sec) from all directions that contribute to both a northward and southward transport of material. Local seas are unaffected by the sheltering islands; however, the swell arriving from beyond the islands must be analyzed in light of sheltering effects.

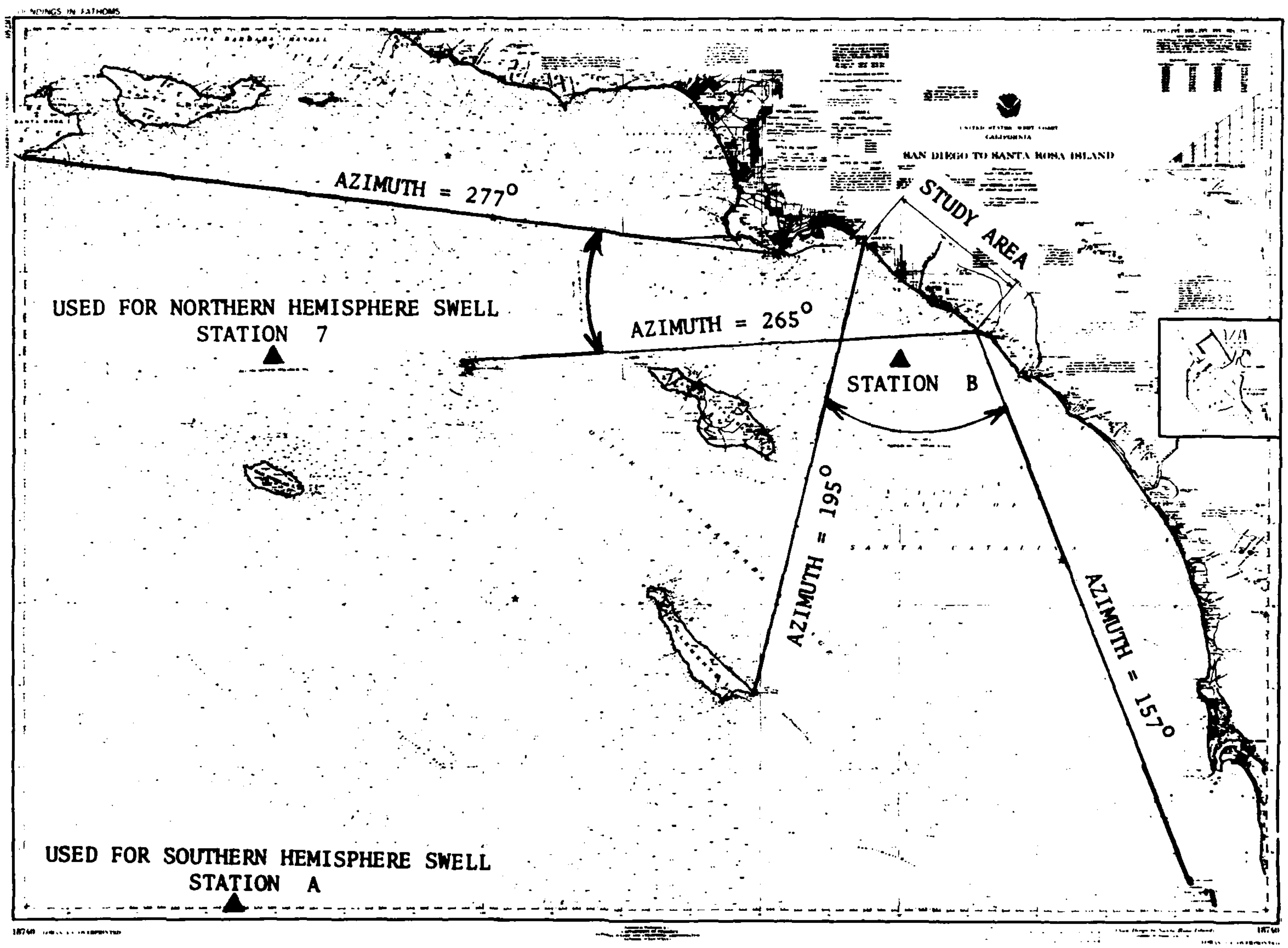

Figure 7. Western and southern wave exposure windows for the study area. Station A was used for southern hemisphere swell, Station 7 was used for northern hemisphere swell, and Station B was used for decayed and local sea waves

Island Sheltering Effects

15. If the southern California coastline from Anaheim Bay to Huntington Beach were not sheltered by the offshore islands, waves would arrive from a wide range of directions, even if the direction of the wind in the generating area were relatively constant. According to Arthur (1951), variability of wave direction makes a path of at least 45 deg on each side of the wind. A directional beam pattern of wave intensity of the form $(1 + \cos 2\theta)$ has been used to approximate this spreading function. The result of sheltering is to prevent certain parts of the wave rose from reaching the protected area.

16. In investigating island sheltering, the first consideration is to determine which directions of approach are open to waves of various periods and which are blocked. This cannot be accomplished by simply inspecting the sea level contours of the islands, for shoal water can act as a barrier just as effectively as an island shore. The blocking action depends on both water depth and wave period, with long-period waves requiring deeper water for passage than short-period waves. As a result, any given opening between two islands will present a narrower portal to a long-period wave than it will to a short-period one. With the aid of precise bottom-contour charts, all such avenues of approach were determined for the coastline between Anaheim Bay and Huntington Beach. The effect of sheltering on the wave climate was evaluated at the midpoint of the section of coastline being considered in this study.

17. The island sheltering theory yields not only height-reduction ratios but indicates modification in direction as well. Periods are assumed to remain unchanged. The direction modifications are necessary because, in some cases, sheltering will block out part or all of the central portion of the direction sector of a train of approaching waves. When this happens, the wave energy reaching the hindcast point will come from around the two ends of the barrier. The resulting modified wave train will come from a direction within the original sector but will be modified toward that end of the barrier around which the larger part of its remaining wave energy came. The island sheltering coefficients, or the percent remaining of the original deepwater wave height, and the direction-of-approach alterations were applied to the deepwater wave climate being used in this analysis. The resulting sheltered deepwater wave climate was then refracted shoreward to the study area. The

sheltered deepwater depth in all cases was 600 ft, which was the depth where the refraction analysis was initiated.

Data Sources

18. In recent years, questions have arisen regarding the applicability of using a singular wave model for the determination of wave statistics. Most knowledgeable researchers agree that the spectral approach should be significantly better, and indeed, the U. S. Army Engineer Waterways Experiment Station (WES) is presently engaged in a 5-year project to provide, through hindcasting, a numerical directional spectral wave climatology for all continental United States coastlines and Hawaii. This wave climatology will ultimately be available to all Corps of Engineers (CE) Districts in the form of a computer-based Sea-State Engineering Applications System (SEAS) with the capability to perform nearshore wave transformations such as those necessary for this study. However, initial computations for the coast of California from this new wave study will not be available until the latter part of 1983; hence it was not possible to delay an investigation of the wave climate and coastal processes taking place between Anaheim Bay and Huntington Beach until this comprehensive data set becomes available. Consequently, the only viable alternative at the present time is to proceed with analyses based upon the best information currently available.

19. For this particular region of coastline, the best available wave data at the present time are believed to be the hindcast wave data of National Marine Consultants (NMC 1960), and Marine Advisers (MA 1961). Data stations from these two investigations are at locations that are more directly representative of the wave climate at the coastal region of interest than hindcast studies of other investigators. Results and conclusions of this study can be revised and updated, if necessary, as more precise wave data become available. Indeed, some results of the postconstruction monitoring program at Surfside-Sunset Beach which was initiated in 1978 (U. S. Army Engineer District, Los Angeles, 1978b) could be used to supplement the existing data base. This monitoring program also has established Littoral Environmental Observations (LEO) stations along the coastline from Anaheim Bay to Huntington Beach; however, the data base is quite limited at the present time and cannot be satisfactorily adapted to this particular study. The Office of the Chief of

Engineers (OCE) also is sponsoring through its Field Data Collection Program a coastal data program along the coast of California. This program, known as the California Coastal Data Program (CCDP), is being implemented to provide a 3-year determination of the wave climate along the entire California coast, and to make an extensive uniform collection of data to identify coastal processes. Again, these data are incomplete at the present time.

20. An evaluation of the adequacy of the hindcast data base upon which wave-height estimates for structure design wave determinations, and longshore computations, are founded would require the establishment of confidence limits during the actual hindcasting procedure. Wave hindcast data in use at the present time have not provided this information because of the inherent limitations. Marine Advisers (1961) discussed the fundamental limitations of hindcasting wave data from weather maps. When weather maps are used, two limiting factors are involved. The first concerns the accuracy of the map. Opportunities for error, both human and mechanical, exist at many places in the chain of activities stretching from the weather itself to the symbols on the map. The initial observation may have been correct, depending upon the skill and experience of the observer and the condition of the instrumentation. The second major limitation concerns the subjectivity of weather analyses in general. In considering the oceanic regions of a weather map, the weather forecaster inevitably encounters large areas where data are scant or nonexistent. Under these circumstances, it is obvious that no two forecasters will produce identical analyses. Such uncertainties can affect a wave hindcast, since moderate differences in isobar spacing can result in significant differences in the wind speeds they imply. The wave hindcasters for Marine Advisers (1961) accepted the work of their meteorological predecessors and on it imposed their own set of subjective interpretations, among which include the size and persistence of fetches, the intensity and direction of winds, and the duration of wind velocities that produce the wave hindcast. Under these limitations, confidence limits for past hindcast efforts are not available.

21. The southern California coastline from Anaheim Bay to Huntington Beach is exposed to deepwater waves propagating from the open ocean from southerly and westerly directions. The orientation of the coastline and offshore islands limits the approach of deepwater waves from other directions. Wave hindcasts have been prepared by Marine Advisers (1961) for three specific

locations, one of which (Station A) is located in open water beyond the sheltering islands (Figure 6). This station is exposed to open-ocean influences from the southeast through west to north-northwest, and is considered to be representative of conditions outside the offshore islands. The other two stations are located between the sheltering islands and the mainland. One of these stations (Station B) is positioned approximately 8 miles directly offshore from Newport Beach, and contains information regarding both local sea generation nearshore and decayed sea transferred past the sheltering islands from Station A. National Marine Consultants (1960) Station 7 is located directly west of the beach of interest, and experiences the wave climate propagating onshore between Santa Catalina and Point Fermin. The information of these three hindcast data stations is indicative of the wave climate along the shore of interest.

22. Marine Advisers (1961) Station A data contain the only information regarding swell waves generated in the Southern Hemisphere. Accordingly, these data were transferred past the islands by sheltering techniques. That Northern Hemisphere swell from a southerly direction was also transferred past the islands from Station A. The Northern Hemisphere swell from a westerly direction was used directly from Station 7 since this station sensed those waves propagating down the San Pedro Channel. Sea (local sea and decayed sea) was obtained from Station B located inside the sheltering islands directly offshore from Newport Beach.

Northern Hemisphere swell

23. The main source of wave energy for southern California waters is Northern Hemisphere swell originating from winds of Japanese-Aleutian storms that move from west to east across the North Pacific at relatively high latitudes, often stagnating in the Gulf of Alaska. Hawaiian storms that also move from west to east in middle latitudes generally do not produce as large a swell as do the Japanese-Aleutian storms. Tropical hurricane-type storms, which develop off the west coast of Mexico, move in a westerly direction at first and then usually curve to the north and northeast. These occur almost exclusively during the months of July through October. The resulting swell rarely exceeds 6 ft, but a strong storm will occasionally move far enough north to cause destructively high waves in portions of southern California. Steep pressure gradients around the Pacific high pressure cells can cause strong and persistent north and northwest winds over the extreme eastern

Pacific Ocean that result in significant Northern Hemisphere swell.

Southern Hemisphere swell

24. Southern Hemisphere swell is generated by winds associated with storms of the austral winter in the South Pacific, storms of even greater size and intensity than those of the Northern Hemisphere. This swell is most common during August and September (Marine Advisers 1961) but occurs significantly from May through October. The frontal storms of the South Pacific that produce Southern Hemisphere swell can be classified as either southern storms which move from west to east across relatively high southern latitudes, or New Zealand storms which originate in the general vicinity of New Zealand and move eastward across the middle latitudes. Other types of Southern Hemisphere storms contribute little or nothing to the swell that affects southern California. The Southern Hemisphere swell that reaches the area of interest has periods which vary from 12 to 20 sec, but with heights which rarely exceed 4 ft.

Sea

25. Sea is the term applied to short, steep waves that are still in or near the area in which they were generated, as distinguished from swell which refers to longer, flatter waves that have left the generating area and have begun to change their physical characteristics through frequency dispersion. In order to forecast sea, it is necessary to have information on the winds over the water area immediately windward of the forecast location. Wind conditions vary greatly offshore from the southern California coast with a characteristic transformation from relatively mild winds over the inner channels to strong, gusty winds outside the islands. The transition zone extends southeastward from Point Conception in a direction roughly corresponding to the California coastline. Station A lies in the region of strong winds, while Station B is in an area where the winds are usually light. Some of the sea waves outside of the islands are of considerable size and even after having been reduced by decay and island sheltering, their effect on mainland coasts is not negligible. In order that the statistics resulting from the hindcast efforts should reflect this phenomenon, decay and island sheltering coefficients were applied to the sea information from Marine Advisers (1961) Station A data and results were added to the sea information which had been obtained for Station B by applying the Sverdrup-Munk-Bretschneider theory to local winds. Hence the sea statistics of Marine Advisers (1961) are actually a

composite of local sea plus decayed sea that has not been sufficiently removed from the generating influences to be called Northern Hemisphere swell.

26. The open-ocean deepwater wave statistics for Northern Hemisphere swell and Southern Hemisphere swell used in this study were extracted directly from National Marine Consultants (1960) and Marine Advisers (1961) and are presented in Appendix A. After these open-ocean deepwater statistics have been transferred past the sheltering islands, the sheltered deepwater wave statistics of Appendix B resulted. This appendix also contains the sheltered deepwater sea statistics (both local and decayed sea) that were available at the sheltered deepwater location a priori, and thus did not require transference past the islands.

Refraction and Shoaling Effects

27. The phase speed of a surface gravity wave depends on the depth of water in which the wave propagates. As the wave celerity decreases with depth, the wavelength must also decrease for the period to remain constant. Variation in phase velocity occurs along the crest of a wave moving at an angle to underwater contours, because that part of the wave in deeper water is moving faster than that part in shallow water. This variation causes the wave crest to bend toward alignment with the contours. This bending effect, called refraction, depends on the relation of water depth to wavelength. It is analogous to refraction of other types of waves, such as light or sound.

28. As waves propagate from deep water into shallow water, changes other than refraction take place. The assumption generally made is that there is not loss of wave energy and negligible reflection. Thus the power being transmitted by the wave train in water of any depth is equal to the power being transmitted by the wave system in deep water. The wave does not experience a lateral flow of energy across orthogonals, and the period remains constant in water of any depth, whereas the wavelength, celerity, and height vary.

29. The transformation of irregular ocean waves is a complex process that is not fully understood. The usual method of treating the problem (which is both practical and relatively successful) is to represent the actual system by a series of sinusoidal waves of different heights, periods, and phases. Such a system now has a two-dimensional energy spectrum. The wave statistics

being analyzed in the present study are treated in this manner by the method of Dobson (1967).

30. Refraction and shoaling effects are important for several reasons. These phenomena determine the wave height at any particular water depth for a given set of incident deepwater wave conditions (i.e., wave height, period, and direction-of-approach in deep water). Refraction and shoaling, therefore, have a significant influence on the distribution of wave energy along the coast. The change in wave direction of different parts of the wave results in convergence or divergence of wave energy and materially affects the forces exerted by waves on structures in varying water depths. Also substantially affected is the wave's capacity to transport sand either alongshore or onshore/offshore.

Wave Climate at Proposed Structure Site

31. The purpose for the construction of a jetty system at locations such as that shown in Figures 4 and 5 is to stabilize navigation (or nonnavigable) channels from the Pacific Ocean to Bolsa Chica Bay and to prevent the channels from closing by an influx of littoral material. The extension of the jetties through the surf zone for a distance sufficient to reach a water depth where wave motion will not be felt on the bottom is, of course, impractical. More realistically, the jetties should extend to a depth such that bottom movement will be experienced for only a small percentage of the time. Thus, because of the low frequency of occurrence, the total volume of material moved will not be untenable, considering the jetty system is conceived to be operated in concert with a weir sand bypassing mechanism if the entrance channel is constructed to allow navigation. The nonnavigable concept envisions an offshore bar bypassing mechanism with an accompanying allowance for a small percentage of material to be bypassed by dredging from the inner bar to nourish the downdrift beach. The proposed layouts of the navigable entrance channels of Figures 4 and 5 assume that the jetties are oriented essentially perpendicular to the offshore contours to minimize jetty length. The amount of wave shadow zone near the jetties, and thus the temporal stability of the fillets that form near structures of this nature, are directly determined by the jetty orientation. Other structure planform layouts may provide varying degrees of wave shadow.

Navigable entrance channel depth

32. The entrance channel to a harbor is intended to provide a pathway for boats free of breaking waves. This requires that either the jetties extend seaward beyond the zone of wave breaking or the channel be deep enough to preclude the breaking process. Additionally, the channel should be deep enough to prevent the keel of the largest boat from striking bottom as it traverses the channel at low tide through the incipient wave climate. The analysis of SPL (in preparation) for determining the depth of a new entrance channel to Bolsa Chica Bay was based primarily on wave effects, but prototype closure experience of other harbors on the Pacific coast of southern California was also considered.

33. A navigation channel can become unsafe as waves approach the breaking process, and complete breaking is not necessary for closure. Ahrens (1977) determined that the Rayleigh distribution was appropriate for wave height distribution in the surf zone. Waves arrive in groups of high and low heights with a statistical distribution of period and direction. Potentially, the most dangerous situation arises when the significant wave height is not breaking, but higher waves in the spectrum arrive in groups. The channel should be dredged or extended to water of sufficient depth to prevent the less frequently occurring waves from breaking in the channel. The entrance channel should be designed with a depth such that less than 1 percent of the waves break in the channel. The number of hours per year that the significant wave, H_s , and the 10 percent and 1 percent of the waves equal or exceed a breaking wave height across the proposed entrance channel locations are given in Table 1. Based on the Rayleigh distribution and the 1 percent exceedance frequency, SPL determined that if the channel were in 16 and 18 ft of water, closure would occur 4 and 2-1/2 days per year, respectively. The channel would be closed by the 1 percent exceedance wave in 20 ft of water about 1-1/2 days per year.

34. These results were comparable with the experience of other prototype marinas along the southern California coast; however, depending on the location, all marinas have slightly different wave exposures due to the sheltering effect of the offshore islands and existing protective structures at the entrance. The marinas of Oceanside, Newport, Ventura, Long Beach, and Marina del Rey all have project design depths of 20 ft mllw. Oceanside is the only one of these five marinas that has ever been officially closed, closing on the average about once each year. Newport experiences about 2 to

Table 1

Average Annual Hours of Wave Breaking
Across Proposed Entrance Channel
Bolsa Chica Bay, California

Depth ft mllw	Duration, hr H_s	H_{10}	H_1
16	4	7	103
18	2	4	63
20	*	1	34
22	*	*	17

* Less than 1 hr per year.
Source: U. S. Army Engineer District, Los Angeles (in preparation)

3 days each year of dangerous conditions, while Ventura reports 5 to 10 days each of dangerous conditions, although the exposure window of swell approaching from the west is greater than that at Bolsa Chica. Long Beach and Marina del Rey experience only minor disturbances each year due to breaking waves.

35. According to Dunham and Finn (1974), the minimum channel depth, d_{min}, should be great enough to allow all craft to safely pass through at low tide. This depth should allow for the draft of the largest vessel, heaving (approximately one-half the wave height), squat, and 1 to 2 ft of overdepth. Hence

$$d_{min} = D + \frac{1}{2} H + z + OD \qquad (1)$$

where

D = vessel draft, ft
H = wave height, ft
z = squat, ft
OD = overdepth, ft

For a typical 8-ft maximum draft operating in a relatively severe 10-ft wave climate, and considering a 1/2-ft squat and a 2-ft overdepth, the minimum channel depth should be about 16 ft. Allowing for possible shoaling or other obstacles, to reduce the occurrences of wave breaking in the entrance channel,

and based on the experience of other nearby marinas, SPL (in preparation) determined that the design channel depth for the proposed new entrance to Bolsa Chica Bay, California, should be 20 ft mllw.

Structure site significant wave height, H_s, estimate

36. Based on wave effects, nearby prototype marina closure experience, and CERC design guidance, the design depth of the entrance channel should be 20 ft mllw. This implies that the stabilization jetties should terminate in a water depth of 20 ft mllw. Due to the fact that additional structures in the form of offshore detached breakwaters of rubble-mound construction may be required to reduce the amount of wave energy propagating through the entrance channel, computations of the significant wave height occurring at the proposed sites of Figures 4 and 5 were extended to a water depth of 30 ft mllw.

37. Wave heights at various locations along the proposed jetty system depend directly on the deepwater wave height, deepwater wave period, and direction of approach. The shallow-water values of wave height and wave angle at locations along the proposed layout were determined by a refraction analysis. Because this study was conducted partially in conjunction with the Santa Ana River enlargement project, the area covered by the refraction analysis is substantially larger than that shown in Figures 4 and 5. The section of southern California coastline and the nearshore zone extending from Anaheim Bay to Abalone Point (near Laguna Beach) were included in the refraction analysis. The latest hydrographic survey data for this region were overlain by a 600-ft-square depth grid covering an area 14.3 miles by 30.0 miles. The 30.0-mile direction was alongshore, and the grid penetrated into the ocean approximately 14.3 miles. This grid size provided adequate detail and permitted the wave ray computations to proceed to the breaker zone for all wave conditions.

38. The entire 30.0-mile section of coastline was included in the ray computations so that the effect of all local topographic effects on wave amplification could be determined. Those rays that approached the shoreline in the vicinity of the proposed structure determined the wave heights to be expected along the structure. The highest waves in the period bands for the various directions of approach were considered, and the refraction and shoaling coefficients for those waves were obtained in water depths of 30, 25, 20, 15, and 10 ft; these data are tabulated in Tables 2-6, respectively. Here it is shown that for the deeper water depths, the product of the refraction and

Table 2

Significant Wave Heights and Frequency of Occurrence at Proposed New Entrance Channel to Bolsa Chica Bay, California, for Structure Design Wave-Height Determination

Water Depth, D = 30 ft, Wave Breaker Height, H_b = 23.4 ft

Sheltered Deepwater Azimuth deg	Wave Period sec	Deepwater Wave Height ft	Refraction Coefficient R_k	Shoaling Coefficient S_k	$R_k \times S_k$	Structure Wave Height ft	Frequency of Occurrence percent	Source
157	6-7.9	8-9.9	0.91	0.94	0.86	6.9-8.5	0.01	Sea
157	10-11.9	14-15.9	0.86	1.03	0.89	12.5-14.2	0.01	Sea
180	8-9.9	12-13.9	0.81	0.99	0.80	9.6-11.1	0.01	Sea
180	12-13.9	2-2.9	0.60	1.09	0.65	1.3-1.9	0.30	S. Swell
180	14-15.9	2-2.9	0.54	1.15	0.62	1.2-1.8	0.20	S. Swell
180	14-15.9	3-3.9	0.54	1.15	0.62	1.9-2.4	0.10	N. Swell
180	16-17.9	2-2.9	0.49	1.22	0.60	1.2-1.7	0.10	S. Swell
180	16-17.9	3-3.9	0.49	1.22	0.60	1.8-2.3	0.10	N. Swell
202	8-9.9	12-13.9	0.95	0.99	0.94	11.3-13.1	0.01	Sea
225	6-7.9	6-7.9	0.97	0.94	0.91	5.5-7.2	0.05	Sea
247	4-5.9	4-4.9	1.03	0.94	0.97	3.8-4.8	0.01	Sea
270	6-7.9	8-9.9	0.96	0.93	0.89	7.1-8.8	0.03	Sea
270	8-9.9	10-11.9	0.88	0.98	0.86	8.6-10.2	0.02	Sea
270	10-11.9	13-14.9	0.79	1.04	0.82	10.7-12.2	0.05	N. Swell
270	12-13.9	13-14.9	0.70	1.09	0.76	9.9-11.3	0.09	N. Swell
270	14-15.9	11-12.9	0.64	1.15	0.74	8.1-9.5	0.07	N. Swell
270	16-17.9	11-12.9	0.57	1.22	0.70	7.7-9.0	0.02	N. Swell

Table 3

Significant Wave Heights and Frequency of Occurrence at Proposed New Entrance Channel to Bolsa Chica Bay, California, for Structure Design Wave-Height Determination

Water Depth, D = 25 ft, Wave Breaker Height, H_b = 19.5 ft

Sheltered Deepwater Azimuth deg	Wave Period sec	Deepwater Wave Height ft	Refraction Coefficient R_k	Shoaling Coefficient S_k	$R_k \times S_k$	Structure Wave Height ft	Frequency of Occurrence percent	Source
157	6-7.9	8-9.9	0.90	0.95	0.86	6.9-8.5	0.01	Sea
157	10-11.9	14-15.9	0.86	1.07	0.92	12.9-14.6	0.01	Sea
180	8-9.9	12-13.9	0.80	1.01	0.81	9.7-11.3	0.01	Sea
180	12-13.9	2-2.9	0.58	1.13	0.66	1.3-1.9	0.30	S. Swell
180	14-15.9	2-2.9	0.53	1.20	0.64	1.3-1.9	0.20	S. Swell
180	14-15.9	3-3.9	0.53	1.20	0.64	1.9-2.5	0.10	N. Swell
180	16-17.9	2-2.9	0.48	1.27	0.61	1.2-1.8	0.10	S. Swell
180	16-17.9	3-3.9	0.48	1.27	0.61	1.8-2.4	0.10	N. Swell
202	8-9.9	12-13.9	0.95	1.01	0.96	11.5-13.3	0.01	Sea
225	6-7.9	6-7.9	0.98	0.95	0.93	5.6-7.3	0.05	Sea
247	4-5.9	4-4.9	1.03	0.95	0.98	3.9-4.8	0.01	Sea
270	6-7.9	8-9.9	0.96	0.95	0.91	7.3-9.0	0.03	Sea
270	8-9.9	10-11.9	0.87	1.01	0.88	8.8-10.5	0.02	Sea
270	10-11.9	13-14.9	0.78	1.07	0.83	10.8-12.4	0.05	N. Swell
270	12-13.9	13-14.9	0.70	1.13	0.79	10.3-11.8	0.09	N. Swell
270	14-15.9	11-12.9	0.64	1.20	0.77	8.5-9.9	0.07	N. Swell
270	16-17.9	11-12.9	0.57	1.27	0.72	7.9-9.3	0.02	N. Swell

Table 4

Significant Wave Heights and Frequency of Occurrence at Proposed New Entrance Channel to Bolsa Chica Bay, California, for Structure Design Wave-Height Determination

Water Depth, D = 20 ft, Wave Breaker Height, H_b = 15.6 ft

Sheltered Deepwater Azimuth deg	Wave Period sec	Deepwater Wave Height ft	Refraction Coefficient R_k	Shoaling Coefficient S_k	$R_k \times S_k$	Structure Wave Height ft	Frequency of Occurrence percent	Source
157	6-7.9	8-9.9	0.87	0.97	0.84	6.7-8.3	0.01	Sea
157	10-11.9	14-15.9	0.86	1.11	0.95	13.3-15.1	0.01	Sea
180	8-9.9	12-13.9	0.79	1.04	0.82	9.8-11.4	0.01	Sea
180	12-13.9	2-2.9	0.58	1.19	0.69	1.4-2.0	0.30	S. Swell
180	14-15.9	2-2.9	0.52	1.26	0.66	1.3-1.9	0.20	S. Swell
180	14-15.9	3-3.9	0.52	1.26	0.66	2.0-2.6	0.10	N. Swell
180	16-17.9	2-2.9	0.47	1.33	0.63	1.3-1.8	0.10	S. Swell
180	16-17.9	3-3.9	0.47	1.33	0.63	1.9-2.5	0.10	N. Swell
202	8-9.9	12-13.9	0.95	1.04	0.99	11.9-13.8	0.01	Sea
225	6-7.9	6-7.9	0.99	0.97	0.96	5.8-7.6	0.05	Sea
247	4-5.9	4-4.9	1.03	0.95	0.98	3.9-4.8	0.01	Sea
270	6-7.9	8-9.9	0.94	0.97	0.91	7.3-9.0	0.03	Sea
270	8-9.9	10-11.9	0.86	1.04	0.89	8.9-10.6	0.02	Sea
270	10-11.9	13-14.9	0.77	1.11	0.85	11.1-12.7	0.05	N. Swell
270	12-13.9	13-14.9	0.70	1.19	0.83	10.8-12.4	0.09	N. Swell
270	14-15.9	11-12.9	0.64	1.26	0.81	8.9-10.4	0.07	N. Swell
270	16-17.9	11-12.9	0.57	1.33	0.76	8.4-9.8	0.02	N. Swell

Table 5

Significant Wave Heights and Frequency of Occurrence at Proposed New Entrance Channel to Bolsa Chica Bay, California, for Structure Design Wave-Height Determination

Water Depth, D = 15 ft, Wave Breaker Height, H_b = 11.7 ft

Sheltered Deepwater Azimuth deg	Wave Period sec	Deepwater Wave Height ft	Refraction Coefficient R_k	Shoaling Coefficient S_k	$R_k \times S_k$	Structure Wave Height ft	Frequency of Occurrence percent	Source
157	6-7.9	8-9.9	0.85	1.00	0.85	6.8-8.4	0.01	Sea
157	10-11.9	14-15.9	0.84	1.17	0.98	11.7*	0.01	Sea*
180	8-9.9	12-13.9	0.78	1.09	0.85	10.2-11.7*	0.01	Sea*
180	12-13.9	2-2.9	0.58	1.26	0.73	1.5-2.1	0.30	S. Swell
180	14-15.9	2-2.9	0.52	1.34	0.70	1.4-2.0	0.20	S. Swell
180	14-15.9	3-3.9	0.52	1.34	0.70	2.1-2.7	0.10	N. Swell
180	16-17.9	2-2.9	0.47	1.43	0.67	1.3-1.9	0.10	S. Swell
180	16-17.9	3-3.9	0.47	1.43	0.67	2.0-2.6	0.10	N. Swell
202	8-9.9	10-13.9	0.95	1.09	1.04	10.4-11.7*	0.02	Sea*
225	6-7.9	6-7.9	0.99	1.00	0.99	5.9-7.8	0.05	Sea
247	4-5.9	4-4.9	1.02	0.95	0.97	3.9-4.8	0.01	Sea
270	6-7.9	8-9.9	0.93	1.00	0.93	7.4-9.2	0.03	Sea
270	8-9.9	10-11.9	0.85	1.08	0.92	9.2-10.9	0.02	Sea
270	10-11.9	13-14.9	0.77	1.17	0.90	11.7*	0.05	N. Swell*
270	12-13.9	13-14.9	0.70	1.26	0.88	11.4-11.7*	0.09	N. Swell*
270	14-15.9	11-12.9	0.64	1.35	0.86	9.5-11.1	0.07	N. Swell
270	16-17.9	11-12.9	0.57	1.43	0.82	9.0-10.6	0.02	N. Swell

* Wave breaks on structure. Maximum wave height, H_{max} , = wave breaker height, H_b = 11.7 .

Table 6

Significant Wave Heights and Frequency of Occurrence at Proposed New Entrance Channel to Bolsa Chica Bay, California, for Structure Design Wave-Height Determination

Water Depth, D = 10 ft, Wave Breaker Height, H_b = 7.8 ft

Sheltered Deepwater Azimuth deg	Wave Period sec	Deepwater Wave Height ft	Refraction Coefficient R_k	Shoaling Coefficient S_k	$R_k \times S_k$	Structure Wave Height ft	Frequency of Occurrence percent	Source
157	6-7.9	8-9.9	0.82	1.07	0.88	7.0-7.8*	0.01	Sea*
157	10-11.9	14-15.9	0.83	1.28	1.06	7.8*	0.01	Sea*
180	6-7.9	8-9.9	0.85	1.07	0.91	7.3-7.8*	0.03	Sea*
180	8-9.9	10-13.9	0.76	1.18	0.90	7.8*	0.04	Sea*
180	12-13.9	2-2.9	0.57	1.39	0.79	1.6-2.3	0.30	S. Swell
180	14-15.9	2-2.9	0.52	1.47	0.76	1.5-2.2	0.20	S. Swell
180	14-15.9	3-3.9	0.52	1.47	0.76	2.3-3.0	0.10	N. Swell
180	16-17.9	2-2.9	0.47	1.56	0.73	1.5-2.1	0.10	S. Swell
180	16-17.9	3-3.9	0.47	1.56	0.73	2.2-2.8	0.10	N. Swell
202	6-7.9	6-9.9	0.97	1.06	1.03	6.2-7.8*	0.04	Sea*
202	8-9.9	10-13.9	0.95	1.17	1.11	7.8*	0.02	Sea*
225	6-7.9	6-7.9	0.99	1.07	1.06	6.4-7.8*	0.05	Sea*
247	4-5.9	4-4.9	1.02	0.98	1.00	4.0-4.9	0.01	Sea
270	6-7.9	8-9.9	0.92	1.07	0.98	7.8*	0.03	Sea*
270	8-9.9	10-11.9	0.85	1.17	0.99	7.8*	0.02	Sea*
270	8-9.9	7-10.9	0.85	1.17	0.99	7.0-7.8*	0.24	N. Swell*
270	10-11.9	7-14.9	0.77	1.28	0.99	7.0-7.8*	0.77	N. Swell*
270	12-13.9	7-14.9	0.70	1.39	0.97	6.8-7.8*	0.47	N. Swell*
270	14-15.9	7-12.9	0.64	1.48	0.95	6.6-7.8*	0.19	N. Swell*
270	16-17.9	11-12.9	0.57	1.56	0.89	7.8*	0.02	N. Swell*

* Wave breaks on structure. Maximum wave height, H_{max} , = wave breaker height, H_b = 7.8 ft .

shoaling coefficients is substantially less than 1.00. The maximum wave height at the structure for all waves is less than the depth-limiting breaker wave height for water depths of 30, 25, and 20 ft. The proposed structure will be subjected to nonbreaking waves in those water depths. As the wave propagates shoreward, however, the product of the refraction and shoaling coefficients increases dramatically; and the wave heights approach the depth-limiting breaker height. Those portions of the structure will be subjected to breaking waves of various periods from certain directions of approach. Hence the design wave height will vary along the structure length, depending upon the water depth. Before construction of the proposed jetty and breakwater system, stability analyses of the structures should be performed through physical model testing.

39. Because the data on which the refraction analyses were performed are significant wave statistics based on a finite period of record, SPL (in preparation) determined that the design wave for the offshore breakwater should be the 50-year return period wave obtained from an analysis of 13 storms occurring from 1900 to 1958. For preliminary design purposes, this wave height is approximately 15.5 ft, and is a nonbreaking wave in 25 ft of water. As this design wave propagates shoreward from the proposed breakwater location to the jetties located in shallower water, the wave shoals and breaks. Hence, portions of the jetties will be subjected to nonbreaking, breaking, and broken waves. The design wave varies along the length of the structure, depending upon water depth. Breaking wave heights of 15.5 and 17.0 ft were determined to be appropriate for the jetty head and truck, respectively.

40. The jetties necessary to stabilize a nonnavigable channel would extend to a water depth of 5 ft below mllw. The design wave used for armor-stone calculations was determined to be a depth-limited, 11.8-ft, breaking wave based on the 50-year return period wave obtained from the analysis of 13 storms occurring between 1900 and 1958.

PART III: POTENTIAL LONGSHORE TRANSPORT

Surfside-Sunset Beach Nourishment Background

41. The supply of beach nourishment material to the San Pedro littoral cell has been severely restricted in recent years by the construction of dams and debris basins on the Los Angeles, San Gabriel, and Santa Ana Rivers. While the Los Angeles-Long Beach Harbor breakwaters prevented much of the material transported into the harbor by the Los Angeles River from being carried downcoast, some of the sediments transported by the San Gabriel River could pass by Anaheim Bay and nourish the Surfside-Sunset Beach area prior to the construction of the Anaheim Bay jetties. Erosion of the shoreline at Surfside-Sunset Beach has been a relatively continuous problem since the mid-1940's, according to the Los Angeles District (1978a). In 1945, the U. S. Navy constructed 600 ft of stone revetment downcoast from the Anaheim Bay east jetty to retard the erosion but had to reinforce it the following year. In 1947, the revetment was extended farther and a wood sheet-pile bulkhead established to strengthen the shore road. Throughout the 1940's, material in the amount of 1,422,000 cu yd was placed on the beach. Additional material placed along the Surfside-Sunset Beach shoreline later included 874,000 cu yd in 1956, 4,000,000 cu yd in 1964, 2,260,000 cu yd in 1971, and 1,644,000 cu yd in 1979. Volumetric analyses of the beach nourishment and downcoast area by the Los Angeles District (1978a) for the 5-year period 1965-1970 show that 1,500,000 cu yd of sand was lost from this stretch of beach by a predominant downcoast littoral drift producing a constant erosion and the area south of 18th Street undergoing minor accretion from upcoast nourishment. This feeder beach nourishment area is shown in Figure 8.

42. The bathymetry of this region, and the sheltering effect of the offshore Islands of San Clemente, Santa Catalina, San Nicholas, and Santa Barbara, is such that waves generated on the open ocean can approach the coast in this region only from the due-west sector and the south-to-southeast sector. The Bolsa Chica Beach State Park region is more protected from southerly waves than is Newport Beach, which is located approximately 17 miles downcoast. Hence the amount of material transported to Bolsa Chica Beach from the south is less than that at Newport Beach. Simultaneously, the orientation of the beach at Newport Beach is such that the divergence of wave energy from the west does not transport nearly as much material in a southerly direction here as at

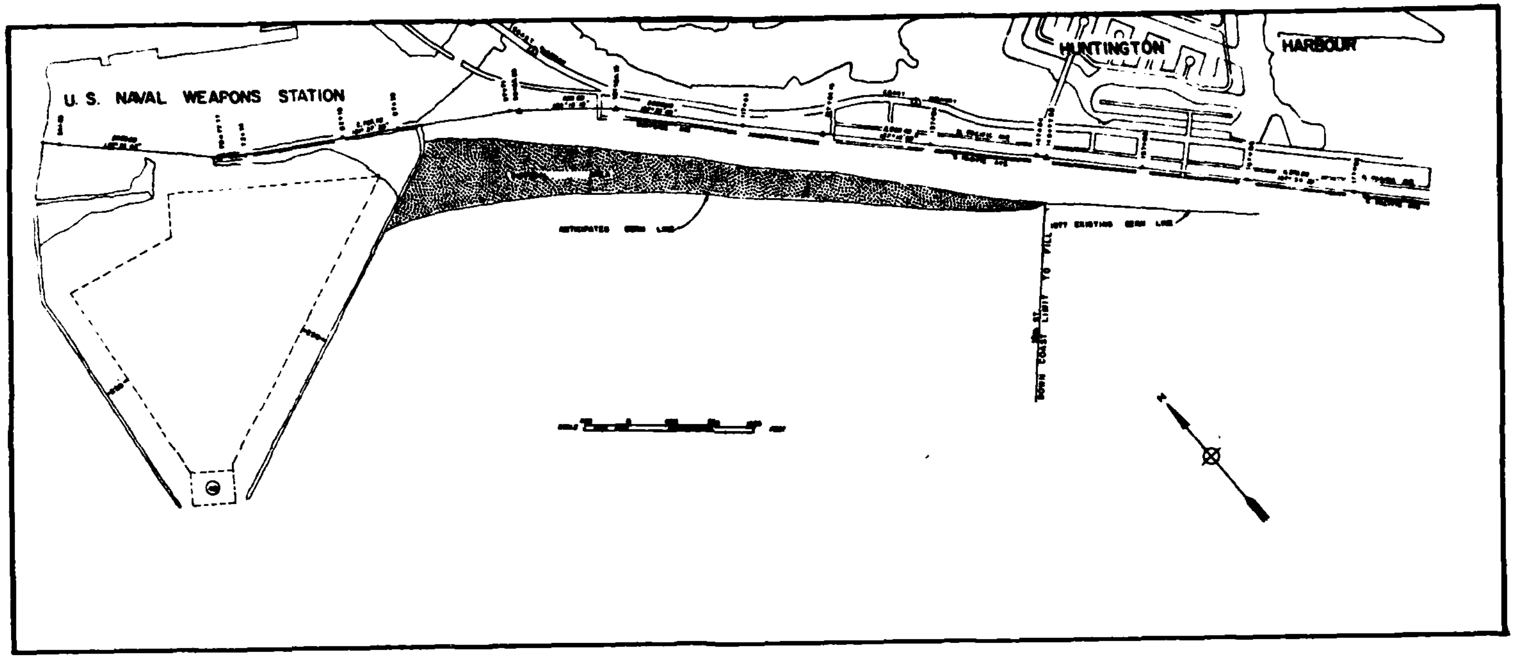

Figure 8. Feeder beach nourishment area at Surfside-Sunset Beach, California. This nourishment region is used to provide a source of beach material for the downcoast beaches to Newport Beach (after U. S. Army Engineer District, Los Angeles, 1978b)

Bolsa Chica Beach. The result is that a loss of material is being experienced at Bolsa Chica Beach consisting of a net downcoast littoral movement. Most of the beach nourishment material placed on the feeder beach at Surfside-Sunset Beach is gradually transferred downcoast and eventually out of the system.

Empirical Longshore Transport Estimation

43. Potential longshore transport is defined as the amount of littoral material that a specific wave climate will transport in the presence of an unlimited source (supply) of material. If the source is not unlimited, then the actual longshore transport will be less than the potential transport. When the feeder beach at Surfside-Sunset Beach has been nourished, an essentially unlimited supply of material exists for transport past Bolsa Chica Beach State Park.

44. Most investigators have attempted a correlation between wave characteristics and measured longshore transport rates. Intuitively, the rate at which a transport process takes place should be related to the total wave power, or energy flux, available for transporting material alongshore in the surf zone. The alongshore energy flux is approximated under the assumptions of conservation of energy in shoaling waves and application of the Airy theory for small amplitude waves. Based on these assumptions (CERC 1977), the energy flux at the breaker zone, P_{1s}, is:

$$P_{1s} = \frac{\rho g}{16} \left(H_b^2 \; C_g \; \sin 2 \alpha_b \right) \tag{2}$$

where

P_{1s} = alongshore component of wave energy flux per unit length of beach, ft-lb/ft/sec

ρ = density of salt water, 1.99 lb-sec^2/ft^4

g = gravitational constant, 32.174 ft/sec^2

H_b = breaking wave height, ft

C_g = group velocity or the velocity of propagation of wave energy, ft/sec (in shallow water, $C_g = C$, the wave celerity)

α_b = breaking angle of wave with shoreline, deg

If the wave speed at breaking can be approximated by solitary theory:

$$C_g = C \simeq (2 \; g \; H_b)^{1/2} \tag{3}$$

where C = wave celerity, ft/sec. Equation 2 can now be expressed in terms of the wave breaking characteristics of breaker height, H_b, and breaker angle, α_b, as:

$$P_{ls} = 32.1\ H_b^{5/2} \sin 2\ \alpha_b \tag{4}$$

following the development of CERC (1977).

45. A number of empirical equations have been advanced since the early 1950's that relate the longshore component of wave energy flux, Equation 4, with measured values of volumetric longshore transport. The relationship developed by CERC, based entirely on 23 field observations and no laboratory data, is:

$$Q_{ls} = 7{,}500\ P_{ls} \tag{5}$$

where Q_{ls} = potential longshore transport, cu yd/yr. Equation 5 is displayed graphically in Figure 9, which also shows the field data.

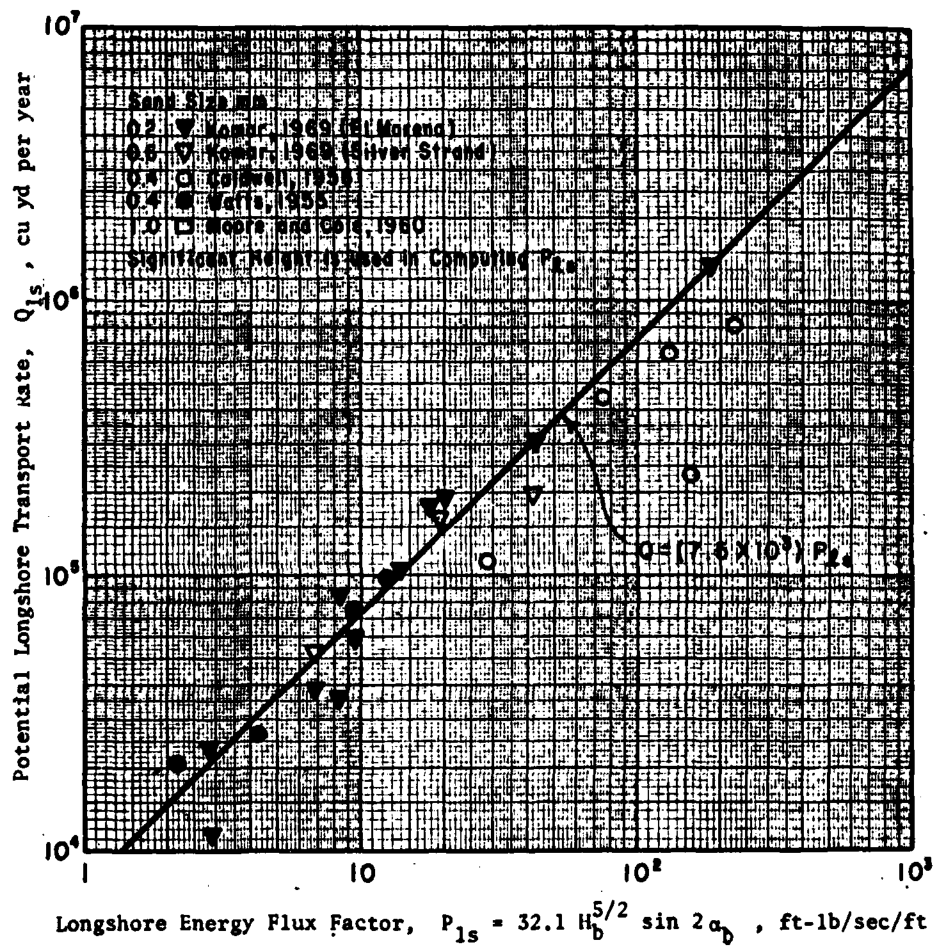

Figure 9. Prototype field data for development of longshore transport relationship (after CERC 1977)

Bolsa Chica Bay Region, California, Potential Longshore Transport Estimate

46. In order to apply Equations 4 and 5 to determine an estimate of the potential longshore transport occurring along the Bolsa Chica Bay region (Surfside-Sunset Beach to Huntington Beach), the wave breaker height, H_b , and the breaker angle, α_b , must be known for each element comprising the sheltered deepwater wave statistics matrix (Appendix B). The breaker height, H_b , depends directly on the deepwater wave height, H_o , and the deepwater wave period, T , as also does the breaker angle, α_b . These breaker values of height and angle were determined by the refraction analysis discussed in PART II. Wave ray computations were conducted from deep water to the breaking point along the entire section of coastline under consideration. Breaker height, H_b , and the corresponding breaker angle, α_b , for each element were determined and are presented in Appendix C, which also shows the potential longshore transport calculated by the use of Equations 4 and 5.

47. Typical examples of the effects of refraction on wave characteristics are shown in Figure 10 for an 18-sec wave approaching from the south and in Figure 11 for an 18-sec wave approaching from the west. These are the two dominant directions of approach for this entire section of coastline, and the bathymetry causes significant convergence and divergence of wave energy at various locations.

48. Summaries of the potential longshore transport computations for the Bolsa Chica Bay region are presented in Table 7, based upon the detailed calculations of Appendix C. This table is arranged to display the influence of sea, Southern Hemisphere swell, and Northern Hemisphere swell on the overall net and gross transport on a monthly basis. The computations indicate a net southerly transport of 275,900 cu yd/yr which is in qualitative agreement with other similar investigations, for example, Emery (1960), Herron and Harris (1962), Inman and Frautschy (1965), and Shepard and Wanless (1971). The gross transport rates also are the same order of magnitude as previously reported.

49. The net southerly transport rate in the vicinity of Bolsa Chica Beach State Park (275,900 cu yd/yr) appears somewhat less than the average amount of beach nourishment material that is known to have historically been placed on the beach (about 350,000 cu yd/yr). It must be understood that the net southerly transport rate of 275,900 cu yd/yr was determined for the

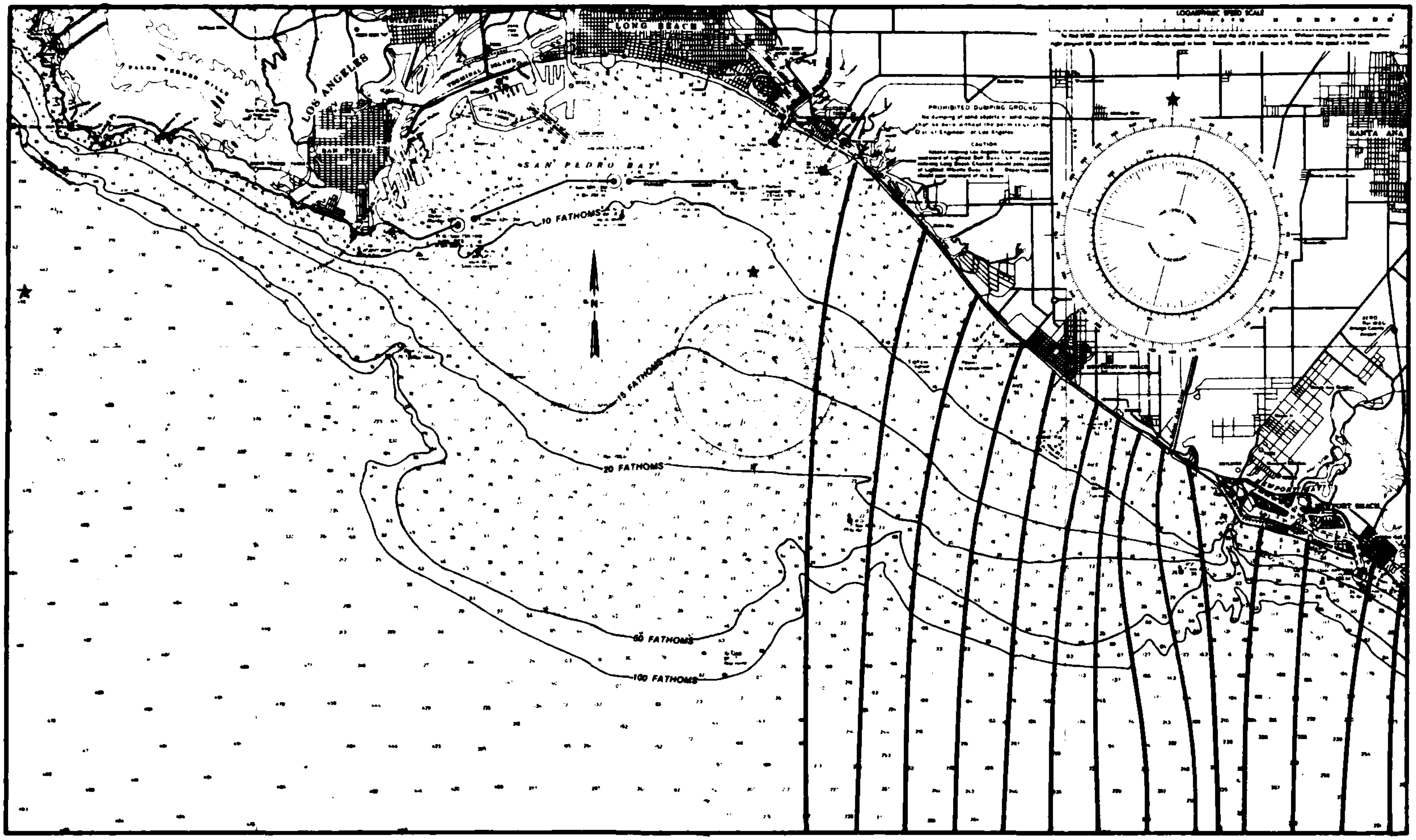

Figure 10. Effects of offshore bathymetry on refraction of 18-sec sheltered deepwater wave propagating from the south

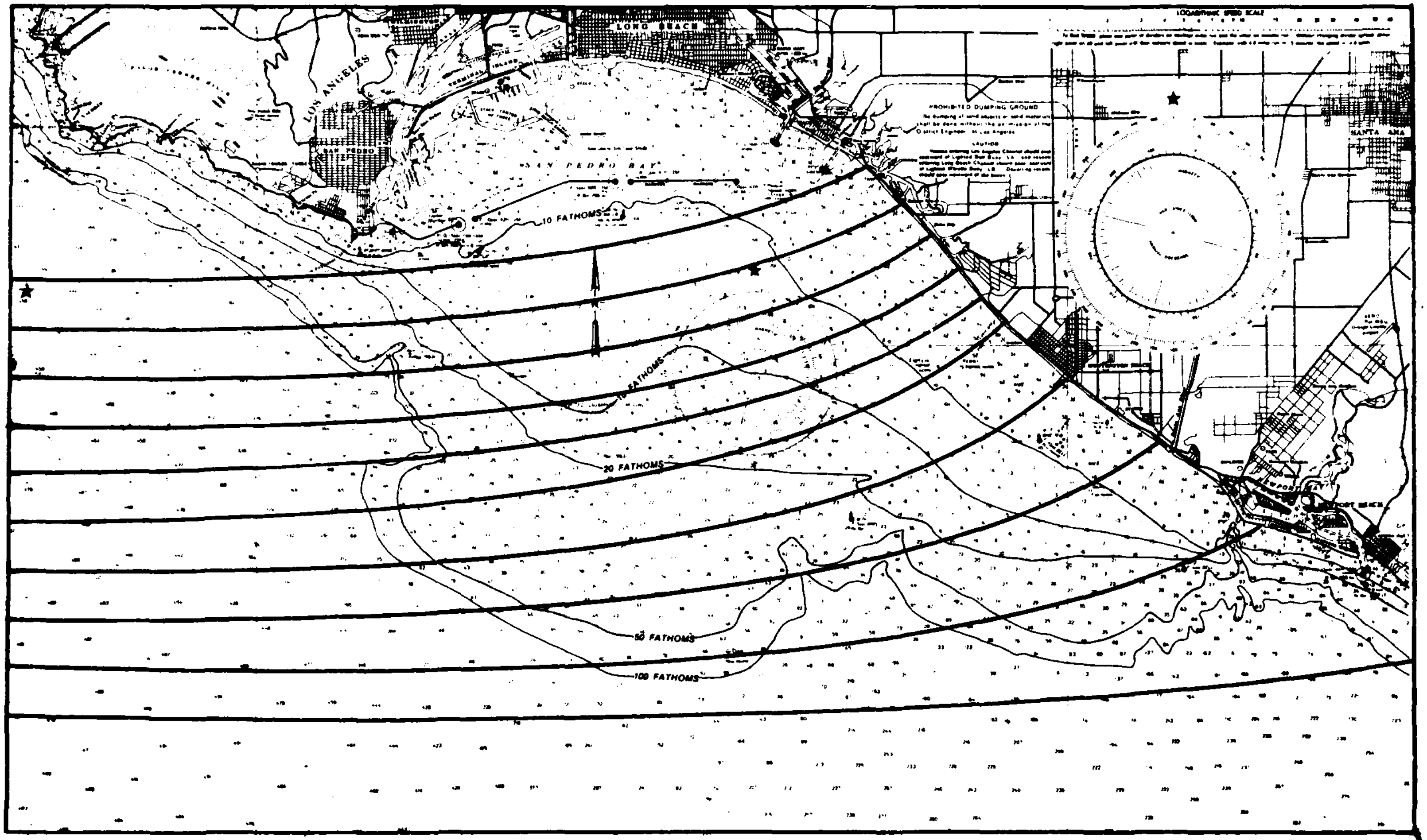

Figure 11. Effects of offshore bathymetry on refraction of 18-sec deepwater wave propagating from the open ocean from the west

Table 7

Summary of Potential Longshore Transport Computations

Bolsa Chica Bay Region, California

(All Values in Cubic Yards)

	Sea		Northern Swell		Southern Swell		Sum		Net		
	+	-	+	-	+	-	+	-	+	-	
Month	North	South	North	South	North	South	North	South	North	South	Gross
Jan	14,700	19,300	0	88,600	0	0	14,700	107,900		93,200	122,600
Feb	74,200	13,100	0	203,800	0	0	74,200	216,900		142,700	291,100
Mar	29,900	24,800	0	57,300	0	0	29,900	82,100		52,200	112,000
Apr	4,900	20,600	0	55,700	0	0	4,900	76,300		71,400	81,200
May	2,100	14,600	0	13,300	20,500	0	22,600	27,900		5,300	50,500
Jun	2,600	12,400	0	3,100	13,200	0	15,800	15,500	300		31,300
Jul	4,200	12,700	3,000	0	37,200	0	44,400	12,700	31,700		57,100
Aug	2,600	10,700	3,900	0	36,800	0	43,300	10,700	32,600		54,000
Sep	1,100	10,500	9,000	600	28,400	0	38,500	11,100	27,400		49,600
Oct	4,700	5,900	2,000	16,600	21,600	0	28,300	22,500	5,800		50,800
Nov	1,100	10,500	0	2,400	0	0	1,100	12,900		11,800	14,000
Dec	27,400	7,500	0	17,000	0	0	27,400	24,500	2,900		51,900
Annual	169,500	162,600	17,900	458,400	157,700	0	345,100	621,000	100,700	376,600	966,100
Net	6,900			440,500	157,700			275,900		275,900	

average (equilibrium) beach orientation for the entire finite section of coastline under consideration. When material is initially placed upon the feeder beach at Surfside-Sunset Beach, the coastline in this region is oriented at a much larger angle with respect to predominant incident waves than is the average coastline where material has not been placed. Thus the rate of transport from this region is initially larger than transport rates along the average coastline. As the feeder beach erodes back toward its equilibrium orientation, transport rates approach those along the normal coastline. However, by that time, the erosion has become so severe in the Surfside-Sunset Beach region that renourishment of the feeder beach must be effected which again accelerates transport from the Surfside-Sunset Beach region. Calculations in PART IV of this report quantify this aspect.

50. Additionally, part of the material disappearing from the feeder beach may be transported out of the system into the Anaheim Bay entrance channel. Based only on dredging records of the Anaheim Bay entrance channel, this material cannot be precisely accounted for, as other deposits take place in the channel from Anaheim Bay proper. A portion of the material placed on Surfside-Sunset Beach also may be transported offshore as fine material and may not return to the littoral zone. Because of the periodic beach nourishment activities in this region (as the need arises), essentially an unlimited amount of material is available for littoral transport. Hence the potential longshore transport computations (which are strictly applicable only to a region where an unlimited source of transportable material exists) should fairly well approximate the actual longshore transport process in this vicinity.

51. In order for potential longshore transport computations to provide useful information for the design and deployment of sand bypassing systems at harbor entrances or beach erosion studies, it is necessary that seasonal or monthly transport rates be determined. Accordingly, the annual quantities were decomposed into the components occurring, on the average on a monthly basis, and those data are displayed in Figure 12. Table 7 indicates that a significant amount of material moves both northwesterly and southeasterly each month of the year, although there is practically no northwesterly transport in April and November, and only relatively minimal southeasterly transport from June to November. The winter and early spring months of January, February, March, and April (particularly February) exhibit the greatest amount of both gross and net potential longshore transport. Figure 12 indicates a

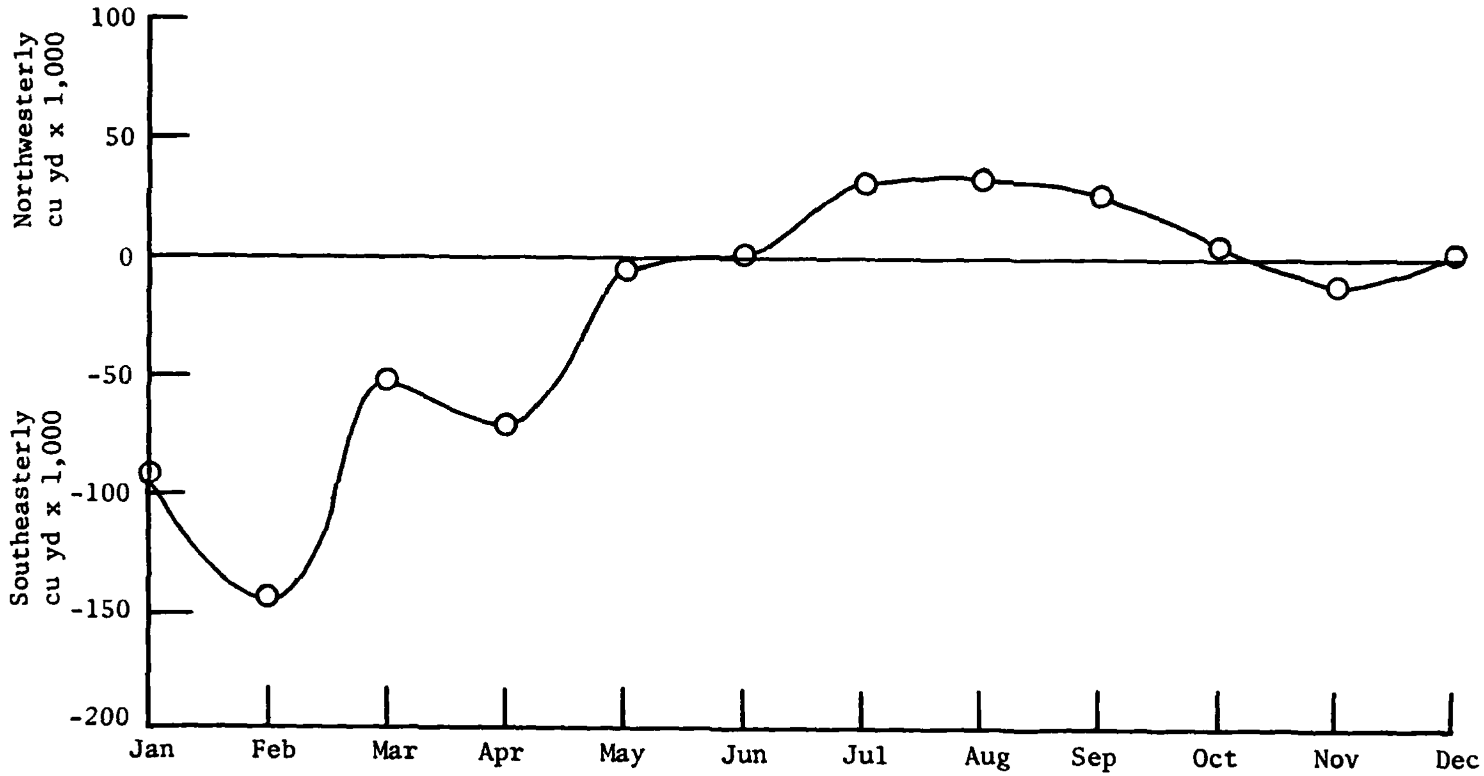

Figure 12. Net monthly potential longshore transport from Surfside-Sunset Beach to Huntington Beach (Bolsa Chica Bay region, California)

large gradient of southeasterly movement during the early months of the year, and this appears to be the appropriate period for bypassing material across the proposed new entrance channel to the downcoast beaches.

PART IV: COMPUTER SIMULATION OF SHORELINE EVOLUTION

Computer Simulation Model

52. The evolution of a shoreline as a result of longshore sediment transport may be estimated by dividing the shoreline into cells, determining the transport in each cell by using Equations 4 and 5 of PART III, and applying continuity conditions. This method has been used in the past by Pelnard-Considere (1956), Komar and Inman (1970), Komar (1973), Rea and Komar (1975), Komar (1976, 1977), and LeMehaute and Soldate (1980). The method divides the shoreline into a series of cells of finite and uniform length, Δx, each with an individual width, y_1, y_2, etc., beyond some arbitrary baseline, in the manner of Komar (1977) (Figure 13). The narrower the cells, the more nearly the series of cells will approximate the existing shoreline at the beginning of computation. Changes in the shoreline location are produced by littoral drift, QIN_i, or $QOUT_i$, which shifts material from cell i to cell $i+1$. The net change in volume of sand in the i^{th} cell is given as

$$\Delta V_i = (QIN_i - QOUT_i)\Delta t \tag{6}$$

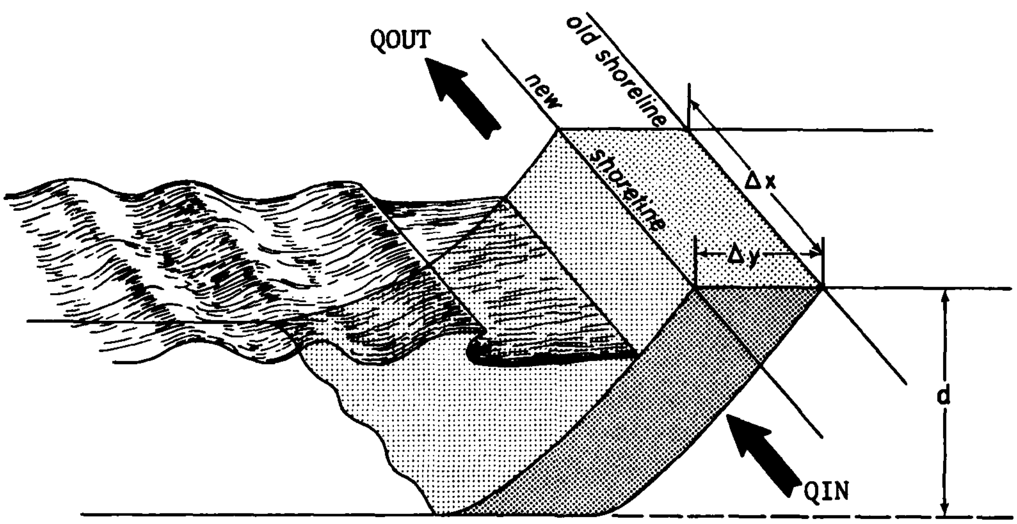

Volume, $\Delta V = d \cdot \Delta x \cdot \Delta y$

Figure 13. Shoreline cell illustrating how a change in sand volume within the cell produced by littoral drift into and out of the cell results in a change in the shoreline position, Δy (after Komar 1977)

where

ΔV_i = net change in volume of sand in cell i

QIN_i = littoral drift of material into cell i from cell i-1

$QOUT_i$ = littoral drift of ma :rial from cell i to cell i+1

Δt = time increment

The change in volume, ΔV_i, will be positive or negative depending on the relative rates at which sand is transported into and out of the cell. When the rate into the cell is equal to the rate out of the cell, $\Delta V_i = 0$.

53. The change in volume, ΔV_i, also equals the change in position of the shoreline, Δy_i, times the length of a cell, Δx, times the average water depth at which erosion or deposition occurs, d.

$$\Delta V_i = d\ \Delta y_i\ \Delta x \tag{7}$$

The parameter, d, is not known a priori, but can be determined by relating known volumes of material erosion or deposition with known values of shoreline changes during historical events. Thus the computer simulation model must be calibrated for a specific location from historical events. From Equations 6 and 7,

$$\Delta y_i = (QIN_i - QOUT_i)\frac{\Delta t}{d\ \Delta x} \tag{8}$$

The littoral drift quantities, QIN_i and $QOUT_i$, are determined from Equations 4 and 5. Thus when the parameters Δt, Δx, and d have been selected for a particular region of coastline under investigation, the values of Δy_i can be determined for each cell. If the cells have other sources of sand supply (such as a river mouth or sand bypassing at an inlet or navigation channel), these quantities are linearly additive.

54. It is important in this computer simulation model that values of Δy_i remain relatively small so that there will be no discontinuities in the shoreline configuration. This restriction implies that the time increment, Δt, be kept small. The proper sign convention must be strictly adhered to in order to obtain the proper breaker angles, α_b, and transport directions. In the longshore transport model, the angle α_i which the shoreline makes with a parallel to the x-axis, between the i and the i+1 cells, is taken as

$$\tan \alpha_i = \frac{y_i - y_{i+1}}{\Delta x} \tag{9}$$

When the breaking waves make an angle α_o with the x-axis direction, then the breaking angle, α_b, at the shoreline is

$$\alpha_b = \alpha_i \pm \alpha_o \tag{10}$$

Thus

$$\tan \alpha_b = \frac{\tan \alpha_i \pm \tan \alpha_o}{1 \pm \tan \alpha_i \tan \alpha_o} \tag{11}$$

This computer simulation model of Komar (1977) is essentially one-dimensional in that it does not allow for onshore or offshore movement of material under wave conditions. For the application to longshore transport mechanisms (the reason for its development), one of the principal advantages is that this model allows the parameters to be varied through time and space. This provides a probabilistic aspect with an otherwise deterministic model.

Calibration at Bolsa Chica Bay Region

55. The computer simulation model for shoreline evolution developed by Komar (1977) was adapted for the beaches of the Bolsa Chica Bay region (Surfside-Sunset Beach to Huntington Beach), and is listed in Appendix D. The section of coastline modeled by this approach is shown in Figures 4 and 5. Three hundred cells, each with a width of 100 ft, were used to model this coastline. A time period of 5 years was considered (the anticipated Surfside-Sunset Beach renourishment interval), and a time increment, Δt, of 1 hr was used. The model shoreline begins with cell 1 adjacent to the east jetty to Anaheim Bay and extends downcoast for a distance of 300 cells to approximately the northwestern limit of the city of Huntington Beach.

56. Three sections of shoreline are being investigated: (a) the erosional coast (Surfside-Sunset Beach region); (b) the depositional coast (the fillet and temporal accretion on the updrift side of the west jetty); and (c) the variational coast downdrift of the east jetty (which oscillates in response to the shifting transport directions). Known quantities of material have been placed on the feeder beach in the Surfside-Sunset Beach region, and

periodic cross-sectional surveys reveal the temporal manner in which the nourishment material is being eroded away. Figure 14 displays typical representative beach profiles indicating the extent of beach fill during the most recent nourishment activities (1979) at Surfside-Sunset Beach. The nourishment region extended from the east jetty at Anaheim Bay for a distance of approximately 6,000 ft downcoast (to about cell 60).

57. The hindcast wave statistics of Appendix C were used to determine the amount of potential longshore transport (net and gross) on a monthly basis. In the absence of knowledge of the time of occurrence of the various waves each month (i.e., which wave came first), it was assumed that the equivalent wave height each month which produced the known quantity of transport would be appropriate for use with the computer simulation model of shoreline evolution. The computed quantities of material of Table 7 have been determined to be the average for the entire section of coastline under consideration (Surfside-Sunset Beach to Huntington Beach), with the breaker angle, α_b , determined from the equilibrium beach orientation. The equivalent breaker angle which produced updrift or downdrift transport was determined by applying the average annual breaker height, H_b , which produced updrift or downdrift transport, respectively, to Equations 5 and 6 (since the total updrift and downdrift transport quantities are known a priori). Then the equivalent monthly wave breaker height was obtained by solving Equations 5 and 6 for wave height with the monthly transport quantities and equivalent breaker angle known. These equivalent wave breaker heights were then used on a monthly basis in 1-hr time increments for determining the shoreline evolution. After each time increment, the shoreline location would be updated, and a new wave breaker angle would be computed.

58. From historical beach-fill records, the Surfside-Sunset Beach region appears to have been filled to acceptable standards in 1956. Since that time, the material quantities of Table 8 have been placed on this beach. On the average for the 22-year time interval since 1956, approximately 7,904,000 cu yd of beach-fill material has been placed in this region, or about 359,300 cu yd per year. The computer simulation model previously described was operated for a time interval of 5 years (the intended periodic beach nourishment interval), starting with the shoreline location in the 1979 postnourishment position and beginning the model operation at the first of January. The computer model (with the parameter d adjusted such that the

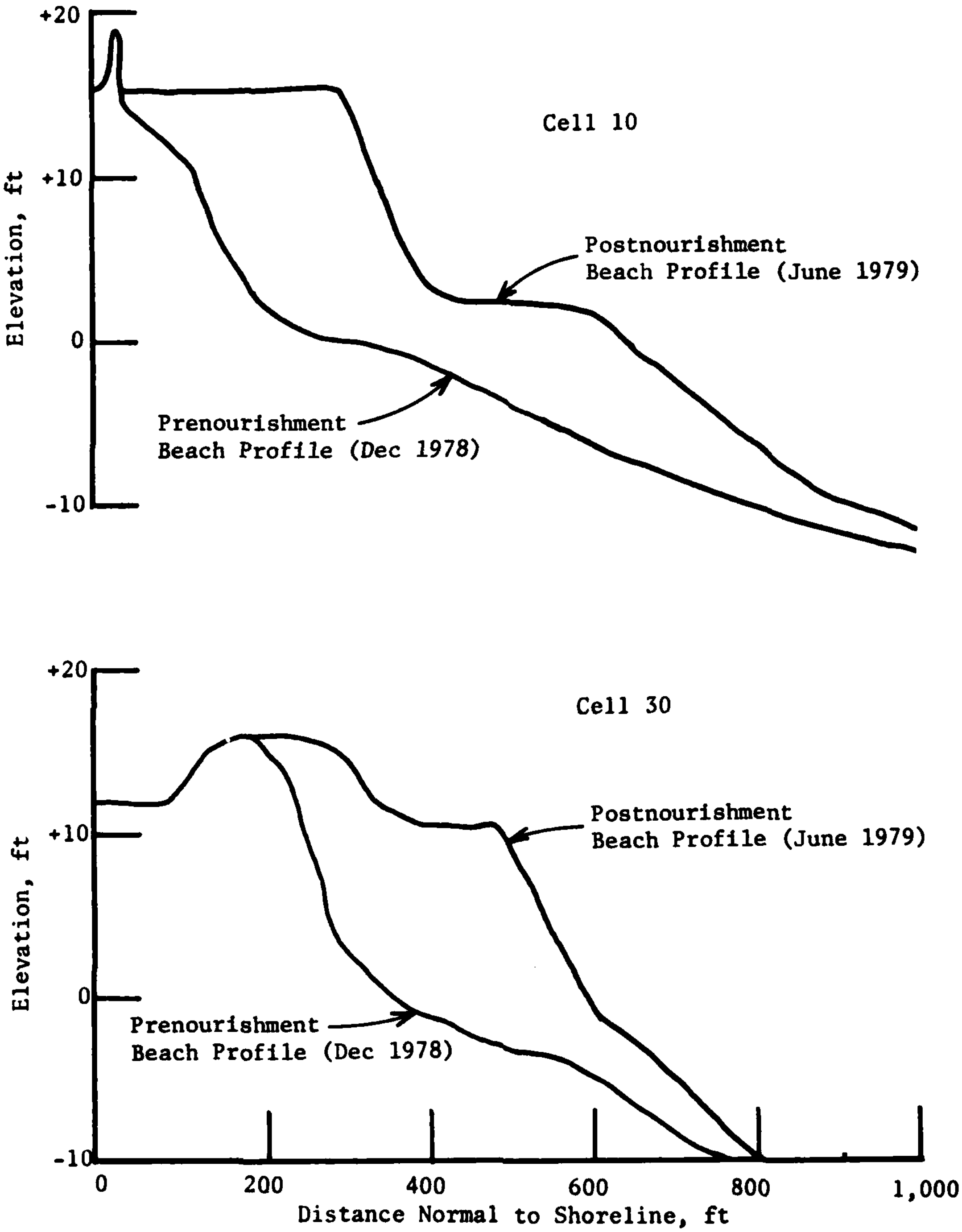

Figure 14. Two typical beach profiles indicating the extent of beach fill during the 1979 nourishment activities at Surfside-Sunset Beach

Table 8

Feeder Beach Nourishment Material

Placed on Surfside-Sunset Beach

Year	Quantity, cu yd
1964	4,000,000
1971	2,260,000
1979	1,644,000
22-year interval since 1956	7,904,000 cu yd placed on Surfside-Sunset Beach
	Average quantity = 359,300 cu yd/yr

total volume over the 5-year interval agrees with known quantities) indicates that the quantities of Table 9 would be removed after the indicated time interval. On the average, for the 5-year interval of operation of the computer model, approximately 1,812,800 cu yd of material was removed from this region, or about 362,600 cu yd/yr. This value appears to compare favorably with the 359,300 cu yd/yr of material known to have been placed on this beach region, on the average, and the computer simulation model was considered to be calibrated within acceptable limits for this region.

Table 9

Computer Simulation Model Indication of Material

Removed from Surfside-Sunset Beach

Year	Quantity, cu yd
1	558,300
2	379,300
3	322,700
4	288,600
5	263,900
5-year interval	1,812,800 cu yd removed from Surfside-Sunset Beach
	Average quantity = 362,600 cu yd/yr

59. Immediately after beach nourishment activities, the feeder beach shoreline location is in a nonequilibrium position. The angle that the beach makes with the winter wave conditions is much greater than the average beach orientation for the Bolsa Chica Bay region. Hence, in the early years after nourishment, the wave climate is capable of removing much greater quantities of material than in later years when the shoreline angle has had an opportunity to moderate and become more nearly equivalent to the average shoreline orientation. With the passage of time, the quantities of material removed from the beach decline in an asymptotic manner, such that after about 5 years the quantitites removed from this region are about equivalent to the potential longshore transport for the entire section of coastline extending to Huntington Beach (Table 9). The rate of beach erosion has decreased significantly after approximately 5 years; however, the extent of the actual beach erosion in the interim has left a severely depleted beach that would be susceptible to property damage in the event of a high-intensity storm occurring under these conditions. For this reason, it is necessary for continued recurring beach nourishment activities along this unstabilized beach region. Figures 15-21 are the computer simulation model indication of the rate and extent of the beach erosion in the Surfside-Sunset Beach region, beginning with the post-construction beach location of June 1979 and operating for a 5-year time interval in 1-hr time increments.

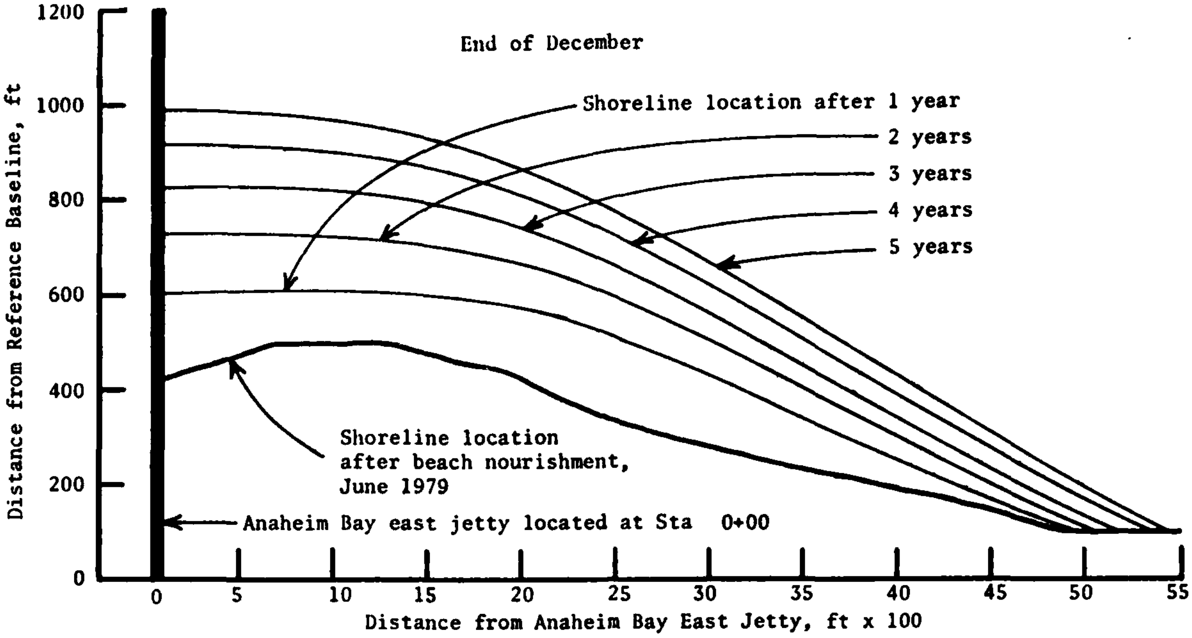

Figure 15. Computer simulation model indication of the rate and extent of beach erosion at the nourishment feeder beach, Surfside-Sunset Beach, California, end of December

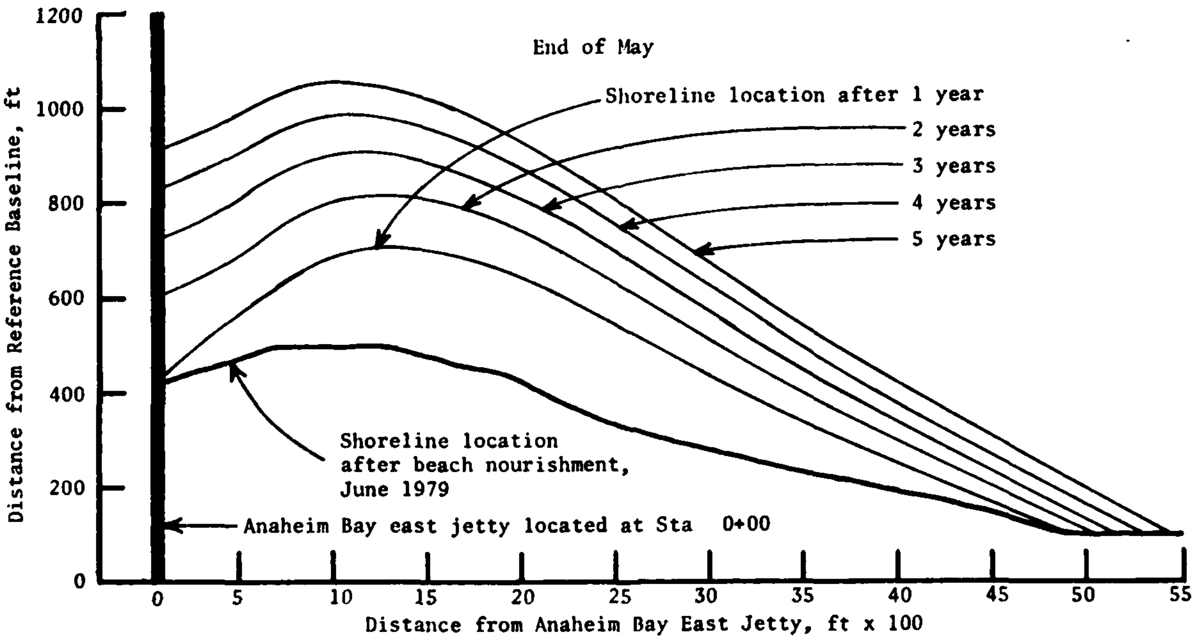

Figure 16. Computer simulation model indication of the rate and extent of beach erosion at the nourishment feeder beach, Surfside-Sunset Beach, California, end of May

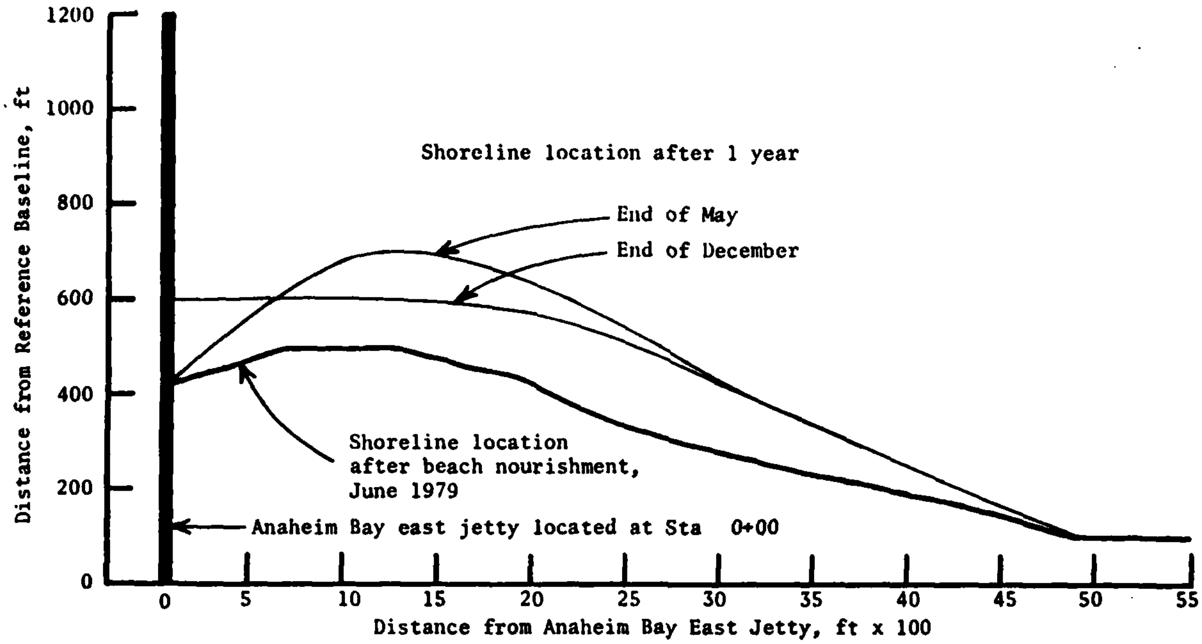

Figure 17. Computer simulation model indication of the rate and extent of beach erosion at the nourishment feeder beach, Surfside-Sunset Beach, California, after 1 year

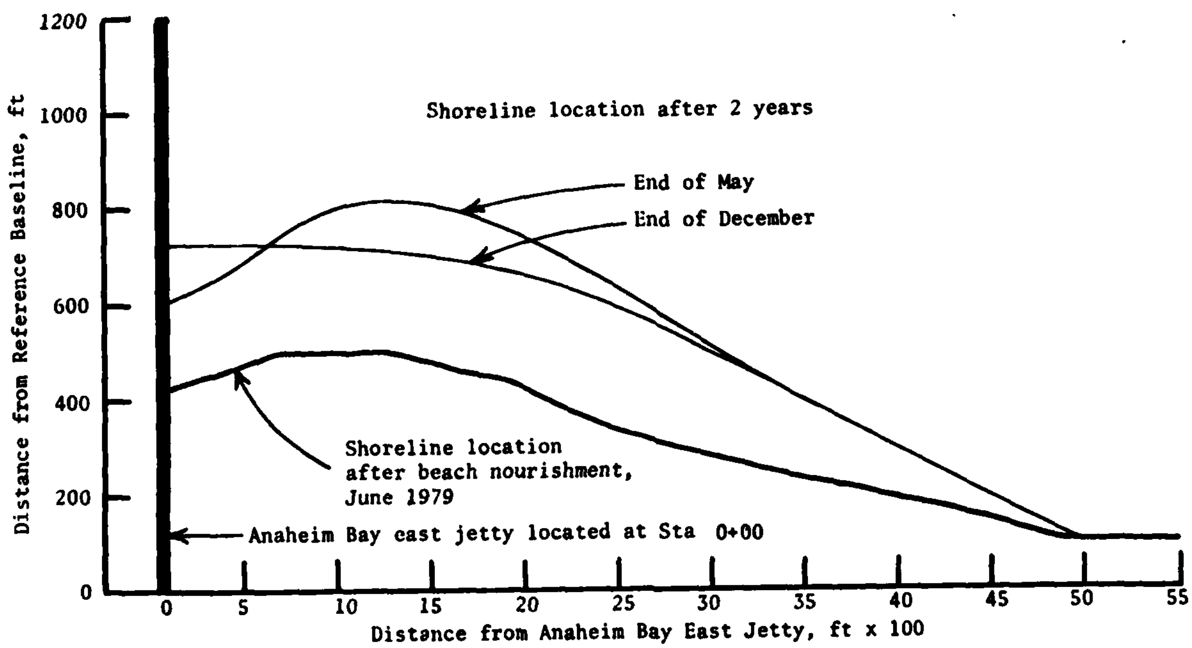

Figure 18. Computer simulation model indication of the rate and extent of beach erosion at the nourishment feeder beach, Surfside-Sunset Beach, California, after 2 years

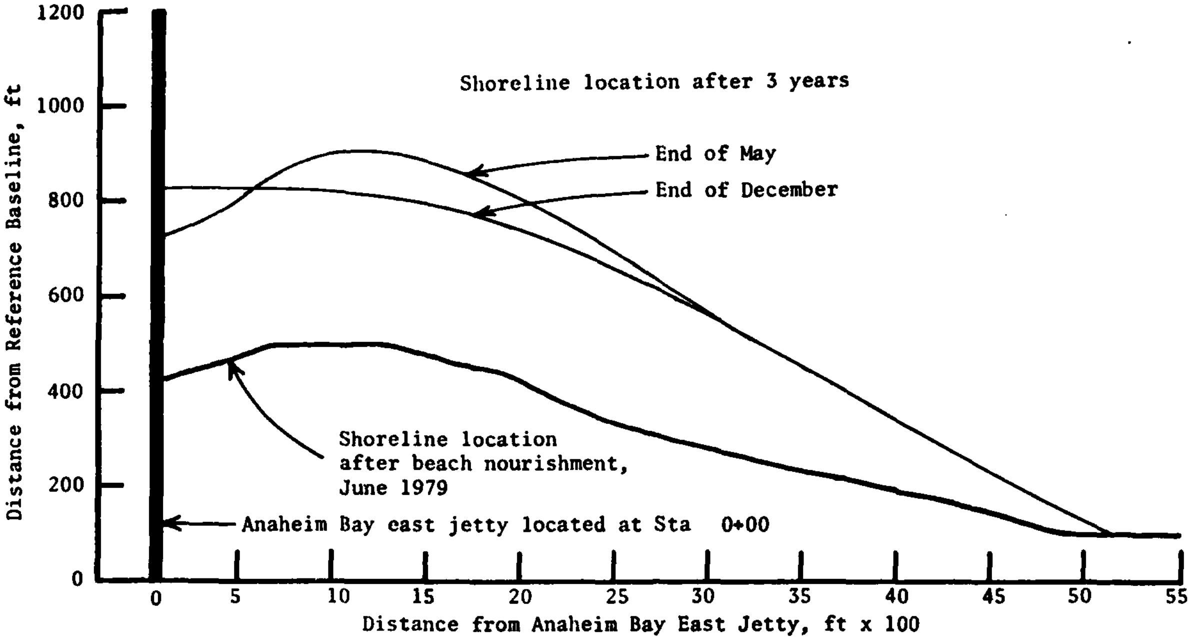

Figure 19. Computer simulation model indication of the rate and extent of beach erosion at the nourishment feeder beach, Surfside-Sunset Beach, California, after 3 years

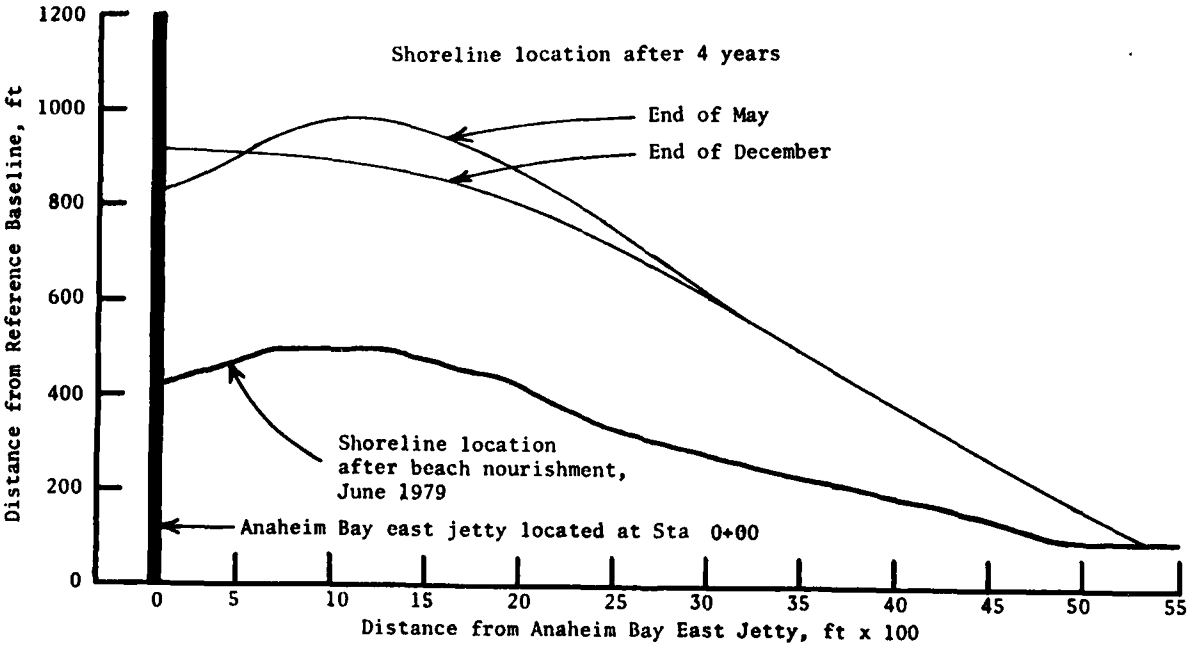

Figure 20. Computer simulation model indication of the rate and extent of beach erosion at the nourishment feeder beach, Surfside-Sunset Beach, California, after 4 years

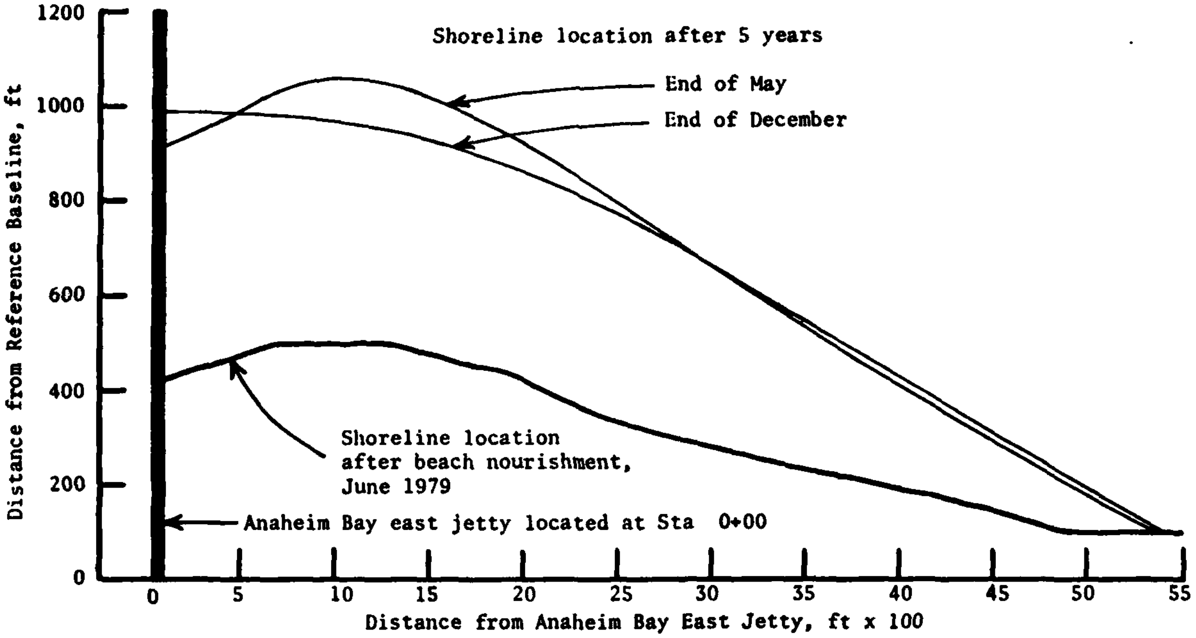

Figure 21. Computer simulation model indication of the rate and extent of beach erosion at the nourishment feeder beach, Surfside-Sunset Beach, California, after 5 years

PART V: PROPOSED SPUR GROIN AT ANAHEIM BAY EAST JETTY

60. The localized region where the Anaheim Bay east jetty connects with the shoreline is subjected to severe scour and erosion by certain wave characteristics and approach directions. There exists the possibility that the east jetty landward end may be breached if the erosion near this jetty is allowed to continue unabated. Similar problem areas have developed at other jetties and groins (i.e., Big Bay Harbor, Michigan; Grand Traverse Bay Harbor, Michigan; Black River Harbor, Michigan; and the upper entrance to the Keeweenaw Waterway, Lake Superior) and appear to be the result of the "Mach-stem" phenomenon (Hales 1980). The problem arises when the wave approach is such that the wave crest propagates along the section of jetty or groin, increases in amplitude along the Mach stem, and terminates as a geyser of water plunging over the crest of the structure at the shore end. Depending on the intensity of the wave attack, the water plume may reach 10 to 12 ft in height. Resulting dynamic forces are seldom sufficient to severely damage or destroy a properly designed rubble-mound breakwater or jetty; but it occasionally is necessary to rehabilitate such structures, and vertical sheet-steel walls have been completely destroyed.

61. For incident angles (the angle between the direction of wave advance and the structure) greater than 45 deg, the reflection pattern is normal (Wiegel 1964). The incident and reflected waves are slightly disturbed near the structure; but the angle of reflection is equal to the angle of incidence, and the reflected wave height is only slightly less than the incident wave height. For angles of incidence less than 20 deg, the wave crest bends so that it becomes perpendicular to the structure and no reflected wave appears.

62. When the angle of incidence is greater than 20 deg but less than 45 deg, the reflection of water waves off structures appears to be of the type called a Mach reflection in acoustics. In this case, three waves are present: (a) the incident wave, (b) the reflected wave, and (c) a wave crest approximately perpendicular to the structure, the extent of which grows in length as the wave travels along the structure. The height of the portion of the wave perpendicular to the structure (called the Mach stem) is greater than the incident wave height, and may reach its maximum height at the structure of twice the incident wave height. The wave climate existing in the Gulf of Santa Catalina and San Pedro Channel is sufficiently adequate to generate

waves that approach the Anaheim Bay east jetty with incident angles varying from essentially 0 to 90 deg. Hence, the Mach-stem and resulting phenomena are expected to exist in this location, and appropriate measures should be taken to preclude breaching of the east jetty at Anaheim Bay.

63. Because continuous nourishment of beach replenishment material is not available for this particular localized region (nourishment is of a periodic nature), any solution of this local scour must be of the structural type. Any existing beach location may probably be stabilized at that position by the construction of a properly designed spur groin erected perpendicularly to the Anaheim Bay east jetty and oriented essentially parallel with the general Surfside-Sunset Beach shoreline. Such a proposed spur groin location is shown in Figure 22, positioned at approximately the after-1979 beach nourishment configuration.

64. The length of the spur groin section should be optimized with respect to extent of stable beach section deemed essential to prevent breaching of the Anaheim Bay east jetty. The existence of such a spur groin should not materially affect the volume of beach nourishment required to maintain the recreation beach in the Surfside-Sunset Beach region. Accordingly, the computer simulation model for shoreline evolution was operated for a 5-year time interval in 1-hr time increments starting with the after-beach nourishment location of 1979. Two different lengths of spur groin were installed in the numerical model (a 500-ft length and a 1,000-ft length). These spur groin sections did not significantly affect the erosion volume from the beach, and these data are presented in Table 10. Because of the influence of the breaker angle on longshore transport, the longer section of spur groin permits a slightly smaller volume of erosion from the beach (approximately 120,000 cu yd over a 5-year time interval); however, this slight reduction in total volume should be optimized with consideration of the initial cost of the spur groin.

65. Results of the computer simulation model indication of the effect of the two sections of spur groin on the rate and extent of erosion of the recreational beach at Surfside-Sunset Beach are presented in Figures 23-46. The effect of the 500-ft length of spur groin is presented in Figures 23-29, and the effect of the 1,000-ft spur groin is shown in Figures 30-36. Comparisons of the existing condition with these two sections of spur groin are presented in Figures 37-41 after 1 to 5 years at the end of December. Similar

Figure 22. Proposed spur groin location to eliminate severe erosion at junction of Anaheim Bay east jetty with shoreline

Table 10

Computer Simulation Model Indication of Material Removed from Surfside-Sunset Beach, Existing Conditions, 500-ft Spur Groin and 1000-ft Spur Groin

Year	Existing Condition cu yd	500-ft Spur Groin cu yd	1,000-ft Spur Groin cu yd
1	558,300	554,900	552,000
2	379,300	367,200	354,500
3	322,700	306,500	290,500
4	288,600	271,600	254,200
5	263,900	246,800	242,100
Total, cu yd	1,812,800	1,747,000	1,693,300
Average, cu yd/yr	362,600	349,400	338,700

comparisons for the end of May are presented in Figures 42-46. While neither groin will eliminate the requirement for periodic beach nourishment, neither adversely impacts significantly on the existing condition situation. It appears either section of spur groin will offer satisfactory protection to the localized scour area where the Anaheim Bay east jetty connects with the shoreline of southern California.

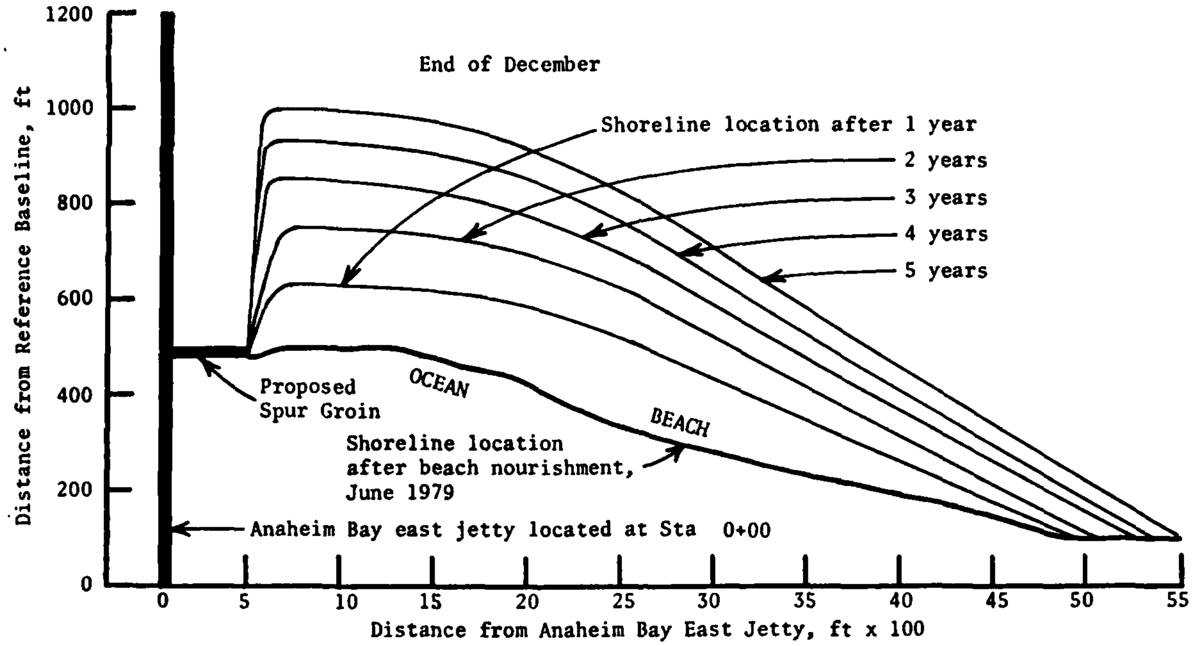

Figure 23. Computer simulation model indication of the rate and extent of beach erosion at the nourishment feeder beach, Surfside-Sunset Beach, California, end of December, for a 500-ft spur groin

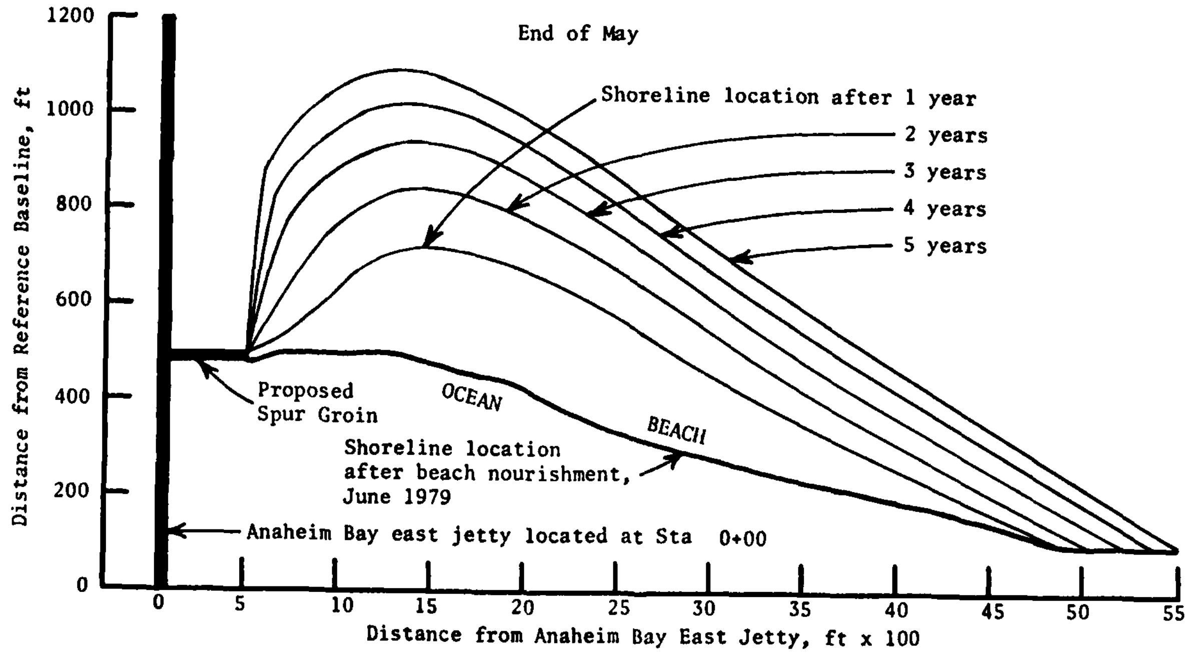

Figure 24. Computer simulation model indication of the rate and extent of beach erosion at the nourishment feeder beach, Surfside-Sunset Beach, California, end of May, for a 500-ft spur groin

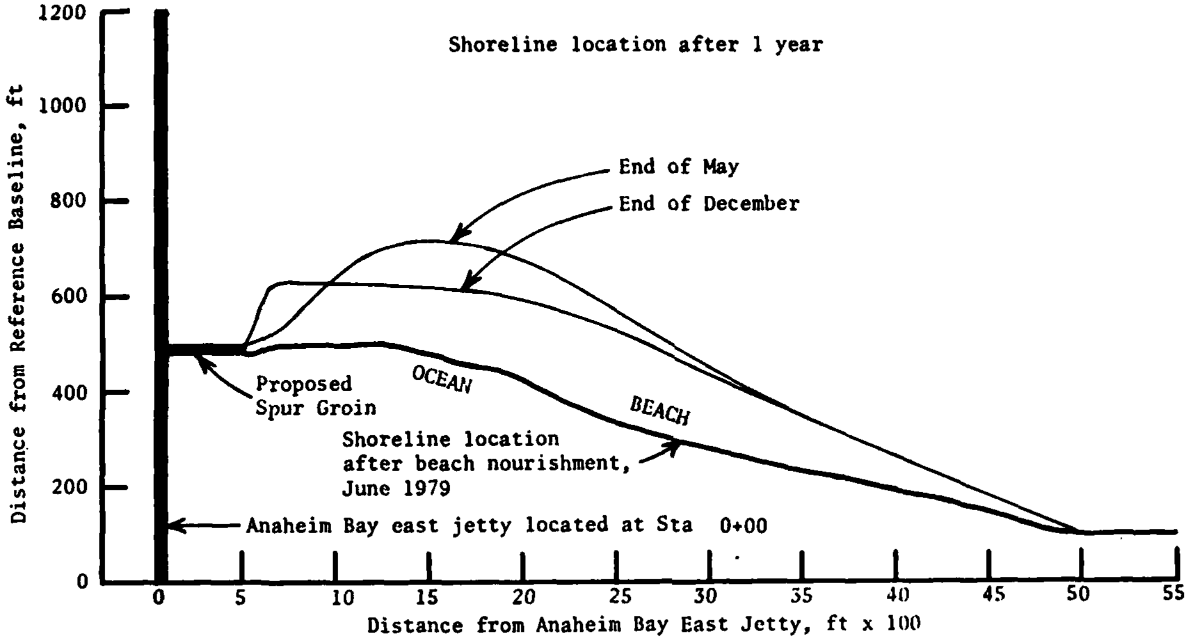

Figure 25. Computer simulation model indication of the rate and extent of beach erosion at the nourishment feeder beach, Surfside-Sunset Beach, California, after 1 year, for a 500-ft spur groin

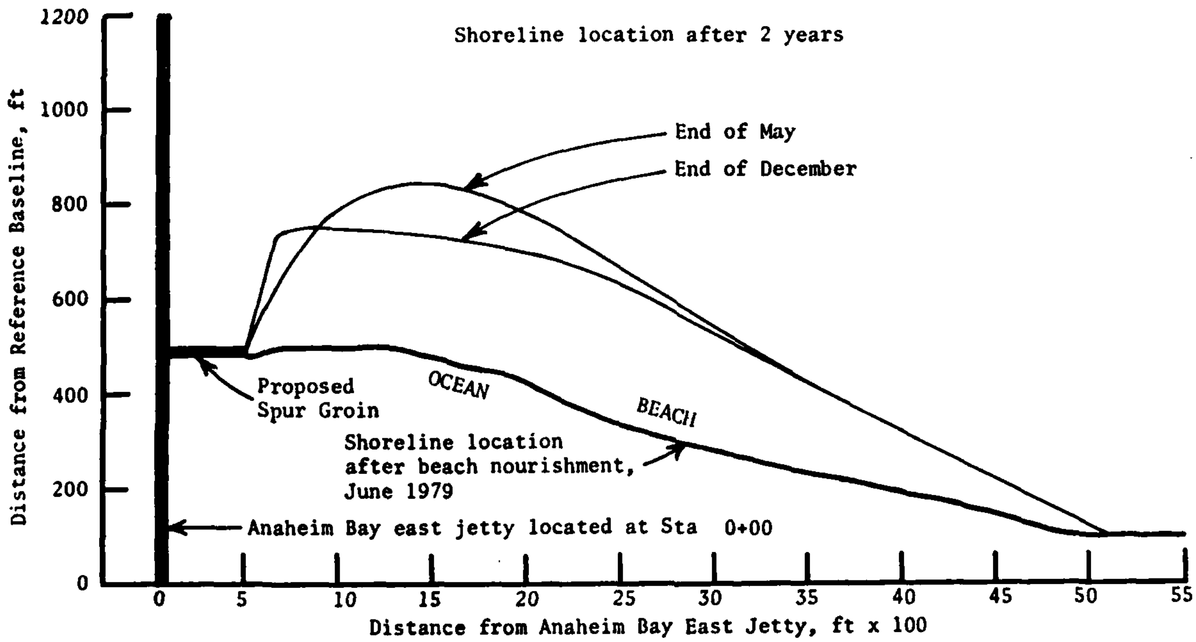

Figure 26. Computer simulation model indication of the rate and extent of beach erosion at the nourishment feeder beach, Surfside-Sunset Beach, California, after 2 years, for a 500-ft spur groin

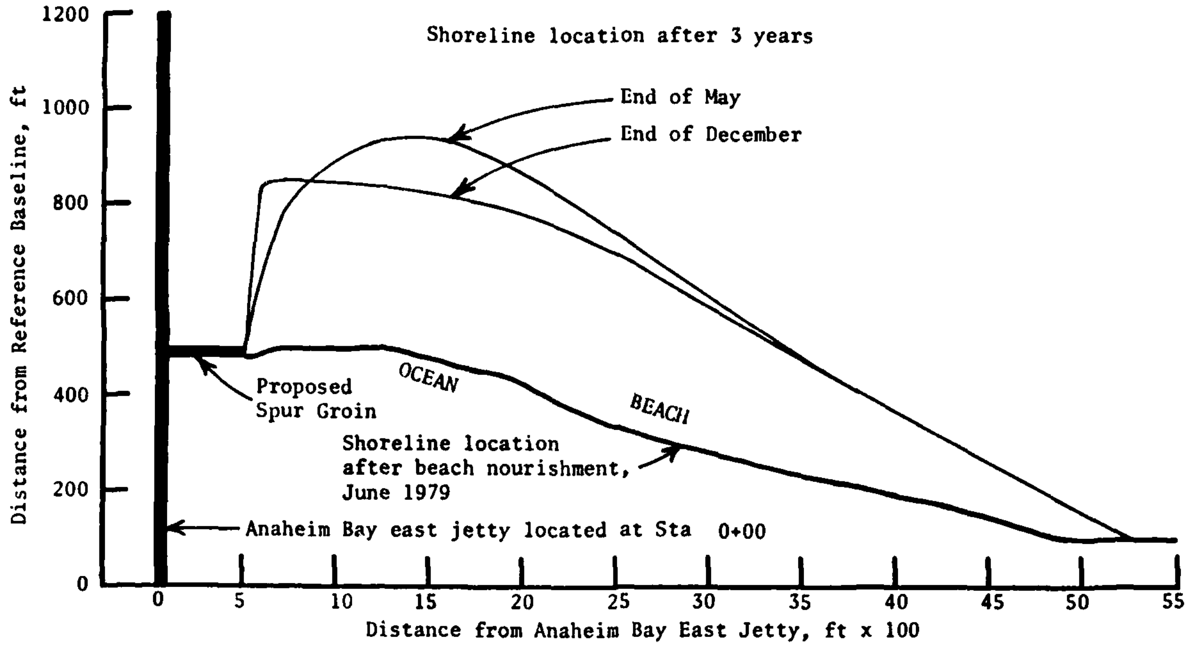

Figure 27. Computer simulation model indication of the rate and extent of beach erosion at the nourishment feeder beach, Surfside-Sunset Beach, California, after 3 years, for a 500-ft spur groin

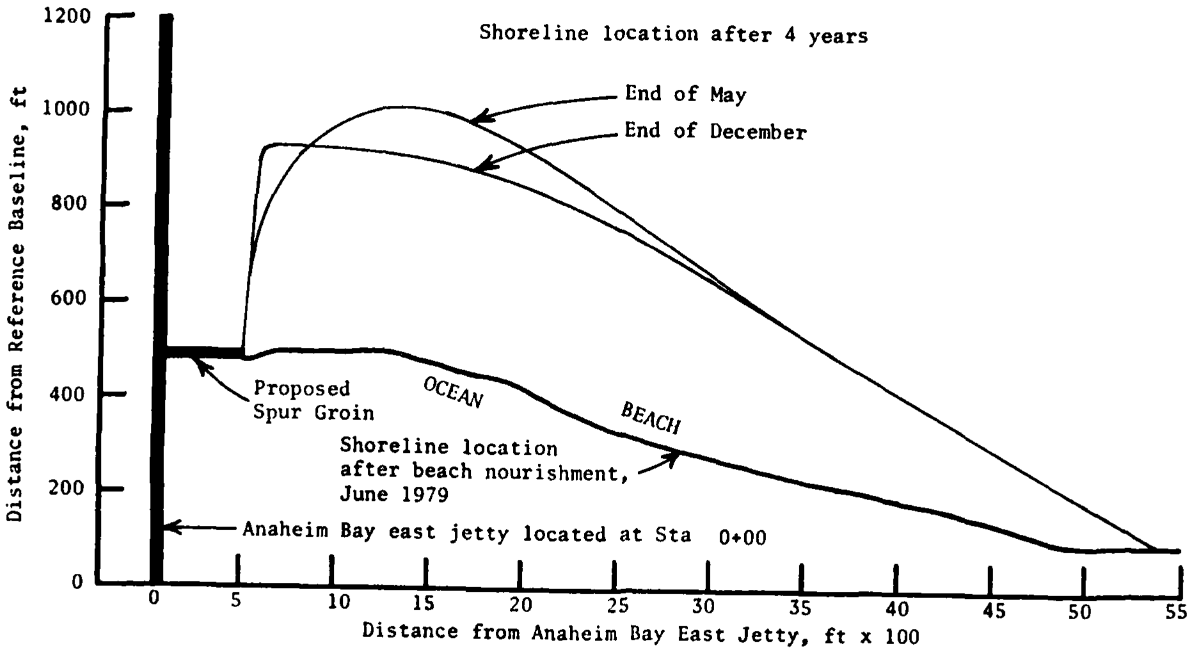

Figure 28. Computer simulation model indication of the rate and extent of beach erosion at the nourishment feeder beach, Surfside-Sunset Beach, California, after 4 years, for a 500-ft spur groin

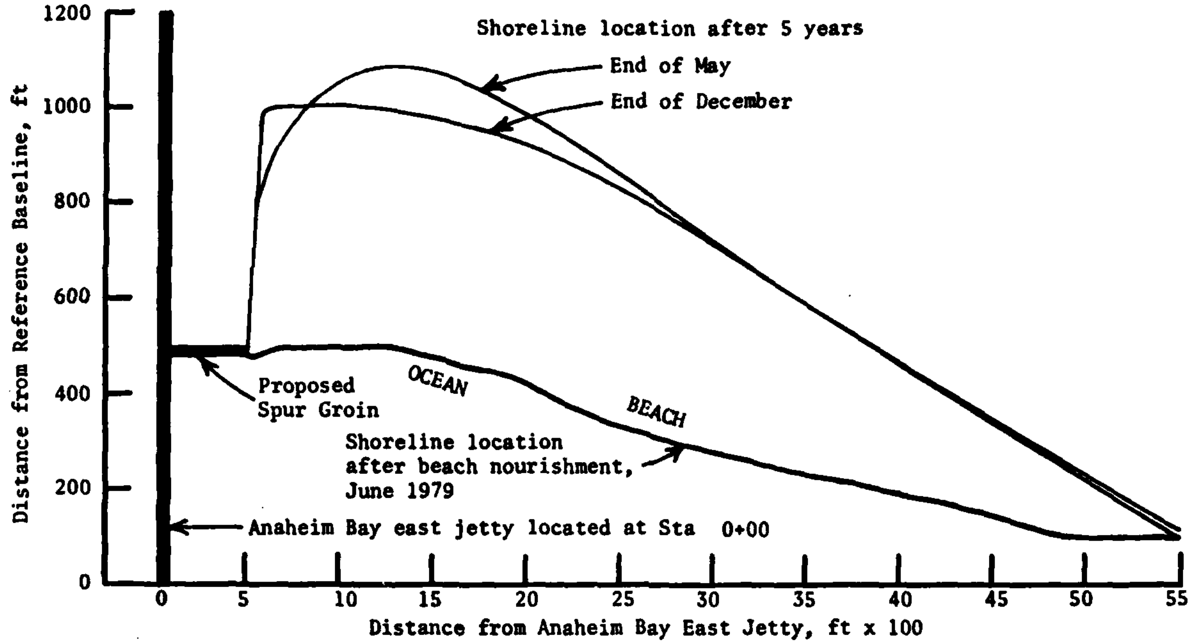

Figure 29. Computer simulation model indication of the rate and extent of beach erosion at the nourishment feeder beach, Surfside-Sunset Beach, California, after 5 years, for a 500-ft spur groin

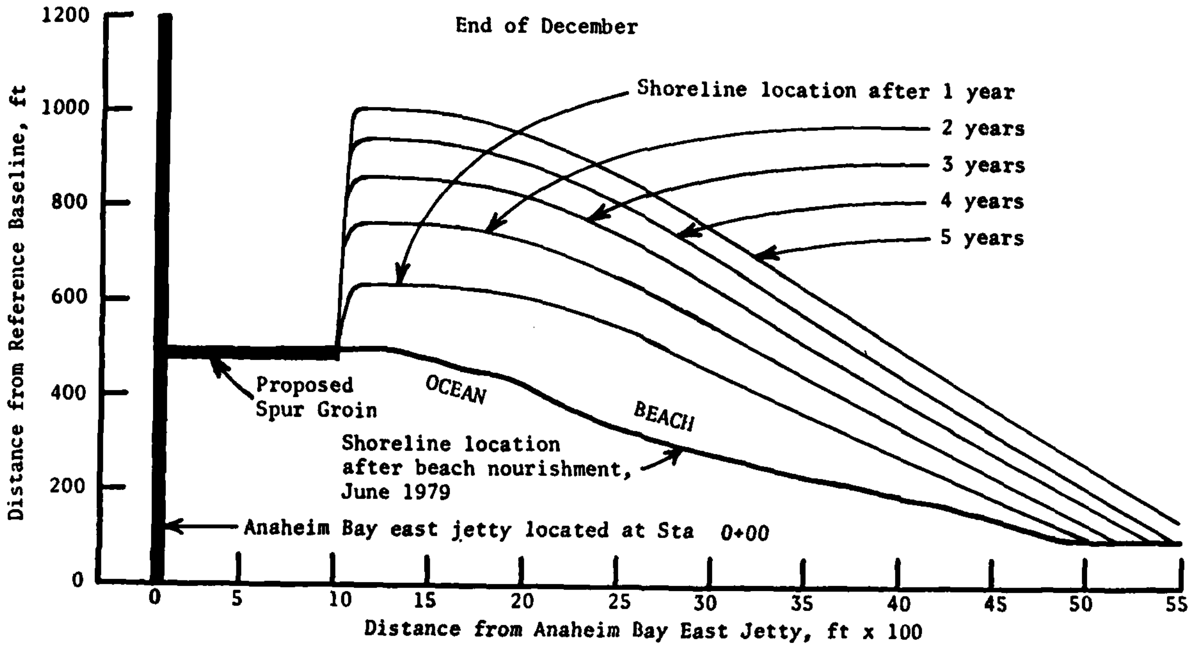

Figure 30. Computer simulation model indication of the rate and extent of beach erosion at the nourishment feeder beach, Surfside-Sunset Beach, California, end of December, for a 1,000-ft spur groin

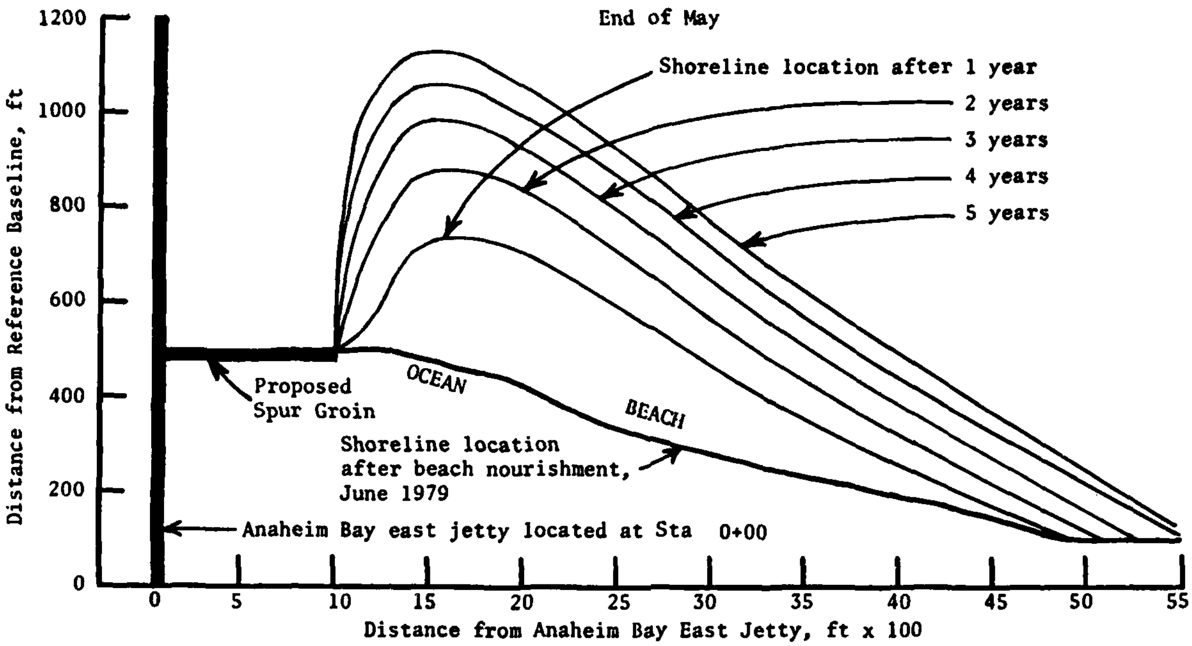

Figure 31. Computer simulation model indication of the rate and extent of beach erosion at the nourishment feeder beach, Surfside-Sunset Beach, California, end of May, for a 1,000-ft spur groin

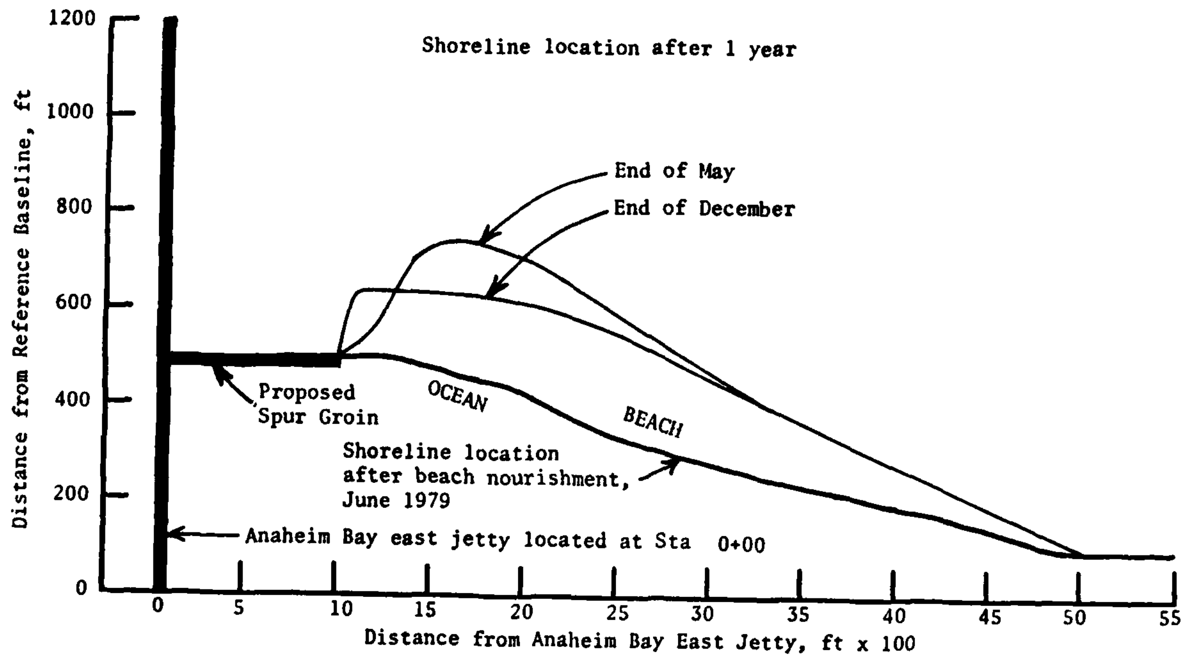

Figure 32. Computer simulation model indication of the rate and extent of beach erosion at the nourishment feeder beach, Surfside-Sunset Beach, California, after 1 year, for a 1,000-ft spur groin

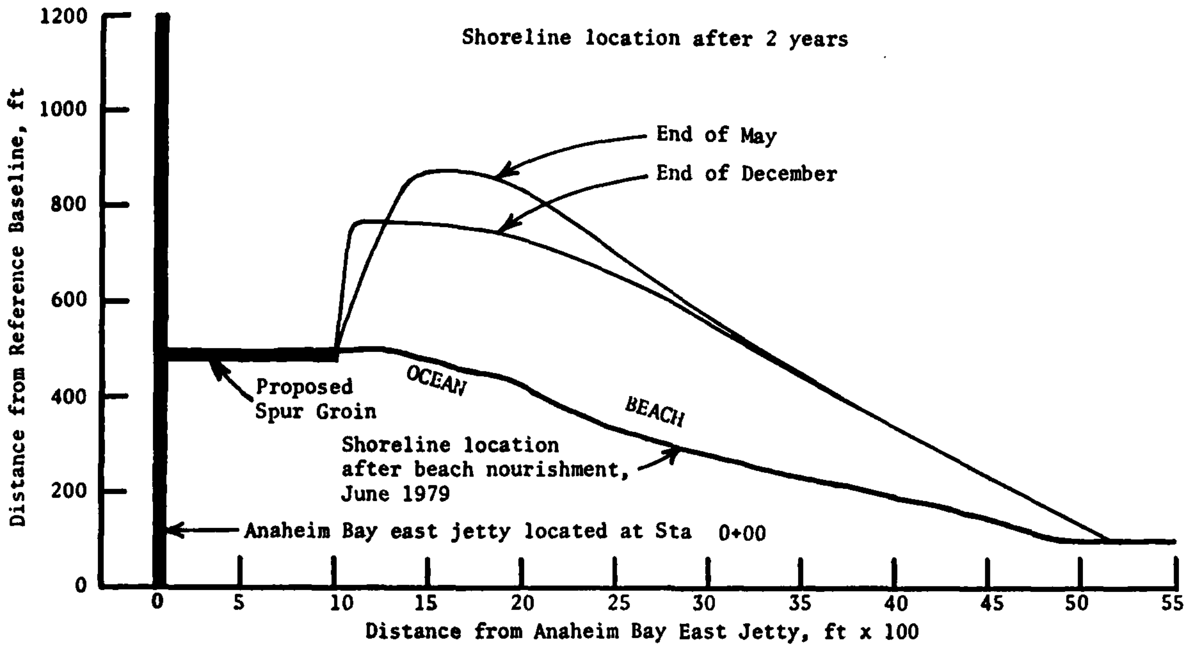

Figure 33. Computer simulation model indication of the rate and extent of beach erosion at the nourishment feeder beach, Surfside-Sunset Beach, California, after 2 years, for a 1,000-ft spur groin

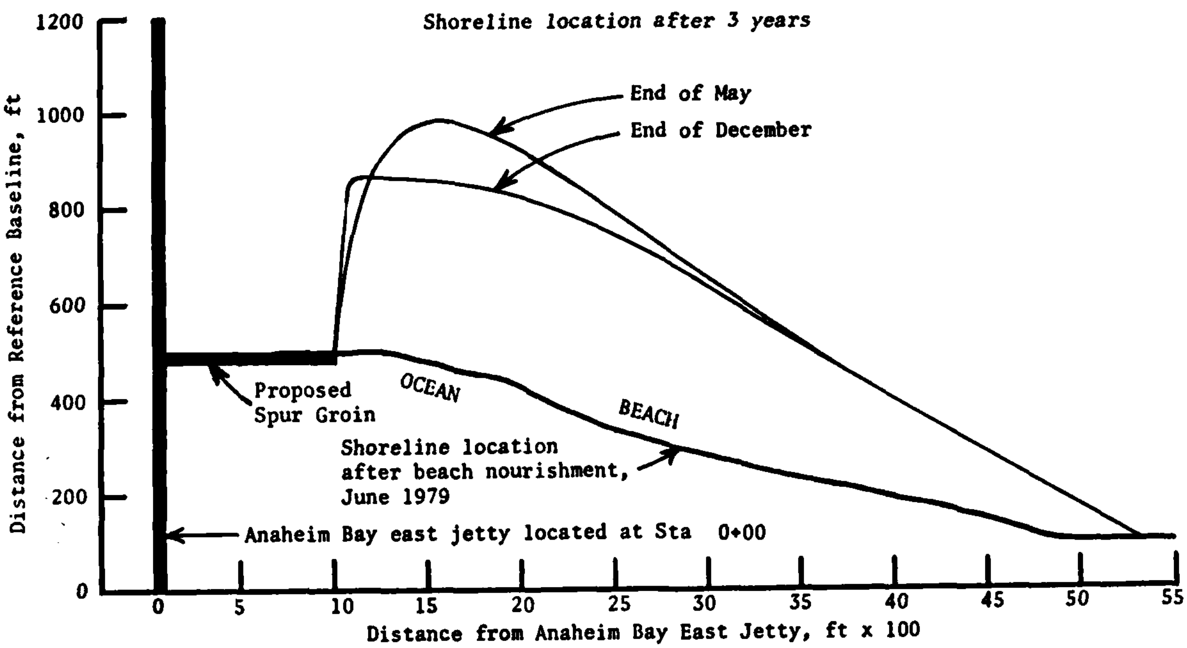

Figure 34. Computer simulation model indication of the rate and extent of beach erosion at the nourishment feeder beach, Surfside-Sunset Beach, California, after 3 years, for a 1,000-ft spur groin

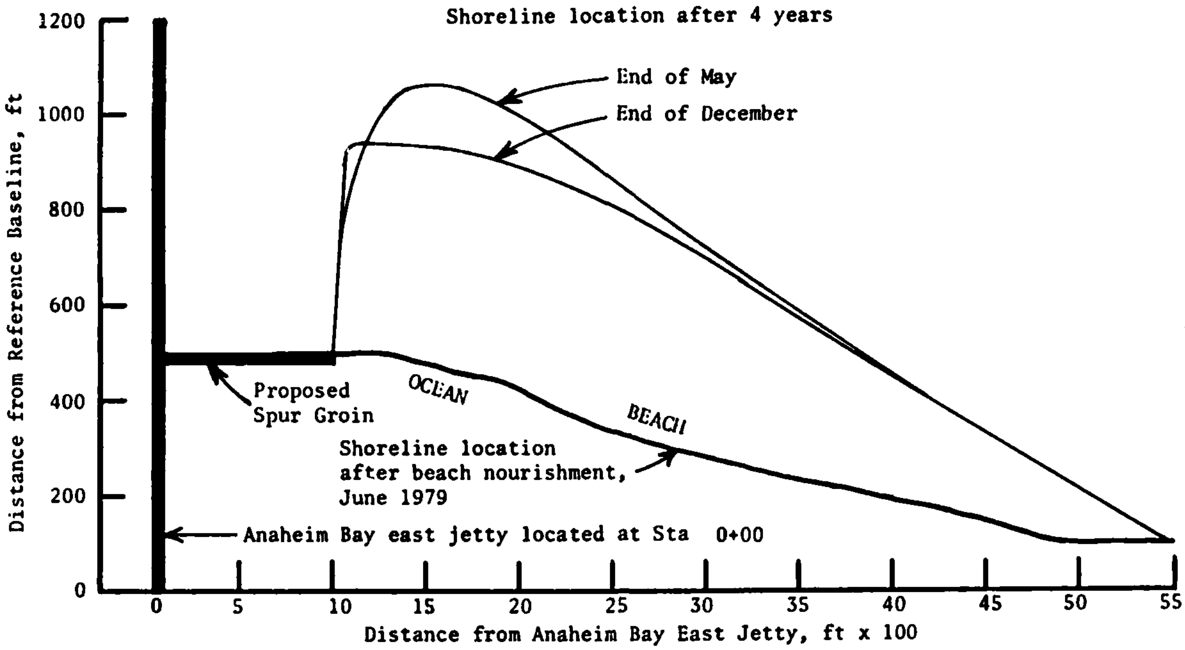

Figure 35. Computer simulation model indication of the rate and extent of beach erosion at the nourishment feeder beach, Surfside-Sunset Beach, California, after 4 years, for a 1,000-ft spur groin

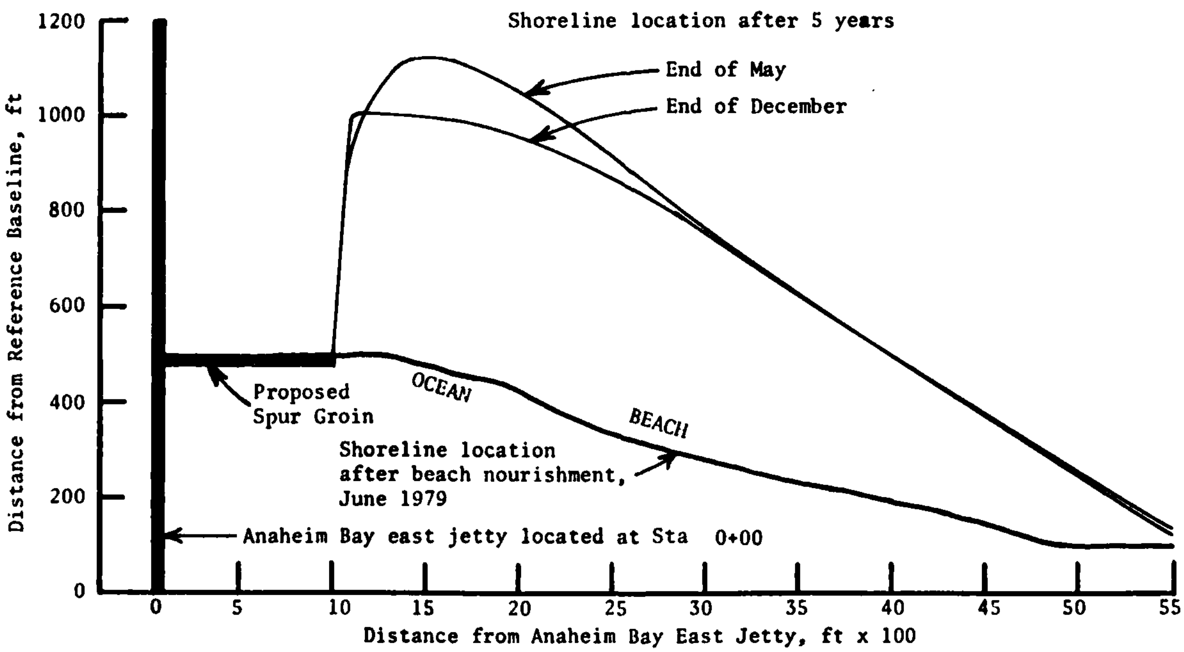

Figure 36. Computer simulation model indication of the rate and extent of beach erosion at the nourishment feeder beach, Surfside-Sunset Beach, California, after 5 years, for a 1,000-ft spur groin

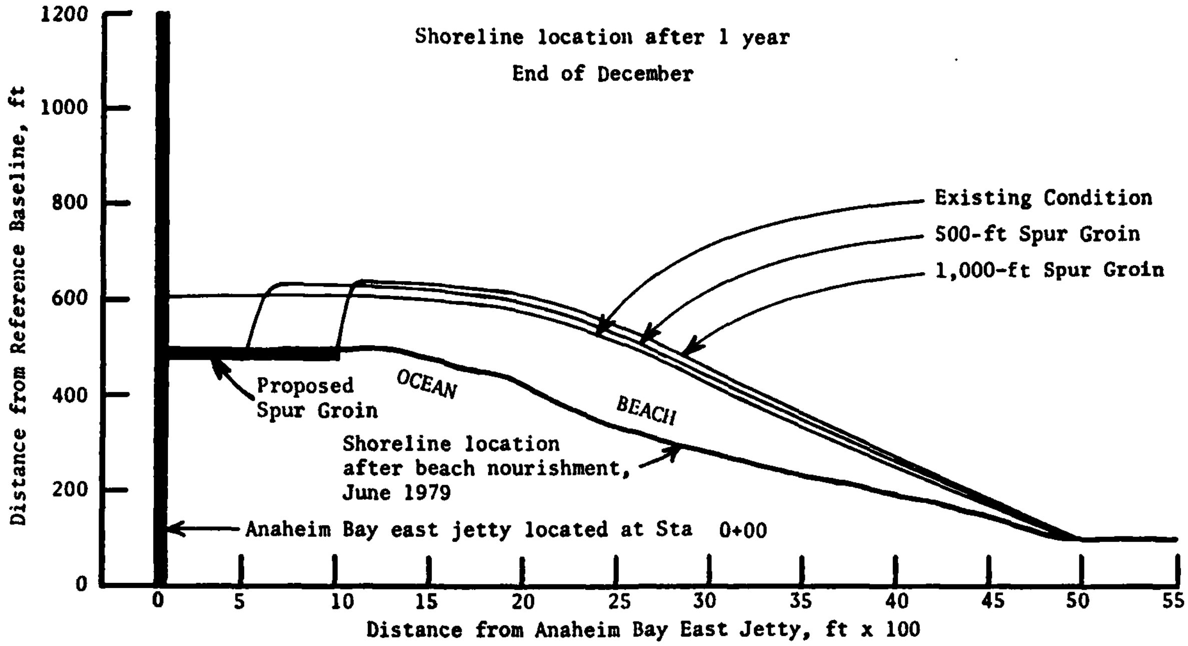

Figure 37. Comparison of computer simulation model indication of the rate and extent of beach erosion at the nourishment feeder beach, Surfside-Sunset Beach, California, after 1 year, end of December, for existing condition, 500-ft spur groin, and 1,000-ft spur groin

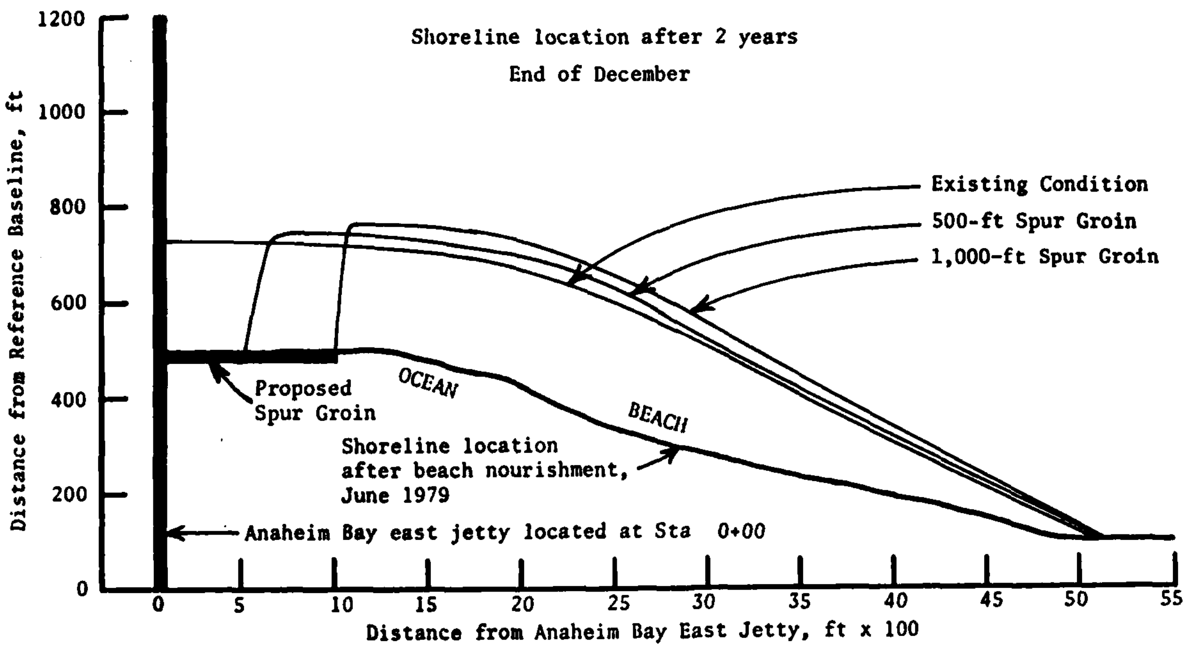

Figure 38. Comparison of computer simulation model indication of the rate and extent of beach erosion at the nourishment feeder beach, Surfside-Sunset Beach, California, after 2 years, end of December, for existing condition, 500-ft spur groin, and 1,000-ft spur groin

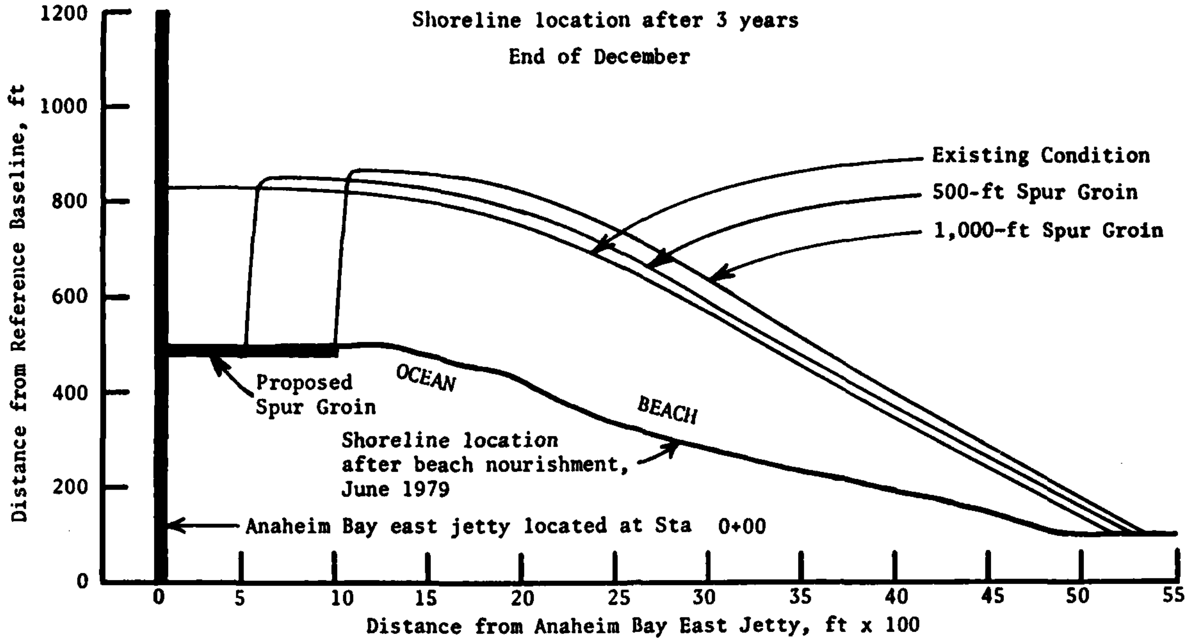

Figure 39. Comparison of computer simulation model indication of the rate and extent of beach erosion at the nourishment feeder beach, Surfside-Sunset Beach, California, after 3 years, end of December, for existing condition, 500-ft spur groin, and 1,000-ft spur groin

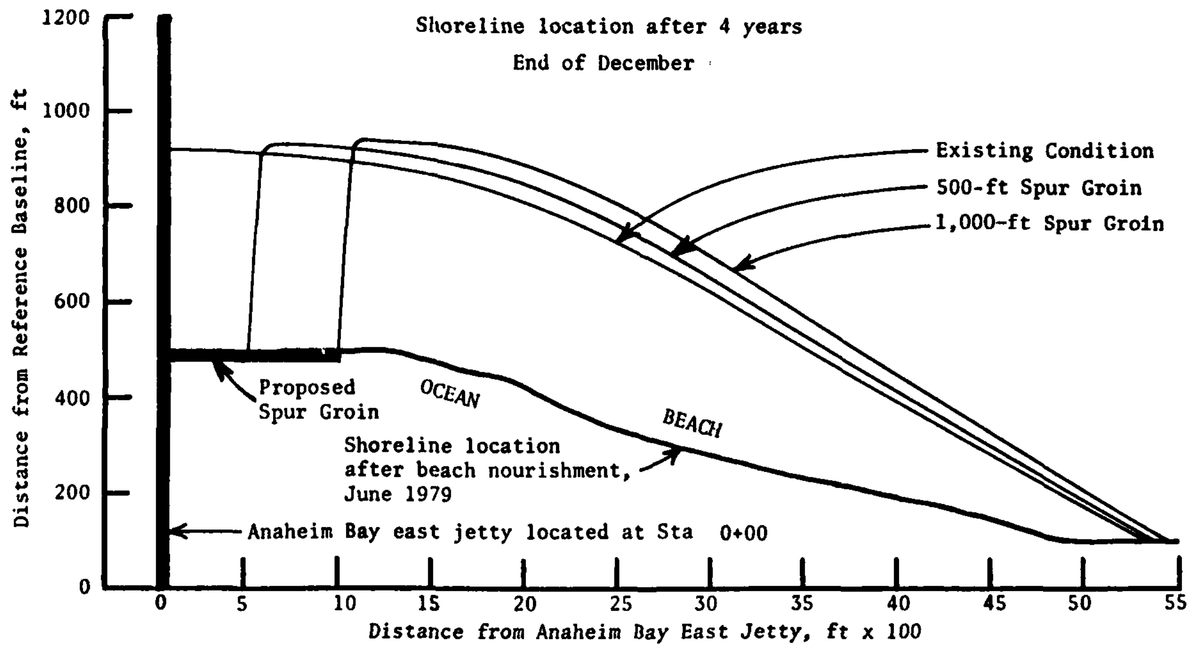

Figure 40. Comparison of computer simulation model indication of the rate and extent of beach erosion at the nourishment feeder beach, Surfside-Sunset Beach, California, after 4 years, end of December, for existing condition, 500-ft spur groin, and 1,000-ft spur groin

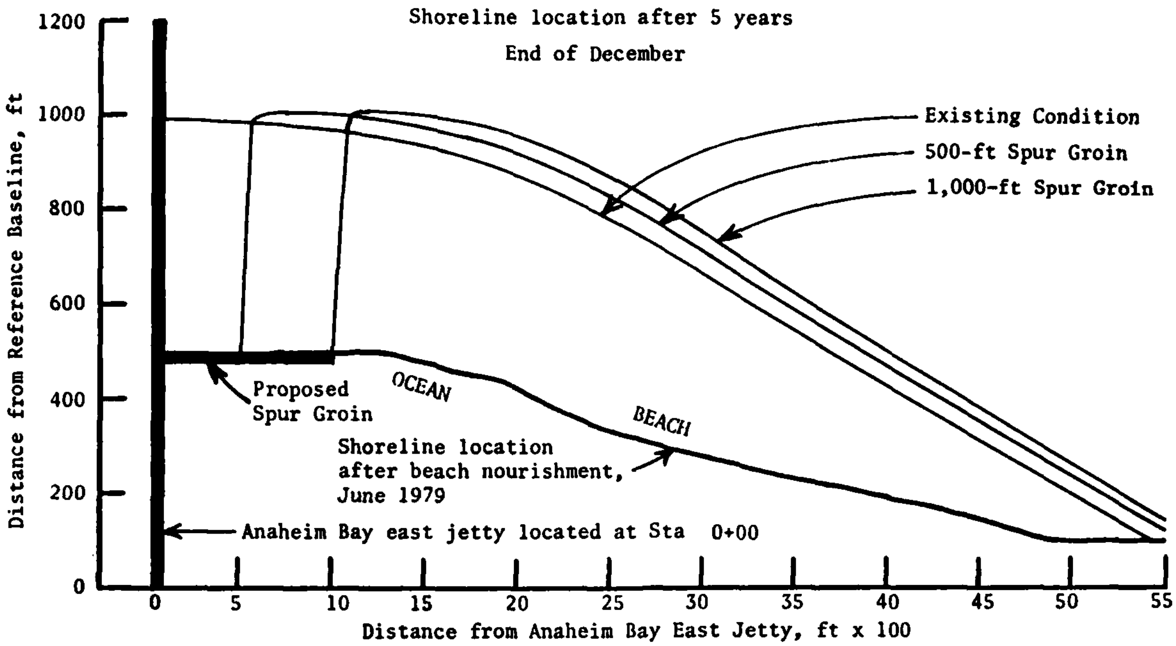

Figure 41. Comparison of computer simulation model indication of the rate and extent of beach erosion at the nourishment feeder beach, Surfside-Sunset Beach, California, after 5 years, end of December, for existing condition, 500-ft spur groin, and 1,000-ft spur groin

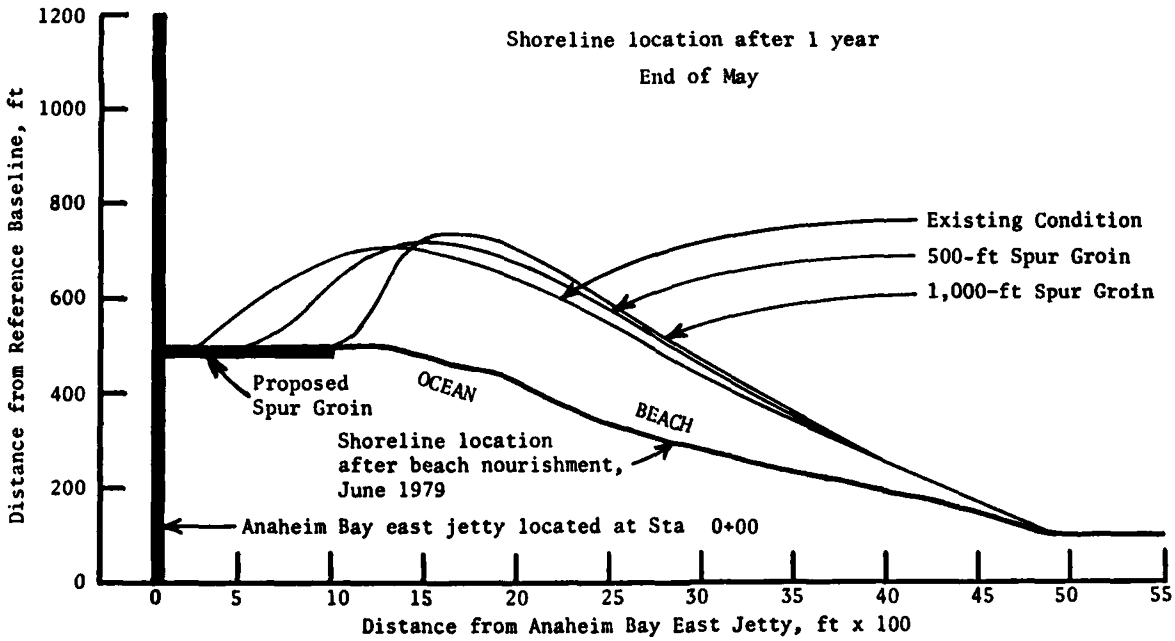

Figure 42. Comparison of computer simulation model indication of the rate and extent of beach erosion at the nourishment feeder beach, Surfside-Sunset Beach, California, after 1 year, end of May, for existing condition, 500-ft spur groin, and 1,000-ft spur groin

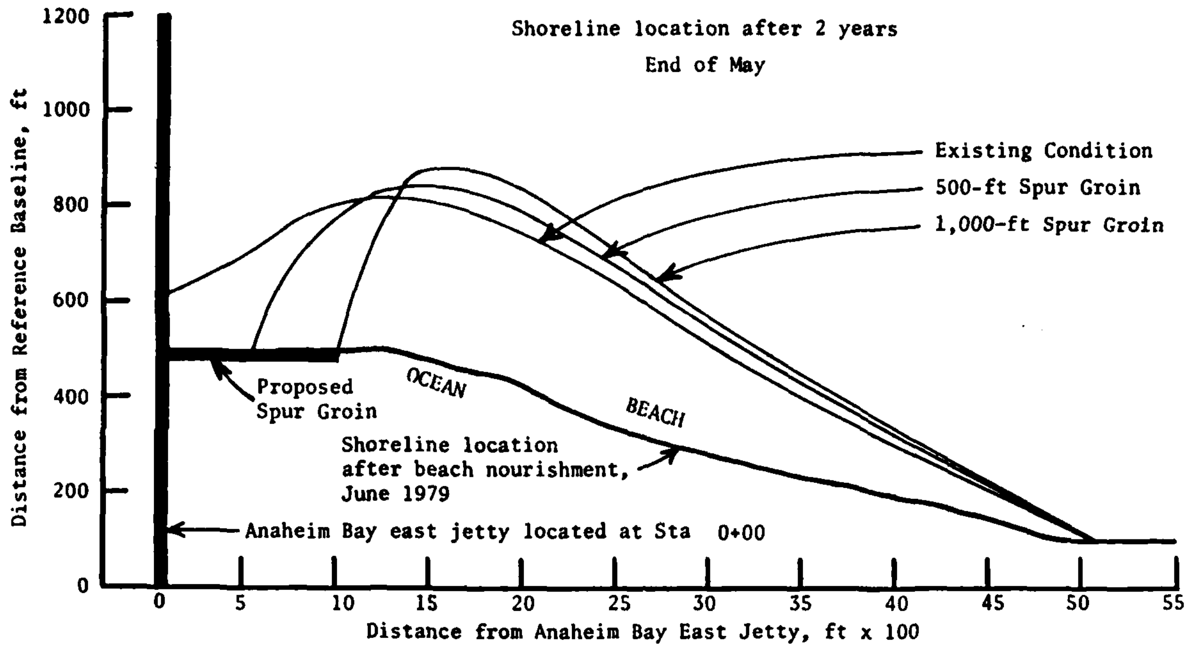

Figure 43. Comparison of computer simulation model indication of the rate and extent of beach erosion at the nourishment feeder beach, Surfside-Sunset Beach, California, after 2 years, end of May, for existing condition, 500-ft spur groin, and 1,000-ft spur groin

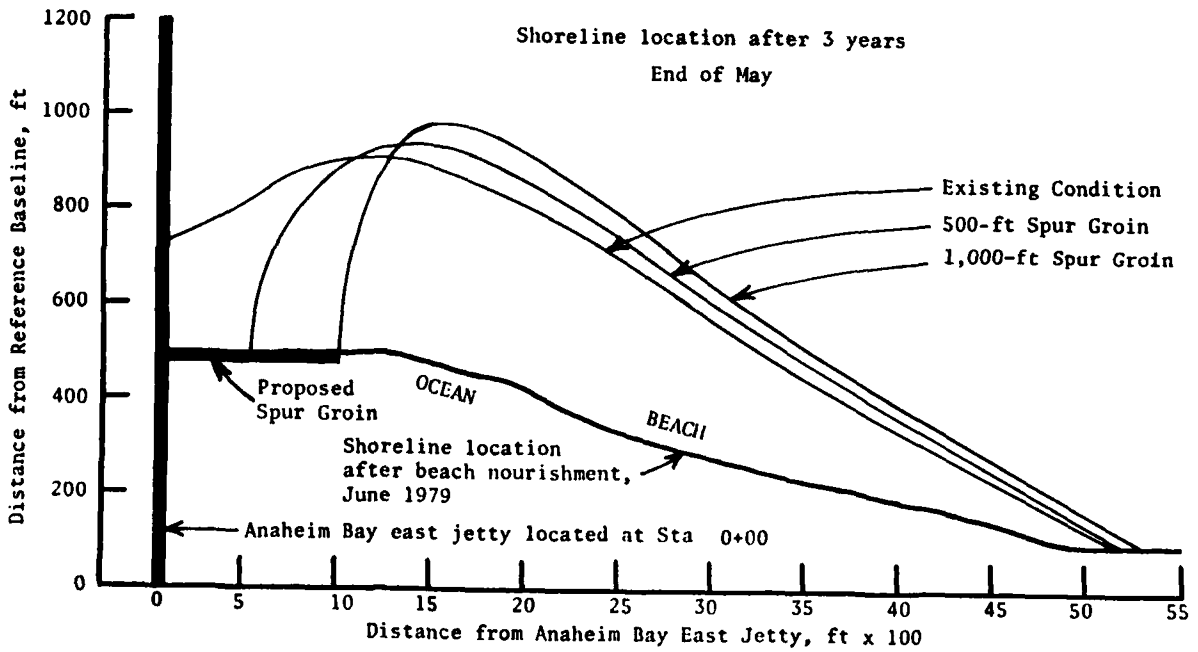

Figure 44. Comparison of computer simulation model indication of the rate and extent of beach erosion at the nourishment feeder beach, Surfside-Sunset Beach, California, after 3 years, end of May, for existing condition, 500-ft spur groin, and 1,000-ft spur groin

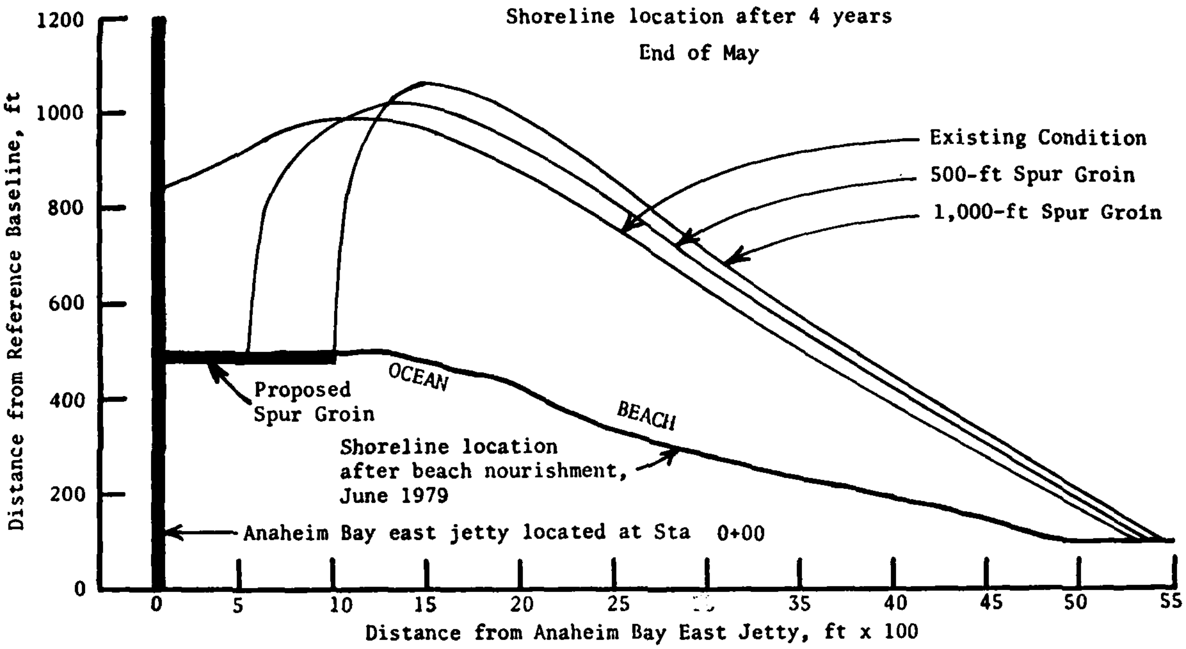

Figure 45. Comparison of computation simulation model indication of the rate and extent of beach erosion at the nourishment feeder beach, Surfside-Sunset Beach, California, after 4 years, end of May, for existing condition, 500-ft spur groin, and 1,000-ft spur groin

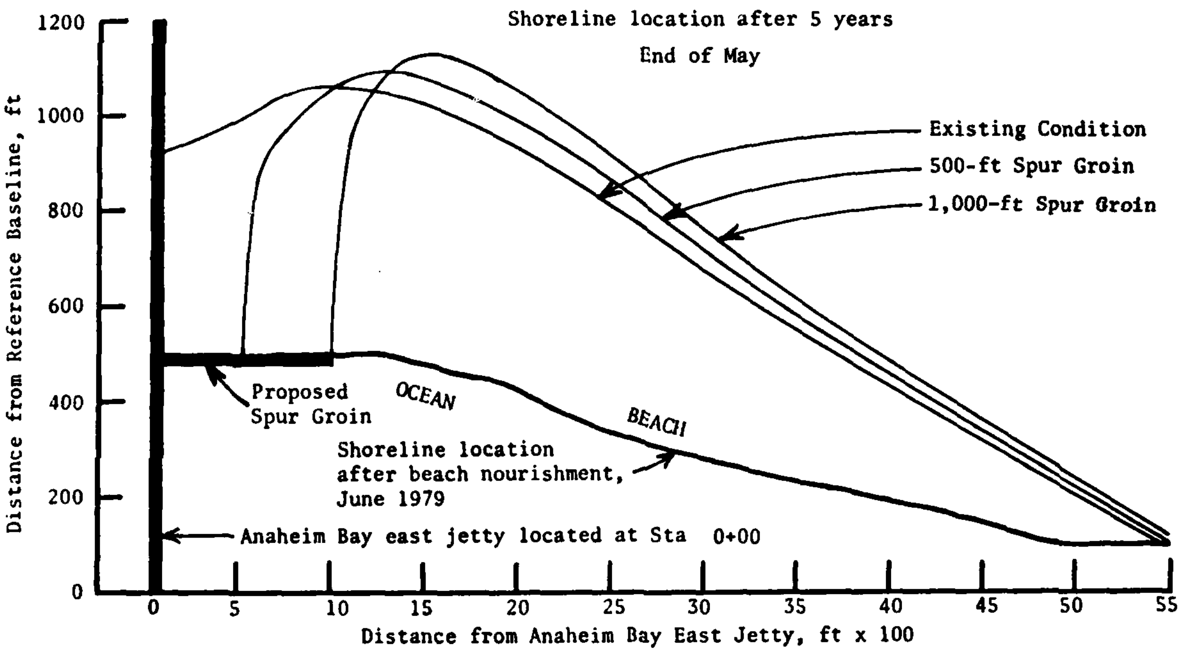

Figure 46. Comparison of computation simulation model indication of the rate and extent of beach erosion at the nourishment feeder beach, Surfside-Sunset Beach, California, after 5 years, end of May, for existing condition, 500-ft spur groin, and 1,000-ft spur groin

PART VI: WEIR JETTY AND SAND BYPASSING CONCEPT

66. Construction of jetties to stabilize entrance channels to bays, harbors, or estuaries usually interrupts the natural longshore transport of sand. The resulting starvation of the downdrift beach may cause serious erosion unless measures are taken to transfer or bypass sand from the updrift side of the entrance channel. One method of accomplishing this sand transfer to the downcoast region is with the construction and operation of a weir jetty, with the accompanying transfer mechanism consisting of a sand bypassing system. Sand that passes over the weir into the deposition basin can be removed from the deposition basin and placed on the downdrift beach during periods of downcoast movement of littoral material in the surf zone. The weir jetty and sand bypassing concept has been discussed by Weggel (1981) for optimum systems operating under idealized conditions.

67. The key elements of the weir jetty system include (Figure 47): (a) an updrift jetty comprised of a sandtight landward section, a weir section with an elevation near mean waterline (mwl), and a seaward section having a typical jetty cross section; (b) a downdrift jetty that normally has a conventional jetty cross section without a weir section; (c) a deposition basin; (d) a navigation channel; (e) an updrift beach; and (f) a downdrift beach that normally also serves as the disposal area for sand removed from the deposition basin. The weir jetty system is intended to keep to a minimum the amount of sand required to be bypassed. Optimally, this amount should be the net sand transport moving downcoast; realistically, the amount of material that requires bypassing was found to be dependent on the length of the sandtight landward section of the updrift jetty and on the time (number of years) since construction of the weir jetty structure. These two factors govern the growth of the updrift fillet to maturity, since the fillet does not completely fill during the first year but continues to grow and asymptotically approaches an ultimate equilibrium configuration. After the fillet reaches maturity, the amount of material passing over the weir will approximate the net downcoast movement of littoral material. Prior to the growth of the fillet to maturity, however, the amount of material entering the deposition basin will be less than the net downcoast movement. Because the net quantity should be placed on the downdrift side of the proposed new entrance channel to prevent erosion of the downcoast beach, any difference between the required net

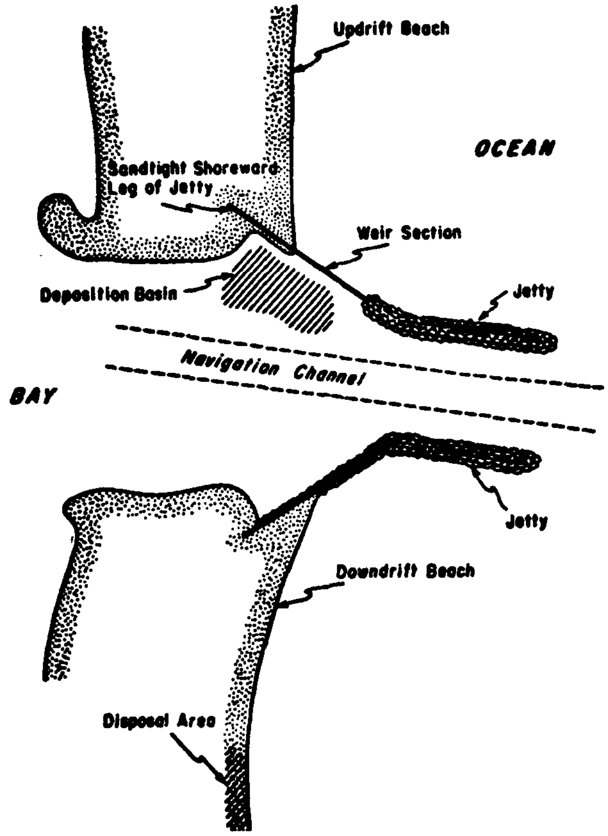

Figure 47. Key elements of a typical weir jetty system (after Weggel 1981)

quantity and that amount actually passing over the weir into the deposition basin should be obtained from an external source.

Quantity of Material to be Bypassed

68. The quantity of material that will pass over the weir section into the deposition basin each year will be the difference between the volume of material which is eroded from the Surfside-Sunset Beach region and the volume of material which accumulates in the updrift fillet (and along the shoreline during the early years after jetty construction until the fillet grows to maturity). This quantity of material, therefore, is governed by the length of the sandtight landward section of jetty between the weir and the existing shoreline (schematized in Figure 48). For the interruption of the littoral drift along an equilibrium coastline such as the location of the proposed new entrance channels to Bolsa Chica Bay (Site A, Figure 4, or Site B, Figure 5),

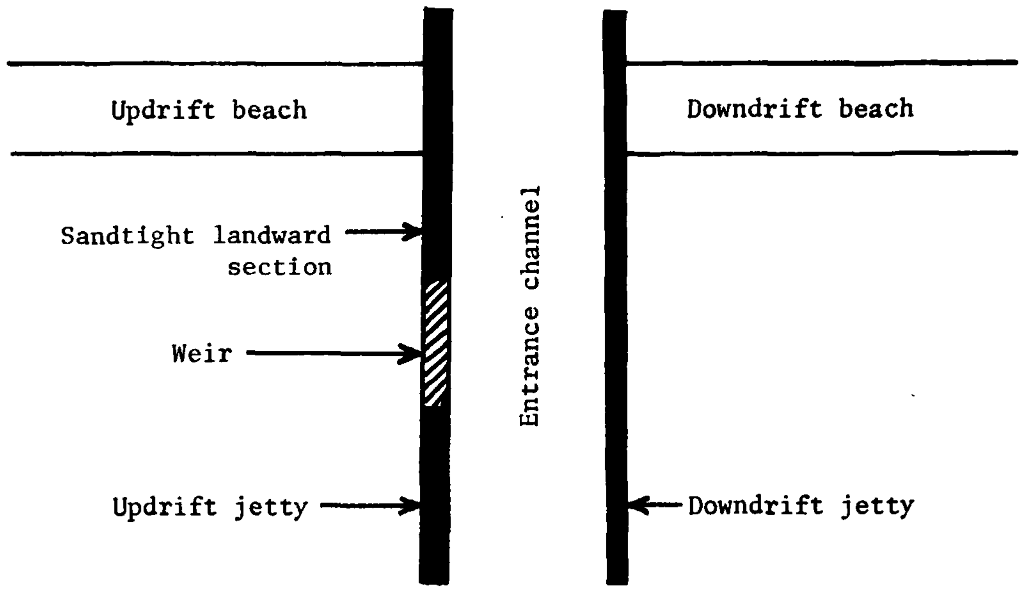

Figure 48. Schematic of weir jetty system prior to fillet growth

the shoreline downcoast will respond in an asymptotic manner to the existing condition (in the absence of any bypassing), as in Figure 49a. Near the Anaheim Bay east jetty, the beach nourishment provides a localized nonequilibrium orientation where material removed is greater than the transport capacity of the equilibrium beach farther downcoast (Figure 49b). The result is a temporal accretion along the existing shoreline that will gradually dissipate with time as the nonequilibrium section returns to an equilibrium condition and the transport out of the Surfside-Sunset Beach region decreases. The situation more nearly approximating that condition which will exist after construction of the proposed new entrance channel at either Site A or Site B (Figures 4 and 5, respectively) is schematized in Figure 49c. Here the temporal accretion along the shoreline will become obscured with time as the fillet near the proposed jetty grows.

69. Starting with the after-nourishment beach orientation of 1979, the computer simulation model was operated for a period of 5 years in 1-hr time increments to observe the effect of proposed new entrance channel structures at Site A and Site B on the unstabilized upcoast shoreline. The quantity of material eroded from the Surfside-Sunset Beach region (Tables 11 and 12), the quantity of material accumulated in the updrift fillet as the fillet grows asymptotically to maturity (Tables 13 and 14), the volume of material passing over the weir into the deposition basin (Tables 15 and 16), and the quantity

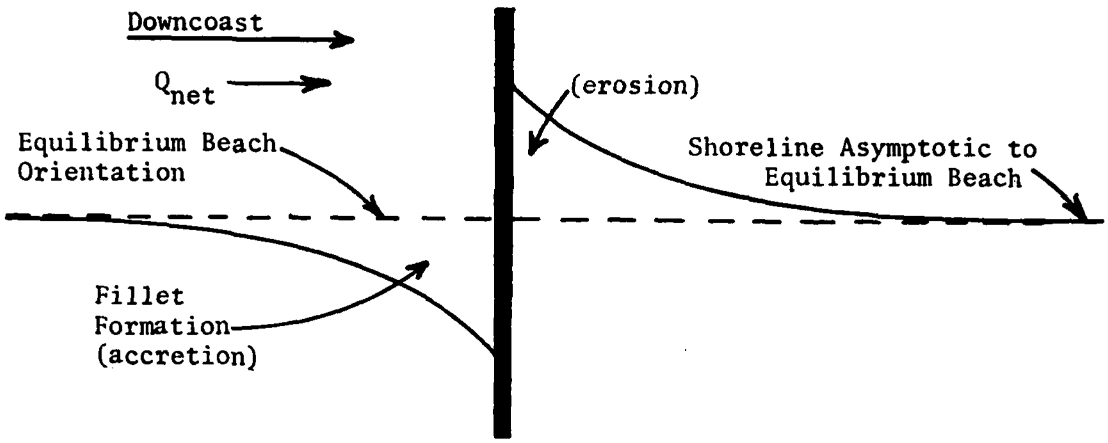

a. Equilibrium Beach

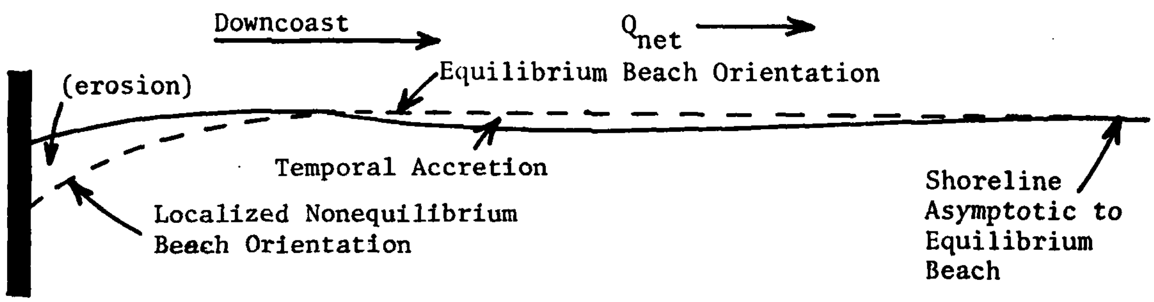

b. Nonequilibrium Beach

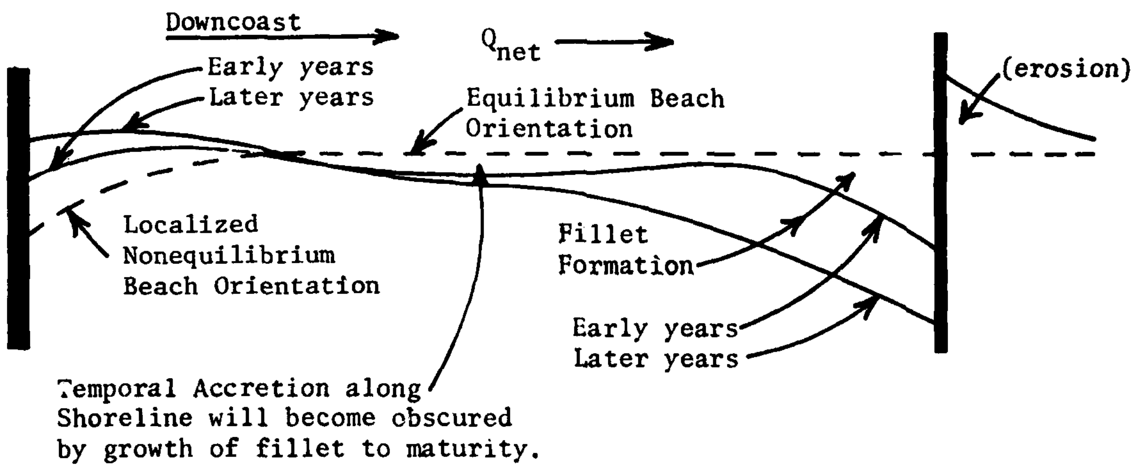

c. Combination Nonequilibrium and Equilibrium Beach

Figure 49. Schematic of shore processes near structures for equilibrium, nonequilibrium, and combination beach orientations

Table 11

Computer Simulation Model Indication of

Erosion from Surfside-Sunset Beach

Proposed Entrance Channel Located at Site A

During Year	Existing Condition cu yd	Length of Sandtight Landward Section 50-ft Section cu yd	100-ft Section cu yd	150-ft Section cu yd	200-ft Section cu yd	250-ft Section cu yd
1	558,300	558,200	558,200	558,200	558,200	558,200
2	379,300	378,000	376,600	375,400	374,600	374,100
3	322,700	319,600	315,000	310,600	306,800	303,600
4	288,600	285,200	277,300	270,200	263,600	257,600
5	263,900	260,700	251,600	242,400	233,900	225,800
Total	1,812,800	1,801,700	1,778,700	1,756,800	1,737,100	1,719,300

Table 12

Computer Simulation Model of

Erosion from Surfside-Sunset Beach

Proposed Entrance Channel Located at Site B

During Year	Existing Condition cu yd	Length of Sandtight Landward Section 50-ft Section cu yd	100-ft Section cu yd	150-ft Section cu yd	200-ft Section cu yd	250-ft Section cu yd
1	558,300	558,300	558,300	558,300	558,300	558,300
2	379,300	379,200	379,100	379,100	379,100	379,000
3	322,700	322,100	321,300	320,600	320,100	319,700
4	288,600	287,400	285,400	283,500	281,700	280,400
5	263,900	262,200	258,800	255,600	252,600	249,800
Total	1,812,800	1,809,200	1,802,900	1,797,100	1,791,800	1,787,200

Table 13

Computer Simulation Model Indication of
Accumulation Upcoast of Proposed New Weir Jetty
Proposed Entrance Channel Located at Site A

		Length of Sandtight Landward Section				
During Year	Existing Condition cu yd	50-ft Section cu yd	100-ft Section cu yd	150-ft Section cu yd	200-ft Section cu yd	250-ft Section cu yd
1	164,200	245,900	325,300	400,000	466,900	522,100
2	78,400	85,800	122,200	159,900	199,700	242,600
3	14,600	12,200	36,600	61,900	88,700	117,800
4	-23,300	-31,000	-14,500	3,300	22,100	42,500
5	-48,300	-56,700	-44,400	-31,900	-18,200	-3,500
Total	185,600	256,200	425,200	593,200	759,200	921,500

Table 14

Computer Simulation Model Indication of
Accumulation Upcoast of Proposed New Weir Jetty
Proposed Entrance Channel Located at Site B

		Length of Sandtight Landward Section				
During Year	Existing Condition cu yd	50-ft Section cu yd	100-ft Section cu yd	150-ft Section cu yd	200-ft Section cu yd	250-ft Section cu yd
1	164,300	246,100	325,500	400,200	467,100	522,300
2	81,800	93,800	131,500	170,200	210,600	253,700
3	23,700	32,200	60,300	89,200	119,100	150,700
4	-12,800	-8,600	13,800	36,600	60,300	85,200
5	-39,600	-38,700	-20,700	-2,200	16,900	37,100
Total	217,400	324,800	510,400	694,000	874,000	1,049,000

Table 15

Computer Simulation Model Indication of

Material Entering Deposition Basin

Prior to Fillet Maturity

Proposed Entrance Channel Located at Site A

		Length of Sandtight Landward Section				
During Year	Existing Condition cu yd	50-ft Section cu yd	100-ft Section cu yd	150-ft Section cu yd	200-ft Section cu yd	250-ft Section cu yd
1	--	312,300	232,900	158,200	91,300	36,100
2	--	292,200	254,300	215,500	174,900	131,500
3	--	307,400	278,400	248,700	218,100	185,800
4	--	316,200	291,800	266,900	241,500	215,100
5	--	317,500	296,000	274,300	252,100	229,200
Total	--	1,545,600	1,353,400	1,163,600	977,900	797,700

Table 16

Computer Simulation Model Indication of

Material Entering Deposition Basin

Prior to Fillet Maturity

Proposed Entrance Channel Located at Site B

		Length of Sandtight Landward Section				
During Year	Existing Condition cu yd	50-ft Section cu yd	100-ft Section cu yd	150-ft Section cu yd	200-ft Section cu yd	250-ft Section cu yd
1	--	312,200	232,700	158,100	91,200	6,000
2	--	285,400	247,600	208,900	168,500	125,300
3	--	289,900	260,900	231,400	201,000	168,900
4	--	296,000	271,600	246,900	221,500	195,200
5	--	300,900	279,500	257,800	235,600	212,800
Total	--	1,484,400	1,292,300	1,103,200	917,800	738,200

of material returned to the Surfside-Sunset Beach region from dynamic storage in the fillet (Tables 17 and 18) were determined for the transition period as the fillet grows. These estimations were obtained for five different lengths of sandtight landward sections of the weir jetty (50, 100, 150, 200, and 250 ft). All computations were performed under the assumption that the structures were instantaneously placed into position at the beginning of January with no initial fillet formation.

70. During the period of time from initial jetty construction to the conclusion of fillet formation, portions of the material moving downcoast as net littoral drift will be retained as fillet growth, and portions will be transmitted over the weir into the deposition basin. That material being deposited in the deposition basin will be removed and placed on the downcoast beach to preclude erosion of this region; however, the material accumulating in the deposition basin during the growth of the fillet to maturity will not be sufficient to completely prevent some erosion of the downcoast region from occurring. Hence, supplemental material will be required to be placed on the downcoast beaches during this transition period. The volume of supplemental material required to satisfy this demand will ideally be the difference between the net downcoast movement of littoral material and the volume of material which accumulates in the deposition basin, assuming this accumulated material will be expeditiously removed and placed on the downcoast beach. These quantities are displayed in tabular form in Tables 19 and 20 for proposed navigation entrance channel locations at Site A and Site B, respectively.

71. From the data of Tables 11-18, it appears that Sites A and B are not significantly different in their effect on the unstabilized upcoast shoreline. Selection of either of these sites as the location for a proposed new navigable entrance channel to Bolsa Chica Bay from the Pacific Ocean will be based on additional criteria. The structures with a 50-ft sandtight landward section do not duplicate the existing conditions; and furthermore, the 100-ft sandtight landward section is only marginal until the updrift fillet matures. After that time (about 4 years) either the 100-, 150-, 200-, or 250-ft sandtight landward section at Site A or Site B will provide a quantity of material for updrift transport from temporary dynamic storage to approximate the existing condition of no structure at the proposed new navigable entrance channel locations. The 150-, 200-, and 250-ft sandtight landward section structures will provide adequate temporary dynamic storage during the first year after

Table 17

Computer Simulation Model Indicatin of

Material Returned to Surfside-Sunset Beach

Proposed Entrance Channel Located at Site A

During Year	Existing Condition cu yd	Length of Sandtight Landward Section 50-ft Section cu yd	100-ft Section cu yd	150-ft Section cu yd	200-ft Section cu yd	250-ft Section cu yd
1	73,900	33,100	65,400	74,100	74,100	74,100
2	89,000	55,700	86,800	91,000	91,500	91,900
3	96,800	68,400	97,800	100,600	101,700	102,600
4	102,600	75,500	104,000	106,900	108,400	109,800
5	106,400	78,600	108,300	111,200	113,200	114,800
Total	468,700	311,300	462,300	483,800	488,900	493,200

Table 18

Computer Simulation Model Indication of

Material Returned to Surfside-Sunset Beach

Proposed Entrance Channel Located at Site B

During Year	Existing Condition cu yd	Length of Sandtight Landward Section 50-ft Section cu yd	100-ft Section cu yd	150-ft Section cu yd	200-ft Section cu yd	250-ft Section cu yd
1	73,900	31,500	64,800	74,600	74,700	74,700
2	89,000	48,400	83,400	89,900	89,900	90,000
3	96,800	59,300	93,600	98,200	98,500	98,700
4	102,600	67,600	101,100	104,600	105,100	105,500
5	106,400	73,200	106,400	109,400	110,100	110,800
Total	468,700	280,000	449,300	476,700	478,300	479,700

Table 19

Computer Simulation Model Indication of
Supplemental Material Required to be Placed on Downcoast Beach
in Addition to Material Removed from Deposition Basin
Proposed Entrance Channel Located at Site A

		Length of Sandtight Landward Section				
During Year	Existing Condition cu yd	50-ft Section cu yd	100-ft Section cu yd	150-ft Section cu yd	200-ft Section cu yd	250-ft Section cu yd
1	--	0	43,200	117,800	184,800	240,000
2	--	0	21,800	60,600	101,200	144,600
3	--	0	0	27,400	58,000	90,300
4	--	0	0	9,100	34,600	61,100
5	--	0	0	1,800	24,000	46,800
Total	--	0	65,000	216,700	402,600	582,800

Table 20

Computer Simulation Model Indication of
Supplemental Material Required to be Placed on Downcoast Beach
in Addition to Material Removed from Deposition Basin
Proposed Entrance Channel Located at Site B

		Length of Sandtight Landward Section				
During Year	Existing Condition cu yd	50-ft Section cu yd	100-ft Section cu yd	150-ft Section cu yd	200-ft Section cu yd	250-ft Section cu yd
1	--	0	43,300	118,000	184,900	240,100
2	--	0	28,400	67,200	107,600	150,800
3	--	0	15,100	44,600	75,100	107,100
4	--	0	4,500	29,200	54,600	80,900
5	--	0	0	18,300	40,500	63,300
Total	--	0	91,300	277,300	462,700	642,200

construction, assuming construction occurs during the summer months so that the southerly transport during January, February, March, April, and May will be retained in the fillet. However, all these sandtight landward section concepts tend to restrict the material which enters the deposition basin. Therefore the 150-ft sandtight landward section may provide the optimum configuration, considering the desirability of passing the net downdrift quantity of littoral material past the proposed new navigable entrance channel and also allowing for temporary dynamic storage of that material which moves northwesterly during the summer months. The data of Tables 11-18 apply only during the period of fillet growth to maturity; after that time, the net downcoast movement of littoral material will enter the deposition basin and will require bypassing to the downcoast region to prevent serious erosion from occurring east of the proposed new navigable entrance channel jetties.

Deposition Basin

72. Characteristics of the deposition area that must be determined include: (a) basin location and shape and (b) basin capacity. Basin location and shape are dictated by navigation channel geometry and desired location of the navigation channel. The deposition area should be adjacent to the weir section so that the eductor system of sand bypassing will function effectively. An important factor in selecting the deposition basin location is the expected response of the navigation channel to the sheltering afforded by the jetties. Providing room for a deposition basin between two jetties usually requires somewhat of an "arrowhead" jetty layout. If the navigation channel has a tendency to meander, its movement into the deposition basin is possible. In that case, a training dike may be required to fix the channel location between the jetties in the reach adjacent to the deposition basin. Two typical examples of the "arrowhead" jetty layout are shown in Figures 50 and 51. Figure 50 shows a weir jetty system that has a sandtight landward section, and Figure 51 presents a system that does not have such a sandtight section connecting the weir portion with the shoreline.

73. Two factors that influence the required deposition basin capacity are: (a) the longshore transport rate over the weir into the basin; and (b) the estimated frequency and rate at which the basin will be excavated. A reserve volume large enough to accommodate the entire downcoast net movement

(March 1972)

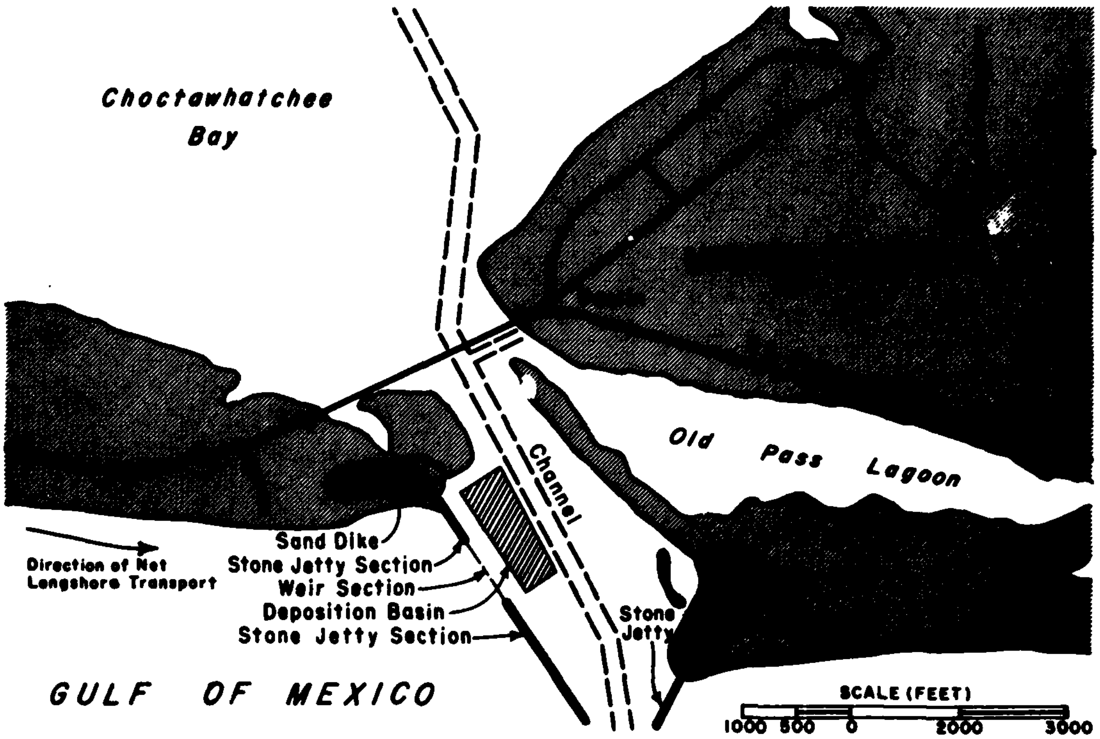

Figure 50. Destin East Pass, Florida, weir jetty alignment and deposition basin. System has a sandtight landward section connecting the weir portion with the shoreline (after CERC 1977)

(October 1970)

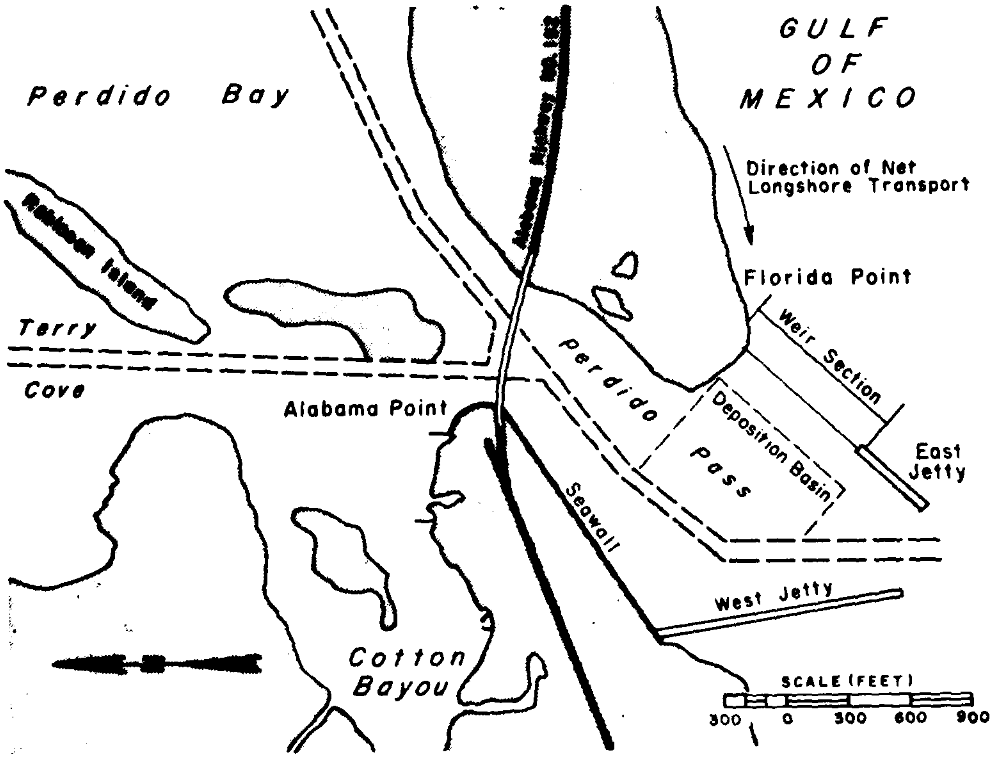

Figure 51. Perdido Pass, Alabama, weir jetty alignment and deposition basin. System does not have a sandtight landward section connecting the weir portion with the shoreline (after CERC 1977)

of littoral material, Q_{net} (275,900 cu yd/yr), is not necessary. Ideally, the deposition basin should only be large enough to hold that material which flows over the weir in excess of the rate of an adequately designed bypassing system. The example sand bypassing program discussed subsequently indicates that the deposition basin in this instance ideally should be required to temporarily store only about 80,000 cu yd of material. Short-term influx rates during storms may be much higher than average values; hence additional storage capacity for unexpected events should be provided. In all cases, the deposition basin capacity should be optimized in conjunction with the bypassing system design rates.

Weir Structure

74. Factors involved in designing the weir section of a jetty include determining weir crest length, orientation, elevation, type of construction, and location of the landward end of the weir itself. The length of the weir section should be selected so that it will extend through the normal surf zone and thus intercept most of the sand in transport along the beach. Experimental studies (Seabergh 1983) indicate that much of the sand transported across a weir structure will cross near the shore face, and that the beach profile adjacent and updrift of the weir will adjust and flatten to allow significant bedload transport over the weir in the region of the beach where the weir and the waterline intersect. The location of maximum transport on the beachface will change with tidal stage. The amount of transport over the weir is sensitive to the weir elevation, tide stage, and level of wave activity. In order to intercept the transport over all ranges of conditions, the weir section should extend beyond the normal breaker location.

75. The length of existing weir jetties reflects the designer's concern about the possible "sanding-in" of the weir section should large slugs of sand move up against the weir during storms and not be effectively transported over the weir into the deposition basin. Observations of the performance of existing weir jetties (Murrells Inlet, South Carolina; Masonboro Inlet, North Carolina; Ponce de Leon Inlet, Florida; Destin East Pass, Florida; Perdido Pass, Alabama) suggest that this may not be as great a problem as first believed. Generally, the weir elevation has been set at mean tide level (mtl) in areas where the tidal range is about 2 ft to 5 ft (Atlantic coast), and at

AD-A147 549 POTENTIAL EFFECTS OF NEW ENTRANCE CHANNEL TO BOLSA CHICA BAY CALIFORNIA O..(U) COASTAL ENGINEERING RESEARCH CENTER VICKSBURG MS L Z HALES OCT 84 2/3

UNCLASSIFIED CERC-MP-84-10 F/G 13/2 NL

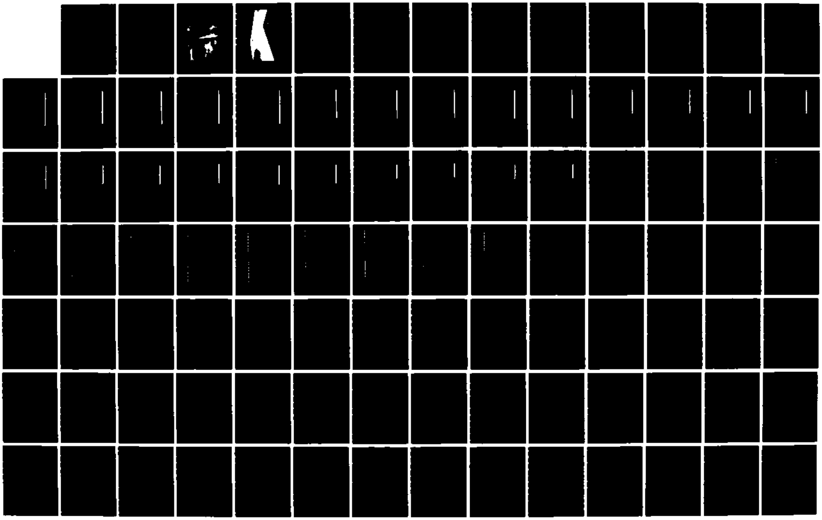

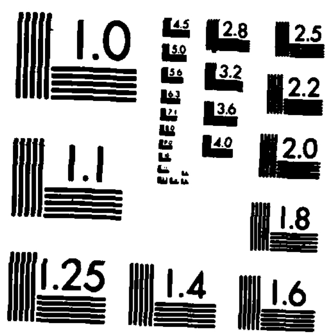
1.0
1.1
1.25
1.4
1.6
1.8
2.0
2.2
2.5
2.8
3.2
3.6
4.0

mean low water (mlw) in areas with a relatively low tidal range (Gulf of Mexico). This appears to have been a satisfactory compromise, and a weir elevation of mwl should be acceptable for the Pacific coast (extrapolating from previous experience).

76. A critical jetty design factor is to establish the location of the landward end of the weir section. The section of jetty connecting the weir with the shoreline should be sandtight to hold the updrift beach in a dynamically stable planform. The length of the sandtight shore section is determined from the desired updrift beach configuration and from the necessity to hold a volume of material in active storage to prevent it from passing over the weir section into the deposition basin. If the sandtight landward section is too short, erosion may occur over a significant area upcoast of the structure; if it is too long, a large volume of sand will be held in permanent storage along the updrift beach. Ideally, the amount of sand in storage along the updrift fillet should be the amount needed to replenish updrift beaches when the longshore sand transport is in the updrift direction.

77. Figure 52 is a 1981 photograph of a weir jetty system located at Murrells Inlet, South Carolina. In this region, it was concluded that the dominant direction of littoral drift was to the south. Since there was believed to be only a limited amount of material moving to the north, the weir section was positioned so that the weir extended all the way to the shoreline; and this configuration appears to be working successfully to this time at this location. WES has performed comprehensive experimental studies of weir jetty systems (Seabergh 1983), and the model configuration of Figure 53 indicated that for large reversals in transport direction a finite sandtight landward section should exist near the desired resultant shoreline.

78. Portions of the material in active storage may accumulate upcoast of the weir section during downcoast movement and then be displaced back upcoast during periods of drift reversal. Hence it appears the landward end of the weir section should start at least 100 to 150 ft seaward of the existing mwl in order to provide a stable attachment at the shoreline. The resulting fillet that will form on the west side of the weir jetty will have sufficient capacity to store, on the average, the volume of material which is presently being transported westerly under existing conditions.

79. It is necessary for a finite weir section to accumulate longshore

Figure 52. 1981 photograph of weir jetty system at Murrells Inlet, South Carolina. In this region of unidirectional littoral transport, the weir section extends all the way to the shoreline

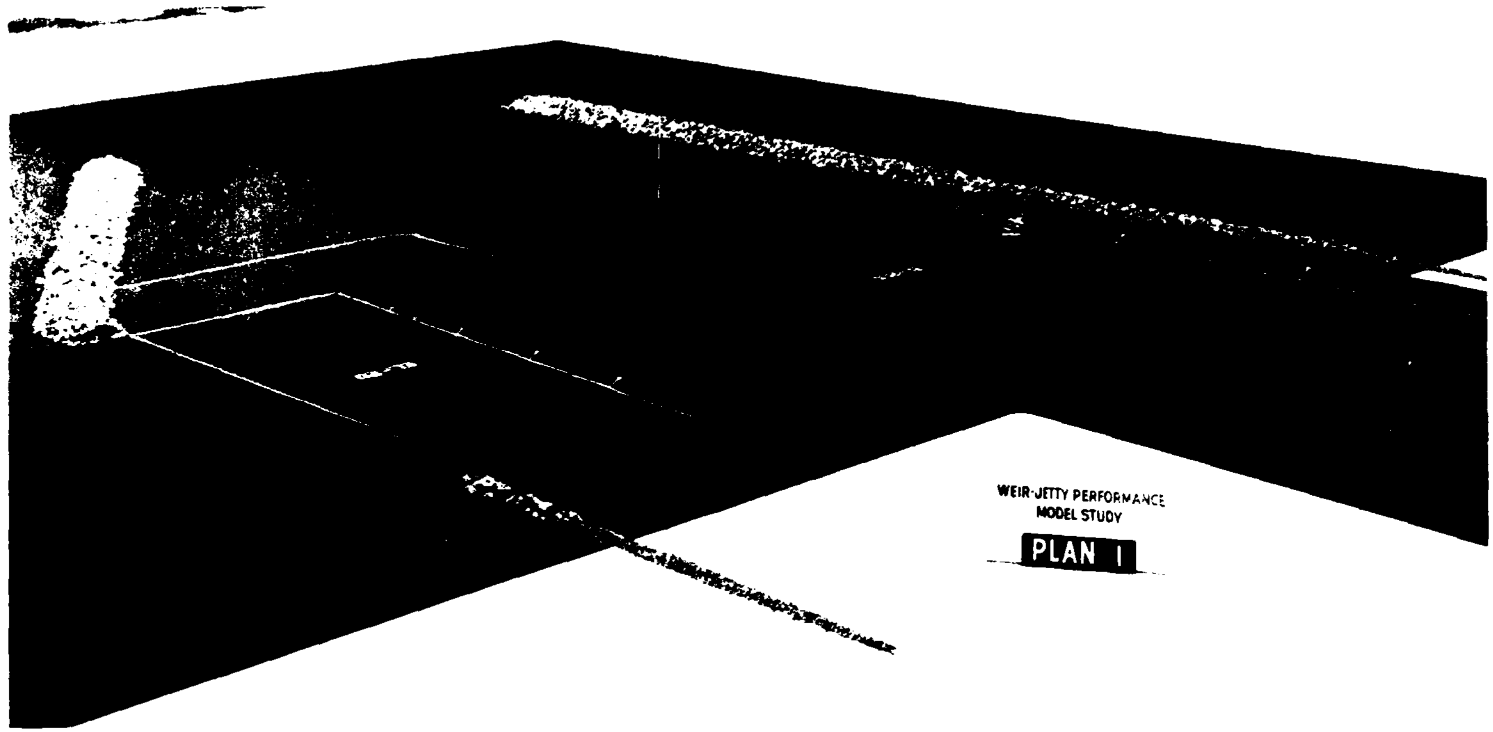

Figure 53. Experimental study of weir jetty system under investigation by WES. Sandtight structure section connects weir with existing shoreline to allow fillet to form on updrift side of jetty so a breach of landward end of jetty will be unlikely to occur (after Seabergh 1983)

material in a localized region for a weir jetty and sand bypassing concept to operate successfully at the proposed new entrance channel to Bolsa Chica Bay, California. The average annual breaking wave height for this region is approximately 2 ft; however, there are waves that break with a height approaching 15 ft. In order to intercept the material transported over this range of wave conditions, the weir crest length should be about 400 ft to cover the range of water depths where this range of wave heights breaks in the vicinity of proposed new entrance channels to Bolsa Chica Bay, California. The jetties for stabilizing the proposed navigation channels probably need not extend beyond the 20-ft water depth contour referenced to mean lower low water (mllw).

Wave Transmission by Weir Structure

80. The amount of wave activity that can be tolerated in a deposition basin is determined by the operation characteristics of the dredge performing the material removal or bypassing operation. When the bypassing system being utilized is a jet pump system, the level of wave action may not be as critical. In either case, the degree of wave action in the deposition basin, for a given weir crest elevation, can be estimated from available wave transmission formulas, following the method of Weggel (1981). Assuming no wave energy enters between the jetties, and none passes through the weir section, wave transmission is by overtopping of the weir crest only. In that case, the expression for wave transmission, H_t/H_i, over the weir crest can be applied (Goda, Takeda, and Moriya 1967; Goda 1969; Seelig 1976).

$$\frac{H_t}{H_i} = 0.5 \left\{1 - \sin\left[\frac{\pi}{2\alpha}\left(\frac{h - d_s}{H_i} + \beta\right)\right]\right\} \qquad (12)$$

where

H_t = transmitted wave height, ft

H_i = incident wave height, ft

h = height of weir structure crest above the bottom, ft

d_s = water depth at the weir structure, ft

α and β are empirical coefficients that depend on the structure's characteristics. For a thin vertical wall (sheet pile) weir section, $\alpha = 1.8$ and $\beta = 0.1$. For rubble-mound structures where transmission is by overtopping of

the weir crest only, the transmission coefficient, H_t/H_i, has been given by Seelig (1980) as:

$$\frac{H_t}{H_i} = \left(0.51 - 0.11\ \frac{B}{h}\right)\left(1 - \frac{h - d_s}{R}\right) \tag{13}$$

where B is the crest width of the structure, and R is the wave runup height above the still-water level that would occur if the structure crest were above the limit of runup. For a rubble-mound structure, the runup is given by Ahrens and McCartney (1975) as:

$$R = \left(\frac{a\varepsilon}{1 + b\varepsilon}\right) H_i \tag{14}$$

where

ε = surf parameter given by:

$$\varepsilon = \frac{\tan\ \theta}{\sqrt{H_i/L_o}} \tag{15}$$

a,b = empirical coefficients equal to 0.692 and 0.504, respectively, for a structure with two layers of rubble armor

θ = angle the seaward face of the weir section makes with the horizontal

L_o = deepwater wavelength given by $L_o = gT^2/2\pi$, with T the incident wave period and g the acceleration due to gravity

81. Wave heights in the deposition basin vary with tidal stage as the weir crest submerges and emerges from the water. Maximum wave transmission occurs at high tide; however, the maximum wave transmitted by the weir at all tide elevations is determined by the depth-limited breaker wave height controlled by the water depth at the structure location. The average beach profile in the vicinity of a potential new navigation entrance channel to Bolsa Chica Bay is given by Los Angeles District (in preparation) as Figure 54. The water depth beneath the weir crest varies with distance along the jetty, with the average depth for the weir section being 5.2 ft below mllw (8.0 ft below the weir crest which is positioned at mean sea level (msl), or 2.8 ft above mllw). The diurnal tide range of 5.4 ft is assumed to vary in a sinusoidal manner above mllw and is displayed in Figure 55.

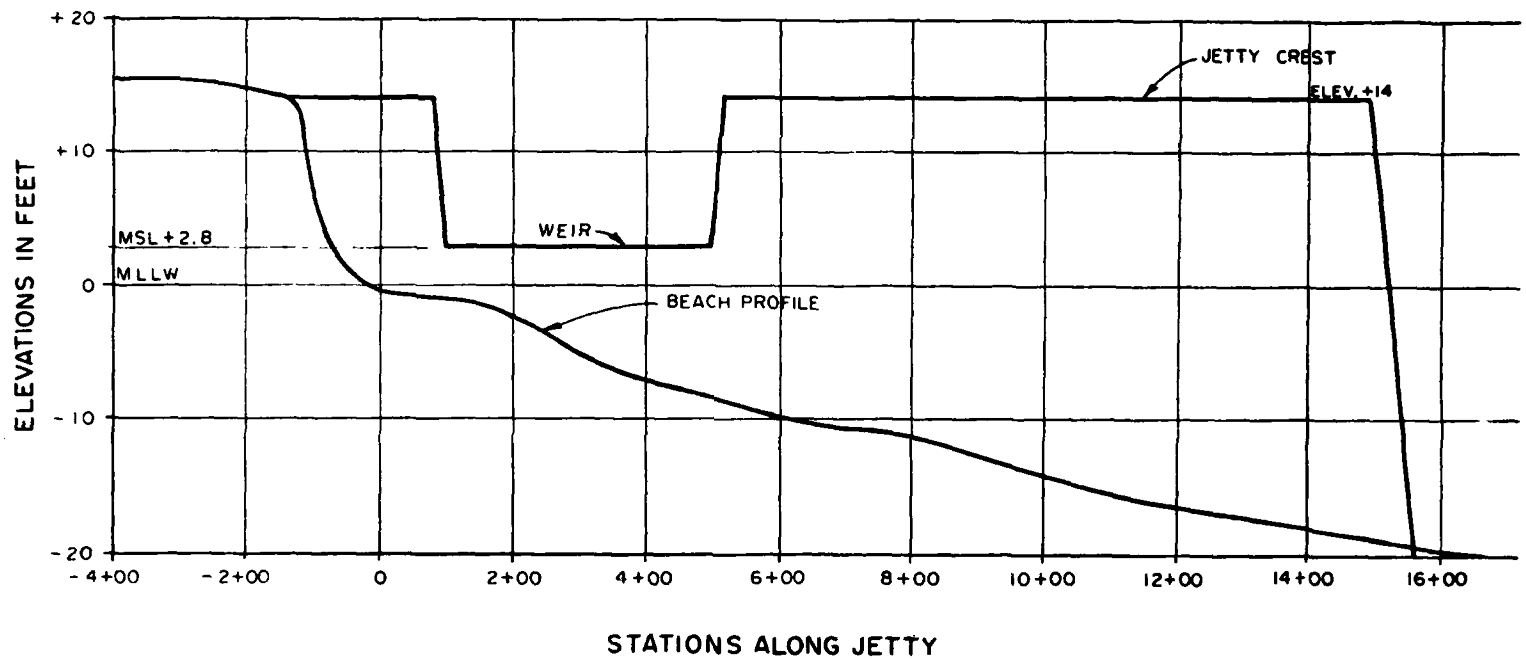

Figure 54. Average beach profile in vicinity of potential new navigation entrance channel weir jetty, *Bolsa Chica Bay*, California (after U. S. Army Engineer District, Los Angeles, in preparation)

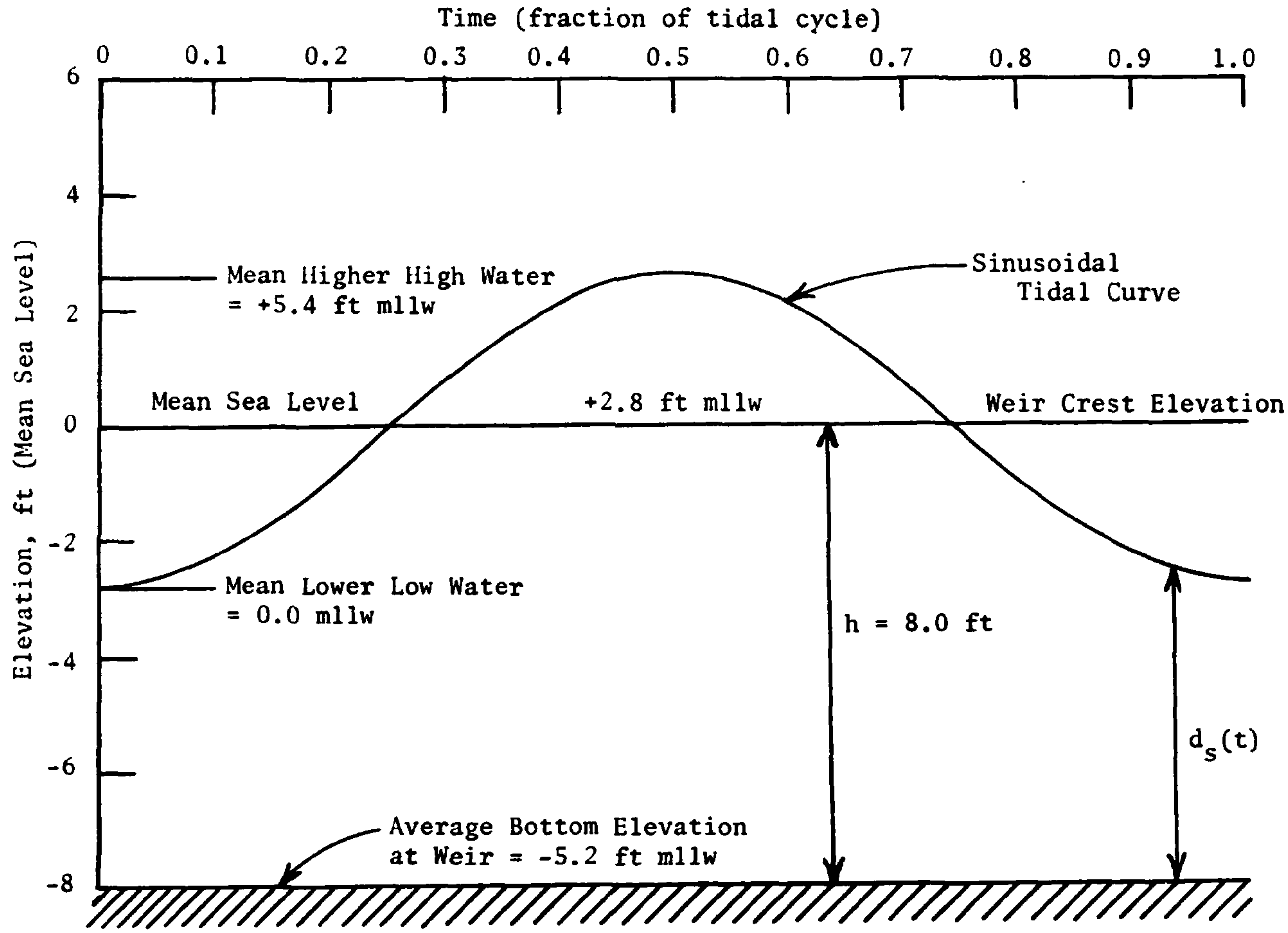

Figure 55. Average water level at weir location as a function of time

82. For a sinusoidally varying tide with an amplitude of 5.4 ft at a vertical sheet-pile weir, the solution of Equation 12 is given in Table 21 and presented graphically in Figure 56. The maximum wave transmission occurs at high tide (d_s = 10.6 ft) with the transmitted wave height, H_t, of 4.9 ft. The maximum wave height which can occur at the weir is given approximately by the condition that $(H_i)_{max} = 0.78\ d_s$. Therefore $(H_i)_{max} = 0.78(10.6)$ = 8.3 ft. The transmission coefficient, H_t/H_i, at this high tide is 0.59. Hence the maximum wave height, $(H_t)_{max}$, transmitted by the sheet-pile weir into the deposition basin region is approximately $(H_t)_{max} = 0.59(8.3)$ = 4.9 ft. Since it is assumed a priori that no other wave energy penetrates the navigation entrance channel, this maximum wave height of 4.9 ft, based on a depth-limited condition, decreases in magnitude as the wave energy disperses away from the weir.

83. If the weir section is constructed of rubble-mound material, the solution of Equation 13 is appropriate and is given in Table 22. This

Table 21

Wave Transmission by Weir Overtopping

Sheet-Pile Weir

Time (Percent of Tidal Period)	Depth Below Weir Crest d_s, ft	Breaker Wave Height H_i, ft	Transmission Coefficient H_t/H_i	Transmitted Wave Height H_t, ft
0	5.2	4.0	0.18	0.7
5	5.3	4.1	0.19	0.8
10	5.7	4.4	0.24	1.1
15	6.3	4.9	0.31	1.5
20	7.1	5.5	0.38	2.1
25	7.9	6.2	0.45	2.8
30	8.7	6.8	0.50	3.4
35	9.5	7.4	0.54	4.0
40	10.1	7.9	0.57	4.5
45	10.5	8.2	0.58	4.8
50*	10.6	8.3	0.59	4.9

* Because of symmetry of tidal curve, solution is symmetric about time = 50 percent.

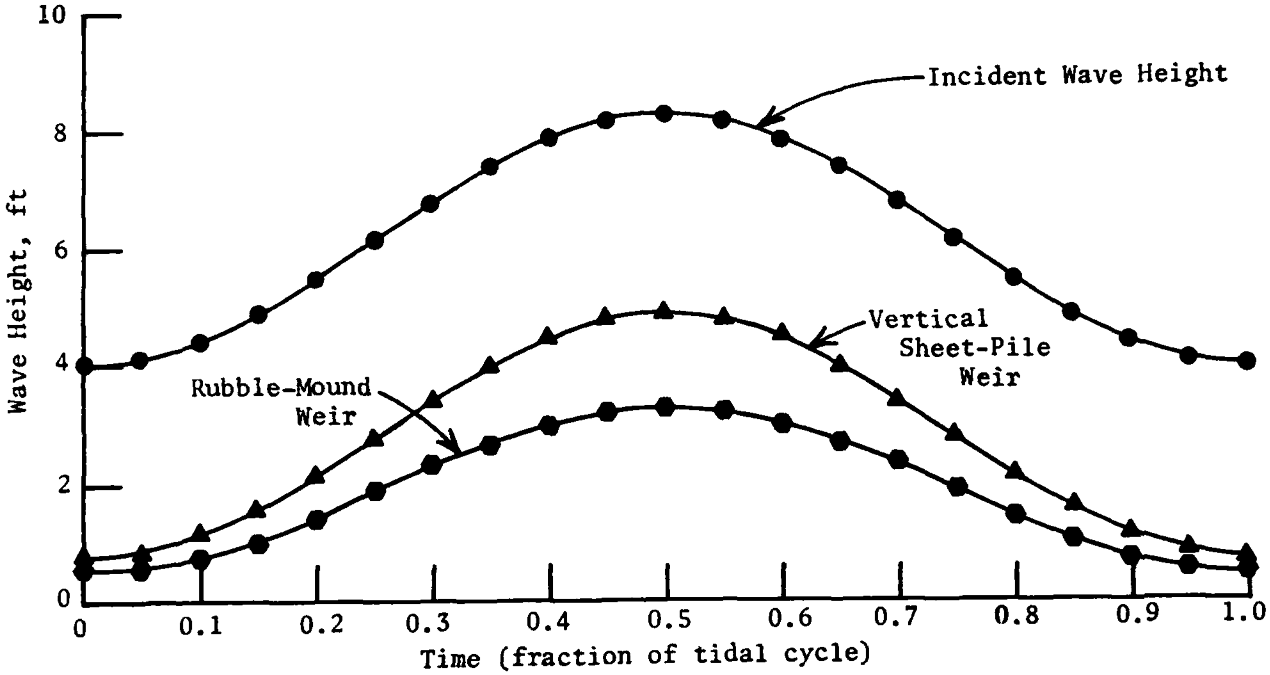

Figure 56. Time variation of maximum wave conditions transmitted by vertical sheet-pile and rubble-mound weirs into the deposition basin, relative to the incident depth-limited wave height

Table 22

Wave Transmission by Weir Overtopping

Rubble-Mound Weir

Time (Percent of Tidal Period)	Surf Parameter ε	Wave Runup ft	Transmission Coefficient H_t/H_i	Transmitted Wave Height H_t , ft
0	10.18	4.60	0.12	0.5
5	10.06	4.70	0.13	0.5
10	9.71	5.02	0.16	0.7
15	9.20	5.53	0.21	1.0
20	8.68	6.15	0.26	1.4
25	8.18	6.85	0.30	1.9
30	7.81	7.45	0.33	2.3
35	7.49	8.03	0.36	2.7
40	7.25	8.52	0.38	3.0
45	7.11	8.80	0.39	3.2
50*	7.07	8.90	0.39	3.3

* Because of symmetry of tidal curve, solution is symmetric about time = 50 percent.

solution is also presented graphically in Figure 56. Here the maximum transmission coefficient, H_t/H_i , produces a maximum transmitted wave height into the deposition basin of $(H_t)_{max}$ = 3.3 ft.

PART VII: ESTIMATED EFFECT OF PROPOSED BOLSA CHICA BAY NAVIGATION ENTRANCE CHANNEL JETTIES ON UNSTABILIZED ADJACENT SHORELINES

84. When channel stabilization jetties are constructed in the sandy nearshore zone, they will alter the natural movements of beach sediments. Such modifications upset the natural equilibrium, and the shoreline undergoes changes in response. These changes are most severe when there is a net drift of sand along the beach under a predominant wave direction. Sand will accumulate on the upcoast side and erosion will occur on the downdrift side. The section of southern California coastline under investigation (Bolsa Chica Bay region) experiences a twice annual reversal, on the average, in net longshore transport direction (Figure 12). Strong southerly transport occurs during the months of January, February, March, and April. Anticipated accretion should occur on the west side of the proposed west jetties at the navigation entrance channels of Site A or Site B. Erosion is expected to occur on the east side of the east jetties unless there is sand bypassing to the eastern side or material input from an external source. During the remainder of the year, mild westerly transport reverses the process, and the east side of the east jetty temporarily becomes the accretion side. Accordingly, the west side of the west jetty then should experience some degree of depletion as material previously accumulated in the fillet will drift upcoast toward the eroding feeder beach at Surfside-Sunset Beach.

Effect on Shoreline West of Proposed Navigation Entrance Channels

85. The two critical times of the year in the Bolsa Chica Bay region are toward the end of May (following a large volume of southerly transport movement) and toward the end of December (at the end of the northerly transport season). At these times, the shoreline will have advanced or retreated to its farthest position during the year's oscillations. The length of the sandtight landward section of the proposed navigation channel west jetty between the preconstruction existing shoreline and the weir determines the extent of fillet formation that will evolve and ultimately the volume of material that will be available for transport back upcoast toward the erosional beach

area. In the early years following construction, the updrift movement of material under average-to-extreme wave conditions may be sufficient to breach the land end of the west jetty. To investigate these phenomena, five different lengths of sandtight landward section (50, 100, 150, 200, and 250 ft) were analyzed. These data from the computer simulation model indicate the rate and extent of the fillet formation on the updrift side of the various potential structures and are displayed in Figures 57-80. Here the data are addressing the formation and growth of the fillet proper, and the dotted portions of the computer-generated lines indicate that region away from the fillet proper which will experience oscillations due to the temporal accretion along the shoreline (even under existing conditions) and is therefore not a part of the fillet per se. All material accumulating in the temporal accretion and fillet are considered as being retained by the west jetty. Similarly, all material that moves westerly into the Surfside-Sunset Beach erosional area (from either the temporal accretion or the fillet) is considered as coming from the accumulation updrift of the west jetty. These quantities have been presented previously in PART V of this report.

86. The computer simulation model computations were commenced at the beginning of January, assuming the jetties were installed immediately prior to that time. Hence the west jetty will initially experience a period of fillet accretion. In the early years following construction, the upcoast drift of material movement under average-to-extreme wave conditions may be sufficient to breach the land end of the west jetty. While all sections (50, 100, 150, 200, and 250 ft) of sandtight landward portions evaluated approached an upper filling limit, the shorter section (50-ft sandtight landward section) suffered a breaching of the existing shoreline and would not provide enough return flow of littoral material to the eroding coast to replicate the existing conditions at the end of the year. The 100-ft sandtight landward section structure reproduces the existing condition after being in operation for approximately 4 years, whereas the 150-ft section and larger structures permit an adequate amount of material during all years, whether the proposed new navigation entrance channel is located at Site A or Site B. The effect of positioning the proposed new entrance channel at Site A is not significantly different from positioning the channel at Site B, with regard to fillet formation. From these considerations, it appears the sandtight landward section existing between the present shoreline and the weir section should be at least 150 ft long.

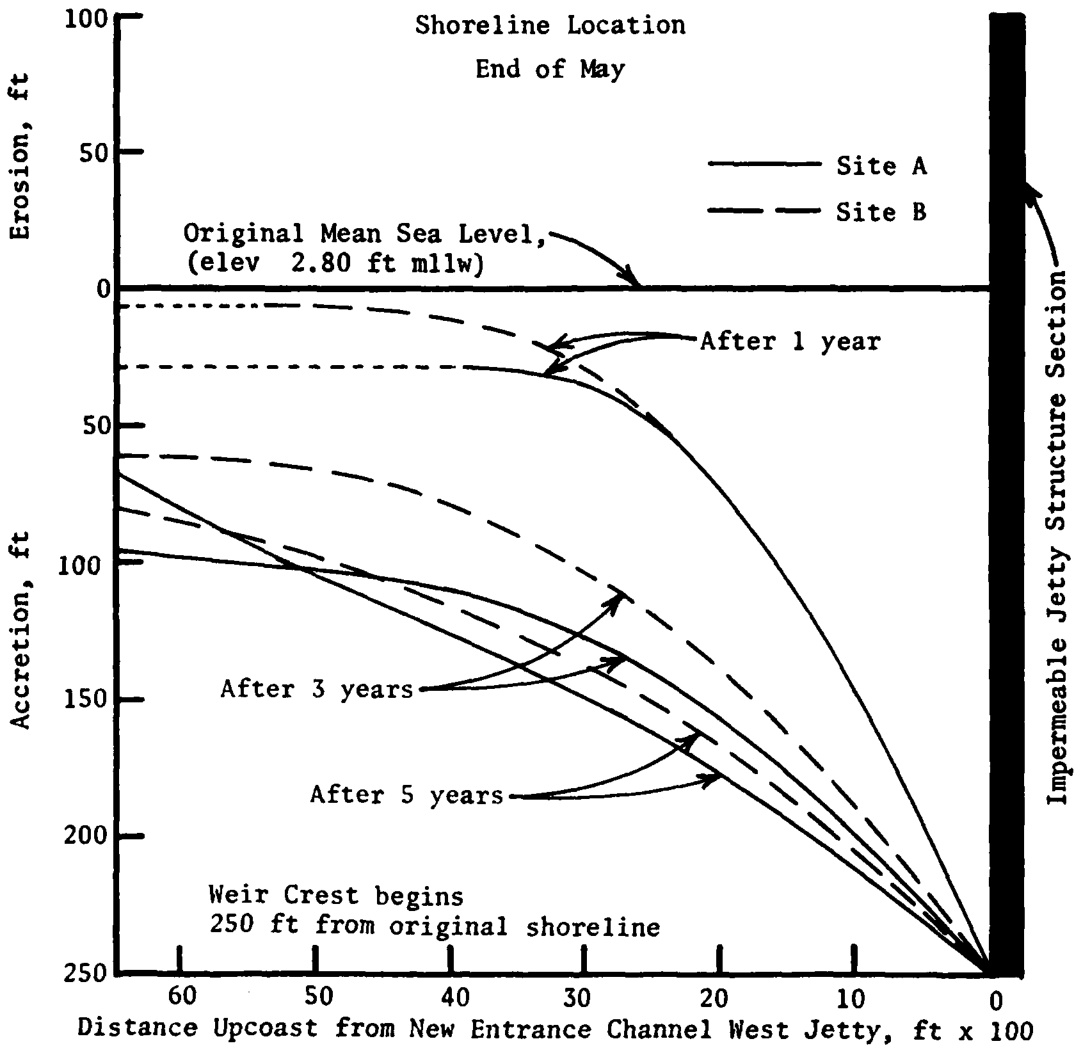

Figure 57. Computer simulation model indication of fillet formation on updrift side of west jetty at proposed new navigation entrance channel locations to Bolsa Chica Bay, California, at the end of May after 1, 3, and 5 years of operation with a 250-ft sandtight landward section

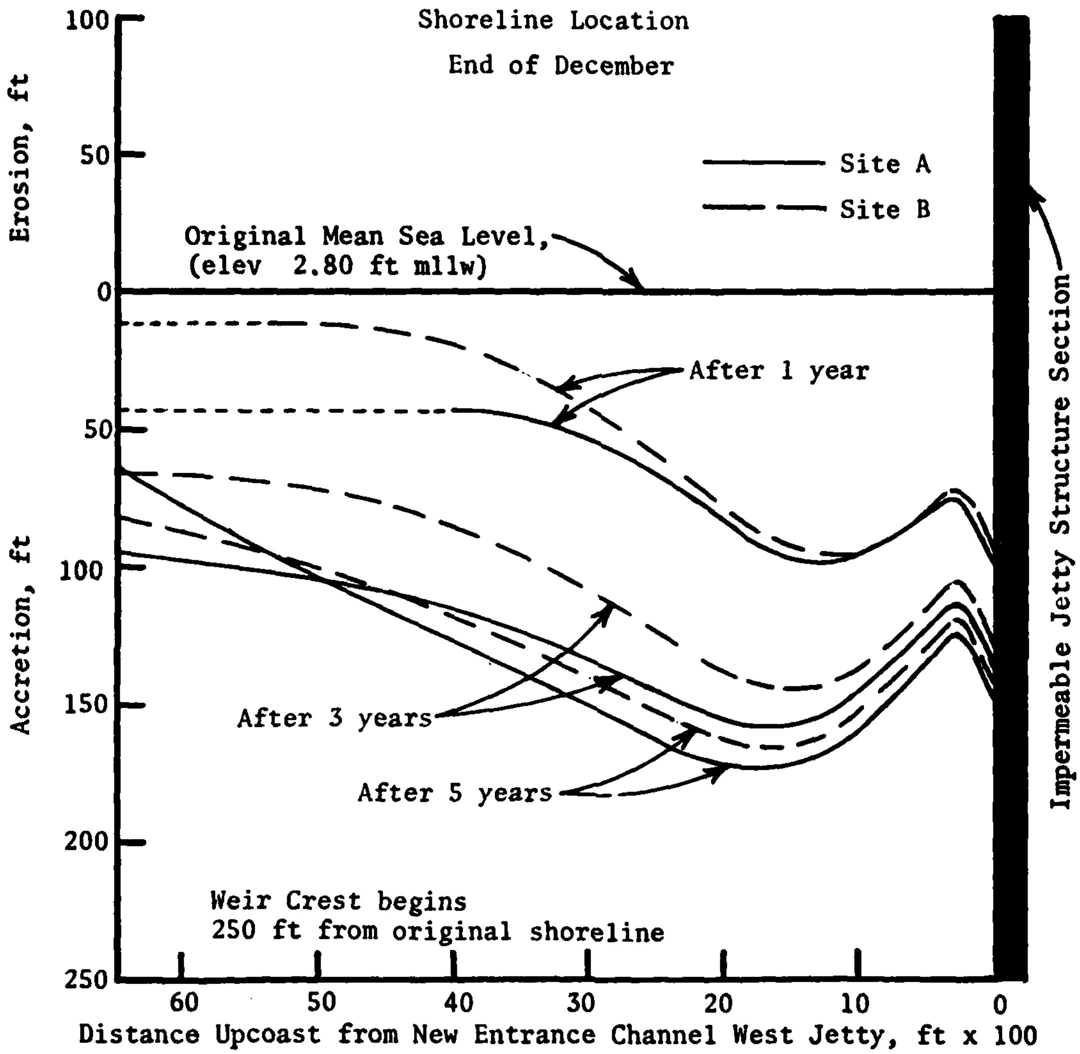

Figure 58. Computer simulation model indication of fillet formation on updrift side of west jetty at proposed new navigation entrance channel locations to Bolsa Chica Bay, California, at the end of December after 1, 3, and 5 years of operation with a 250-ft sandtight landward section

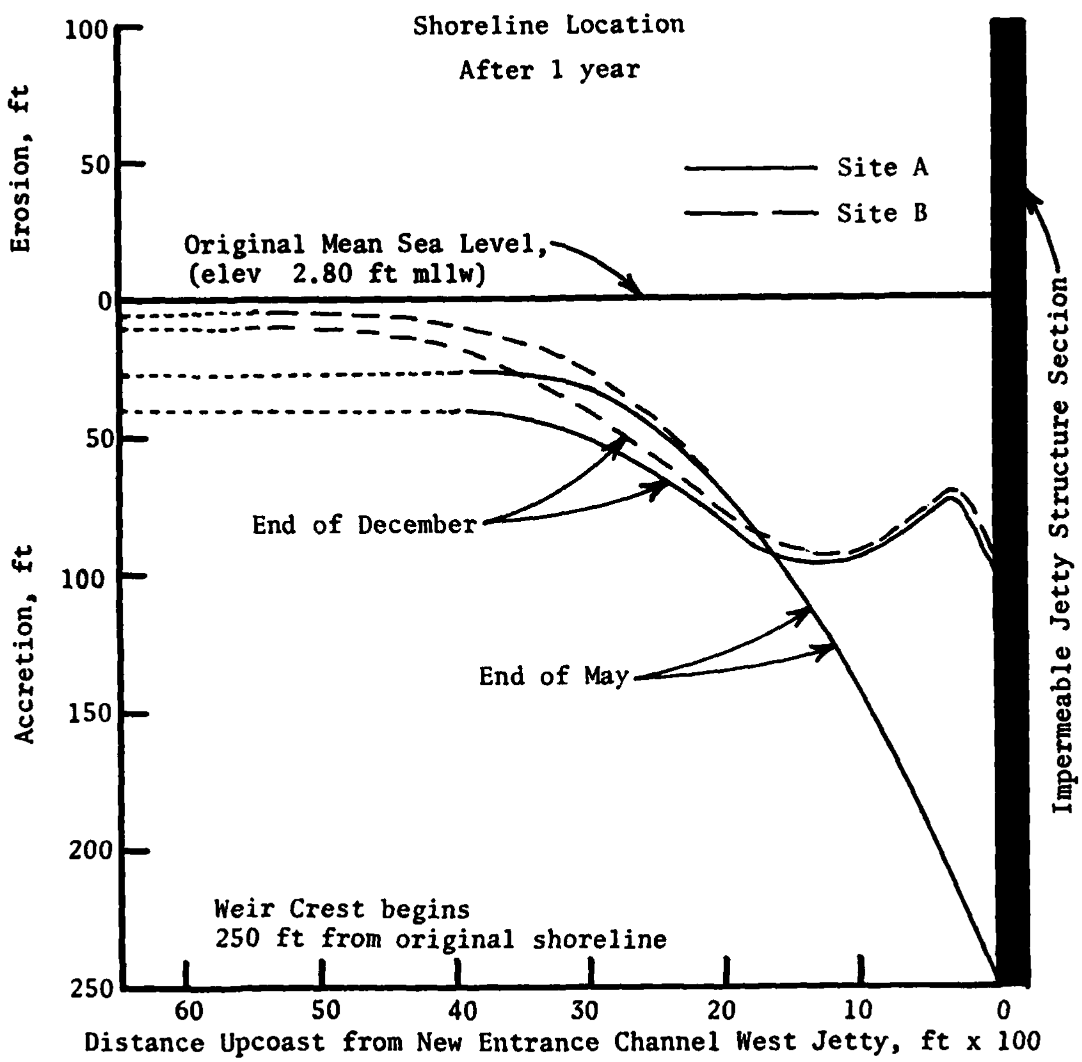

Figure 59. Computer simulation model indication of fillet formation on updrift side of west jetty at proposed new navigation entrance channel locations to Bolsa Chica Bay, California, at the end of May and December after 1 year of operation with a 250-ft sandtight landward section

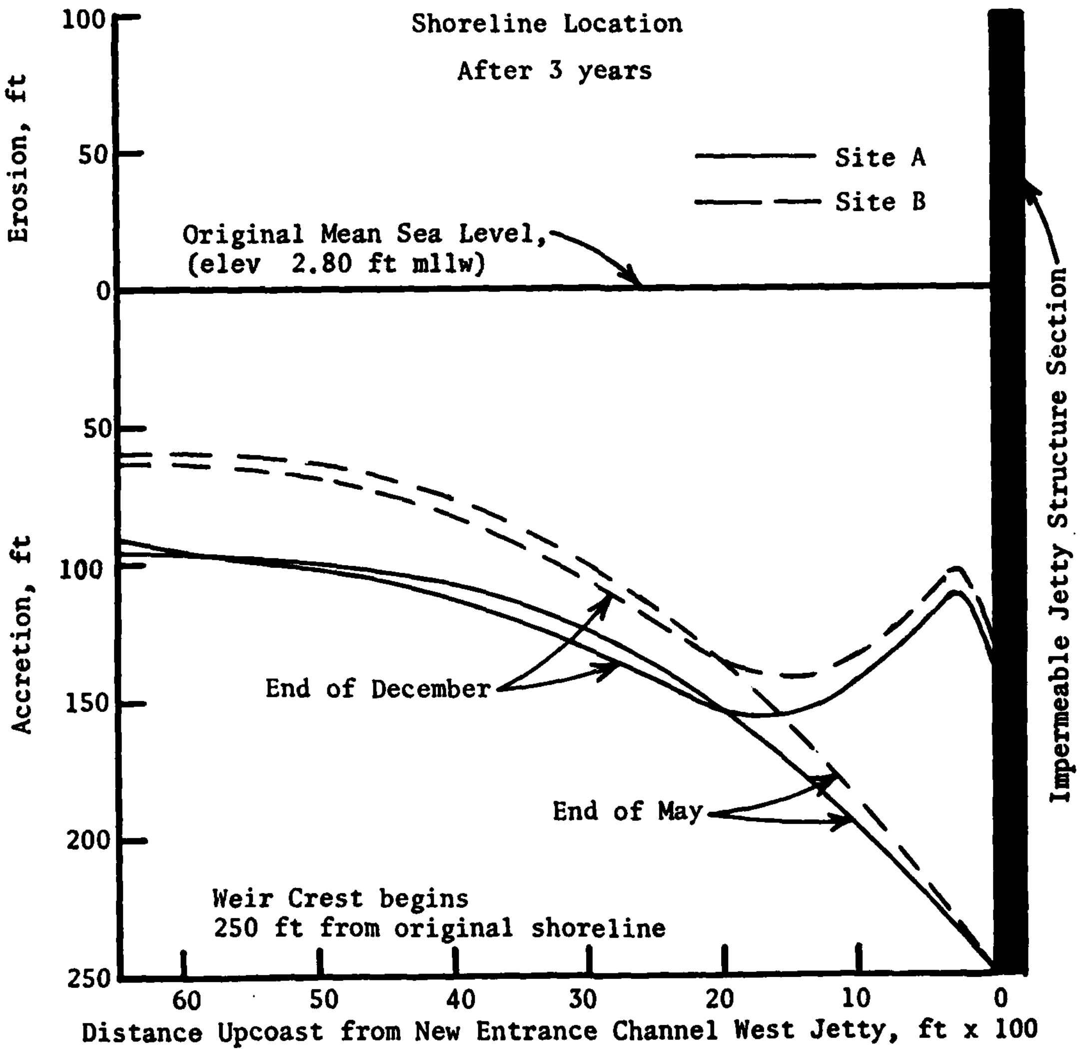

Figure 60. Computer simulation model indication of fillet formation on updrift side of west jetty at proposed new navigation entrance channel locations to Bolsa Chica Bay, California, at the end of May and December after 3 years of operation with a 250-ft sandtight landward section

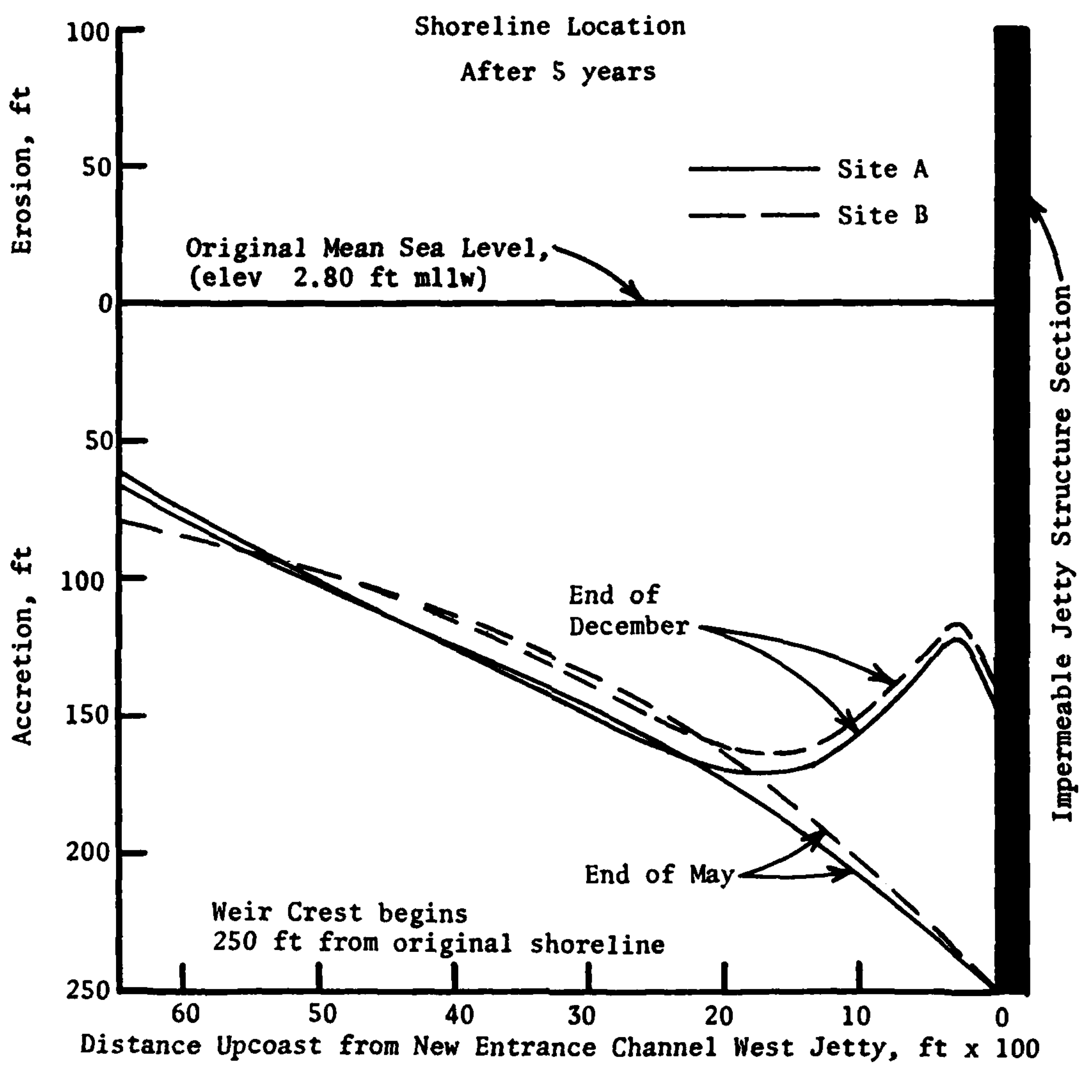

Figure 61. Computer simulation model indication of fillet formation on updrift side of west jetty at proposed new navigation entrance channel locations to Bolsa Chica Bay, California, at the end of May and December after 5 years of operation with a 250-ft sandtight landward section

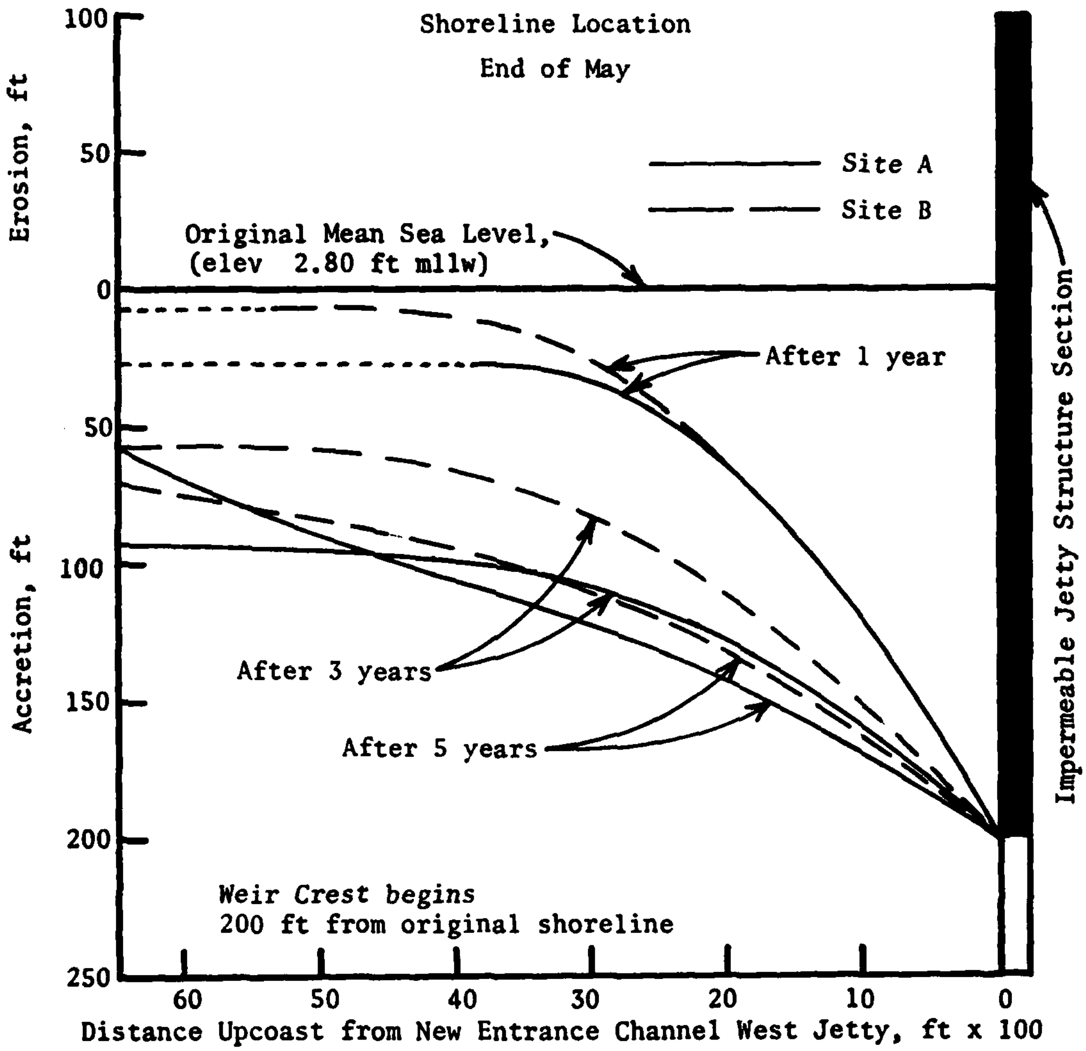

Figure 62. Computer simulation model indication of fillet formation on updrift side of west jetty at proposed new navigation entrance channel locations to Bolsa Chica Bay, California, at the end of May after 1, 3, and 5 years of operation with a 200-ft sandtight landward section

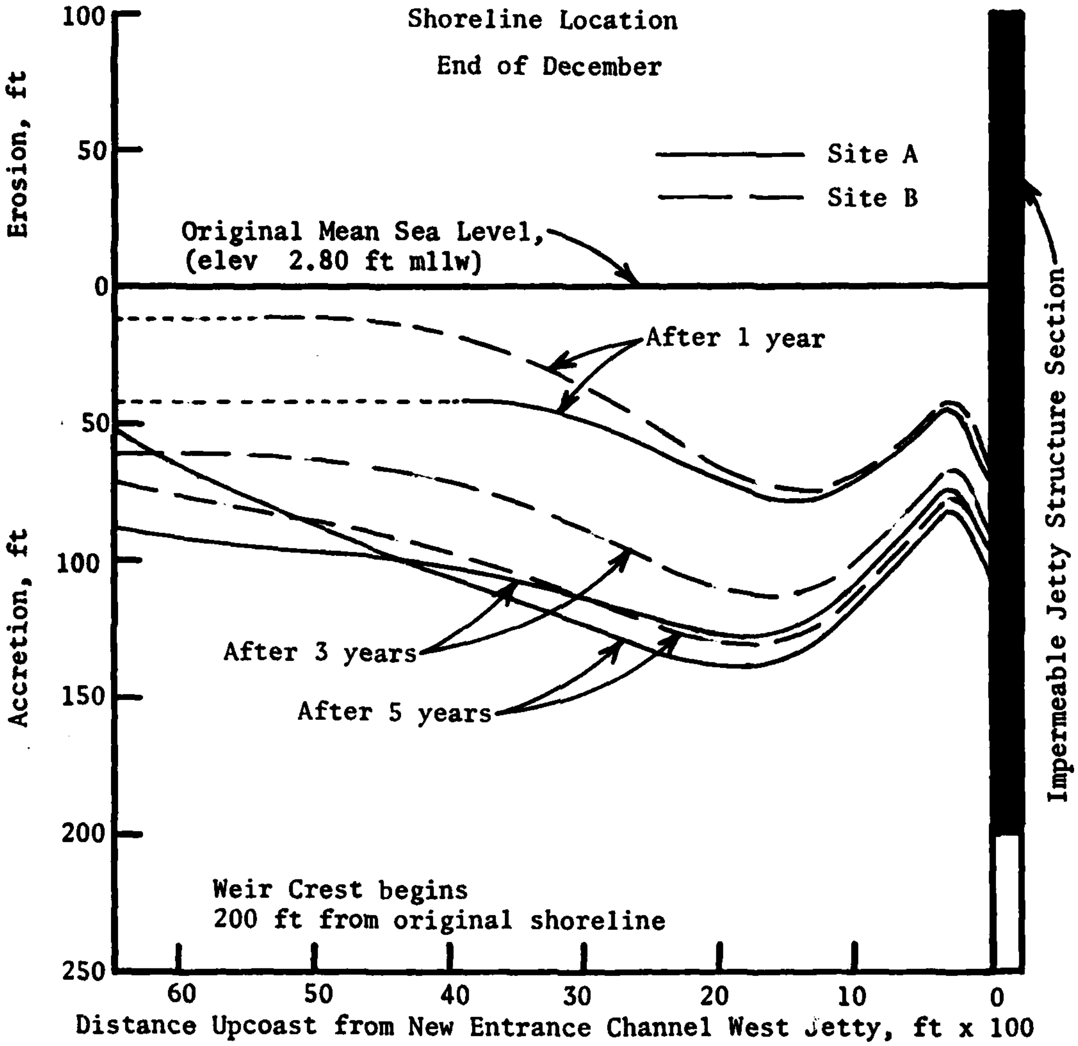

Figure 63. Computer simulation model indication of fillet formation on updrift side of west jetty at proposed new navigation entrance channel locations to Bolsa Chica Bay, California, at the end of December after 1, 3, and 5 years of operation with a 200-ft sandtight landward section

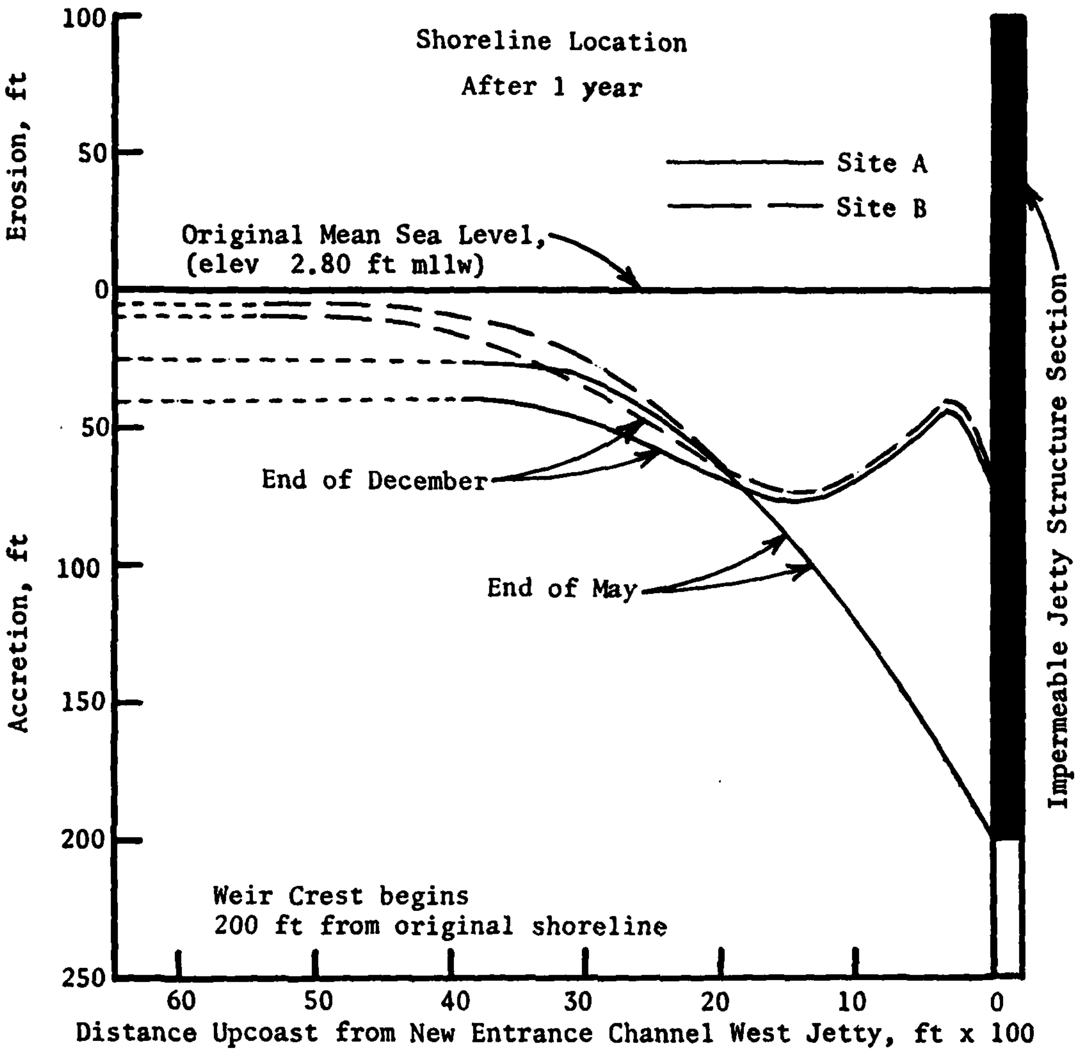

Figure 64. Computer simulation model indication of fillet formation on updrift side of west jetty at proposed new navigation entrance channel locations to Bolsa Chica Bay, California, at the end of May and December after 1 year of operation with a 200-ft sandtight landward section

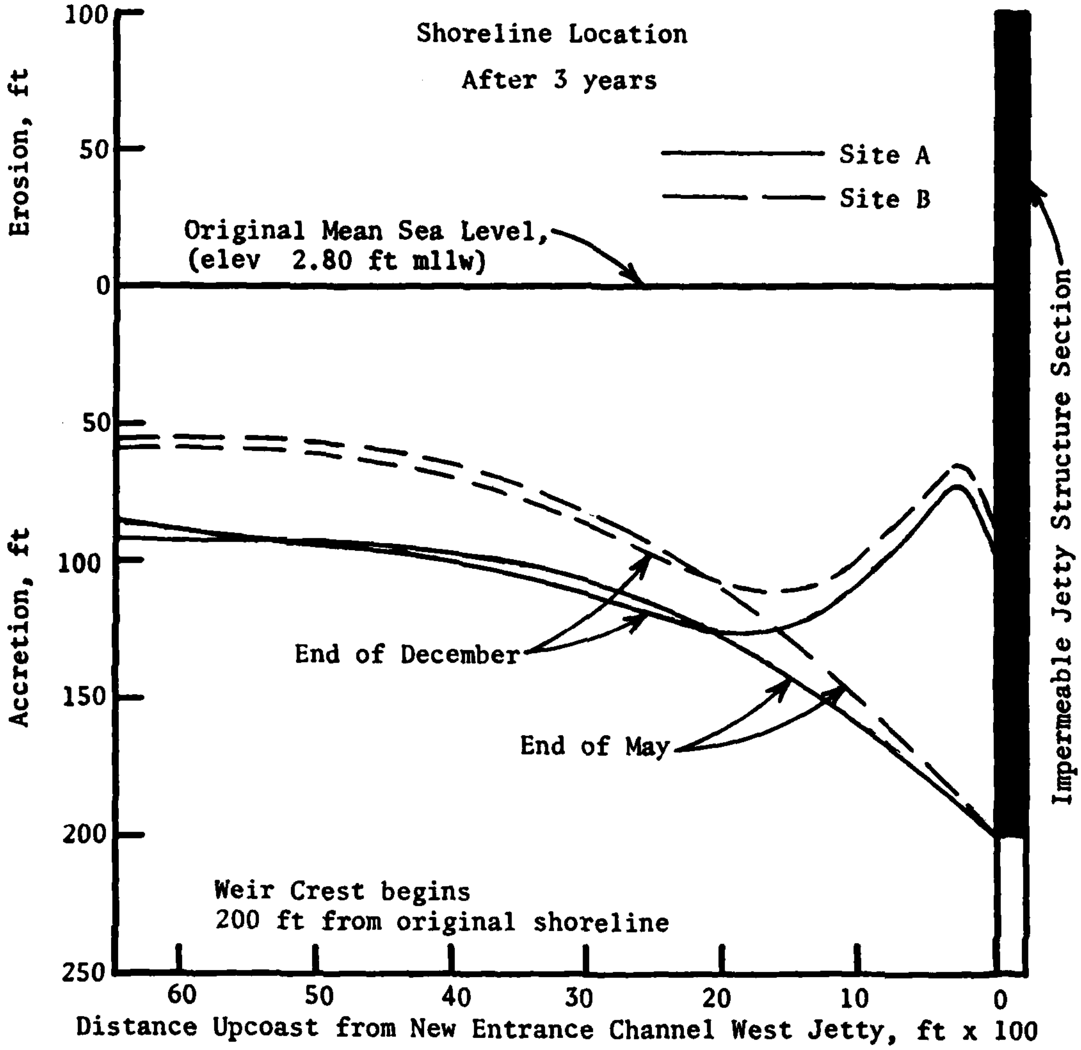

Figure 65. Computer simulation model indication of fillet formation on updrift side of west jetty at proposed new navigation entrance channel locations to Bolsa Chica Bay, California, at the end of May and December after 3 years of operation with a 200-ft sandtight landward section

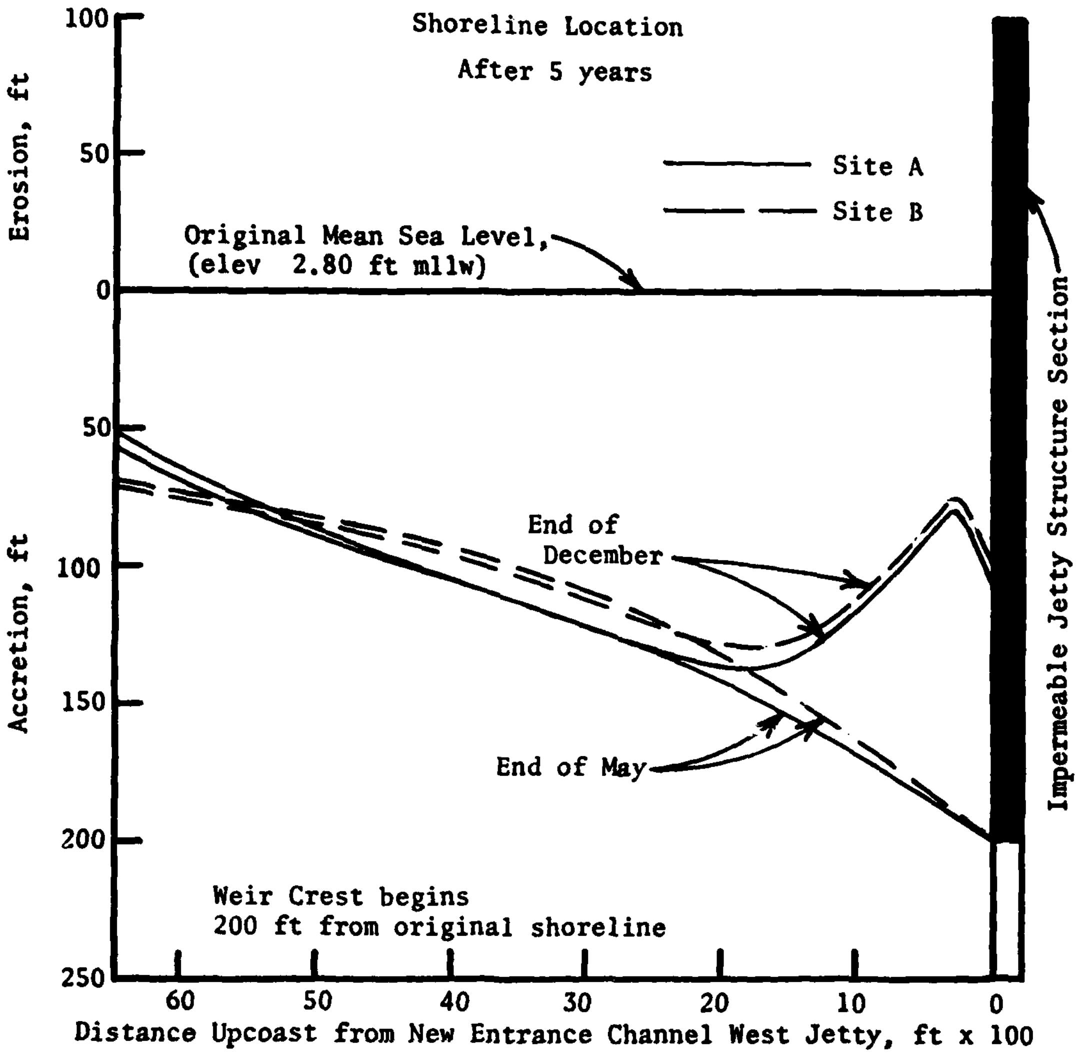

Figure 66. Computer simulation model indication of fillet formation on updrift side of west jetty at proposed new navigation entrance channel locations to Bolsa Chica Bay, California, at the end of May and December after 5 years of operation with a 200-ft sandtight landward section

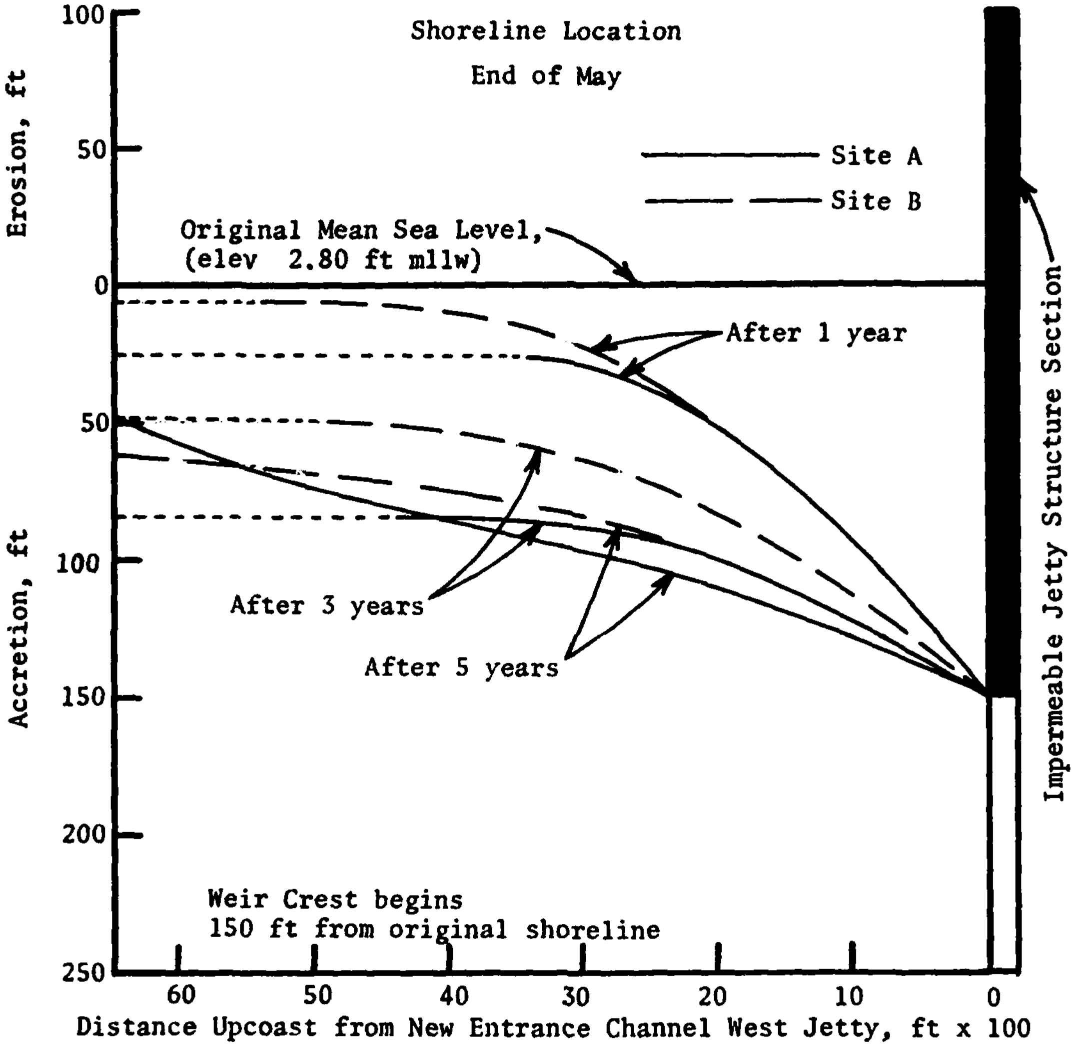

Figure 67. Computer simulation model indication of fillet formation on updrift side of west jetty at proposed new navigation entrance channel locations to Bolsa Chica Bay, California, at the end of May after 1, 3, and 5 years of operation with a 150-ft sandtight landward section

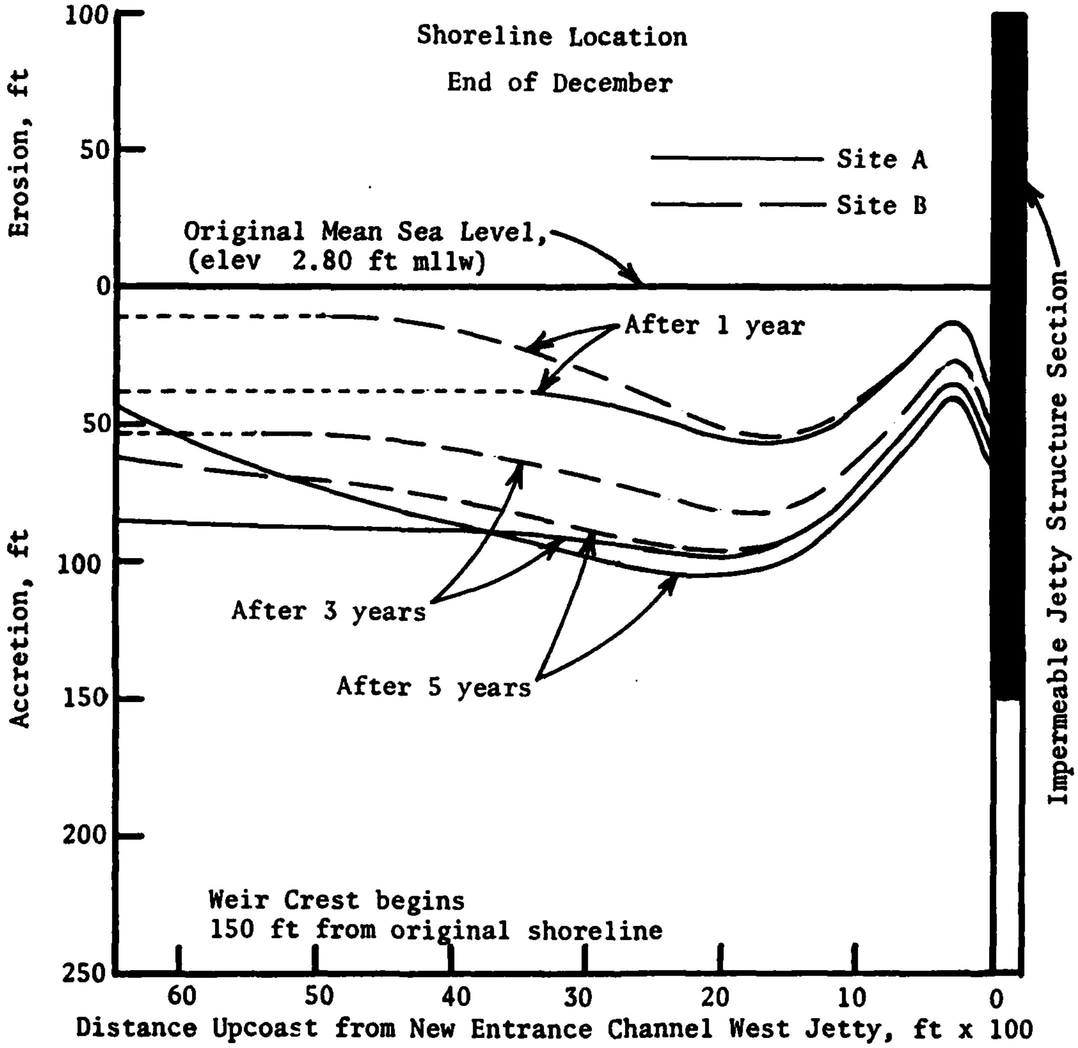

Figure 68. Computer simulation model indication of fillet formation on updrift side of west jetty at proposed new navigation entrance channel locations to Bolsa Chica Bay, California, at the end of December after 1, 3, and 5 years of operation with a 150-ft sandtight landward section

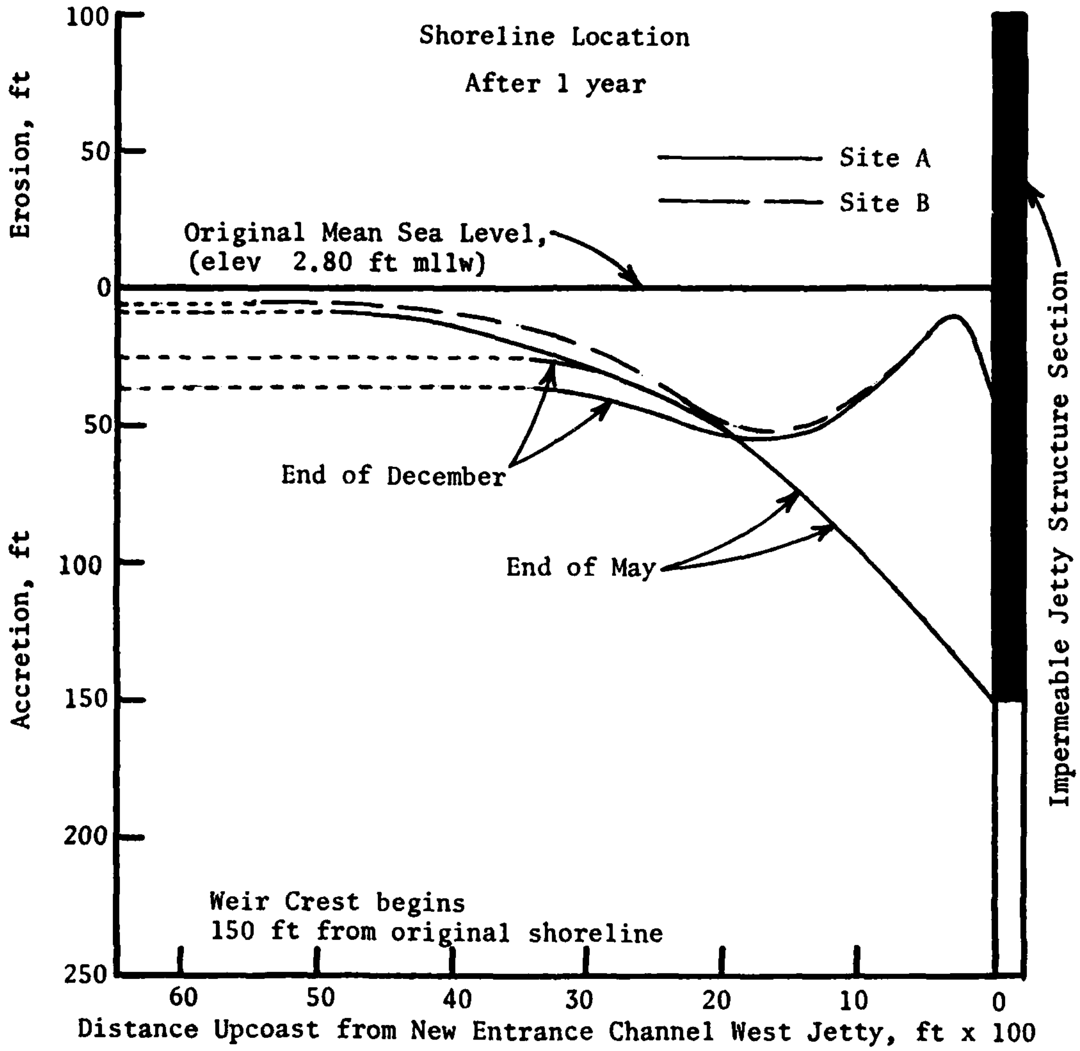

Figure 69. Computer simulation model indication of fillet formation on updrift side of west jetty at proposed new navigation entrance channel locations to Bolsa Chica Bay, California, at the end of May and December after 1 year of operation with a 150-ft sandtight landward section

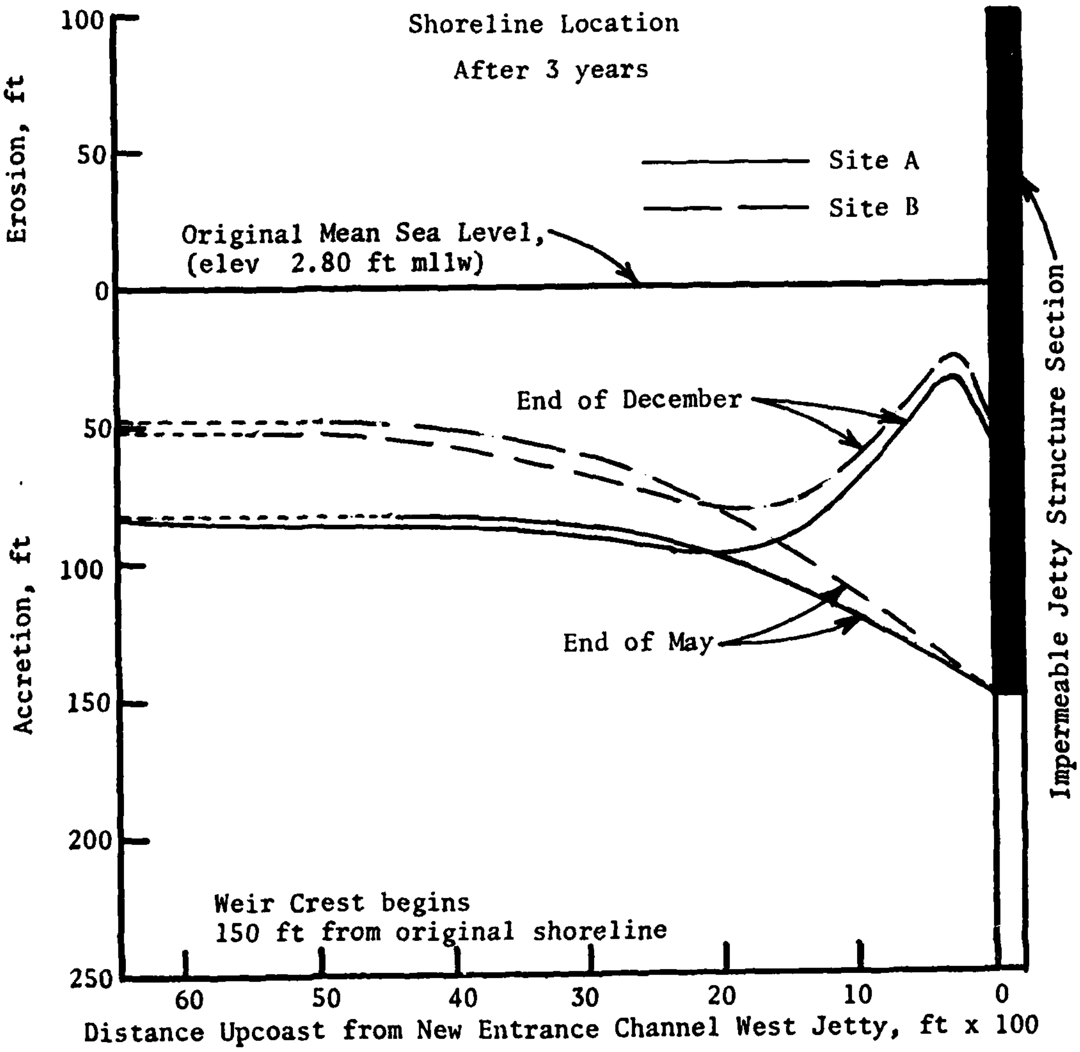

Figure 70. Computer simulation model indication of fillet formation on updrift side of west jetty at proposed new navigation entrance channel locations to Bolsa Chica Bay, California, at the end of May and December after 3 years of operation with a 150-ft sandtight landward section

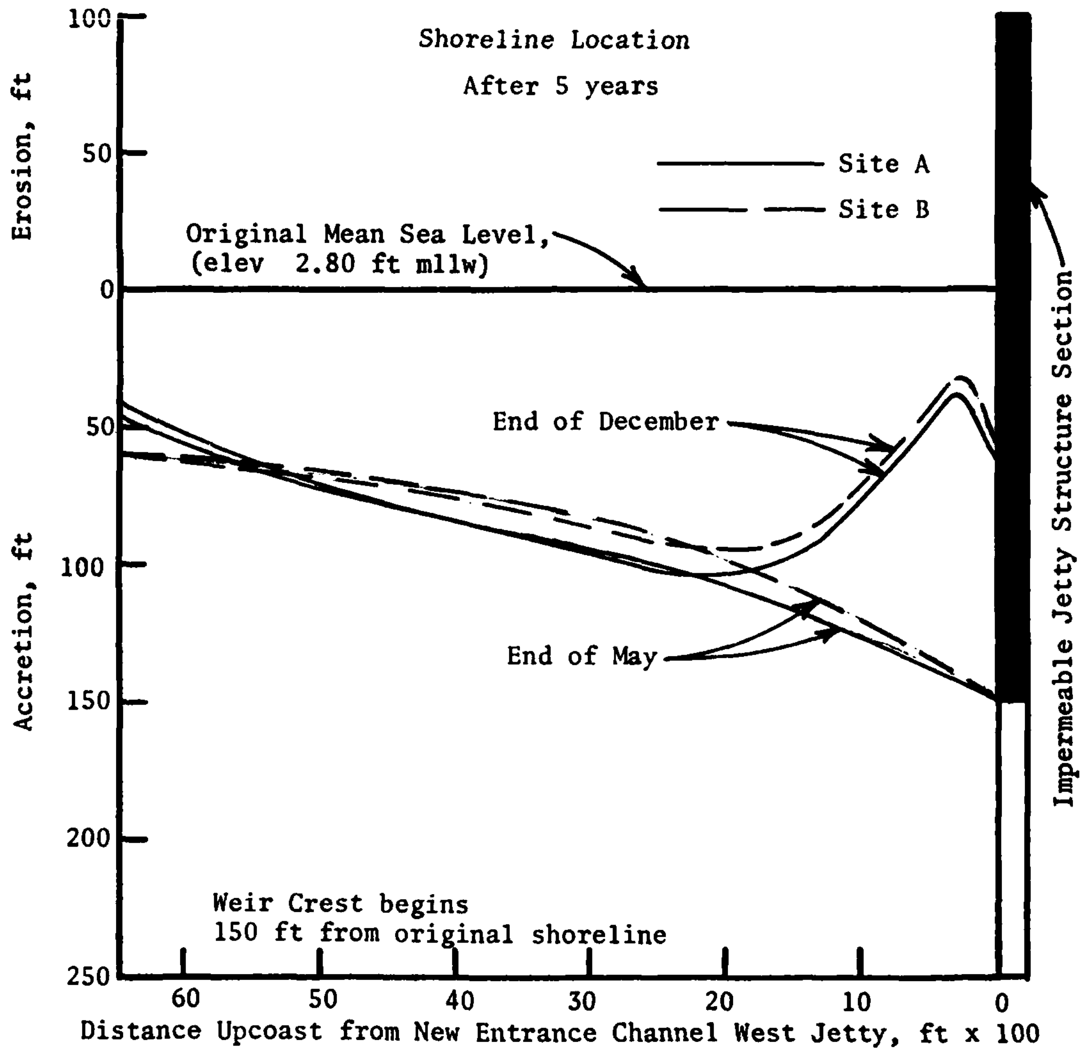

Figure 71. Computer simulation model indication of fillet formation on updrift side of west jetty at proposed new navigation entrance channel locations to Bolsa Chica Bay, California, at the end of May and December after 5 years of operation with a 150-ft sandtight landward section

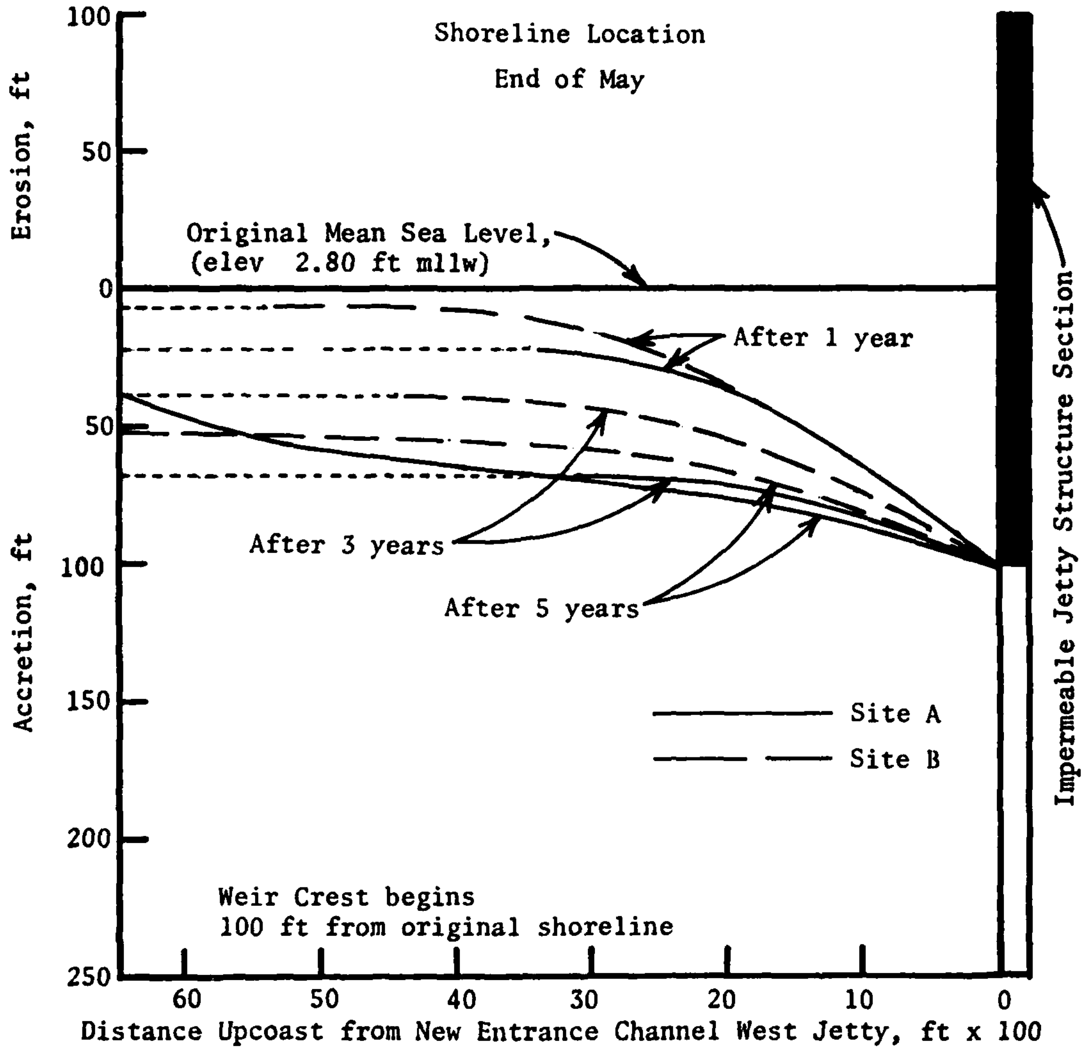

Figure 72. Computer simulation model indication of fillet formation on updrift side of west jetty at proposed new navigation entrance channel locations to Bolsa Chica Bay, California, at the end of May after 1, 3, and 5 years of operation with a 100-ft sandtight landward section

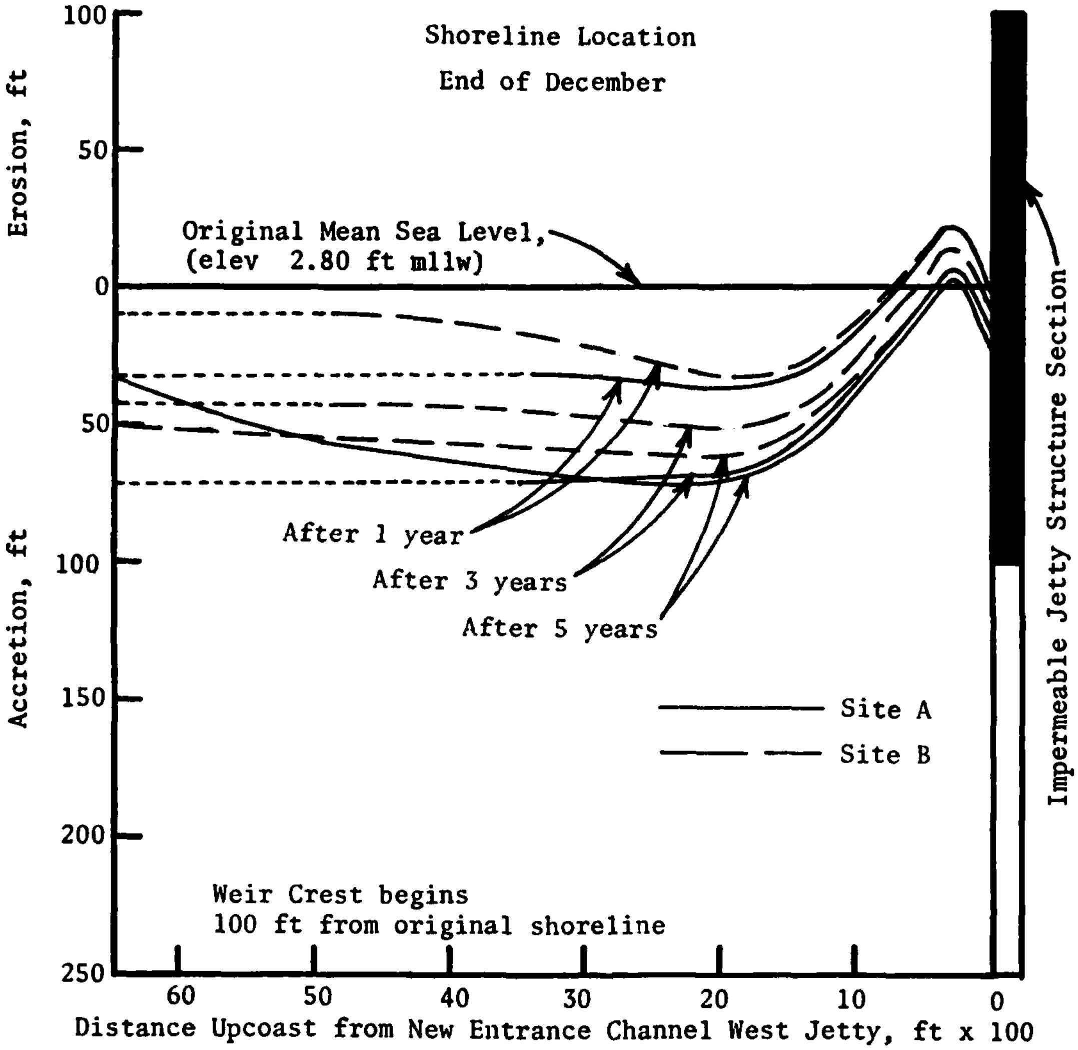

Figure 73. Computer simulation model indication of fillet formation on updrift side of west jetty at proposed new navigation entrance channel locations to Bolsa Chica Bay, California, at the end of December after 1, 3, and 5 years of operation with a 100-ft sandtight landward section

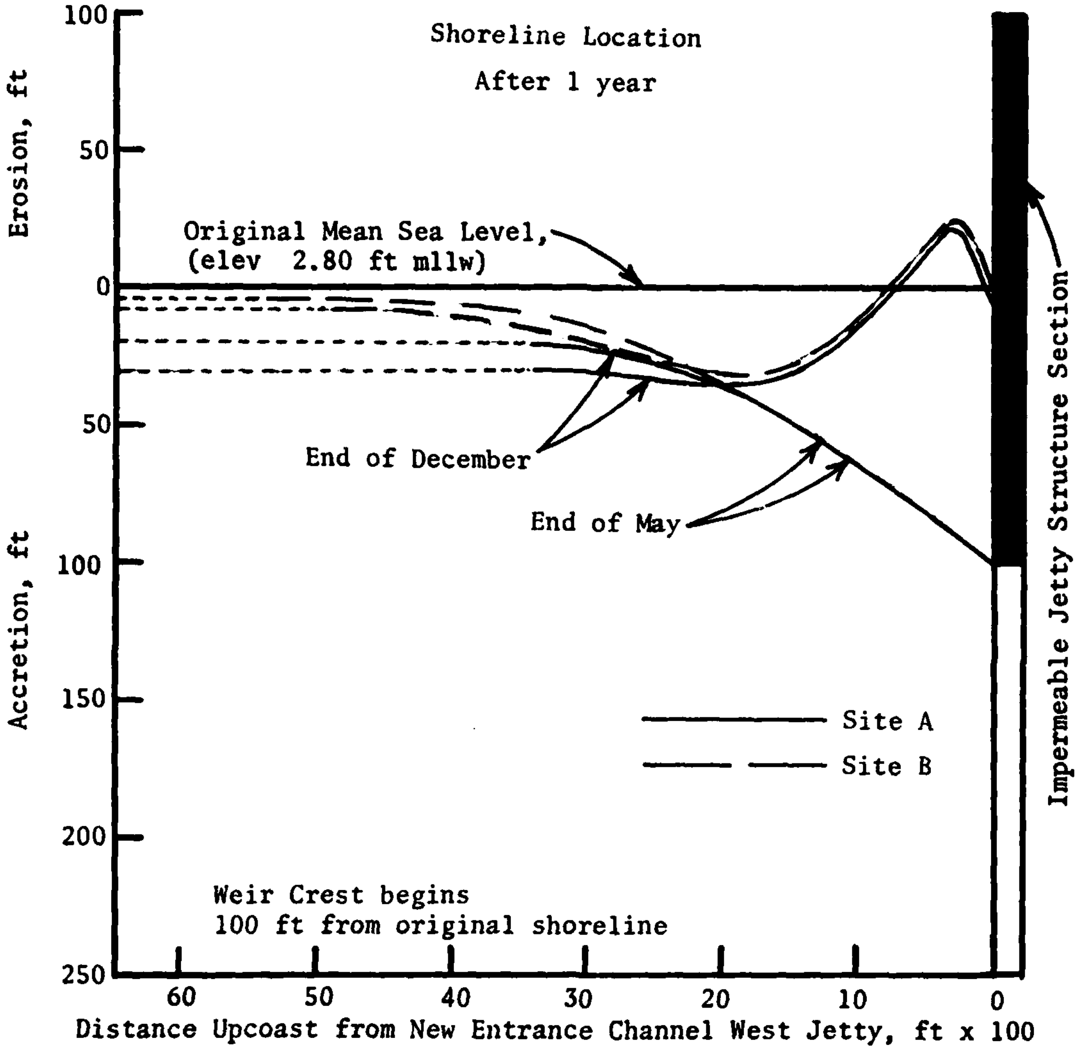

Figure 74. Computer simulation model indication of fillet formation on updrift side of west jetty at proposed new navigation entrance channel locations to Bolsa Chica Bay, California, at the end of May and December after 1 year of operation with a 100-ft sandtight landward section

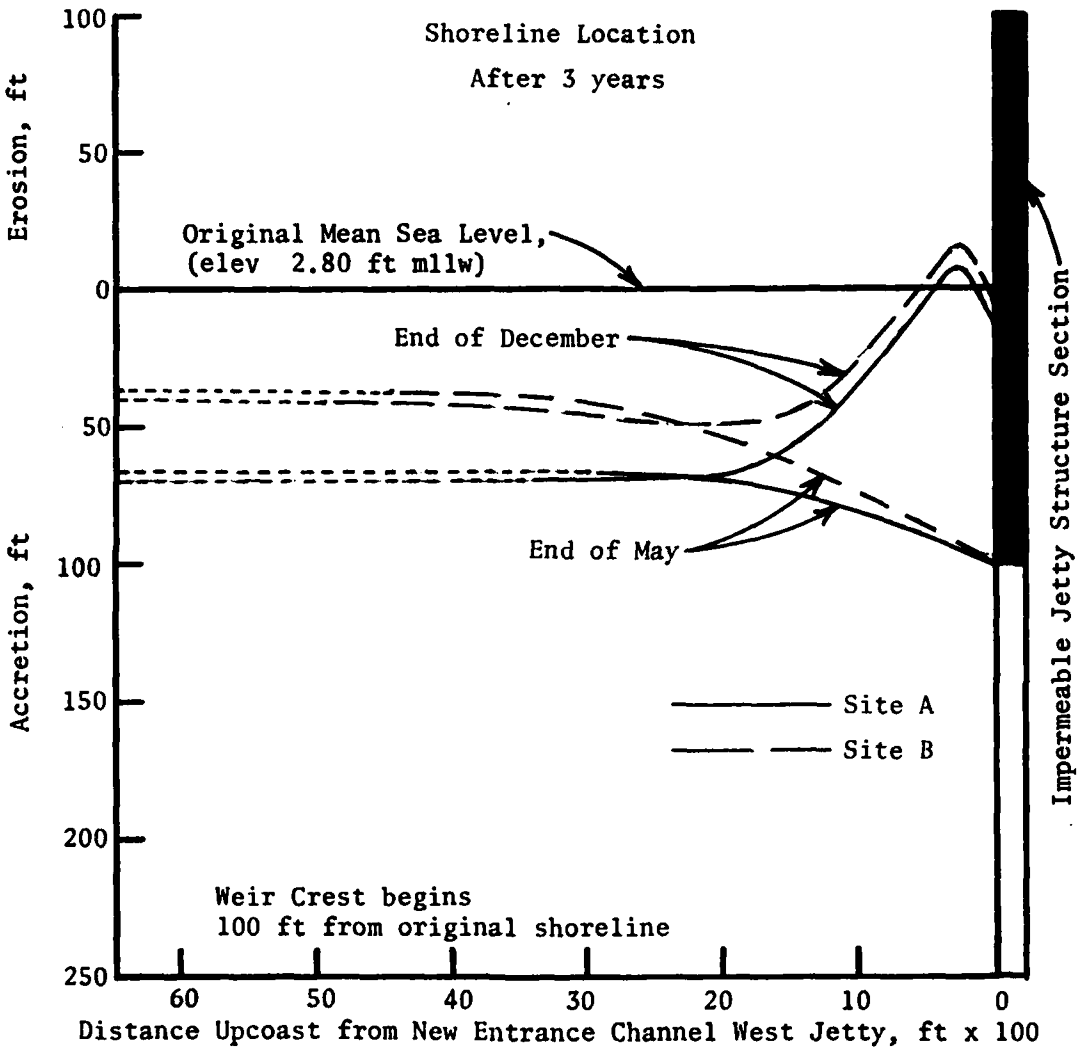

Figure 75. Computer simulation model indication of fillet formation on updrift side of west jetty at proposed new navigation entrance channel locations to Bolsa Chica Bay, California, at the end of May and December after 3 years of operation with a 100-ft sandtight landward section

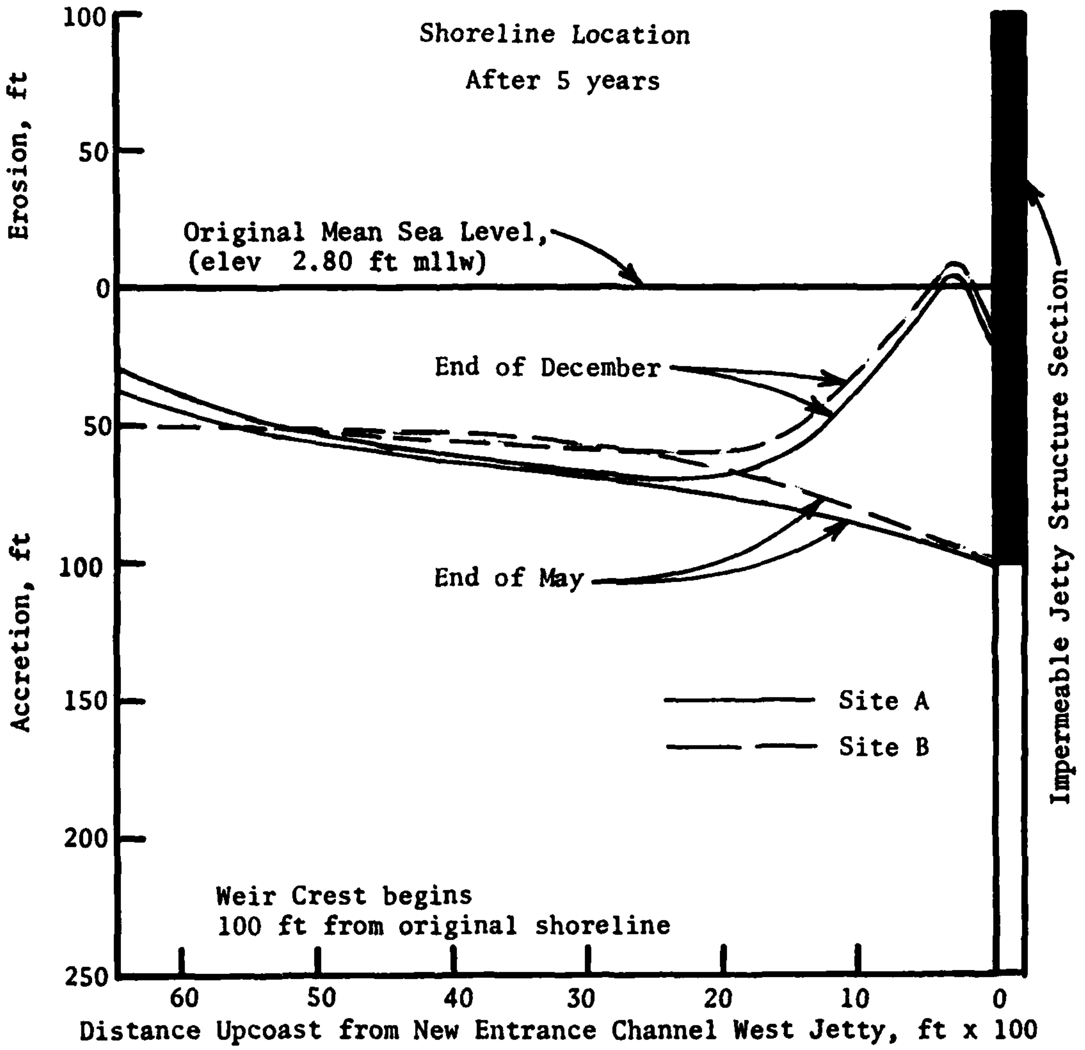

Figure 76. Computer simulation model indication of fillet formation on updrift side of west jetty at proposed new navigation entrance channel locations to Bolsa Chica Bay, California, at the end of May and December after 5 years of operation with a 100-ft sandtight landward section

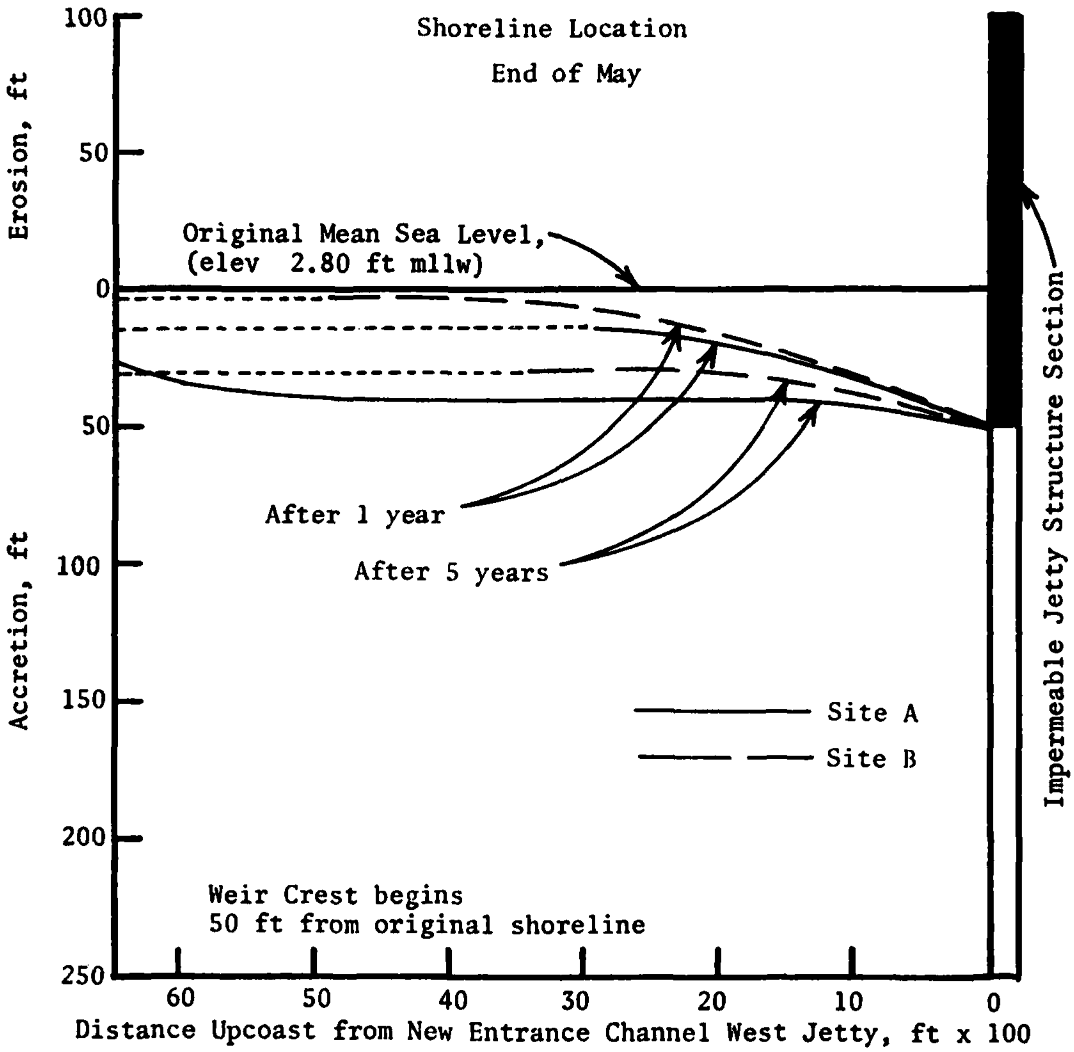

Figure 77. Computer simulation model indication of fillet formation on updrift side of west jetty at proposed new navigation entrance channel locations to Bolsa Chica Bay, California, at the end of May after 1 and 5 years of operation with a 50-ft sandtight landward section

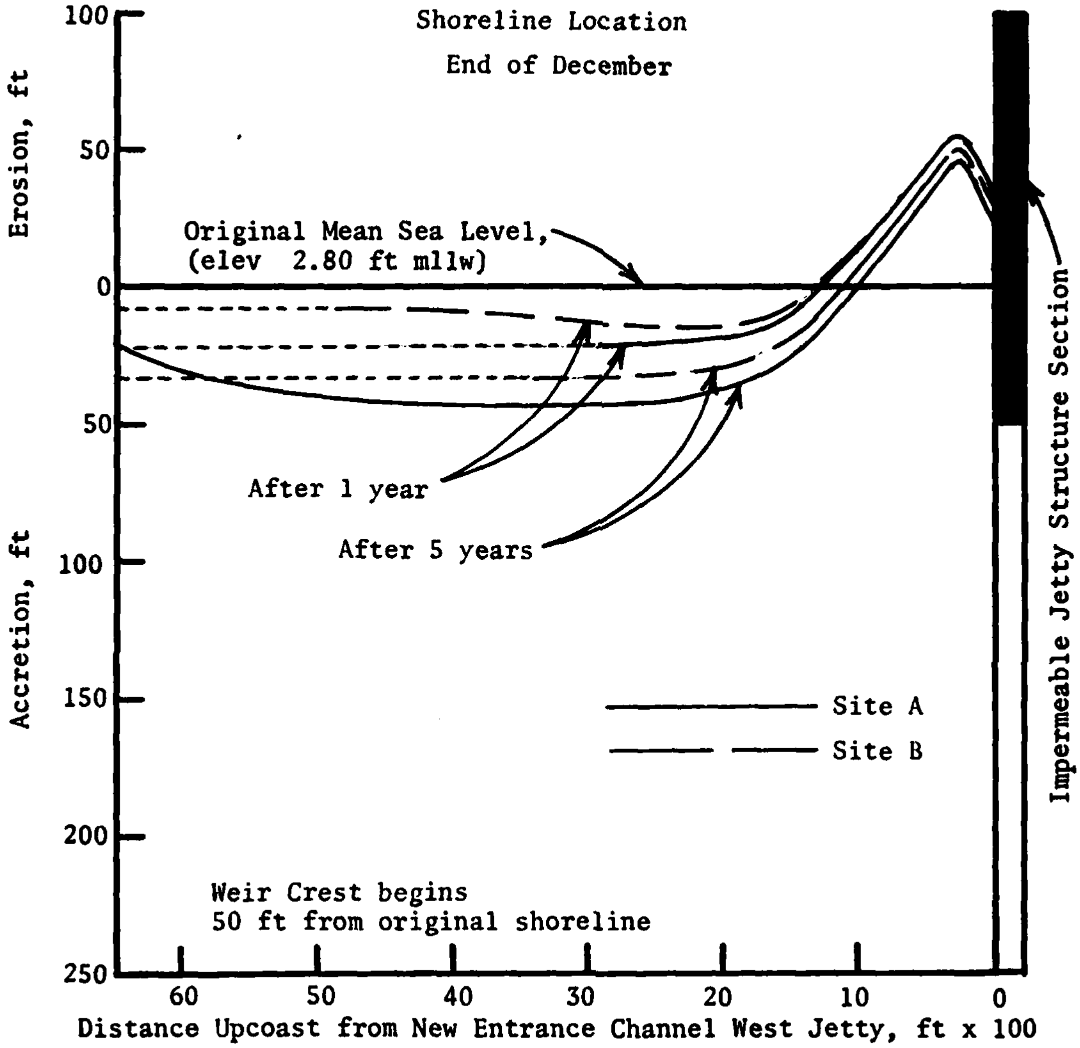

Figure 78. Computer simulation model indication of fillet formation on updrift side of west jetty at proposed new navigation entrance channel locations to Bolsa Chica Bay, California, at the end of December after 1 and 5 years of operation with a 50-ft sandtight landward section

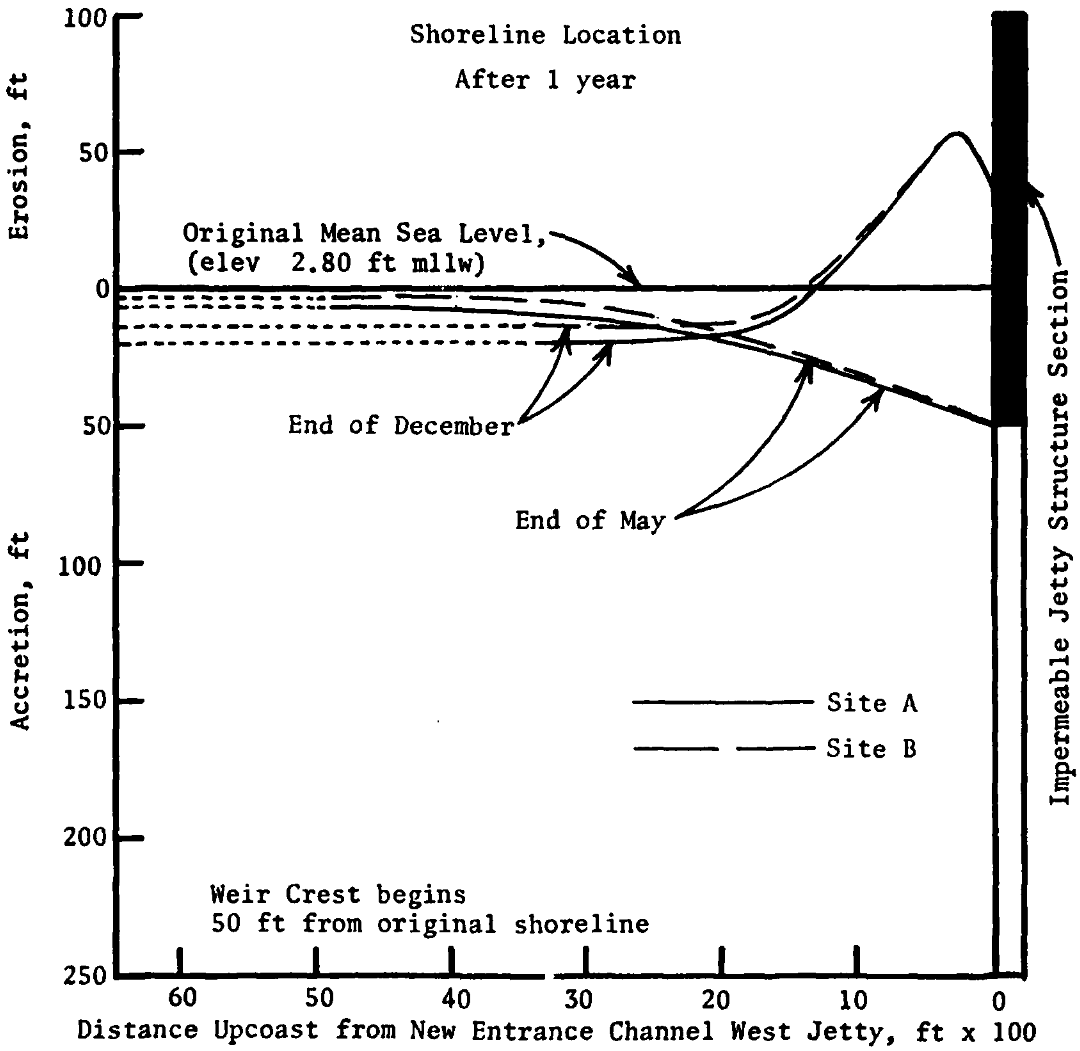

Figure 79. Computer simulation model indication of fillet formation on updrift side of west jetty at proposed new navigation entrance channel locations to Bolsa Chica Bay, California, at the end of May and December after 1 year of operation with a 50-ft sandtight landward section

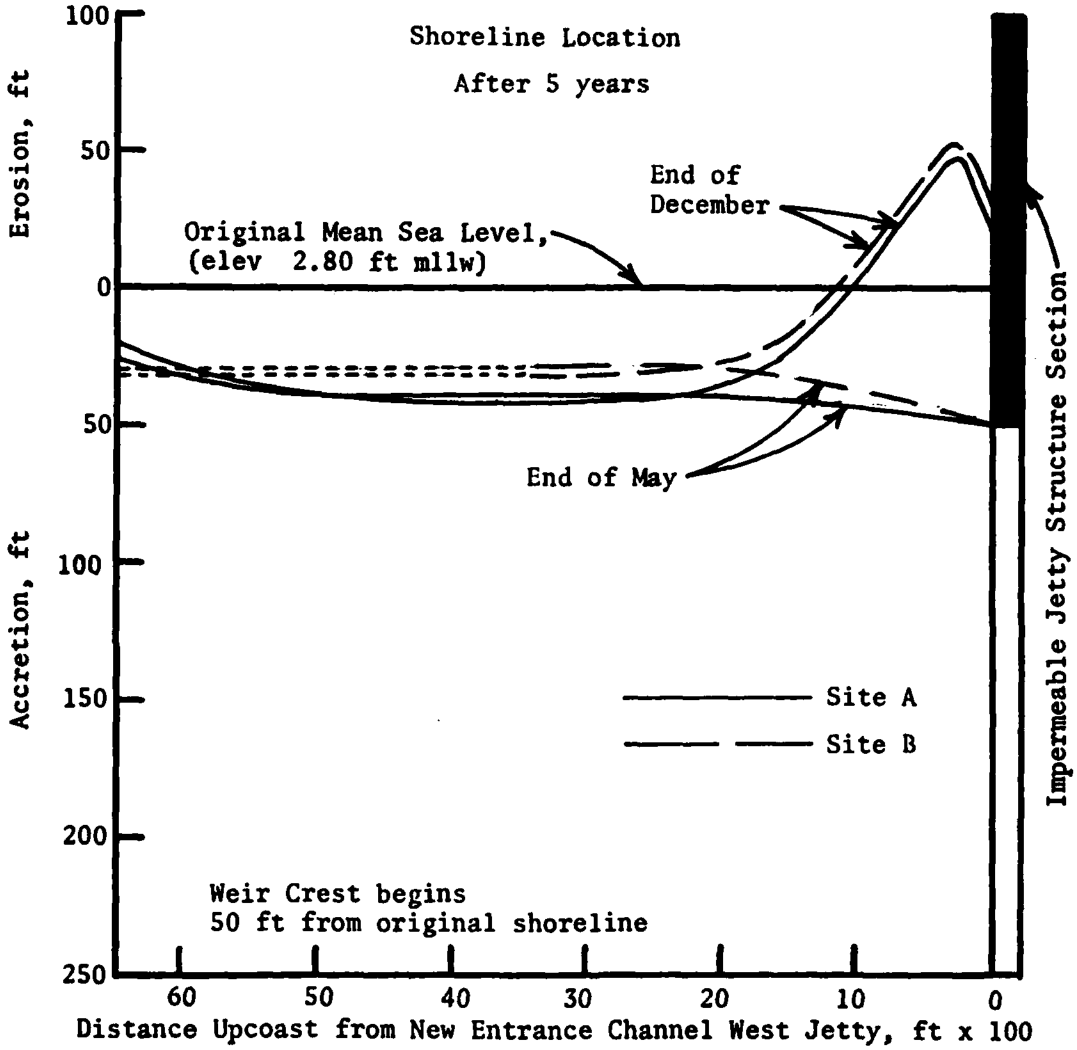

Figure 80. Computer simulation model indication of fillet formation on updrift side of west jetty at proposed new navigation entrance channel locations to Bolsa Chica Bay, California, at the end of May and December after 5 years of operation with a 50-ft sandtight landward section

87. It is pertinent to realize that the longer the sandtight landward section becomes, the more material will accumulate in the updrift fillet which was originally provided as beach nourishment material for Surfside-Sunset Beach. Hence, to maintain a noneroding coastline southeast of the downcoast jetty, additional quantities of beach fill material must be placed from external sources. Because the structures with the longer sandtight landward sections retain a greater amount of the downcoast drift, less material actually passes over the weir into the deposition basin for transfer to the starved downcoast beach during the process of fillet growth to maturity. Thus an optimization must be performed under the dual considerations of an adequate storage of material for return flow upcoast and a sufficient supply of bypassed material for beach nourishment downcoast.

Effect on Shoreline East of Proposed Navigation Entrance Channels

88. Existing conditions indicate that the construction of a weir jetty system at the proposed new navigation entrance channel locations (Site A or Site B) to Bolsa Chica Bay, with a sandtight landward section, will institute the formation of an updrift fillet of littoral material which would otherwise be transported into the deposition basin. The precise location of the weir section will govern the ultimate equilibrium shoreline configuration that develops. Without sand bypassing to the downdrift beach from the deposition basin, the average wave climate is sufficient to erode the downdrift coastline (analogous to the situation at Surfside-Sunset Beach). Even with an effective bypassing program (one which transfers all the net southerly transport), the existing regime will have been interrupted, and the gross oscillations of material movement will not occur under the same conditions as when the proposed new jetties did not exist. Northerly transport of material during the summer months will create a fillet on the east side of the east jetty, and the shoreline orientation will be altered in that region. This directly affects the rate of transport into and out of the area. With systematic bypassing annually (assuming repetitive wave conditions each year), the beach will ultimately respond with a new equilibrium configuration.

89. The computer simulation model developed by Komar (1977) and adapted for this study was utilized to ascertain the effect on the shoreline east of

the potential new navigation entrance channels of a representative example bypassing program and placement distributions. These computations were performed under the basic assumption that the structure was installed during the summer months and thus retained on the east side of the east jetty all littoral material that would have been transported northward during this time, starting with the shoreline at the existing condition location. The same result would have been deduced by assuming that the computations were initiated at the beginning of January, with the placement of enough material on the beach east of the proposed new east jetty to maintain the shoreline at the existing condition location.

90. Technology exists in the area of materials handling by slurry processes to adequately design a satisfactorily operating sand bypassing system at this location. Detailed designs have not been performed at this time, however, and the following example bypassing program is presented for illustrative purposes only. Many other rates of transfer can be handled by the equipment and techniques presently available, and all bypassing programs should be evaluated to ascertain their effects on the shoreline downcoast of the proposed new navigation channel. This example bypassing program recognizes that during the month of January the downcoast movement of littoral material from the Surfside-Sunset Beach region will be entirely utilized in replenishing the available dynamic storage capacity of the fillet on the west side of the west jetty. If the deposition basin is empty at the beginning of January, no material will be available during this month for placement on the beach east of the entrance channel. The majority of the material to be transferred will be bypassed during the months of February, March, April, and May. A relatively small amount of material will be bypassed to the downcoast beach during June in order to empty the deposition basin in anticipation of the next southerly transport season.

91. The example bypassing program evaluated consists of the following transfer rates: (a) February 98,500 cu yd; (b) March 50,200 cu yd; (c) April 50,200 cu yd; (d) May 50,200 cu yd; and (e) June 26,800 cu yd. Results of the computer simulation model application of this example bypassing program to ascertain the effect on shoreline configuration east of the proposed east jetty are presented in Figures 81-100 for uniform placement distributions of 300, 500, 1,000, and 2,000 ft. As the distribution of the bypassed material is extended farther and farther downcoast, those cells nearer the east jetty

will experience an increased depletion of material. It appears from the results of this one-dimensional numerical analysis that the bypassed material should be placed as near to the east jetty as practical while remaining outside the structure wave shadow zone. For the average wave climate utilized in this study, the effective equivalent structure wave shadow zone is quite narrow. The actual wave climate existing under prototype conditions will contain perturbations about this average that will cause fluctuations of the shoreline in the bypassing disposal area not accounted for by this computer simulation model. The actual equilibrium shoreline orientation that develops will be in response to the effectiveness of the bypassing program and in response to the actual wave climate.

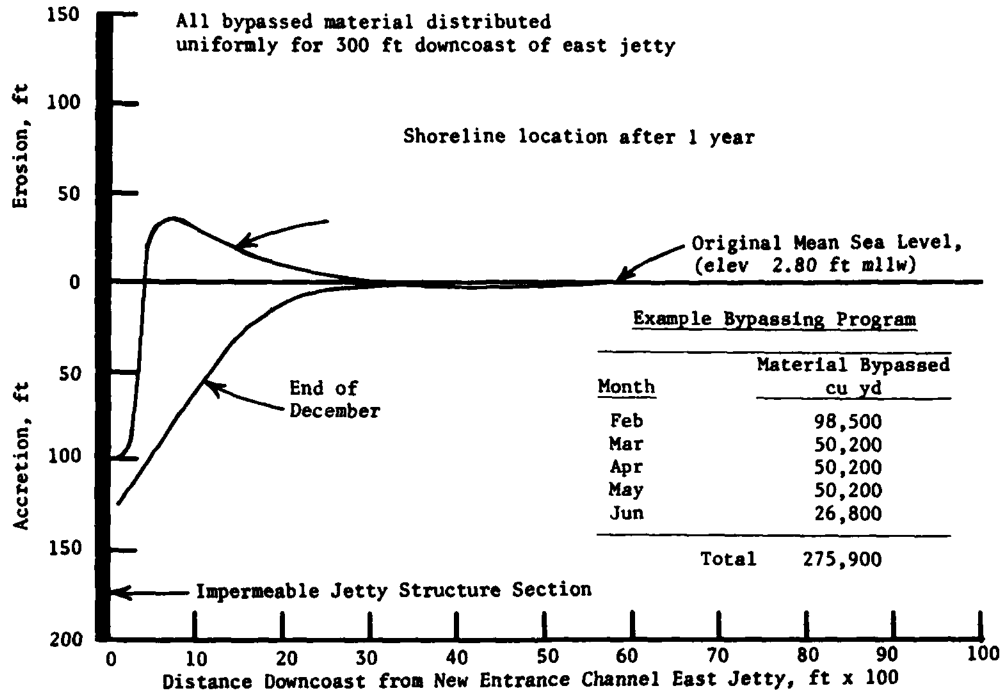

Figure 81. Computer simulation model indication of shoreline configuration on downdrift side of east jetty at proposed new navigation entrance channel to Bolsa Chica Bay, California, at the end of May and December after 1 year of operation with a 300-ft material distribution

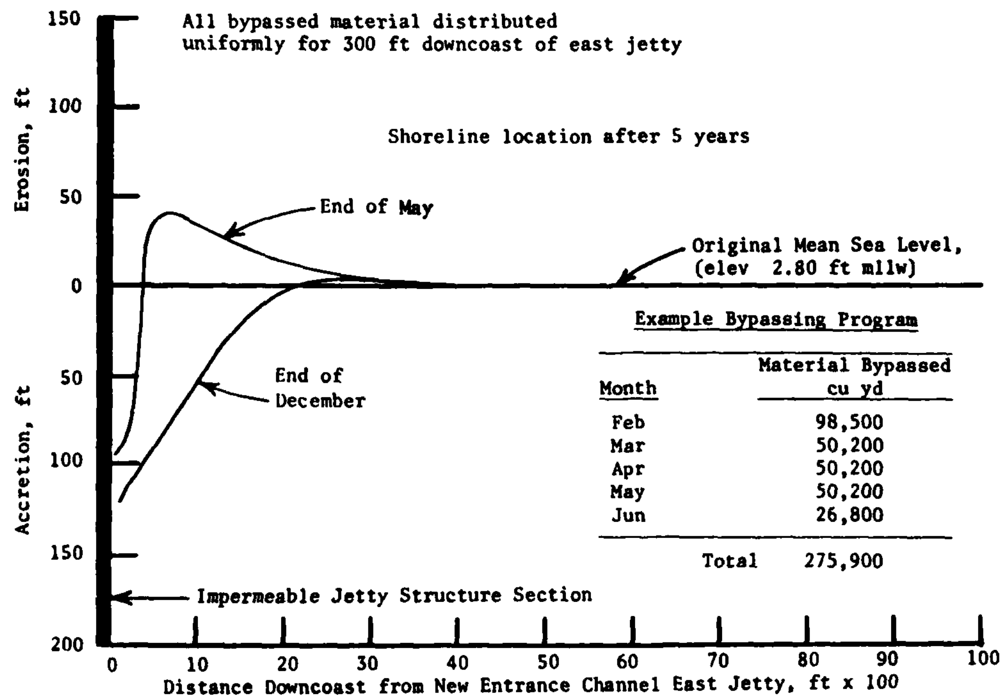

Figure 82. Computer simulation model indication of shoreline configuration on downdrift side of east jetty at proposed new navigation entrance channel to Bolsa Chica Bay, California, at the end of May and December after 5 years of operation with a 300-ft material distribution

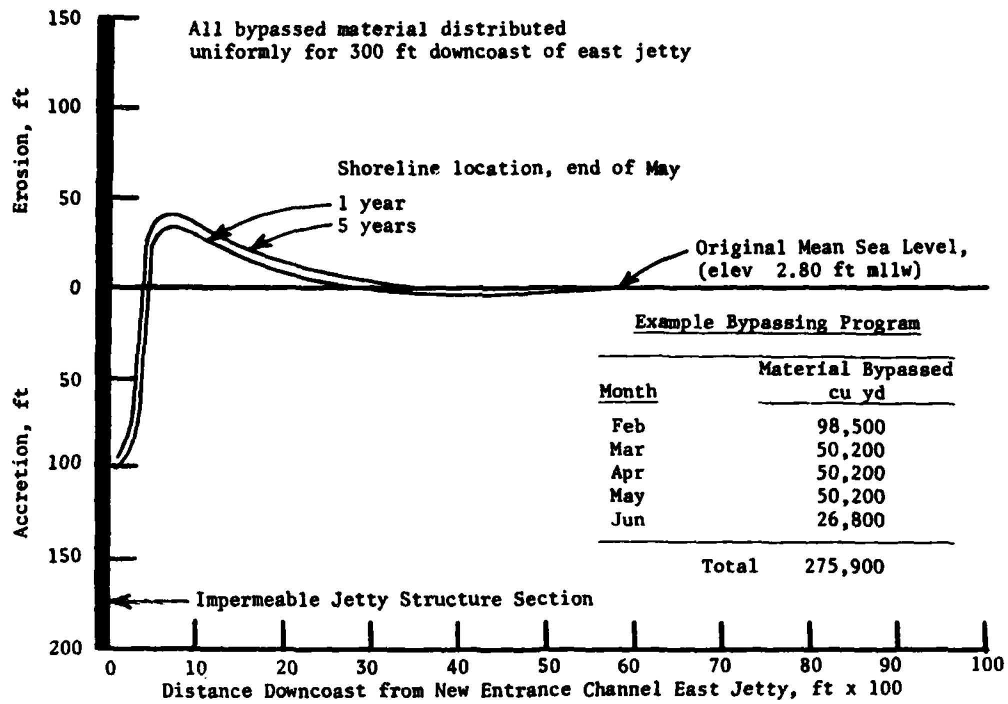

Figure 83. Computer simulation model indication of shoreline configuration on downdrift side of east jetty at proposed new navigation entrance channel to Bolsa Chica Bay, California, at the end of May after 1 and 5 years of operation with a 300-ft material distribution

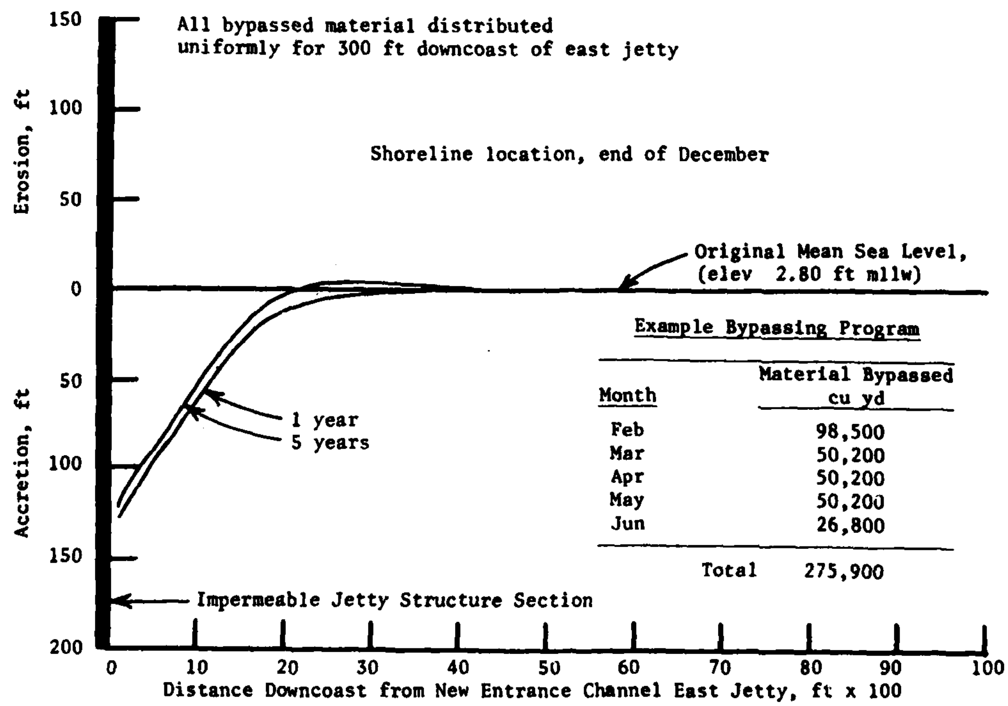

Figure 84. Computer simulation model indication of shoreline configuration on downdrift side of east jetty at proposed new navigation entrance channel to Bolsa Chica Bay, California, at the end of December after 1 and 5 years of operation with a 300-ft material distribution

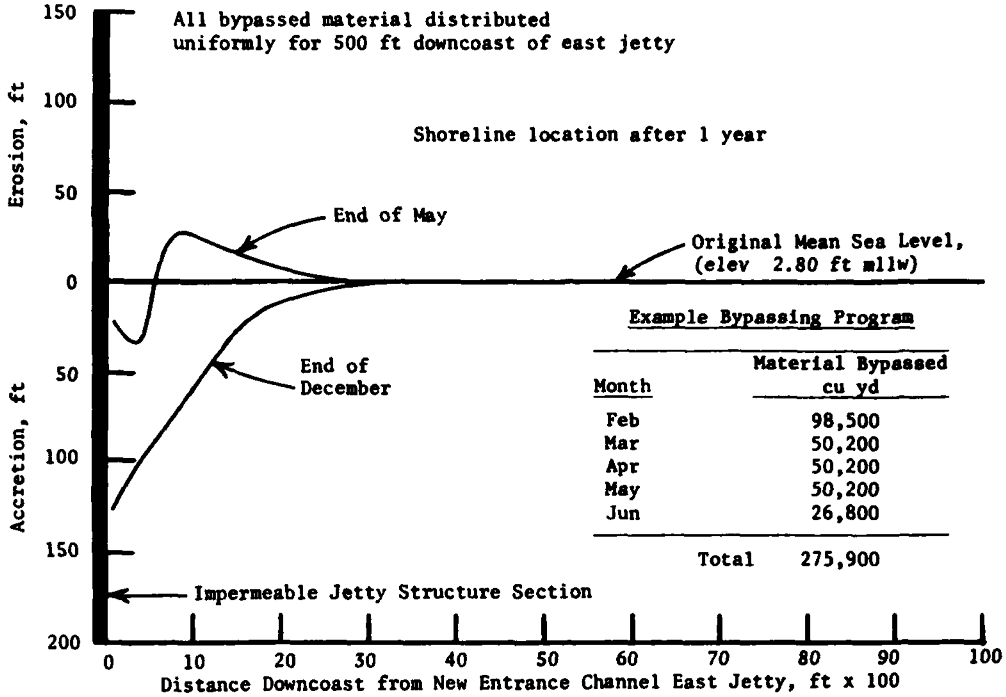

Figure 85. Computer simulation model indication of shoreline configuration on downdrift side of east jetty at proposed new navigation entrance channel to Bolsa Chica Bay, California, at the end of May and December after 1 year of operation with a 500-ft material distribution

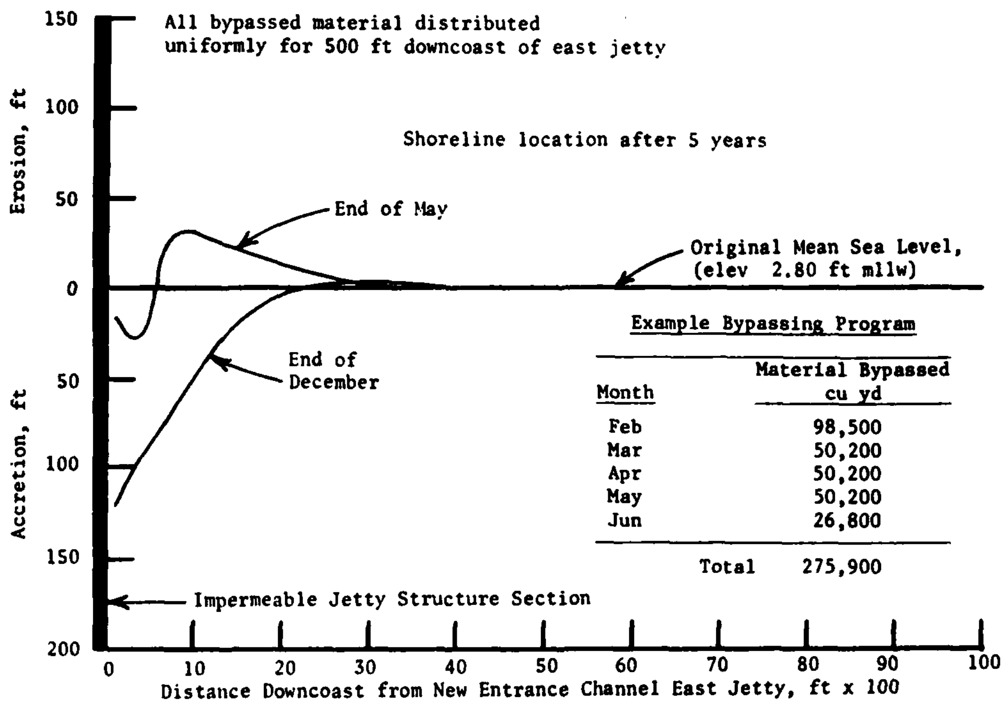

Figure 86. Computer simulation model indication of shoreline configuration on downdrift side of east jetty at proposed new navigation entrance channel to Bolsa Chica Bay, California, at the end of May and December after 5 years of operation with a 500-ft material distribution

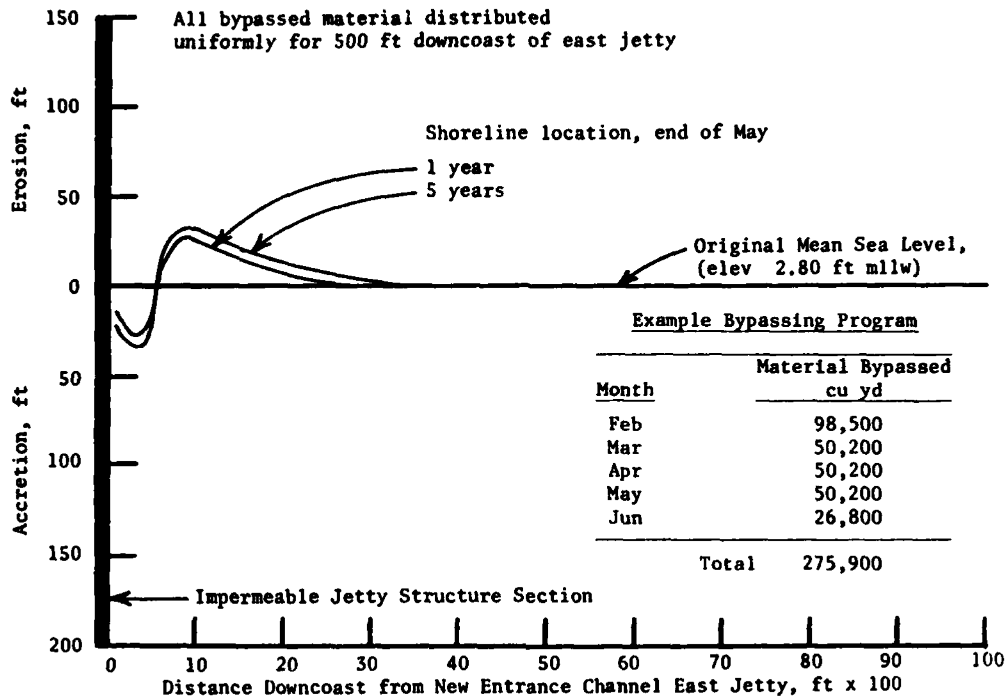

Figure 87. Computer simulation model indication of shoreline configuration on downdrift side of east jetty at proposed new navigation entrance channel to Bolsa Chica Bay, California, at the end of May after 1 and 5 years of operation with a 500-ft material distribution

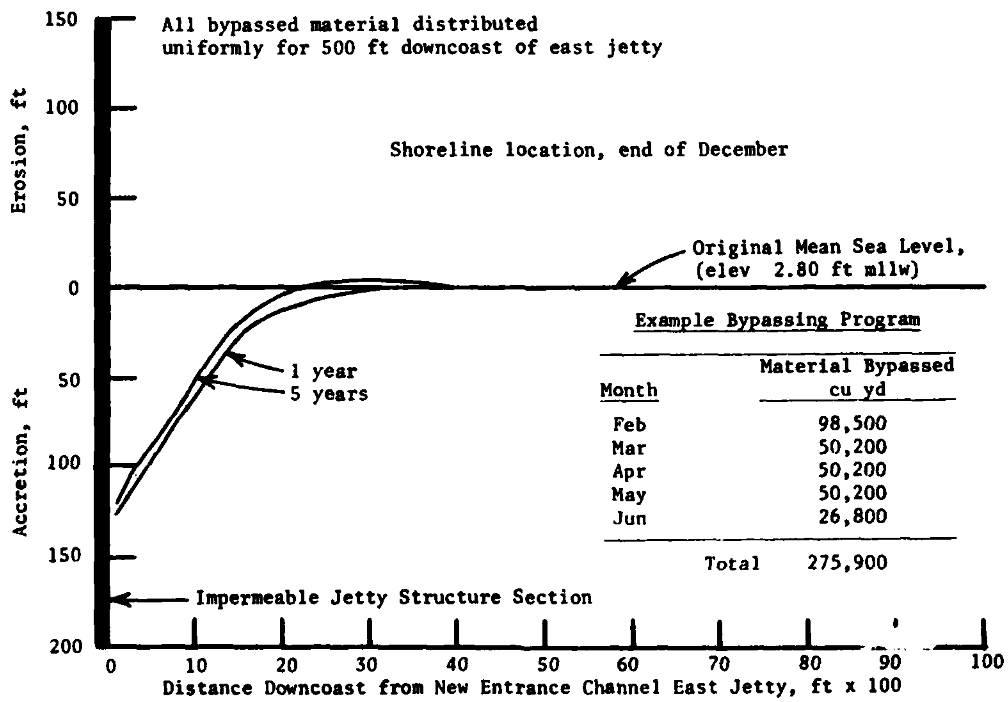

Figure 88. Computer simulation model indication of shoreline configuration on downdrift side of east jetty at proposed new navigation entrance channel to Bolsa Chica Bay, California, at the end of December after 1 and 5 years of operation with a 500-ft material distribution

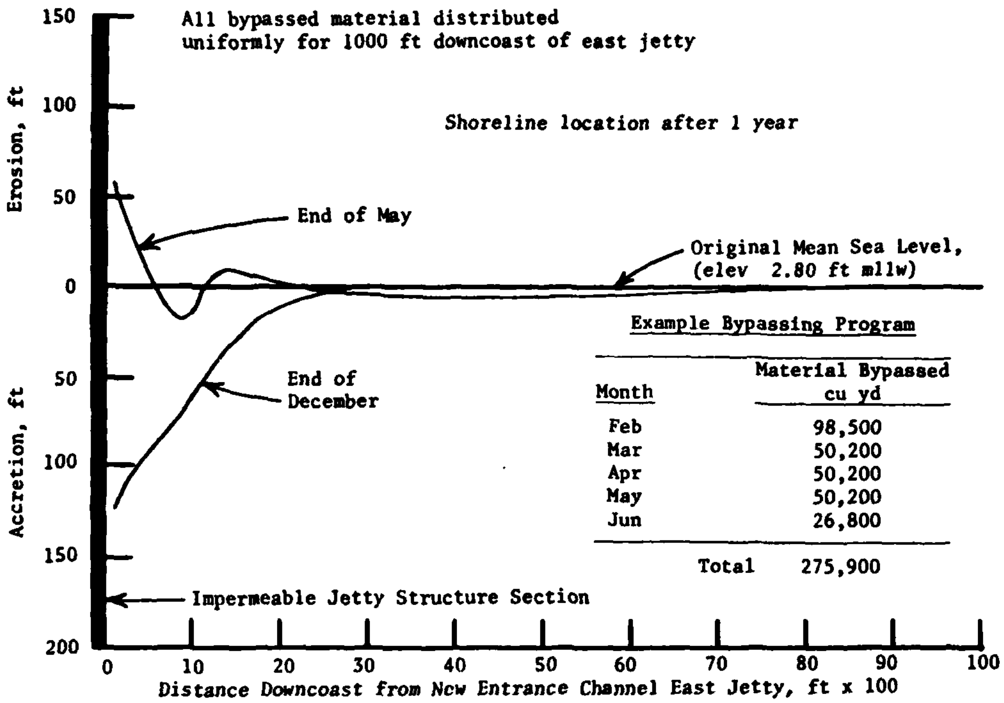

Figure 89. Computer simulation model indication of shoreline configuration on downdrift side of east jetty at proposed new navigation entrance channel to Bolsa Chica Bay, California, at the end of May and December after 1 year of operation with a 1,000-ft material distribution

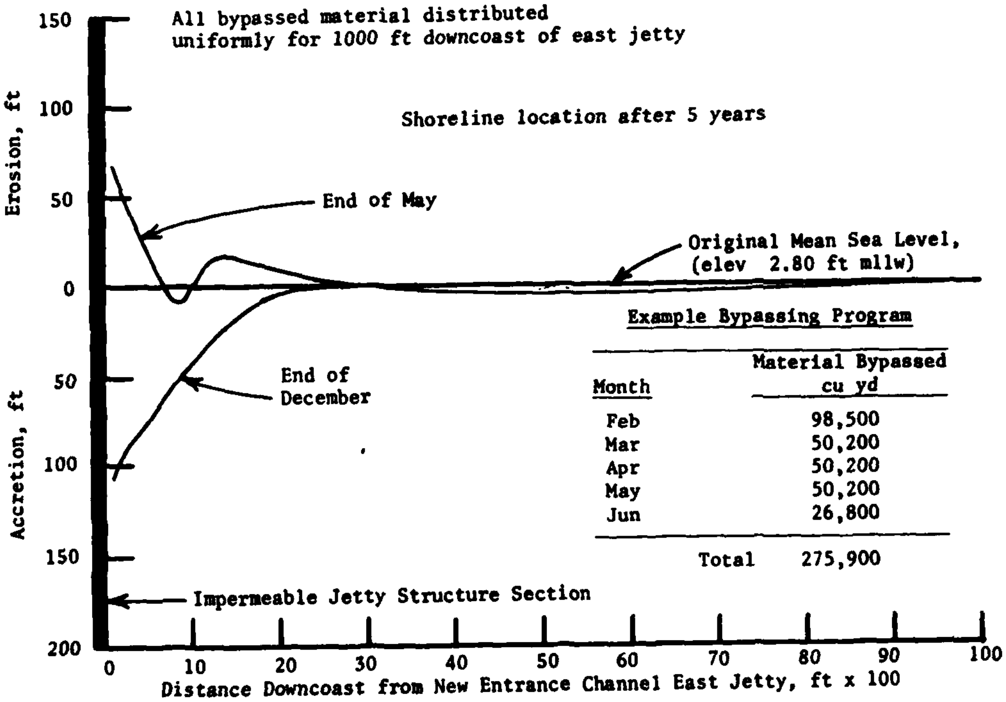

Figure 90. Computer simulation model indication of shoreline configuration on downdrift side of east jetty at proposed new navigation entrance channel to Bolsa Chica Bay, California, at the end of May and December after 5 years of operation with a 1,000-ft material distribution

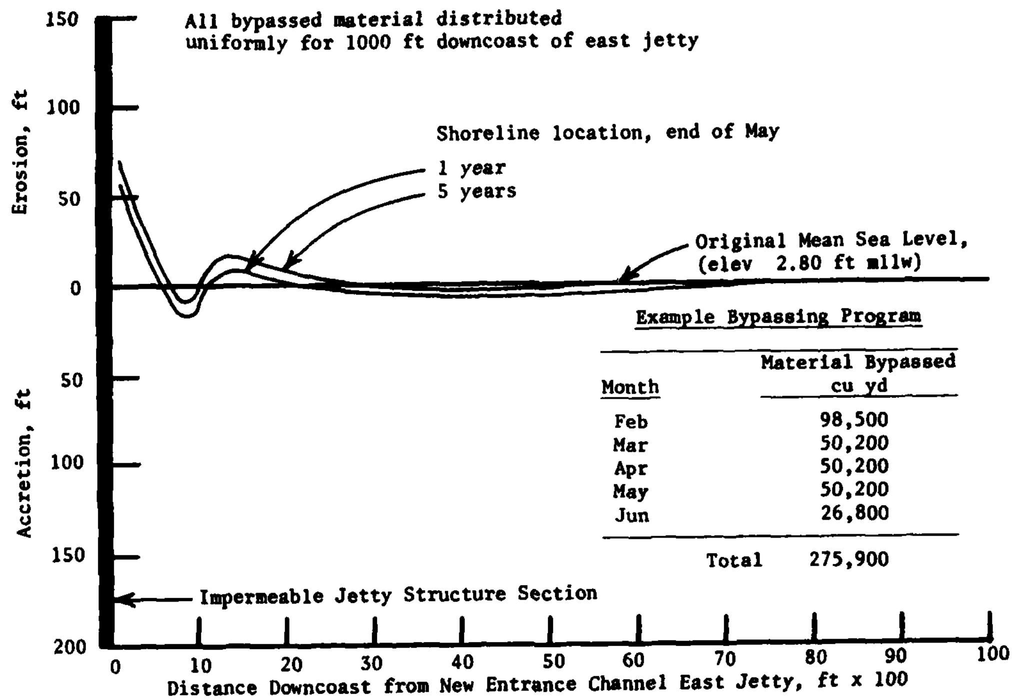

Figure 91. Computer simulation model indication of shoreline configuration on downdrift side of east jetty at proposed new navigation entrance channel to Bolsa Chica Bay, California, at the end of May after 1 and 5 years of operation with a 1,000-ft material distribution

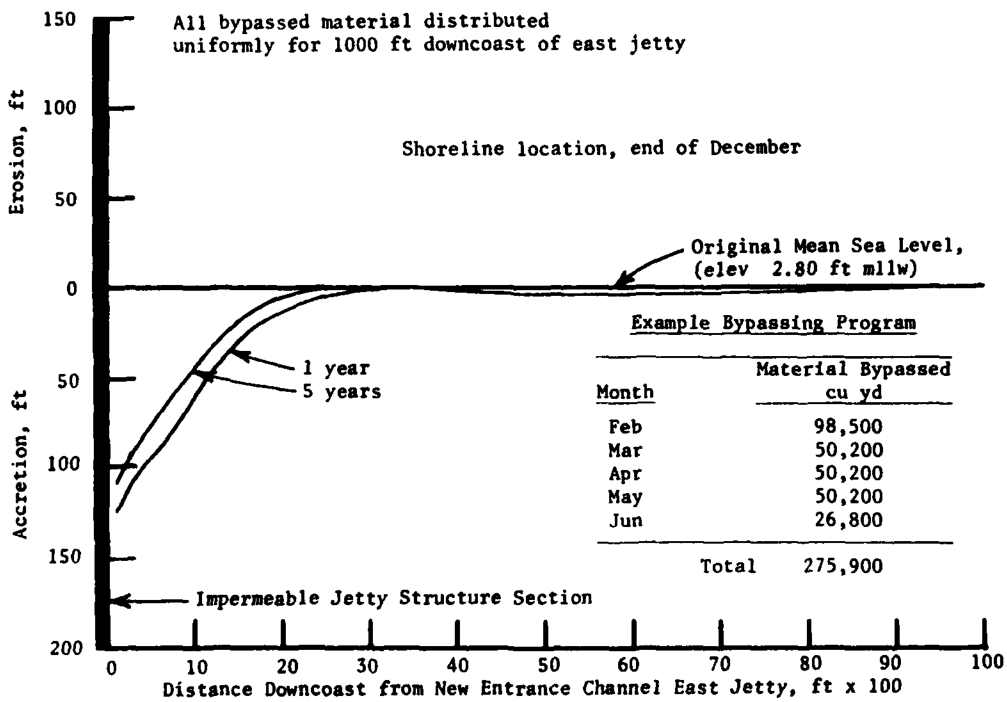

Figure 92. Computer simulation model indication of shoreline configuration on downdrift side of east jetty at proposed new navigation entrance channel to Bolsa Chica Bay, California, at the end of December after 1 and 5 years of operation with a 1,000-ft material distribution

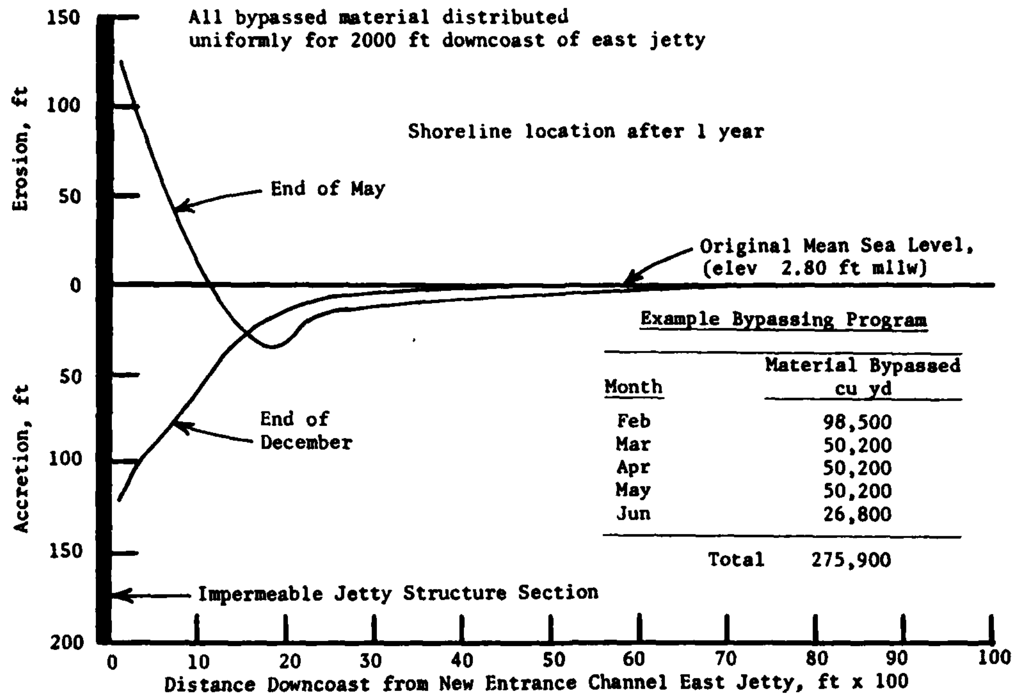

Figure 93. Computer simulation model indication of shoreline configuration on downdrift side of east jetty at proposed new navigation entrance channel to Bolsa Chica Bay, California, at the end of May and December after 1 year of operation with a 2,000-ft material distribution

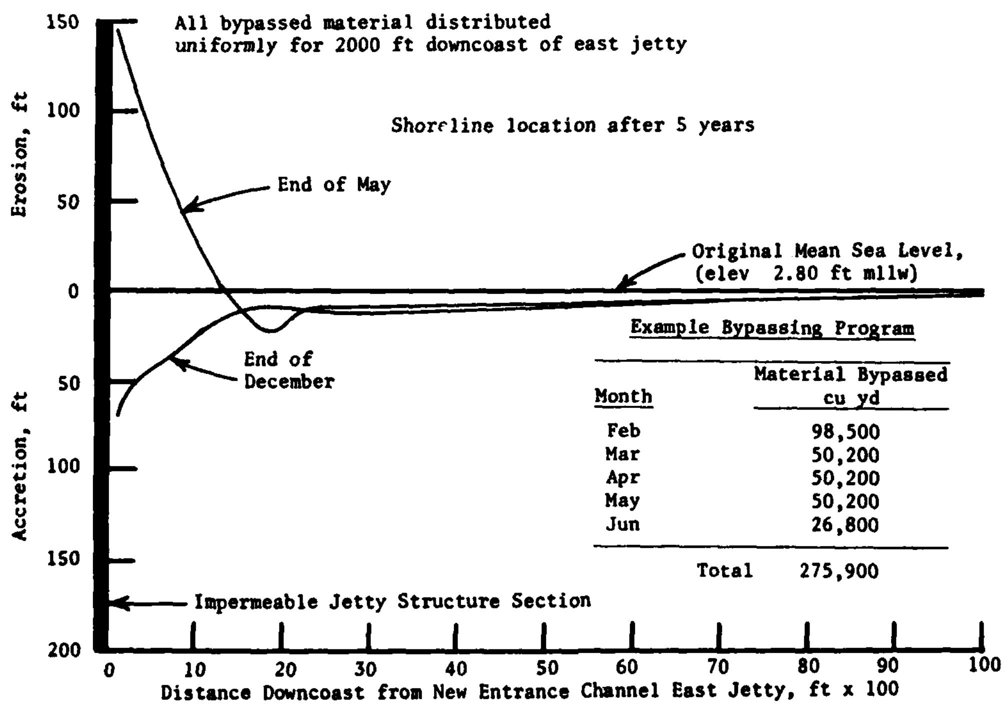

Figure 94. Computer simulation model indication of shoreline configuration on downdrift side of east jetty at proposed new navigation entrance channel to Bolsa Chica Bay, California, at the end of May and December after 5 years of operation with a 2,000-ft material distribution

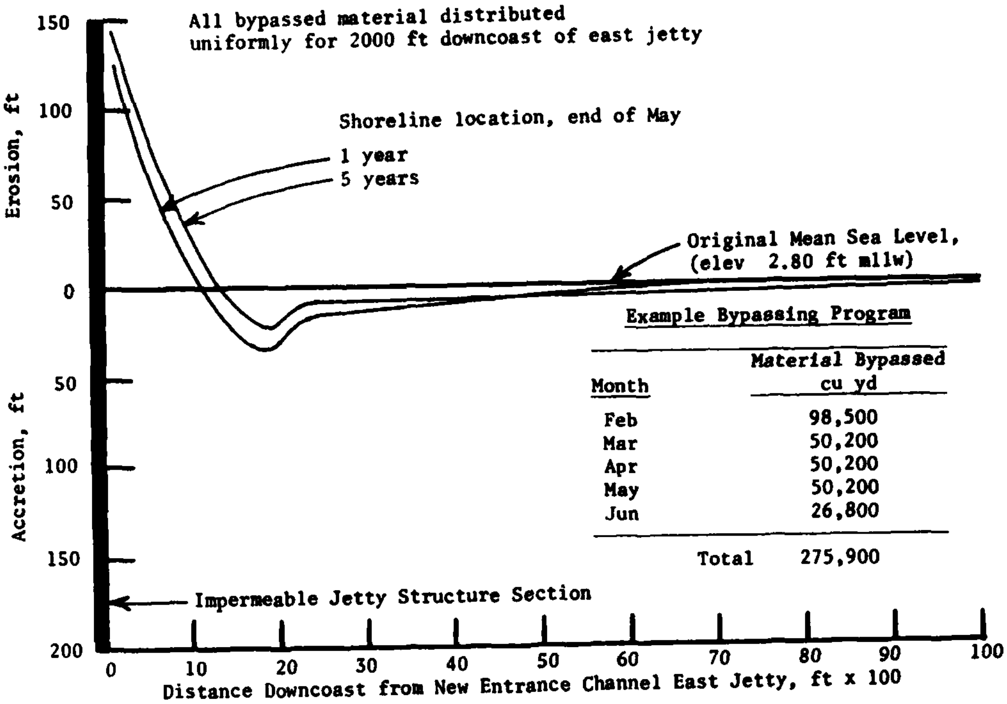

Figure 95. Computer simulation model indication of shoreline configuration on downdrift side of east jetty at proposed new navigation entrance channel to Bolsa Chica Bay, California, at the end of May after 1 and 5 years of operation with a 2,000-ft material distribution

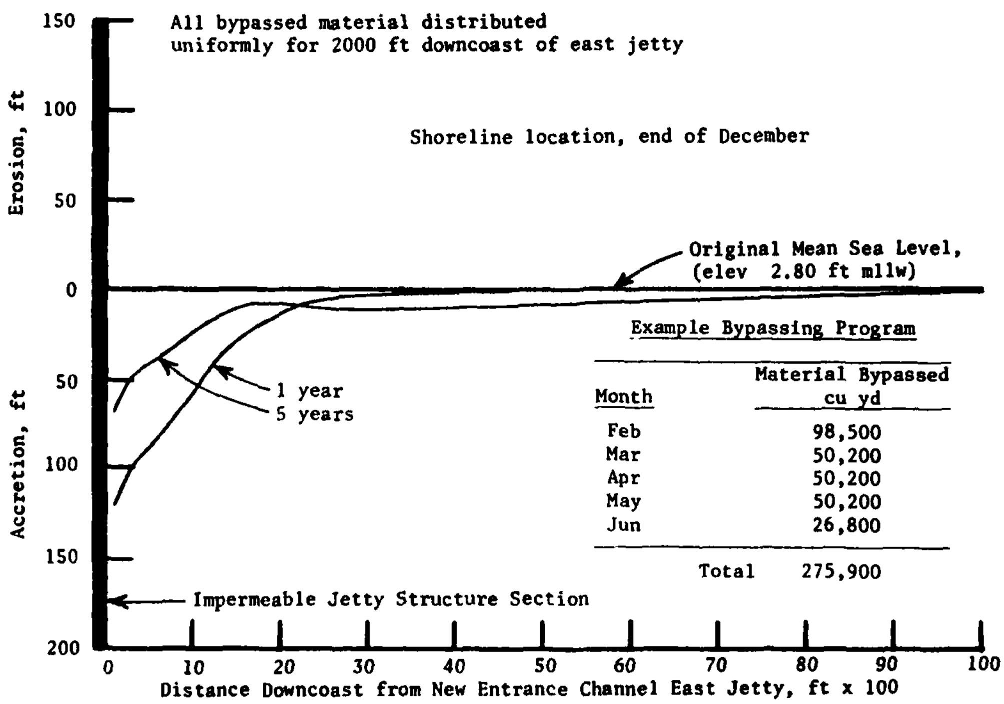

Figure 96. Computer simulation model indication of shoreline configuration on downdrift side of east jetty at proposed new navigation entrance channel to Bolsa Chica Bay, California, at the end of December after 1 and 5 years of operation with a 2,000-ft material distribution

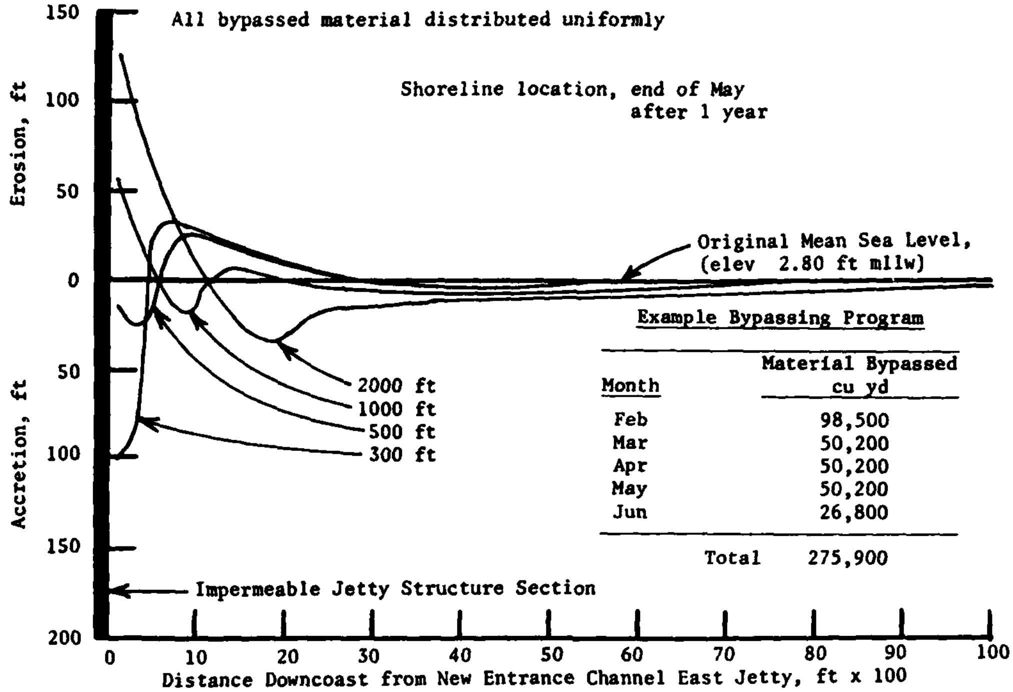

Figure 97. Comparison of computer simulation model indication of shoreline configuration on downdrift side of east jetty at proposed new navigation entrance channel to Bolsa Chica Bay, California, at the end of May after 1 year of operation with four material distributions

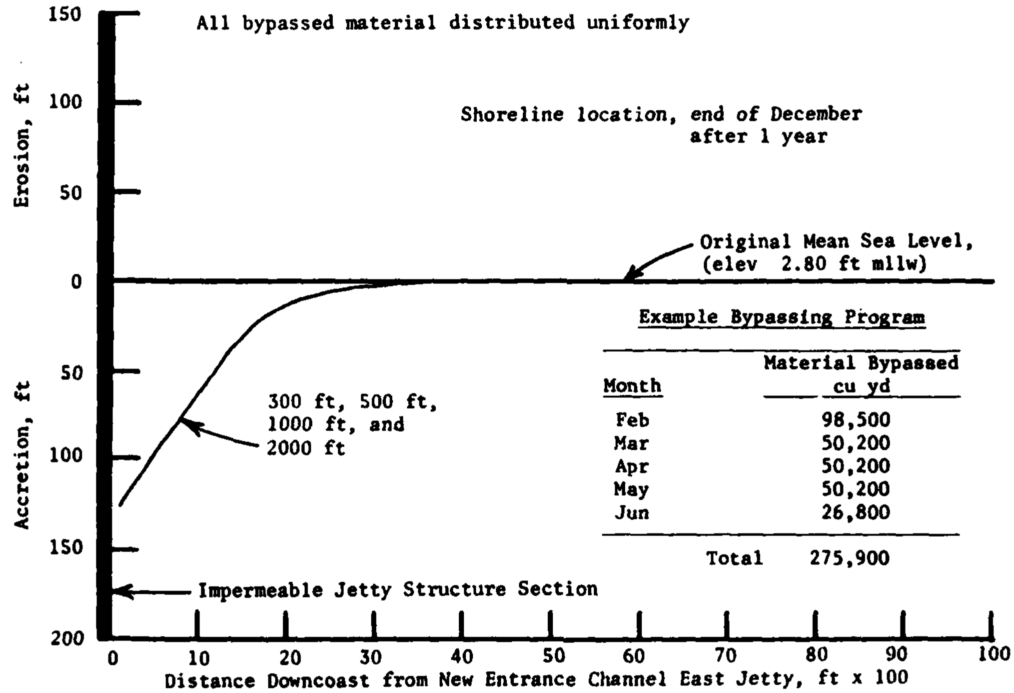

Figure 98. Comparison of computer simulation model indication of shoreline configuration on downdrift side of east jetty at proposed new navigation entrance channel to Bolsa Chica Bay, California, at the end of December after 1 year of operation with four material distributions

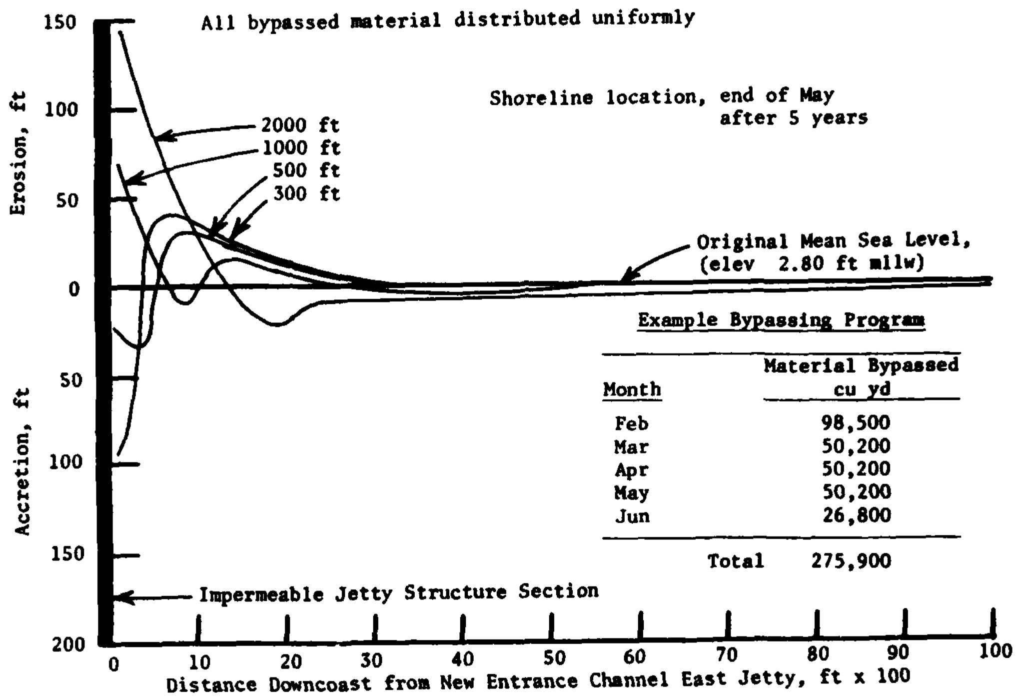

Figure 99. Comparison of computer simulation model indication of shoreline configuration on downdrift side of east jetty at proposed new navigation entrance channel to Bolsa Chica Bay, California, at the end of May after 5 years of operation with four material distributions

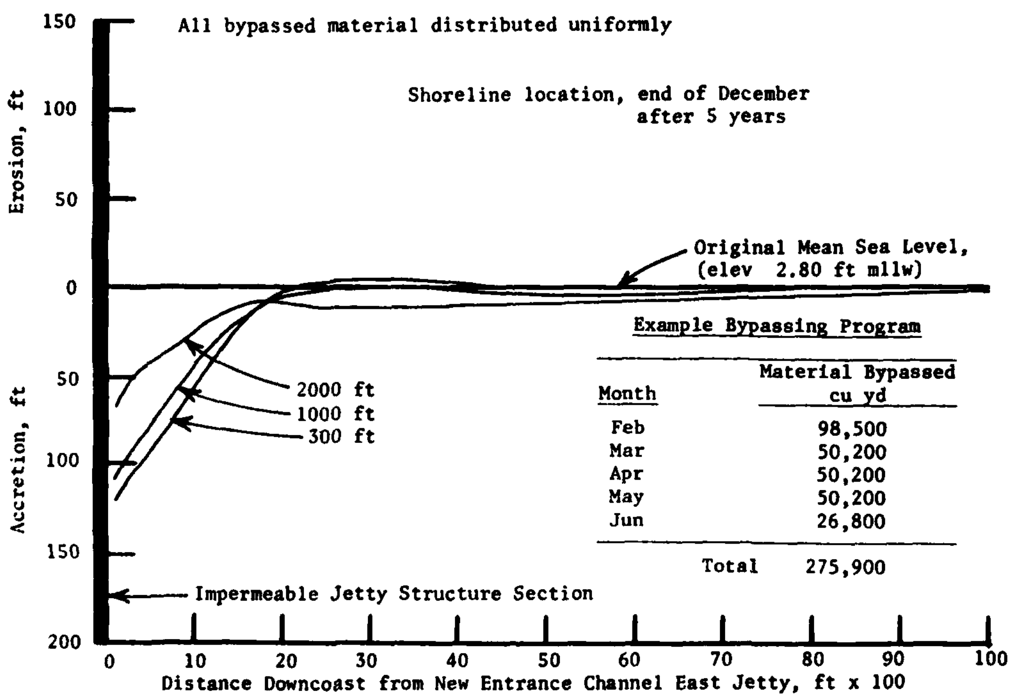

Figure 100. Comparison of computer simulation model indication of shoreline configuration on downdrift side of east jetty at proposed new navigation entrance channel to Bolsa Chica Bay, California, at the end of December after 5 years of operation with four material distributions

PART VIII: SUMMARY AND CONCLUSIONS

Purposes of the Study

92. Access to the open ocean from Huntington Harbor, California, is obtained by passage through Anaheim Bay which is heavily used by the U. S. Naval Weapons Station, Seal Beach. Concern has existed for many years about the possibility of accidental encounters between civilian and military craft in this area where ammunition off-loading and storage are routine practices. Local interests have requested the SPL to investigate the practicality of the construction of a new navigation entrance channel connecting Bolsa Chica Bay with the Pacific Ocean.

93. In August 1972, the State of California executed a land agreement with Signal Property, Incorporated, regarding tidal lands in Bolsa Chica Bay. Points of the agreement pertinent to this study are: (a) the State will receive fee title to a 327.5-acre area of the Bolsa Chica Bay along the Pacific Coast Highway, (b) Signal Property, Incorporated, provided to the State the right to use, starting in 1973 and for a period of 14 years, an additional 230-acre area of Bolsa Chica Bay adjacent to the 327.5-acre area, and (c) the State will receive fee title to the 230-acre area provided a navigational channel with a minimum width of 300 ft be constructed connecting the Pacific Ocean to the Signal Property land during the 14-year period. In 1973, the State of California developed a conceptual plan utilizing the 557.5-acre area of the Bolsa Chica Bay for a public marina and saltwater marsh restoration. Navigable entrances located at two possible sites along the Bolsa Chica Bay shoreline (Figures 4 and 5), and a nonnavigable entrance for the purpose of tidal exchange with a saltwater marsh, are considered in this study.

94. Functional requirements of such a proposed new navigation entrance channel will necessitate stabilization by the use of a parallel or arrowhead jetty system. Otherwise, the large net downcoast drift of littoral material will rapidly close the entrance channel and preclude navigation. At the same time, any jetty system will interrupt the transport of littoral material in the surf zone and deplete the downcoast (in terms of net transport) beaches of their nourishment from upcoast sources. Consequently, a sand bypassing concept must be developed to operate in concert with a weir jetty system. The jetty system is necessary for navigational channel stabilization and a sand

bypassing system is required to mitigate effects of the jetties on the recreational beaches of Bolsa Chica Beach State Park.

95. The purposes of this study were to: (a) estimate the nearshore wave climate in the vicinity of potential new navigation entrance channel construction for structure design wave determination, and (b) to adapt computer simulation modeling of longshore transport of littoral material to estimate the resulting unstabilized shoreline evolution from jetty construction and example representative material bypassing at Bolsa Chica Beach State Park, California.

Structure Wave Height

96. Damage to flexible rubble-mound structures is usually progressive, and for short duration of extreme wave action, waves higher than the significant wave height, H_s, impinging on such structures seldom create serious damage. The significant wave height, H_s, appears to be a reasonable design wave height for this locality. The best deepwater wave data for this region at the present time are believed to be the hindcast data of National Marine Consultants (1960) and Marine Advisors (1961), and these data were used in this analysis.

97. The wave height at various locations along the proposed jetty system depends directly on the deepwater wave height, deepwater wave period, and direction of approach. The shallow-water values of wave height at all points along the structure were determined by a detailed refraction analysis which propagated the deepwater waves shoreward to their breaking location. The wave heights and their frequency of occurrence were determined at five locations along the potential new structure site (10-, 15-, 20-, 25-, and 30-ft water depths). The maximum wave height at the structure for all waves is less than the breaking wave height for water depths of 30, 25, and 20 ft, and the proposed structure will be subjected to nonbreaking waves in these water depths. In shallower water, however, the combined effect of refraction and shoaling increases and the waves may break. These portions of the structure will be subjected to breaking waves of various periods from certain directions of approach. These data are presented in Tables 2-6.

Potential Longshore Transport

98. In order to estimate the effects of a weir jetty system and sand bypassing techniques on the adjacent unstabilized shorelines, it is necessary to have an understanding of the potential longshore transport of littoral material in the surf zone. The refraction analysis and wave hindcast data used for estimating the structure design wave were extended to calculate the potential longshore transport for the region of coastline extending from Surfside-Sunset Beach to Huntington Beach. It was determined that on the average, approximately 376,600 cu yd of material moves toward the southeast each year, and about 100,700 cu yd of material is transported northwesterly each year, resulting in a net southerly transport of about 275,900 cu yd/yr.

99. The section of southern California coastline investigated in this study experiences a twice annual reversal, on the average, in net longshore transport direction (Figure 12). Strong southerly transport occurs during the months of January, February, March, and April. Anticipated accretion should occur on the west side of the proposed west jetties at the navigation entrance channels of Site A or Site B. Erosion is expected to occur on the east side of the east jetties unless there is sand bypassing to the eastern side or material input from an external source. During the remainder of the year, mild westerly transport reverses the process, and the east side of the east jetty temporarily becomes the accretion side. Accordingly, the west side of the west jetty then will experience some degree of depletion as material previously held in dynamic storage in the fillet will drift upcoast toward the eroding feeder beach at Surfside-Sunset Beach. When the fillet has grown to maturity (approximately 4 years after jetty construction), it will be capable of returning the northwesterly transport of littoral material (100,700 cu yd annually) toward the erosional beach at Surfside-Sunset Beach.

Computer Simulation Model

100. A computer simulation model for shoreline evolution developed by Komar (1977) was adapted to this region. The model was calibrated for known movement of material from the feeder beach located at Surfside-Sunset Beach. Because the renourishment interval for the feeder beach is expected to be about 5 years, the numerical model was operated for this period of time (with a time

increment for computational purposes of 1 hr). The two critical times of the year in this region are toward the end of May (following a large volume of southerly transport movement) and toward the end of December (at the end of the northerly transport season). At these times, the shoreline will have advanced or retreated to its farthest position during the year's oscillations. The length of the sandtight landward section of the proposed navigation entrance channel west jetty between the preconstruction existing shoreline and the weir determines the extent of fillet formation that will evolve and ultimately the volume of material that will be available for transport back upcoast toward the erosional beach area.

Spur Groin at Anaheim Bay East Jetty

101. The localized region where the Anaheim Bay east jetty connects with the shoreline is subjected to severe scour and erosion by certain wave characteristics and approach directions. There exists the possibility that the east jetty landward end may be breached if the erosion near this jetty is allowed to continue unabated. The problem appears to be the result of the "Mach-stem" phenomenon and arises when the wave approach is such that the wave crest propagates along the section of jetty, increases in amplitude along the Mach stem, and terminates as a geyser of water plunging on the shore at the land end of the structure. Because continuous nourishment of beach replenishment material is not available for this particular localized region (nourishment is of a periodic nature), any solution of this local scour must be of a structural type. Any existing beach location may probably be stabilized at that position by the construction of a properly designed spur groin erected perpendicularly to the Anaheim Bay east jetty and oriented essentially parallel with the general Surfside-Sunset Beach shoreline.

102. The length of spur groin section should be optimized with respect to extent of stable beach section deemed essential to prevent breaching of the Anaheim Bay east jetty. The existence of such a spur groin should not materially affect the volume of beach nourishment required to maintain the recreation beach in the Surfside-Sunset Beach Region. The computer simulation model for shoreline evolution was operated for a 5-year time interval in 1-hr time increments starting with the after-beach-nourishment location of 1979. Two different lengths of spur groin were installed in the numerical model (a

500-ft length and a 1,000-ft length). Because of the influence of the breaker angle on longshore transport, the longer section of spur groin permits a slightly smaller volume of erosion from the beach (approximately 120,000 cu yd over a 5-year time interval); however, this slight reduction in total volume should be optimized with consideration of the initial cost of the spur groin. While neither groin will eliminate the requirement for periodic beach nourishment, neither adversely impacts significantly on the existing condition situation. It appears that either section of spur groin will offer satisfactory protection to the localized scour area where the Anaheim Bay east jetty connects with the shoreline.

Sandtight Landward Section and Fillet Formation

103. In the early years following construction, the updrift movement of material under average-to-extreme wave conditions may be sufficient to breach the land end of the west jetty. To investigate these phenomena, five different lengths of sandtight landward section (50, 100, 150, 200, and 250 ft) were analyzed at Site A and Site B. These data indicate the rate and extent of the fillet formation on the updrift side of the various potential structures and are displayed in Figures 57-80.

104. While all sections of sandtight landward portions evaluated approached an upper filling limit, the shorter section (50-ft sandtight landward section) suffered a breaching of the existing shoreline and would not provide enough return flow of littoral material to the eroding coast to replicate the existing conditions at the end of the year. The 100-ft sandtight landward section structure reproduces the existing condition after being in operation for approximately 4 years, whereas the 150-ft section and larger structures permit an adequate amount of material during all years, whether the proposed new navigation entrance channel is located at Site A or Site B. The effect of positioning the proposed new entrance channel at Site A is not significantly different from positioning the channel at Site B, with regard to fillet formation. From these considerations, it appears that the sandtight landward section should be at least 150 ft long.

Deposition Basin Capacity

105. Two factors that influence the required deposition basin capacity are: (a) the longshore transport rate over the weir into the basin; and (b) the estimated frequency and rate at which the basin will be excavated. A reserved volume large enough to accommodate the entire downcoast net movement of littoral material, Q_{net} (275,900 cu yd/yr), is not necessary. The deposition basin should only be large enough to hold that material that flows over the weir in excess of the rate of bypassing. With the assumed pumping capacity of the example sand bypassing program, the deposition basin ideally should be required to temporarily store only about 80,000 cu yd. Short-term influx rates during storms may be much higher than average values; hence additional storage capacity for unexpected events should be provided. The deposition basin capacity should be optimized in conjunction with the bypassing system design rates.

Weir Crest Length

106. It is necessary for a finite weir section to accumulate longshore material in a localized region for a weir jetty and sand bypassing concept to operate successfully at the proposed new entrance channel to Bolsa Chica Bay, California. The average annual breaking wave height for this region is approximately 2 ft; however, there are waves that break with a height approaching 15 ft. In order to intercept the material transported over this range of wave conditions, the weir crest length should be about 400 ft to cover the range of water depths where this range of wave heights breaks in the vicinity of proposed new navigation entrance channels to Bolsa Chica Bay, California. The jetties for stabilizing the proposed navigation channels probably need not extend beyond the 20-ft water depth contour (mllw).

Distribution of Bypassed Material

107. Results of the computer simulation model application of an example bypassing program to ascertain the effect on shoreline evolution east of the proposed east jetty are presented in Figures 81-100 for uniform placement distributions of 300, 500, 1,000, and 2,000 ft. As the distribution of the

bypassed material is extended farther and farther downcoast, those cells nearer the east jetty will experience an increased depletion of material. It appears from the results of this one-dimensional numerical analysis that the bypassed material should be placed as near to the east jetty as practical while remaining outside the structure wave shadow zone. For the average wave climate utilized in this study, the effective equivalent structure wave shadow zone is quite narrow. The actual wave climate existing under prototype conditions will contain perturbations about this average that will cause fluctuations of the shoreline in the bypassing disposal area not accounted for by this computer simulation model. The actual equilibrium shoreline orientation that develops will be in response to the effectiveness of the bypassing program and in response to the actual wave climate.

Nonnavigable Entrance Channel

108. The Los Angeles District (in preparation) has proposed as an alternative to a navigable entrance channel, a nonnavigable channel for tidal exchange between the Pacific Ocean and Bolsa Chica Bay. The concept, which is intended to be self-maintaining by flushing away sediment accumulation by tidal flow, has not been specifically addressed in this study. Because of the large volume of gross transport of littoral material (966,100 cu yd/yr), and the relatively small tidal prism (1,110 acre-ft), the bar bypassing mechanism may become overwhelmed by littoral material during unusually large wave conditions. All potential concepts should be investigated by physical model studies for stability and functional adequacy.

REFERENCES

Ahrens, J. P. 1977 (Jul). "Prediction of Irregular Wave Runup," Coastal Engineering Technical Aid No. 77-2, U. S. Army Coastal Engineering Research Center, CE, Fort Belvoir, Va.

Ahrens, J., and McCartney, B. 1975. "Wave Period Effect on the Stability of Rip Rap," Proceedings, Specialty Conference on Civil Engineering in the Ocean III, American Society of Civil Engineers, Vol II, pp 1019-1034.

Arthur, R. S. 1951 (Oct). "Wave Forecasting and Hindcasting," Proceedings, First Conference on Coastal Engineering, Long Beach, Calif., pp 82-87.

Brownlie, W. R., and Taylor, B. D. 1981 (Feb). "Sediment Management for Southern California Mountains, Coastal Plains and Shoreline; Part C, Coastal Sediment Delivery by Major Rivers in Southern California," EQL Report No. 17-C, California Institute of Technology, Pasadena, Calif.

Dobson, R. S. 1967 (Jun). "Some Applications of a Digital Computer to Hydraulic Engineering Problems," Technical Report No. 80, Stanford University, Stanford, Calif.

Dunham, J. W., and Finn, A. A. 1974 (Dec). "Small-Craft Harbors: Design, Construction, and Operation," Special Report No. 2, U. S. Army Coastal Engineering Research Center, CE, Fort Belvoir, Va.

Emery, K. O. 1960. The Sea off Southern California, Wiley, New York.

Goda, Y. 1969 (Sep). "Reanalysis of Laboratory Data on Wave Transmission over Breakwaters," Report of the Port and Harbor Research Institute, Yokosuka, Japan, Vol 8, No. 3, pp 3-18.

Goda, Y., Takeda, H., and Moriya, Y. 1967 (Apr). "Laboratory Investigation of Wave Transmission over Breakwaters," Report of the Port and Harbor Research Institute, Yokosuka, Japan, No. 13, pp 1-38.

Hales, L. Z. 1980 (Mar). "Erosion Control of Scour During Construction; Present Design and Construction Practice," Technical Report HL-80-3, Report 1, U. S. Army Engineer Waterways Experiment Station, CE, Vicksburg, Miss.

Herron, W. J., and Harris, R. L. 1962 (Jan). "New Methods of Conserving Beach Sand," Shore and Beach, Vol 30, No. 1, pp 34-37.

Inman, D. L. 1976 (Nov). "Man's Impact on the California Coastal Zone," California Department of Navigation and Ocean Development, Sacramento, Calif.

Inman, D. L., and Frautschy, J. D. 1965 (Oct). "Littoral Processes and the Development of Shorelines," Proceedings, Conference on Coastal Engineering, Santa Barbara, Calif., Part 2, pp 511-536.

Komar, P. D. 1973. "Computer Models of Delta Growth due to Sediment Input from Rivers and Longshore Transport," Bulletin, Geological Society of America, Vol 84, pp 2217-2226.

__________. 1976. Beach Processes and Sedimentation, Prentice-Hall, Englewood Cliffs, N. J.

Komar, P. D. 1977. "Modeling of Sand Transport on Beaches and the Resulting Shoreline Evolution," Chap 11, The Sea: Ideas and Observations on Progress in Study of the Seas, E. D. Goldberg, ed., Wiley, New York.

Komar, P. D., and Inman, D. L. 1970. "Longshore Sand Transport on Beaches," Journal of Geophysical Research, Vol 75, pp 5914-5927.

Kroll, D. G. 1975 (Feb). "Estimate of Sediment Discharges, Santa Ana River at Santa Ana and Santa Maria River at Guadalupe, California," Water Resources Investigations 40-74, U. S. Geological Survey, Menlo Park, Calif.

LeMehaute, B., and Soldate, M. 1980 (Jul). "A Numerical Model for Predicting Shoreline Changes," Miscellaneous Report No. 80-6, U. S. Army Coastal Engineering Research Center, CE, Fort Belvoir, Va.

Marine Advisers. 1961 (Jan). "A Statistical Survey of Ocean Wave Characteristics in Southern California Waters," La Jolla, Calif.

National Marine Consultants. 1960 (Dec). "Wave Statistics for Seven Deep Water Stations Along the California Coast," Santa Barbara, Calif.

Pelnard-Considere, R. 1956. "Essai de Theorie de l'Evolution des Formes de Rivage en Plages de Sable et de Galets," Fourth Journees de l'Hydraulique, Les Energies de la Mer, Question III, Rapport No. 1.

Rea, C. C., and Komar, P. D. 1975 (Dec). "Computer Simulation Models of a Hooked Beach Shoreline Configuration," Journal of Sedimentary Petrology, Vol 45, No. 4, pp 866-872.

Seabergh, W. C. 1983 (Mar). "Weir Jetty Performance Model Study; Hydraulic Model Investigation," Technical Report HL-83-5, U. S. Army Engineer Waterways Experiment Station, CE, Vicksburg, Miss.,

Seelig, W. N. 1976 (May). "A Simplified Method for Determining Vertical Breakwater Crest Elevation Considering Wave Height Transmitted by Overtopping," CDM 76-1, U. S. Army Coastal Engineering Research Center, CE, Fort Belvoir, Va.

__________. 1980 (Dec). "Estimation of Wave Transmission Coefficients for Overtopping of Impermeable Breakwaters," CETA 77-9, U. S. Army Coastal Engineering Research Center, CE, Fort Belvoir, Va.

Shepard, F. P., and Wanless, H. R. 1971. Our Changing Coastline, McGraw-Hill, New York.

U. S. Army Coastal Engineering Research Center, CE. 1977. Shore Protection Manual, Vols 1 and 2, Fort Belvoir, Va.

U. S. Army Engineer District, Los Angeles, CE. 1978a (Jun). "Shore Protection, Improvement Design Analysis for Stage 7 Construction, Surfside-Sunset Beach, California," Los Angeles, Calif.

__________. 1978b (Oct). "Monitoring Program for Stage 7 Construction, Surfside-Sunset Beach, California," Los Angeles, Calif.

__________. "Sunset Harbor-Bolsa Chica Bay Feasibility Study, Engineering and Cost Estimate" (in preparation), Los Angeles, Calif.

Weggel, J. R. 1981 (Apr). "Weir Sand-Bypassing Systems," Special Report No. 8, U. S. Army Coastal Engineering Research Center, CE, Fort Belvoir, Va.

Wiegel, R. L., 1964. Oceanographical Engineering, Prentice-Hall, Inc., Englewood Cliffs, N. J.

APPENDIX A: OPEN-OCEAN DEEPWATER WAVE STATISTICS SOUTHERN HEMISPHERE AND NORTHERN HEMISPHERE SWELL

Table A1

Frequency of Annual Occurrence, Open-Ocean Deepwater, Southern Hemisphere

Swell Characteristics (Frequency in Percent of Year)

Deepwater Approach Azimuth = 155° to 164°

Significant Wave Height ft	Wave Period, sec 12-13.9	14-15.9	16-17.9	18-19.9	20+
0.0-0.9	2.1	1.2	1.0	0.1	
1.0-1.9	3.5	3.0	1.7	0.2	
2.0-2.9	1.2	1.1	0.5	0.1	
3.0-3.9	0.2	0.2	0.1		
4.0-4.9					
5.0-5.9					
6.0-6.9					

Note: These data are Station A data from "A Statistical Survey of Ocean Wave Characteristics in Southern California Waters," Marine Advisers (1961).

Table A2

Frequency of Annual Occurrence, Open-Ocean Deepwater, Southern Hemisphere

Swell Characteristics (Frequency in Percent of Year)

Deepwater Approach Azimuth = 165° to 174°

Significant Wave Height ft	Wave Period, sec 12-13.9	14-15.9	16-17.9	18-19.9	20+
0.0-0.9	1.1	1.1	0.5		
1.0-1.9	2.5	1.8	0.8	0.2	0.2
2.0-2.9	0.3	0.5			
3.0-3.9	0.1				
4.0-4.9					
5.0-5.9					
6.0-6.9					

Note: These data are Station A data from "A Statistical Survey of Ocean Wave Characteristics in Southern California Waters," Marine Advisers (1961).

Table A3

Frequency of Annual Occurrence, Open-Ocean Deepwater, Southern Hemisphere

Swell Characteristics (Frequency in Percent of Year)

Deepwater Approach Azimuth = 175° to 184°

Significant Wave Height ft	Wave Period, sec				
	12-13.9	14-15.9	16-17.9	18-19.9	20+
0.0-0.9	1.8	1.0	0.4	0.1	0.1
1.0-1.9	2.2	1.4	0.5		
2.0-2.9	0.4	0.1	0.1		
3.0-3.9					
4.0-4.9					
5.0-5.9					
6.0-6.9					

Note: These data are Station A data from "A Statistical Survey of Ocean Wave Characteristics in Southern California Waters," Marine Advisers (1961).

Table A4

Frequency of Annual Occurrence, Open-Ocean Deepwater, Southern Hemisphere

Swell Characteristics (Frequency in Percent of Year)

Deepwater Approach Azimuth = 185° to 194°

Significant Wave Height ft	Wave Period, sec				
	12-13.9	14-15.9	16-17.9	18-19.9	20+
0.0-0.9	0.4	0.3	0.2		
1.0-1.9	0.5	0.3	0.1		
2.0-2.9		0.1			
3.0-3.9					
4.0-4.9					
5.0-5.9					
6.0-6.9					

Note: These data are Station A data from "A Statistical Survey of Ocean Wave Characteristics in Southern California Waters," Marine Advisers (1961).

Table A5

Frequency of Annual Occurrence, Open-Ocean Deepwater, Southern Hemisphere

Swell Characteristics (Frequency in Percent of Year)

Deepwater Approach Azimuth = 195° to 204°

Significant Wave Height ft	Wave Period, sec				
	12-13.9	14-15.9	16-17.9	18-19.9	20+
0.0-0.9	1.2	0.5		0.2	
1.0-1.9	1.2	0.9	0.2		
2.0-2.9	0.5	0.7	0.2	0.1	
3.0-3.9		0.2	0.2	0.1	
4.0-4.9					
5.0-5.9					
6.0-6.9					

Note: These data are Station A data from "A Statistical Survey of Ocean Wave Characteristics in Southern California Waters," Marine Advisers (1961).

Table A6

Frequency of Annual Occurrence, Open-Ocean Deepwater, Southern Hemisphere

Swell Characteristics (Frequency in Percent of Year)

Deepwater Approach Azimuth = 205° to 214°

Significant Wave Height ft	Wave Period, sec				
	12-13.9	14-15.9	16-17.9	18-19.9	20+
0.0-0.9	1.1	0.5			
1.0-1.9	3.1	2.4	0.3		
2.0-2.9	0.3	0.5	0.2		
3.0-3.9	0.1	0.2	0.2		
4.0-4.9					
5.0-5.9					
6.0-6.9					

Note: These data are Station A data from "A Statistical Survey of Ocean Wave Characteristics in Southern California Waters," Marine Advisers (1961).

Table A7

Frequency of Annual Occurrence, Open-Ocean Deepwater, Northern Hemisphere

Swell Characteristics (Frequency in Percent of Year)

Deepwater Approach Azimuth = 150° to 159°

Significant Wave Height ft	Wave Period, sec 8-9.9	10-11.9	12-13.9	14-15.9	16-17.9
0.0-0.9					
1.0-1.9		0.1			
2.0-2.9			0.1		
3.0-3.9			0.2		
4.0-4.9					
5.0-5.9					
6.0-7.9					
8.0-9.9					

Note: These data are Station A data from "A Statistical Survey of Ocean Wave Characteristics in Southern California Waters," Marine Advisers (1961).

Table A8

Frequency of Annual Occurrence, Open-Ocean Deepwater, Northern Hemisphere

Swell Characteristics (Frequency in Percent of Year)

Deepwater Approach Azimuth = 160° to 169°

Significant Wave Height ft	Wave Period, sec 8-9.9	10-11.9	12-13.9	14-15.9	16-17.9
0.0-0.9					
1.0-1.9					
2.0-2.9					
3.0-3.9					
4.0-4.9					0.1
5.0-5.9					
6.0-7.9					
8.0-9.9					

Note: These data are Station A data from "A Statistical Survey of Ocean Wave Characteristics in Southern California Waters," Marine Advisers (1961).

Table A9

Frequency of Annual Occurrence, Open-Ocean Deepwater, Northern Hemisphere

Swell Characteristics (Frequency in Percent of Year)

Deepwater Approach Azimuth = 170° to 179°

Significant Wave Height ft	Wave Period, sec				
	8-9.9	10-11.9	12-13.9	14-15.9	16-17.9
0.0-0.9					
1.0-1.9	0.1				
2.0-2.9					
3.0-3.9				0.1	
4.0-4.9				0.1	
5.0-5.9					
6.0-7.9					
8.0-9.9					

Note: These data are Station A data from "A Statistical Survey of Ocean Wave Characteristics in Southern California Waters," Marine Advisers (1961).

Table A10

Frequency of Annual Occurrence, Open-Ocean Deepwater, Northern Hemisphere

Swell Characteristics (Frequency in Percent of Year)

Deepwater Approach Azimuth = 180° to 189°

Significant Wave Height ft	Wave Period, sec				
	8-9.9	10-11.9	12-13.9	14-15.9	16-17.9
0.0-0.9					
1.0-1.9	0.1	0.1			
2.0-2.9		0.1	0.1		
3.0-3.9					
4.0-4.9					
5.0-5.9					
6.0-7.9					
8.0-9.9					

Note: These data are Station A data from "A Statistical Survey of Ocean Wave Characteristics in Southern California Waters," Marine Advisers (1961).

Table A11

Frequency of Annual Occurrence, Open-Ocean Deepwater, Northern Hemisphere

Swell Characteristics (Frequency in Percent of Year)

Deepwater Approach Azimuth = 190° to 199°

Significant Wave Height ft	Wave Period, sec				
	8-9.9	10-11.9	12-13.9	14-15.9	16-17.9
0.0-0.9					
1.0-1.9					
2.0-2.9		0.1	0.1		
3.0-3.9					
4.0-4.9					
5.0-5.9					
6.0-7.9					
8.0-9.9					

Note: These data are Station A data from "A Statistical Survey of Ocean Wave Characteristics in Southern California Waters," Marine Advisers (1961).

Table A12

Frequency of Annual Occurrence, Open-Ocean Deepwater, Northern Hemisphere

Swell Characteristics (Frequency in Percent of Year)

Deepwater Approach Azimuth = 200° to 209°

Significant Wave Height ft	Wave Period, sec				
	8-9.9	10-11.9	12-13.9	14-15.9	16-17.9
0.0-0.9					
1.0-1.9			0.1		
2.0-2.9			0.1		
3.0-3.9					
4.0-4.9					
5.0-5.9					
6.0-7.9					
8.0-9.9					

Note: These data are Station A data from "A Statistical Survey of Ocean Wave Characteristics in Southern California Waters," Marine Advisers (1961).

Table A13

Frequency of Annual Occurrence, Open-Ocean Deepwater, Northern Hemisphere

Swell Characteristics (Frequency in Percent of Year)

Deepwater Approach Azimuth = 259° to 281°

Significant Wave Height ft	Wave Period, sec						
	6-7.9	8-9.9	10-11.9	12-13.9	14-15.9	16-17.9	18+
1.0-1.9	0.02	0.48	0.23	0.02	0.05		
2.0-2.9	0.88	2.07	1.06	0.62	0.35	0.11	0.02
3.0-3.9	0.42	0.87	0.50	0.35	0.02	0.09	0.02
4.0-4.9	0.16	0.48	0.23	0.09	0.12	0.02	
5.0-5.9	0.12	0.28	0.32	0.14	0.10		
6.0-6.9		0.31	0.32	0.12	0.07	0.05	
7.0-8.9		0.22	0.32	0.20	0.02		
9.0-10.9		0.02	0.23	0.16	0.10		
11.0-12.9			0.17	0.02	0.07	0.02	
13.0-14.9			0.05	0.09			
15.0-16.9							

Note: These data are Station 7 data from "Wave Statistics for Seven Deep Water Stations Along the California Coast," National Marine Consultants (1960).

APPENDIX B: SHELTERED DEEPWATER WAVE STATISTICS
SOUTHERN HEMISPHERE AND NORTHERN HEMISPHERE SWELL AND SEA

Table B1

Frequency of Annual Occurrence, Sheltered Deepwater, Southern Hemisphere

Swell Characteristics (Frequency in Percent of Year)

Sheltered Deepwater Approach Azimuth = 180°

Significant Wave Height ft	Wave Period, sec				
	12-13.9	14-15.9	16-17.9	18-19.9	20+
0.0-0.9	5.0	3.6	2.1	0.2	0.1
1.0-1.9	10.6	8.3	3.7	0.5	0.2
2.0-2.9	0.3	0.2	0.1		
3.0-3.9					
4.0-4.9					
5.0-5.9					
6.0-6.9					

Note: These data were developed from Station A data from "A Statistical Survey of Ocean Wave Characteristics in Southern California Waters," Marine Advisers (1961).

Table B2

Frequency of Annual Occurrence, Sheltered Deepwater, Northern Hemisphere

Swell Characteristics (Frequency in Percent of Year)

Sheltered Deepwater Approach Azimuth = 180°

Significant Wave Height ft	Wave Period, sec				
	8-9.9	10-11.9	12-13.9	14-15.9	16-17.9
0.0-0.9					
1.0-1.9	0.2	0.4	0.3		
2.0-2.9			0.1	0.1	
3.0-3.9				0.1	0.1
4.0-4.9					
5.0-5.9					
6.0-7.9					
8.0-9.9					

Note: These data were developed from Station A data from "A Statistical Survey of Ocean Wave Characteristics in Southern California Waters," Marine Advisers (1961).

Table B3

Frequency of Annual Occurrence, Sheltered Deepwater, Northern Hemisphere

Swell Characteristics (Frequency in Percent of Year)

Sheltered Deepwater Approach Azimuth = 270°

Significant Wave Height ft	Wave Period, sec 6-7.9	8-9.9	10-11.9	12-13.9	14-15.9	16-17.9	18+
1.0-1.9	0.02	0.48	0.23	0.02	0.05		
2.0-2.9	0.88	2.07	1.06	0.62	0.35	0.11	0.02
3.0-3.9	0.42	0.87	0.50	0.35	0.02	0.09	0.02
4.0-4.9	0.16	0.48	0.23	0.09	0.12	0.02	
5.0-5.9	0.12	0.28	0.32	0.14	0.10		
6.0-6.9		0.31	0.32	0.12	0.07	0.05	
7.0-8.9		0.22	0.32	0.20	0.02		
9.0-10.9		0.02	0.23	0.16	0.10		
11.0-12.9			0.17	0.02	0.07	0.02	
13.0-14.9			0.05	0.09			
15.0-16.9							

Note: These data were developed from Station 7 data from "Wave Statistics for Seven Deep Water Stations Along the California Coast," National Marine Consultants (1960).

Table B4

Frequency of Annual Occurrence, Sheltered Deepwater,

Sea Characteristics (Frequency in Percent of Year)

Sheltered Deepwater Approach Azimuth = 157°

Significant Wave Height ft	Wave Period, sec				
	2-3.9	4-5.9	6-7.9	8-9.9	10-11.9
0.0-0.9	1.21				
1.0-1.9	0.48				
2.0-2.9	0.15	0.06			
3.0-3.9		0.13			
4.0-4.9		0.03			
5.0-5.9		0.03	0.01		
6.0-7.9			0.02		
8.0-9.9			0.01		
10.0-11.9					
12.0-13.9					
14.0-15.9					0.01

Note: These data are Station B data from "A Statistical Survey of Ocean Wave Characteristics in Southern California Waters," Marine Advisers (1961).

Table B5

Frequency of Annual Occurrence, Sheltered Deepwater,

Sea Characteristics (Frequency in Percent of Year)

Sheltered Deepwater Approach Azimuth = 180°

Significant Wave Height ft	Wave Period, sec				
	2-3.9	4-5.9	6-7.9	8-9.9	10-11.9
0.0-0.9	4.18				
1.0-1.9	0.61	0.49	0.04		
2.0-2.9	0.02	0.25	0.03		
3.0-3.9		0.15			
4.0-4.9		0.12			
5.0-5.9			0.05		
6.0-7.9			0.06		
8.0-9.9			0.03		
10.0-11.9				0.03	
12.0-13.9				0.01	
14.0-15.9					

Note: These data are Station B data from "A Statistical Survey of Ocean Wave Characteristics in Southern California Waters," Marine Advisers (1961).

Table B6

Frequency of Annual Occurrence, Sheltered Deepwater,

Sea Characteristics (Frequency in Percent of Year)

Sheltered Deepwater Approach Azimuth = 202°

Significant Wave Height ft	Wave Period, sec 2-3.9	4-5.9	6-7.9	8-9.9	10-11.9
0.0-0.9	0.28				
1.0-1.9	0.13	0.01	0.26		
2.0-2.9		0.08			
3.0-3.9		0.06			
4.0-4.9		0.03			
5.0-5.9			0.01		
6.0-7.9			0.02		
8.0-9.9			0.02		
10.0-11.9				0.01	
12.0-13.9				0.01	
14.0-15.9					

Note: These data are Station B data from "A Statistical Survey of Ocean Wave Characteristics in Southern California Waters," Marine Advisers (1961).

Table B7

Frequency of Annual Occurrence, Sheltered Deepwater, Sea Characteristics (Frequency in Percent of Year) Sheltered Deepwater Approach Azimuth = 225°

Significant Wave Height ft	Wave Period, sec				
	2-3.9	4-5.9	6-7.9	8-9.9	10-11.9
0.0-0.9	4.94				
1.0-1.9	1.12				
2.0-2.9		0.38			
3.0-3.9		0.18			
4.0-4.9		0.11			
5.0-5.9		0.03			
6.0-7.9			0.05		
8.0-9.9					
10.0-11.9					
12.0-13.9					
14.0-15.9					

Note: These data are Station B data from "A Statistical Survey of Ocean Wave Characteristics in Southern California Waters," Marine Advisers (1961).

Table B8

Frequency of Annual Occurrence, Sheltered Deepwater,

Sea Characteristics (Frequency in Percent of Year)

Sheltered Deepwater Approach Azimuth = 247°

Significant Wave Height ft	Wave Period, sec				
	2-3.9	4-5.9	6-7.9	8-9.9	10-11.9
0.0-0.9	2.01				
1.0-1.9	0.33		0.27	0.08	
2.0-2.9	0.14			0.04	0.03
3.0-3.9		0.12			
4.0-4.9		0.01			
5.0-5.9					
6.0-7.9					
8.0-9.9					
10.0-11.9					
12.0-13.9					
14.0-15.9					

Note: These data are Station B data from "A Statistical Survey of Ocean Wave Characteristics in Southern California Waters," Marine Advisers (1961).

Table B9

Frequency of Annual Occurrence, Sheltered Deepwater, Sea Characteristics (Frequency in Percent of Year)

Sheltered Deepwater Approach Azimuth = 270°

Significant Wave Height ft	Wave Period, sec				
	2-3.9	4-5.9	6-7.9	8-9.9	10-11.9
0.0-0.9	15.53				
1.0-1.9	2.53		1.91	0.53	0.03
2.0-2.9		1.03		0.21	0.17
3.0-3.9		0.52			
4.0-4.9		0.35			
5.0-5.9			0.13		
6.0-7.9			0.12		
8.0-9.9			0.03		
10.0-11.9				0.02	
12.0-13.9					
14.0-15.9					

Note: These data are *Station B data from* "A Statistical Survey of Ocean Wave Characteristics in Southern California Waters," Marine Advisers (1961).

APPENDIX C: ANNUAL POTENTIAL LONGSHORE TRANSPORT

Table C1

Annual Potential Longshore Transport

Southern Hemisphere Swell Characteristics

Sheltered Deepwater Approach Azimuth = 180°

Significant Wave Height ft		Wave Period, sec				
		12-13.9	14-15.9	16-17.9	18-19.9	20+
0.0-0.9	T =	5.0	3.6	2.1	0.2	0.1
	H_b =	1.0	1.0	1.0	1.0	1.0
	α_b =	+7.5	+8.2	+8.7	+9.3	+10.0
	Q =	+3,150	+2,480	+1,540	+160	+80
1.0-1.9	T =	10.6	8.3	3.7	0.5	0.2
	H_b =	2.2	2.2	2.2	2.1	2.1
	α_b =	+9.7	+10.0	+10.2	+10.8	+11.1
	Q =	+62,020	+50,060	+22,760	+2,900	+1,190
2.0-2.9	T =	0.3	0.2	0.1		
	H_b =	3.3	3.2	3.2		
	α_b =	+11.6	+11.7	+11.9		
	Q =	+5,780	+3,600	+1,830		
3.0-3.9						

Legend

t = time, percent of year

H_b = breaker height, ft

α_b = breaker angle, deg

Q = potential longshore transport, cu yd/yr

Table C2

Annual Potential Longshore Transport

Northern Hemisphere Swell Characteristics

Sheltered Deepwater Approach Azimuth = 180°

Significant Wave Height ft		Wave Period, sec 8-9.9	10-11.9	12-13.9	14-15.9	16-17.9
0.0-0.9						
1.0-1.9	T =	0.2	0.4	0.3		
	H_b =	2.1	2.2	2.2		
	α_b =	+12.0	+10.7	+9.7		
	Q =	+1,290	+2,580	+1,760		
2.0-2.9	T =			0.1	0.1	
	H_b =			3.3	3.2	
	α_b =			+11.6	+11.7	
	Q =			+1,930	+1,800	
3.0-3.9	T =				0.1	0.1
	H_b =				4.3	4.2
	α_b =				+13.2	+13.2
	Q =				+4,250	+4,010

Legend

t = time, percent of year

H_b = breaker height, ft

α_b = breaker angle, deg

Q = potential longshore transport, cu yd/yr

Table C3

Annual Potential Longshore Transport

Northern Hemisphere Swell Characteristics

Sheltered Deepwater Approach Azimuth = 270°

Significant Wave Height ft		Wave Period, sec 6-7.9	8-9.9	10-11.9	12-13.9	14-15.9	16-17.9	18+
1.0-1.9	T =	0.02	0.48	0.23	0.02	0.05		
	H_b =	1.9	1.9	1.9	1.9	1.9		
	α_b =	-10.0	-6.7	-3.2	-1.2	-0.9		
	Q =	-80	-1,350	-310	-10	-20		
2.0-2.9	T =	0.88	2.07	1.06	0.62	0.35	0.11	0.02
	H_b =	2.9	2.9	2.9	2.9	2.9	2.9	2.9
	α_b =	-12.5	-8.5	-4.4	-2.0	-1.3	-0.8	-0.5
	Q =	-13,240	-21,170	-5,610	-1,490	-550	-110	-10
3.0-3.9	T =	0.42	0.87	0.50	0.35	0.02	0.09	0.02
	H_b =	3.8	3.8	3.7	3.7	3.8	3.8	3.8
	α_b =	-14.5	-9.9	-5.3	-2.6	-1.7	-1.0	-0.5
	Q =	-14,400	-20,370	-5,860	-2,010	-80	-210	-20
4.0-4.9	T =	0.16	0.48	0.23	0.09	0.12	0.02	
	H_b =	4.7	4.7	4.6	4.6	4.7	4.7	
	α_b =	-15.7	-10.8	-5.9	-3.0	-2.0	-1.2	
	Q =	-10,110	20,869	-5,170	-1,030	-970	-100	
5.0-5.9	T =	0.12	0.28	0.32	0.14	0.10		
	H_b =	5.8	5.8	5.7	5.7	5.7		
	α_b =	-16.7	-11.6	-6.3	-3.3	-2.2		
	Q =	-13,640	-22,110	-13,140	-3,010	-1,430		
6.0-6.9	T =		0.31	0.32	0.12	0.07	0.05	
	H_b =		6.4	6.3	6.3	6.3	6.3	
	α_b =		-12.3	-6.8	-3.5	-2.3	-1.3	
	Q =		-33,200	-18,210	-3,520	-1,350	-540	

(Continued)

Table C3 (Concluded)

Significant Wave Height ft		Wave Period, sec 6-7.9	8-9.9	10-11.9	12-13.9	14-15.9	16-17.9	18+
7.0-8.9	T =		0.22	0.32	0.20	0.02		
	H_b =		7.5	7.4	7.4	7.4		
	α_b =		-13.1	-7.3	-3.8	-2.4		
	Q =		-37,300	-29,240	-9,510	-600		
9.0-10.9	T =		0.02	0.23	0.16	0.10		
	H_b =		9.1	8.9	8.9	9.0		
	α_b =		-14.2	-8.0	-4.3	-2.7		
	Q =		-5,960	-36,530	-13,660	-5,510		
11.0-12.9	T =			0.17	0.02	0.07	0.02	
	H_b =			10.4	10.3	10.3	10.3	
	α_b =			-8.5	-4.5	-2.8	-1.3	
	Q =			-42,350	-2,580	-5,610	-740	
13.0-14.9	T =			0.05	0.09			
	H_b =			11.6	11.5			
	α_b =			-9.0	-4.8			
	Q =			-17,330	-16,280			
15.0-16.9								

Legend

t = time, percent of year

H_b = breaker height, ft

α_b = breaker angle, deg

Q = potential longshore transport, cu yd/yr

Table C4

Annual Potential Longshore Transport

Sea Characteristics

Sheltered Deepwater Approach Azimuth = 157°

Significant Wave Height ft		Wave Period, sec 2-3.9	4-5.9	6-7.9	8-9.9	10-11.9
0.0-0.9	T =	1.21				
	H_b =	0.5				
	α_b =	+20.5				
	Q =	+370				
1.0-1.9	T =	0.48				
	H_b =	1.1				
	α_b =	+27.0				
	Q =	+1,380				
2.0-2.9	T =	0.15	0.06			
	H_b =	1.7	2.3			
	α_b =	+33.0	+25.2			
	Q =	+1,570	+1,020			
3.0-3.9	T =		0.13			
	H_b =		3.1			
	α_b =		+28.7			
	Q =		+5,300			
4.0-4.9	T =		0.03			
	H_b =		3.9			
	α_b =		+31.3			
	Q =		+2,370			
5.0-5.9	T =		0.03	0.01		
	H_b =		4.7	5.1		
	α_b =		+33.7	+26.5		
	Q =		+4,070	+1,310		

(Continued)

Table C4 (Concluded)

Significant Wave Height ft		Wave Period, sec 2-3.9	4-5.9	6-7.9	8-9.9	10-11.9
6.0-7.9	T =			0.02		
	H_b =			6.3		
	α_b =			+28.3		
	Q =			+4,740		
8.0-9.9	T =			0.01		
	H_b =			8.0		
	α_b =			+31.6		
	Q =			+4,810		
10.0-11.9						
12.0-13.9						
14.0-15.9	T =					0.01
	H_b =					12.4
	α_b =					+28.8
	Q =					+13,100

Legend

t = time, percent of year

H_b = breaker height, ft

α_b = breaker angle, deg

Q = potential longshore transport, cu yd/yr

Table C5

Annual Potential Longshore Transport

Sea Characteristics

Sheltered Deepwater Approach Azimuth = 180°

Significant Wave Height ft		Wave Period, sec 2-3.9	4-5.9	6-7.9	8-9.9	10-11.9
0.0-0.9	T =	4.18				
	H_b =	0.6				
	α_b =	+17.0				
	Q =	+1,670				
1.0-1.9	T =	0.61	0.49	0.04		
	H_b =	1.4	1.7	1.9		
	α_b =	+22.0	+16.5	+13.0		
	Q =	+2,620	+2,560	+220		
2.0-2.9	T =	0.02	0.25	0.03		
	H_b =	2.1	2.6	2.9		
	α_b =	+22.0	+20.0	+15.7		
	Q =	+240	+4,580	+570		
3.0-3.9	T =		0.15			
	H_b =		3.6			
	α_b =		+23.0			
	Q =		+7,130			
4.0-4.9	T =		0.12			
	H_b =		4.5			
	α_b =		+25.0			
	Q =		+10,830			
5.0-5.9	T =			0.05		
	H_b =			5.4		
	α_b =			+21.5		
	Q =			+6,120		

(Continued)

Table C5 (Concluded)

Significant Wave Height ft		Wave Period, sec 2-3.9	4-5.9	6-7.9	8-9.9	10-11.9
6.0-7.9	T =			0.06		
	H_b =			7.1		
	α_b =			+23.5		
	Q =			+15,910		
8.0-9.9	T =			0.03		
	H_b =			9.0		
	α_b =			+25.5		
	Q =			+15,620		
10.0-11.9	T =				0.03	
	H_b =				11.0	
	α_b =				+24.2	
	Q =				+24,480	
12.0-13.9	T =				0.01	
	H_b =				12.6	
	α_b =				+25.6	
	Q =				+12,120	
14.0-15.9						

Legend

t = time, percent of year

H_b = breaker height, ft

α_b = breaker angle, deg

Q = potential longshore transport, cu yd/yr

Table C6

Annual Potential Longshore Transport

Sea Characteristics

Sheltered Deepwater Approach Azimuth = 202°

Significant Wave Height ft		Wave Period, sec 2-3.9	4-5.9	6-7.9	8-9.9	10-11.9
0.0-0.9	T =	0.28				
	H_b =	0.7				
	α_b =	+9.5				
	Q =	+90				
1.0-1.9	T =	0.13	0.01	0.26		
	H_b =	1.5	1.9	2.2		
	α_b =	+12.5	+9.7	+8.0		
	Q =	+380	+40	+1,260		
2.0-2.9	T =		0.08			
	H_b =		2.9			
	α_b =		+11.6			
	Q =		+1,120			
3.0-3.9	T =		0.06			
	H_b =		3.8			
	α_b =		+13.2			
	Q =		+1,870			
4.0-4.9	T =		0.03			
	H_b =		4.8			
	α_b =		+14.5			
	Q =		+1,850			
5.0-5.9	T =			0.01		
	H_b =			5.9		
	α_b =			+12.7		
	Q =			+900		

(Continued)

Table C6 (Concluded)

Significant Wave Height ft		Wave Period, sec 2-3.9	4-5.9	6-7.9	8-9.9	10-11.9
6.0-7.9	T =			0.02		
	H_b =			7.3		
	α_b =			+13.7		
	Q =			+3,320		
8.0-9.9	T =			0.02		
	H_b =			9.1		
	α_b =			+15.0		
	Q =			+6,300		
10.0-11.9	T =				0.01	
	H_b =				10.7	
	α_b =				+14.8	
	Q =				+4,660	
12.0-13.9	T =				0.01	
	H_b =				12.3	
	α_b =				+15.7	
	Q =				+7,000	
14.0-15.9						

Legend

t = time, percent of year

H_b = breaker height, ft

α_b = breaker angle, deg

Q = potential longshore transport, cu yd/yr

Table C7

Annual Potential Longshore Transport

Sea Characteristics

Sheltered Deepwater Approach Azimuth = 225°

Significant Wave Height ft		Wave Period, sec 2-3.9	4-5.9	6-7.9	8-9.9	10-11.9
0.0-0.9	T =	4.94				
	H_b =	0.7				
	α_b =	+1.3				
	Q =	+220				
1.0-1.9	T =	1.12				
	H_b =	1.5				
	α_b =	+1.2				
	Q =	+310				
2.0-2.9	T =		0.38			
	H_b =		2.9			
	α_b =		+1.7			
	Q =		+780			
3.0-3.9	T =		0.18			
	H_b =		3.9			
	α_b =		+1.8			
	Q =		+820			
4.0-4.9	T =		0.11			
	H_b =		4.9			
	α_b =		+2.0			
	Q =		+980			
5.0-5.9	T =		0.03			
	H_b =		5.8			
	α_b =		+2.1			
	Q =		+430			

(Continued)

Table C7 (Concluded)

Significant Wave Height ft		Wave Period, sec 2-3.9	4-5.9	6-7.9	8-9.9	10-11.9
6.0-7.9	T =			0.05		
	H_b =			7.3		
	α_b =			+3.2		
	Q =			+1,940		
8.0-9.9						
10.0-11.9						
12.0-13.9						
14.0-15.9						

Legend

t = time, percent of year

H_b = breaker height, ft

α_b = breaker angle, deg

Q = potential longshore transport, cu yd/yr

Table C8

Annaul Potential Longshore Transport

Sea Characteristics

Sheltered Deepwater Approach Azimuth = 247°

Significant Wave Height ft		Wave Period, sec				
		2-3.9	4-5.9	6-7.9	8-9.9	10-11.9
0.0-0.9	T =	2.01				
	H_b =	0.8				
	α_b =	-7.5				
	Q =	-730				
1.0-1.9	T =	0.33		0.27	0.08	
	H_b =	1.6		2.2	2.4	
	α_b =	-10.5		-4.6	-1.4	
	Q =	-940		-750	-80	
2.0-2.9	T =	0.14			0.04	0.03
	H_b =	2.4			3.6	3.9
	α_b =	-12.8			-2.0	+1.3
	Q =	-1,340			-170	+100
3.0-3.9	T =		0.12			
	H_b =		4.0			
	α_b =		-10.4			
	Q =		-3,360			
4.0-4.9	T =		0.01			
	H_b =		4.9			
	α_b =		-11.2			
	Q =		-500			

Legend

t = time, percent of year

H_b = breaker height, ft

α_b = breaker angle, deg

Q = potential longshore transport, cu yd/yr

Table C9

Annual Potential Longshore Transport

Sea Characteristics

Sheltered Deepwater Approach Azimuth = 270°

Significant Wave Height ft		Wave Period, sec 2-3.9	4-5.9	6-7.9	8-9.9	10-11.9
0.0-0.9	T =	15.53				
	H_b =	0.7				
	α_b =	-15.4				
	Q =	-8,240				
1.0-1.9	T =	2.53		1.91	0.53	0.03
	H_b =	1.4		1.9	1.9	1.9
	α_b =	-20.7		-10.0	-6.7	-3.2
	Q =	-10,210		-7,990	-1,490	-40
2.0-2.9	T =		1.03		0.21	0.17
	H_b =		2.8		2.9	2.9
	α_b =		-18.5		-8.5	-4.5
	Q =		-21,000		-2,150	-920
3.0-3.9	T =		0.52			
	H_b =		3.6			
	α_b =		-20.9			
	Q =		-22,450			
4.0-4.9	T =		0.35			
	H_b =		4.5			
	α_b =		-22.6			
	Q =		-28,550			
5.0-5.9	T =			0.13		
	H_b =			5.6		
	α_b =			-16.7		
	Q =			-13,540		

(Continued)

Table C9 (Concluded)

Significant Wave Height ft		Wave Period, sec 2-3.9	4-5.9	6-7.9	8-9.9	10-11.9
6.0-7.9	T =			0.12		
	H_b =			6.9		
	α_b =			-18.1		
	Q =			-22,820		
8.0-9.9	T =			0.03		
	H_b =			8.6		
	α_b =			-19.6		
	Q =			-10,720		
10.0-11.9	T =				0.02	
	H_b =				10.0	
	α_b =				-14.6	
	Q =				-7,760	
12.0-13.9						
14.0-15.9						

Legend

t = time, percent of year

H_b = breaker height, ft

α_b = breaker angle, deg

Q = potential longshore transport, cu yd/yr

APPENDIX D: APPLICATION OF KOMAR'S COMPUTER SIMULATION MODEL FOR SHORELINE EVOLUTION

SHORELINE CHANGES
ANAHEIM BAY EAST JETTY TO HUNTINGTON BEACH, CALIFORNIA

```
      DIMENSION Z(301),Y(301),ZZ(301),QIN(301),QOUT(301),DANG(301),1ANG(301),
     H(301),VOL(301),DELS(301),YY(301),YYY(301),ZZZ(301),1DDANG(301)
     AANG(301),QQOUT(301),QQIN(301),VVOL(301),DDELS(301),1YYYY(301),
     EFFEC(301),SC(301)
      T=0.
      DELT=1.
      DELX=100.
      READ (5,100)(Z(I),I=301)
  100 FORMAT (8F10.2)
      DO 120 I=1,300
      YYY(I)=(Z(I)+Z(I+1))/2.
  120 Y(I)=(Z(I)+Z(I+1))/2.
      DO 140 I=1,300
      ZZZ(I)=YYY(I)
  140 ZZ(I)=Y(I)
      DO 200 I=1,143
      DANG(I)=(Y(I+1)-Y(I))
      DANG(I)=ATAN(DANG(I)/100.)*57.2958
  200 ANG(I)=21.+DANG(I)
      ANG(144)=ANG(143)/2.
      DO 10200 I=1,299
      DDANG(I)=(YYY(I+1)-YYY(I))
      DDANG(I)=ATAN(DDANG(I)/100.)*57.2958
10200 AANG(I)=21.+DDANG(I)
      AANG(300)=AANG(299)
      DO 250 I=151,299
      DANG(I)=(Y(I+1)-Y(I))
      DANG(I)=ATAN(DANG(I)/100.)*57.2958
  250 ANG(I)=21.+DANG(I)
      DO 270 I=145,150
      ANG(I)=0.
      Y(I)=0.
      DELS(I)=0.
      ZZ(I)=0.
      QOUT(I)=0.
  270 QIN(I)=0.
      ANG(300)=ANG(299)
  500 READ (5,515) G
  515 FORMAT (1F10.3)
      IF (G .EQ. 0.) GO TO 915
      DO 527 I=1,300
  527 H(I)=0.
      H(1)=0.04*H(I)
      H(2)=0.08*H(I)
      H(3)=0.12*H(I)
      H(4)=0.16*H(I)
      H(5)=0.20*H(I)
      H(6)=0.24*H(I)
      H(7)=0.28*H(I)
```

```
      H(8)=0.32*H(I)
      H(9)=0.36*H(I)
      H(10)=0.40*H(I)
      H(11)=0.44*H(I)
      H(12)=0.48*H(I)
      H(13)=0.52*H(I)
      H(14)=0.56*H(I)
      H(15)=0.60*H(I)
      H(16)=0.64*H(I)
      H(17)=0.68*H(I)
      H(18)=0.72*H(I)
      H(19)=0.76*H(I)
      H(20)=0.80*H(I)
      H(21)=0.84*H(I)
      H(22)=0.88*H(I)
      H(23)=0.92*H(I)
      H(24)=0.96*H(I)
      QIN(1)=0.
      QQIN(1)=0.
      QOUT(144)=0.
      DO 3600 I=1,143
      DANG(I)=(Y(I+1)-Y(I))
      DANG(I)=ATAN(DANG(I)/100.)*57.2958
 3600 ANG(I)=21.+DANG(I)
      ANG(144)=ANG(143)/2.
      DO 3650 I=145,150
      AVG(I)=0.
      Y(I)=0.
      YY(I)=0.
 3650 ZZ(I)=0.
      DO 3800 I=151,299
      DANG(I)=(Y(I+1)-Y(I))
      DANG(I)=ATAN(DANG(I)/100.)*57.2958
 3800 ANG(I)=21.+DANG(I)
      ANG(300)=ANG(299)
      DO 110 K=1,720
      T=T+DELT
      DO 550 I=1.143
      QOUT(I)=27.861739*(H(I)**2.5)*SIN(2.*ANG(I)*0.0174533)
  550 QIN(I+1)=QOUT(I)
      DO 10550 I=1,300
      QQOUT(I)=27.861739*(H(I)**2.5)*SIN(2.*AANG(I)*0.0174533)
10550 QQIN(I+1)=QQOUT(I)
      DO 10750 I=1,300
      VVOL(I)=QQIN(I)-QQOUT(I)
      DDELS(I)=(VVOL(I)*27.)/2500.
      YYY(I)=YYY(I)-DDELS(I)
10750 YYYY(I)=YYY(I)-ZZZ(I)
      DO 10800 I=1,299
      DDANG(I)=(YYY(I+1)-YYY(I))
      DDANG(I)+ATAN(DDANG(I)/100.)*57.2958
10800 AANG(I)=21.+DDANG(I)
      AANG(300)=AANG(299)
```

```
      DO 560 I=1,144
      VOL(I)=QIN(I)-QOUT(I)
      DELS(I)=(VOL(I)*27.)/2500.
      Y(I)=Y(I)-DELS(I)
      IF (Y(144) .LT. 4280.83)THEN
      Y(144)=4280.83
      ENDIF
      QIN(151)=0.
560   YY(I)=Y(I)-ZZ(I)
      DO 600 I=1,143
      DANG(I)=(Y(I+1)-Y(I))
      DANG(I)=ATAN(DANG(I)/100.)*57.2958
600   ANG(I)=21.+DANG(I)
      ANG(144)=ANG(143)/2.
      DO 650 I=145,150
      ANG(I)=0.
      Y(I)=0.
      YY(I)=0.
650   ZZ(I)=0.
      DO 700 I=151,300
      ANG(300)=ANG(299)
      QOUT(I)=27.861739*(H(I)**2.5)*SIN(2.*ANG(I)*0.0174533)
700   QIN(I+1)=QOUT(I)
      IF (H(151) .EQ. 2.873) THEN
      QIN(151)=QIN(151)+96.
      ENDIF
      IF (H(151) .EQ. 3.405) THEN
      QIN(151)=QIN(151)+96
      ENDIF
      IF (H(151) .EQ. 2.278) THEN
      QIN(151)=QIN(151)+96.
      ENDIF
      IF (H(151) .EQ. 2.582) THEN
      QIN(151)=QIN(151)+96.
      ENDIF
      DO 750 I=151,300
      VOL(I)=QIN(I)-QOUT(I)
      DELS(I)=(VOL(I)*27.)/2500.
      Y(I)=Y(I)-DELS(I)
750   YY(I)=Y(I)-ZZ(I)
      DO 800 I=151,299
      DANG(I)=(Y(I+1)-Y(I))
      DANG(I)=ATAN(DANG(I)/100.)*57.2928
800   ANG(I)=21.+DANG(I)
      ANG(300)=ANG(299)
110   CONTINUE
      WRITE (6,405) T, G
405   FORMAT (1H1,//,30X,@TIME=@F8.0,1X,@HOURS@,20X,F10.3,/)
      WRITE (6,426)
426   FORMAT (1X,@ELEMENT@,6X,@QIN@,7X,@QOUT@,7X,@ANGLE@,4X,1@SHORE CHANGE@,/)
      DO 900 I=1,300
      YY(I)=0.-YY(I)
      YYYY(I)=0.-YYYY(I)
```

```
  900 EFFEC(I)=YY(I)-YYYY(I)
      DO 18000 I=1,150
      SC(I)=YY(I)
18000 CONTINUE
      DO 17050 I=151,300
17050 SC(I)=EFFEC(I)
      CONTINUE
      DO 6913 I=150,300
      WRITE (6,540) I,QIN(I),QOUT(I),ANG(I),SC(I)
  540 FORMAT(3X,I3,5X,F6.1,5X,F6.1,6X,F6.2,7X,F7.1)
 6913 CONTINUE
  115 CONTINUE
      GO TO 500
  915 CONTINUE
 3000 READ (5,515) G
      IF (G .EQ. 0.) GO TO 500
      IF (G .EQ. 100.) GO TO 1915
      DO 1527 I=1,300
 1527 H(I)=G
      H(142)=0.80*H(142)
      H(143)=0.60*H(143)
      H(144)=0.40*H(144)
      QQOUT(1)=0.
      QOUT(1)=0.
      QOUT(151)=0.
      QIN(144)=0.
      DO 1600 I=2,144
      DANG(I)=(Y(I-1)-Y(I))
      DANG(I)=ATAN(DANG(I)/100.)*57.2958
 1600 ANG(I)=DANG(I)
      ANG(1)=ANG(2)/2.
      DO 11600 I=2,300
      DDANG(I)=(YYY(I-1)-YYY(I))
      DDANG(I)=ATAN(DDANG(I)/100.)*57.2958
11600 AANG(I)=DDANG(I)
      AANG(1)=AANG(2)/2.
      DO 1620 I=152,300
      DANG(I)=(Y(I-1)-Y(I))
      DANG(I)=ATAN(DANG(I)/100.)*57.2958
 1620 ANG(I)=DANG(I)
      ANG(151)=ANG(152)/2.
      DO 1640 I=145,150
      ANG(I)=0.
      Y(I)=0.
      YY(I)=0.
 1640 ZZ(I)=0.
      DO 2110 K=1,720
      T=T+DELT
      DO 2550 I=2,144
      QOUT(I)=27.861739*(H(I)**2.5)*SIN(2.*ANG(I)*0.0174533)
 2550 QIN(I-1)=QOUT(I)
      DO 12550 I=2,300
      QQOUT(I)=27.861739*(H(I)**2.5)*SIN(2.*AANG(I)*0.0174533)
```

AD-A147 549 POTENTIAL EFFECTS OF NEW ENTRANCE CHANNEL TO BOLSA CHICA BAY CALIFORNIA O..(U) COASTAL ENGINEERING RESEARCH CENTER VICKSBURG MS L Z HALES OCT 84 3/3

UNCLASSIFIED CERC-MP-84-10 F/G 13/2 NL

END

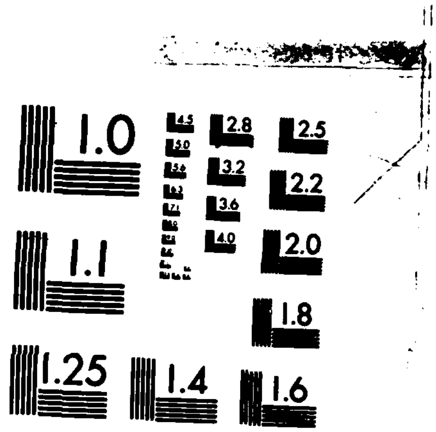
1.0
1.1
1.25
1.4
1.6
1.8
2.0
2.2
2.5
2.8
3.2
3.6
4.0
4.5
5.0

```
12550 QQIN(I-1)=QQOUT(I)
      QQIN(300)=QQOUT(300)
      DO 12560 I=1,300
      VVOL(I)=QQIN(I)-QQOUT(I)
      DDELS(I)=(VVOL(I)*27.)/2500.
      YYY(I)=YYY(I)-DDELS(I)
12560 YYYY(I)=YYY(I)-ZZZ(I)
      DO 12570 I=2,300
      DDANG(I)=(YYY(I-1)-YYY(I))
      DDANG(I)=ATAN(DDANG(I)/100.)*57.2958
12570 AANG(I)=DDANG(I)
      AANG(1)=AANG(2)/2.
      DO 2560 I=1,144
      VOL(I)=QIN(I)-QOUT(I)
      DELS(I)=(VOL(I)*27.)/2500.
      Y(I)=Y(I)-DELS(I)
 2560 YY(I)=Y(I)-ZZ(I)
      DO 2570 I=2,144
      DANG(I)=(Y(I-1)-Y(I))
      DANG(I)=ATAN(DANG(I)/100.)*57.2958
 2570 ANG(I)=DANG(I)
      ANG(1)=ANG(2)/2.
      DO 6640 I=145,150
      ANG(I)=0.
      Y(I)=0.
      YY(I)=0.
 6640 ZZ(I)=0.
      ANG(151)=ANG('52)/2.
      DO 2600 I=152,300
      QQOUT(I)=27.861739*(H(I)**2.5)*SIN(2.*ANG(I)*0.0174533)
 2600 QIN(I-1)=QOUT(I)
      QIN(300)=QOUT(300)
      DO 2620 I=151,300
      VOL(I)=QIN(I)-QOUT(I)
      DELS(I)=(VOL(I)*27.)/2500.
      Y(I)=Y(I)-DELS(I)
 2620 YY(I)=Y(I)-ZZ(I)
      DO 7000 I=152,300
      DANG(I)=(Y(I-1)-Y(I))
      DANG(I)=ATAN(DANG(I)/100.)*57.2958
 7000 ANG(I)=DANG(I)
      ANG(151)=ANG(152)/2.
 2110 CONTINUE
      WRITE (6,405) T, G
      WRITE (6,426)
      DO 2900 I=1,300
      YY(I)=0.-YY(I)
      YYYY(I)=0.-YYYY(I)
 2900 EFFEC(I)=YY(I)-YYYY(I)
      DO 78000 I=1,150
      SC(I)=YY(I)
78000 CONTINUE
      DO 77050 I=151,300
```

```
77050 SC(I)=EFFEC(I)
      CONTINUE
      DO 7913 I=150,300
      WRITE (6,540) I,QIN(I),QOUT(I),ANG(I),SC(I)
 7913 CONTINUE
      GO TO 3000
 1915 CONTINUE
      STOP
      END
```

Input Parameters

Z(I) = Distance from arbitrary baseline to original shoreline prior to model operation

G = Equivalent monthly wave height producing a known quantity of longshore transport

APPENDIX E: NOTATION

a	Rubble-mound weir structure empirical coefficient, dimensionless
b	Rubble-mound weir structure empirical coefficient, dimensionless
B	Weir structure crest width, ft
C	Wave celerity, ft/sec
C_g	Propagation velocity of wave energy, ft/sec
d	Depth parameter in Komar's computer simulation model, ft
d_{min}	Minimum channel depth, ft
d_s	Water depth at weir structure, ft
D	Local water depth, ft; vessel draft, ft
g	Gravitational constant, 32.174 ft/sec^2
h	Height of weir structure crest above bottom, ft
H	Wave height, ft
H_b	Breaking wave height, ft
H_i	Incident wave height, ft
H_o	Deepwater wave height, ft
H_s	Significant wave height, ft
H_t	Transmitted wave height, ft
L_o	Deepwater wavelength, ft
OD	Overdepth, ft
P_{ls}	Longshore component of wave energy flux, ft-lb/ft/sec
Q_n	Longshore transport in a northerly direction, cu yd/yr
Q_s	Longshore transport in a southerly direction, cu yd/yr
Q_{ls}	Longshore transport, cu yd/yr
Q_{net}	Net longshore transport, cu yd/yr
QIN	Longshore transport into a cell, cu yd
QOUT	Longshore transport out of a cell, cu yd
R	Wave runup on rubble-mound structure, ft
R_k	Refraction coefficient, dimensionless
S_k	Shoaling coefficient, dimensionless
t	Time, sec
T	Wave period, sec
y_i	Deviation of shoreline from equilibrium at i^{th} cell, ft
Y_i, y_2	Individual width
z	Ship squat, ft
α	Weir structure empirical coefficient, dimensionless

α_b	Breaking angle of wave with shoreline, deg
α_i	Angle of shoreline with respect to x-axis , deg
α_o	Breaking angle of wave with respect to x-axis , deg
β	Weir structure empirical coefficient, dimensionless
Δt	Time increment, hr
Δx	Length of cell along beachline, ft
Δy	Width of cell perpendicular to beachline, ft
ΔV	Incremental volume, cu ft
ε	Surf parameter, dimensionless
θ	Angle the seaward face of rubble-mound weir makes with horizontal, deg
π	3.14159, dimensionless
ρ	Density of salt water, 1.99 $lb\text{-}sec^2/ft^4$

END

FILMED

12-84

DTIC